



# University of HUDDERSFIELD

## University of Huddersfield Repository

Lepiarz-Raba, Izabela

Anti-Inflammatory and Neuroprotective Properties of Isoflavones Analogues

### Original Citation

Lepiarz-Raba, Izabela (2020) Anti-Inflammatory and Neuroprotective Properties of Isoflavones Analogues. Doctoral thesis, University of Huddersfield.

This version is available at <http://eprints.hud.ac.uk/id/eprint/35487/>

The University Repository is a digital collection of the research output of the University, available on Open Access. Copyright and Moral Rights for the items on this site are retained by the individual author and/or other copyright owners. Users may access full items free of charge; copies of full text items generally can be reproduced, displayed or performed and given to third parties in any format or medium for personal research or study, educational or not-for-profit purposes without prior permission or charge, provided:

- The authors, title and full bibliographic details is credited in any copy;
- A hyperlink and/or URL is included for the original metadata page; and
- The content is not changed in any way.

For more information, including our policy and submission procedure, please contact the Repository Team at: [E.mailbox@hud.ac.uk](mailto:E.mailbox@hud.ac.uk).

<http://eprints.hud.ac.uk/>



*University of*  
**HUDDERSFIELD**

**ANTI-INFLAMMATORY AND NEUROPROTECTIVE PROPERTIES  
OF ISOFLAVONES ANALOGUES**

by

**Izabela Edyta Lepiarz-Raba**

A thesis submitted to the University of Huddersfield in partial fulfilment of the  
requirements for the degree of Doctor of Philosophy

Department of Pharmacy

School of Applied Sciences

The University of Huddersfield

November 2020

## **COPYRIGHT STATEMENT**

- i. The author of this thesis (including any appendices and/or schedules to this thesis) owns any copyright in it (the “Copyright”) and s/he has given The University of Huddersfield the right to use such Copyright for any administrative, promotional, educational and/or teaching purposes.
- ii. Copies of this thesis, either in full or in extracts, may be made only in accordance with the regulations of the University Library. Details of these regulations may be obtained from the Librarian. This page must form part of any such copies made.
- iii. The ownership of any patents, designs, trademarks and any and all other intellectual property rights except for the Copyright (the “Intellectual Property Rights”) and any reproductions of copyright works, for example graphs and tables (“Reproductions”), which may be described in this thesis, may not be owned by the author and may be owned by third parties. Such Intellectual Property Rights and Reproductions cannot and must not be made available for use without permission of the owner(s) of the relevant Intellectual Property Rights and/or Reproductions.

## ABSTRACT

Chronic neuroinflammation leads to excessive production of pro-inflammatory mediators and consequently neurodegeneration. The alleviation of neuroinflammation may mitigate neurodegenerative disorders, including AD which incidence is higher in women due to decrease of oestrogen during menopause. This hypothesis indicates oestrogens as important neuroprotective factors. However, they may cause detrimental side effects in periphery. Therefore, oestrogens can be substituted by natural compounds such as isoflavones which resemble oestrogen structure but lack detrimental side effects. Presented research investigated anti-inflammatory and neuroprotective properties of four novel isoflavone analogues: biochanin A derivatives with carbamate and dodecenoyl ester moiety (compounds 1 and 2) and daidzein derivatives with ethyl ester and chloropropyl triazole moiety (compounds 3 and 4). The research concluded that compounds 1, 2, 3 and 4 reduced LPS-upregulated levels of  $\text{TNF}\alpha$ , IL-6, IL-1 $\beta$ , NO and iNOS in BV2 microglia. Biochanin A derivatives were less effective in inhibition of pro-inflammatory cytokines compared to daidzein derivatives. All tested compounds did not affect LPS-induced production of COX-2 and PGE<sub>2</sub> and do not possess free radical scavenging properties. Only compound 4 decreased NF- $\kappa$ B activity. All tested compounds did not reduce phosphorylation of p38, JNK and ERK1/2 and upregulated ERE activity. Moreover, the anti-inflammatory properties of compounds 3 and 4 are Nrf2-, SIRT1- and ER-independent. Compounds 3 and 4 diminished H<sub>2</sub>O<sub>2</sub>-induced apoptosis in SH-SY5Y neuroblastoma and reduced caspase-3/-7 and -9 activity. Compound 3 upregulated Bcl-2 level. In summary, compounds 3 and 4 inhibited neuroinflammation and protected neurons against oxidative damage. Additionally, this study investigated the validity of HMC3 cells as a cellular model to study neuroinflammation. Amongst ODN 2006, IFN $\gamma$ , LPS, and TNF $\alpha$ , TNF $\alpha$  induced the broadest inflammatory response in HMC3, upregulating Iba1, IL-6, and activating NF- $\kappa$ B and p38 signalling pathways. HMC3 microglia express ER $\alpha$  and ER $\beta$  therefore this cell line can be used to investigate properties of anti-inflammatory compounds acting via ERs.

## **PUBLICATIONS AND CONFERENCE PROCEEDINGS BASED ON THIS STUDY**

### **Conference proceedings:**

**Lepiarz-Raba, I.**, Menghereş G., Hemming, K., Javid, F., Olajide, O. Neuroprotective effects of daidzein derivative on hydrogen peroxide-induced apoptosis in SH-SY5Y cells. Abstract accepted for poster presentation at Neuronus IBRO 2020 Neuroscience Forum in Krakow, Poland - postponed due to COVID-19 to December 2020

**Lepiarz, I.**, Boluda Navarro M., Javid, F., Hemming, K., Olajide O. (2018). NF- $\kappa$ B independent anti-inflammatory properties of biochanin A analogue. Selected Abstracts from Pharmacology 2018. *British Journal of Pharmacology*, 176(16), 3023-3023. doi: 10.1111/bph.14681; poster presentation at the BPS Pharmacology 2018, Annual Meeting of the British Pharmacological Society; 18th – 20th December 2018 at Queen Elizabeth II Conference Centre Westminster London, UK

### **Under preparation:**

**Lepiarz-Raba, I.**, Menghereş, G., Javid, F., Hemming, K., Olajide, O. Anti-inflammatory and neuroprotective properties of ethyl ester and chloropropyl triazole daidzein derivatives

## ACKNOWLEDGEMENTS

I would like to express my special thanks to my research supervisors Dr Olumayokun Olajide and Dr Farideh Javid for their valuable guidance and supervision. Especially I would like to thank Dr Mayo who gave me golden opportunity to start my research journey investigating neuroinflammation during my placement year and also for introducing me into the world of neuroscience.

I would like to express my gratitude to Dr Gabriel Menghereş, Dr Heidi Joao and Dr Karl Hemming for chemical synthesis of compounds examined in this study.

I would like to thank the School of Applied Sciences at the University of Huddersfield for funding this project and my studentship.

I also would like to thank my friends for their inspiration, motivation and constant source of positive energy.

No words can sum up the gratitude I owe my mom. I appreciate your patience, understanding and support. I am deeply grateful for your strength and constant caring even if I am so far away (Żadne słowa nie mogą podsumować wdzięczności, jaką jestem winna mojej mamie. Dziękuję za cierpliwość, zrozumienie i wsparcie. Jestem głęboko wdzięczna za Twoją siłę i ciągłą opiekę, nawet jeśli jestem tak daleko).

Special thanks to my siblings, especially my sister for your constant encouragement and sense of humour.

My deepest appreciation belongs to my husband. Thank you for believing in me and for continuous encouragement through years of study, and the process of research and writing this thesis.

## TABLE OF CONTENTS

<b>1 Chapter I – General introduction .....</b>	<b>22</b>
1.1 Neuroinflammation .....	22
1.2 Neuroinflammation in the pathogenesis of neurodegeneration .....	23
1.3 Microglia .....	25
1.4 Mediators of neuroinflammation .....	27
1.4.1 Cytokines .....	27
1.4.1.1 Tumour Necrosis Factor $\alpha$ .....	27
1.4.1.2 Interleukin-6 .....	30
1.4.1.3 Interleukin-1 $\beta$ .....	31
1.4.2 Reactive Oxygen and Nitrogen Species.....	34
1.4.3 Prostaglandins .....	37
1.5 Signalling pathways modulating neuroinflammation .....	39
1.5.1 NF- $\kappa$ B transcription factor.....	39
1.5.2 MAPKs.....	41
1.5.2.1 p38 MAPK.....	41
1.5.2.2 ERK1/2.....	42
1.5.2.3 JNK.....	43
1.5.3 Nrf2 antioxidant transcription factor.....	44
1.5.4 SIRT1 in the regulation of inflammatory responses .....	45
1.6 Oestrogens in neuroinflammation and neurodegeneration .....	46
1.6.1 Oestrogen signalling pathways .....	48
1.6.2 Beneficial effects of oestrogens in the brain.....	50
1.7 Isoflavones .....	51
1.8 Aims and objectives of this study .....	53
<b>2 Chapter II - Anti-inflammatory Properties and Mechanism of Action of Biochanin A Derivatives .....</b>	<b>55</b>
2.1 Introduction.....	55
2.1.1 Biochanin A .....	55
2.1.2 Biochanin A derivatives.....	56
2.2 Methodology.....	57
2.2.1 BV2 cell culture .....	57
2.2.2 Treatment of BV2 cells with compounds 1 and 2.....	58

2.2.2.1	Determination of non-toxic and active concentrations of compounds 1 and 2 for BV2 cells	59
2.2.2.2	Optimisation of non-toxic concentration of DMSO for BV2 microglia	60
2.2.2.3	Evaluation of optimal LPS concentration to activate BV2 microglia	61
2.2.3	XTT cell viability assay	62
2.2.4	TNF- $\alpha$ , IL-1 $\beta$ and IL-6 ELISA	63
2.2.5	Griess assay	64
2.2.6	Western blotting	65
2.2.6.1	Whole-cell lysate preparation	66
2.2.6.2	Bradford assay	66
2.2.6.3	Immunoblotting	66
2.2.7	DPPH assay	69
2.2.8	PGE <sub>2</sub> enzyme immunoassay	70
2.2.9	Immunofluorescence	71
2.2.10	InstantOne™ ELISA for p-NF- $\kappa$ B and p-p38	72
2.2.11	Reporter gene assay	73
2.2.11.1	Optimisation of magnetofection	73
2.2.11.2	NF- $\kappa$ B and ERE reporter gene assay	77
2.2.12	Statistical analysis	78
2.3	Results	79
2.3.1	The effect of compounds 1 and 2 on the viability of BV2 cells using XTT	79
2.3.2	The effects of compounds 1 and 2 on the production of TNF $\alpha$ , IL-6, and IL-1 $\beta$ in LPS-activated BV2 microglia	80
2.3.3	The effects of compounds 1 and 2 on iNOS and nitrite expression in LPS-activated BV2 cells	82
2.3.4	Evaluation of the free-radical scavenging properties of compounds 1 and 2	84
2.3.5	The effects of compounds 1 and 2 on PGE <sub>2</sub> production and COX-2 expression in LPS-activated BV2 cells	84
2.3.6	The effects of compounds 1 and 2 on NF- $\kappa$ B signalling pathway in LPS-activated BV2 microglia	86
2.3.6.1	The effect of compounds 1 and 2 on phosphorylation of NF- $\kappa$ B p65	86
2.3.6.2	The effect of compounds 1 and 2 on the nuclear localisation of NF- $\kappa$ B p65 in LPS-activated BV2 cells	88
2.3.6.3	The effect of compounds 1 and 2 on NF- $\kappa$ B activity in LPS challenged BV2 cells	90



2.3.7	The effect of compounds 1 and 2 on ERE activity in BV2 microglial cells .....	91
2.3.8	The effect of compounds 1 on LPS-induced MAPKs phosphorylation in BV2 microglial cells .....	92
2.3.8.1	The effect of compound 1 on p38 phosphorylation induced by LPS in BV2 microglial cells.....	92
2.3.8.2	The effect of compound 1 on JNK phosphorylation in LPS challenged BV2 cells	93
2.3.8.3	The effect of compound 1 on LPS-induced ERK1/2 phosphorylation in BV2 microglial cells.....	94
2.4	Discussion .....	96
<b>3</b>	<b><i>Chapter III - Anti-inflammatory Properties and Mechanism of Action of Daidzein Derivatives.....</i></b>	<b>103</b>
3.1	Introduction.....	103
3.1.1	Daidzein .....	103
3.1.2	Daidzein derivatives.....	105
3.2	Methodology.....	106
3.2.1	BV2 cell culture .....	106
3.2.2	Treatment of BV2 microglia with ICI 182,780, ML385 and EX527 .....	106
3.2.3	Treatment of BV2 cells with compounds 3 and 4.....	106
3.2.4	XTT cell viability assay .....	107
3.2.5	TNF $\alpha$ , IL-6 and IL-1 $\beta$ ELISAs.....	107
3.2.6	Griess assay .....	107
3.2.7	Western blotting .....	108
3.2.8	DPPH assay.....	108
3.2.9	PGE <sub>2</sub> enzyme immunoassay .....	108
3.2.10	InstantOne™ ELISA for p-NF- $\kappa$ B and p-p38.....	108
3.2.11	Reporter gene assay .....	108
3.2.12	siRNA mediated knockdown of ER $\beta$ in BV2 cells.....	108
3.2.13	Statistical analysis .....	109
3.3	Results.....	110
3.3.1	The effect of compounds 3 and 4 on BV2 cell viability using XTT.....	110
3.3.2	The effects of compounds 3 and 4 on TNF $\alpha$ , IL-6 and IL-1 $\beta$ production in LPS activated BV2 cells .....	111

3.3.3	The effects of compounds 3 and 4 on nitrite and iNOS production in LPS-activated BV2 microglia .....	113
3.3.4	Evaluation of free-radical scavenging properties of compounds 3 and 4.....	115
3.3.5	The effects of compounds 3 and 4 on PGE <sub>2</sub> and COX-2 expression in LPS-induced BV2 microglia .....	115
3.3.6	The effect of compounds 3 and 4 on LPS-induced NF- $\kappa$ B activation in BV2 cells	117
3.3.6.1	The effect of compounds 3 and 4 on LPS-induced phosphorylation of NF- $\kappa$ B p65 in BV2 cells.....	117
3.3.6.2	The effect of compounds 3 and 4 on NF- $\kappa$ B LPS-induced activity in BV2 microglia	118
3.3.7	The effect of compounds 3 and 4 on LPS-induced MAPKs activation in BV2 microglia .....	119
3.3.7.1	The effect of compounds 3 and 4 on LPS-induced p-38 phosphorylation .....	119
3.3.7.2	The effect of compounds 3 and 4 on LPS-induced JNK phosphorylation .....	120
3.3.7.3	The effect of compounds 3 and 4 on LPS-induced ERK1/2 phosphorylation..	121
3.3.8	The effect of compounds 3 and 4 on ERE activity in BV2 microglia .....	122
3.3.9	The impact of ER antagonism on anti-inflammatory properties of compounds 3 and 4 in BV2 microglia .....	123
3.3.10	The effect of ER $\beta$ knockdown on anti-inflammatory activity of compounds 3 and 4 in BV2 microglia .....	124
3.3.11	The impact of Nrf2 antagonism on anti-inflammatory properties of compounds 3 and 4 in LPS-activated BV2 cells .....	126
3.3.12	The impact of SIRT1 antagonism on anti-inflammatory properties of compounds 3 and 4 in LPS-activated BV2 microglia.....	128
3.4	Discussion .....	130
<b>4</b>	<b><i>Chapter IV - Neuroprotective Properties of Daidzein Derivatives and their Molecular Mechanism</i></b> .....	<b>138</b>
4.1	Introduction.....	138
4.1.1	Neurons .....	138
4.1.2	Neuronal death in neuroinflammation .....	139
4.1.3	Neuroprotective properties of daidzein.....	141
4.2	Methods.....	142
4.2.1	HT22 cell culture .....	142

4.2.2	BV2 cell culture .....	142
4.2.3	HMC3 cell culture.....	142
4.2.4	SH-SY5Y cell culture .....	143
4.2.4.1	Differentiation of SH-SY5Y cells.....	143
4.2.5	XTT cell viability assay .....	144
4.2.6	Selection of the cell model and neurotoxicity-inducing agent for neuroprotection experiments.....	144
4.2.6.1	Conditioned medium experiments.....	144
4.2.6.2	The impact of Amyloid $\beta_{25-35}$ on SH-SY5Y viability .....	147
4.2.6.3	The impact of H <sub>2</sub> O <sub>2</sub> on SH-SY5Y viability.....	148
4.2.7	Treatment of SH-SY5Y cells with compounds 3 and 4.....	148
4.2.8	Annexin V-FITC /PI .....	149
4.2.9	Caspase-3/-7 and -9 activity.....	151
4.2.10	Bcl-2 ELISA .....	152
4.2.11	Pre-treatment of cells with ER antagonist – ICI 182,780.....	152
4.2.12	Statistical analysis .....	153
4.3	Results.....	154
4.3.1	The effect of compounds 3 and 4 on the viability of SH-SY5Y cells .....	154
4.3.2	The effect of compounds 3 and 4 on H <sub>2</sub> O <sub>2</sub> -induced reduction of SH-SY5Y viability using XTT .....	155
4.3.3	The effect of compounds 3 and 4 on H <sub>2</sub> O <sub>2</sub> -induced SH-SY5Y cell death using Annexin V/PI flow cytometry.....	155
4.3.4	The effect of compounds 3 and 4 on H <sub>2</sub> O <sub>2</sub> -induced caspase-3/-7 activity in SH-SY5Y cells .....	158
4.3.5	The effect of compounds 3 and 4 on the H <sub>2</sub> O <sub>2</sub> -induced caspase-9 activity in SH-SY5Y cells.....	159
4.3.6	The effect of compounds 3 and 4 on the Bcl-2 level in SH-SY5Y cells .....	160
4.3.7	The impact of ER antagonist on neuroprotective properties of compounds 3 and 4 in SH-SY5Y cells .....	161
4.4	Discussion .....	162
<b>5</b>	<b><i>Chapter V - Development of the Human Microglia (HMC3) as a Cellular Model of Neuroinflammation.....</i></b>	<b>166</b>
5.1	Introduction.....	166
5.1.1	Microglial cell models .....	166

5.1.2	The human microglial clone 3 cell line.....	167
5.2	Methods.....	169
5.2.1	HMC3 cell culture.....	169
5.2.2	Stimulation of HMC3 cells with LPS, IFN $\gamma$ , TNF $\alpha$ and ODN 2006.....	169
5.2.3	Treatment of HMC3 microglia with 17 $\beta$ -oestradiol .....	169
5.2.4	Immunofluorescence .....	169
5.2.5	Griess assay .....	170
5.2.6	TNF $\alpha$ and IL-6 ELISAs.....	170
5.2.7	Western blotting.....	170
5.2.8	ROS immunofluorescence .....	170
5.2.9	Statistical analysis .....	171
5.3	Results.....	172
5.3.1	Expression of Iba1 in HMC3 .....	172
5.3.2	Expression of CD14 in HMC3.....	175
5.3.3	Expression of ER $\beta$ and ER $\alpha$ in HMC3 cells.....	176
5.3.4	Expression of TLR4 and TLR9.....	178
5.3.5	ROS production in HMC3 .....	179
5.3.6	The effect of ODN 2006, IFN $\gamma$ , LPS, and TNF $\alpha$ on the production nitrite, IL-6 and TNF $\alpha$ .....	180
5.3.7	NF- $\kappa$ B activation in HMC3 cells .....	181
5.3.7.1	The effect of LPS on NF- $\kappa$ B nuclear localisation in HMC3 cells.....	182
5.3.7.2	The effect of IFN $\gamma$ on NF- $\kappa$ B activation.....	183
5.3.7.3	The effect of TNF $\alpha$ on NF- $\kappa$ B activation.....	186
5.3.8	MAPK activation in HMC3 cells.....	187
5.3.8.1	The impact of IFN $\gamma$ on ERK1/2 in HMC3 cells.....	187
5.3.8.2	The effect of IFN $\gamma$ on p38 in HMC3 cells.....	188
5.3.8.3	The effect of TNF $\alpha$ on ERK1/2 activation in HMC3 cells .....	189
5.3.8.4	The effect TNF $\alpha$ on p38 activation in HMC3.....	190
5.4	Discussion .....	191
<b>6</b>	<b><i>Concluding Remarks.....</i></b>	<b><i>196</i></b>
6.1	Directions for future research .....	201
<b>7</b>	<b><i>Appendices.....</i></b>	<b><i>203</i></b>
7.1	Appendix 1: Anti-inflammatory properties of compounds 3 and 4 using HMC3 activated with TNF $\alpha$ .....	203

7.1.1	Treatment of HMC3 with compounds 3 and 4 .....	203
7.1.2	The effect of compounds 3 and 4 on the viability of HMC3 cells .....	204
7.1.3	The effect of compounds 3 and 4 on IL-6 production in TNF $\alpha$ activated HMC3 microglia .....	204
7.2	Appendix 2: Figure illustrating the experimental variation that occurs in LPS control .....	206
7.3	Appendix 3: List of materials used in this study.....	207
<b>References.....</b>		<b>211</b>

## LIST OF FIGURES

Figure 1.1 Morphology of microglial cells .....	26
Figure 1.2 TNF $\alpha$ cytokine production and signalling via TNFR1 and TNFR2.....	29
Figure 1.3 IL-6 cytokine secretion and classical and trans-signalling pathways.....	31
Figure 1.4 Pro-IL-1 $\beta$ production, activation and its pathological effects.....	33
Figure 1.5 Enzymatic synthesis of nitric oxide.....	35
Figure 1.6 Oxidative/nitrosative damage caused to cells by peroxynitrite .....	36
Figure 1.7 The biosynthesis of PGE <sub>2</sub> and its signalling .....	38
Figure 1.8 Canonical and alternative NF- $\kappa$ B signalling pathway.....	40
Figure 1.9 MAPK signalling pathways.....	43
Figure 1.10 Nrf2 signalling in homeostasis and stress conditions.....	45
Figure 1.11 The structural representation of oestrogens.....	47
Figure 1.12 Cell-specific 17 $\beta$ -oestradiol production in a brain .....	48
Figure 1.13 Oestrogenic signalling pathways .....	49
Figure 1.14 The structural representation of isoflavones.....	52
Figure 2.1 The chemical structure of biochanin A. ....	56
Figure 2.2 The structural formula of biochanin A derivatives – compounds 1 and 2.....	56
Figure 2.3 Determination of maximum non-toxic and active concentrations of compounds 1 and 2 for BV2 cells .....	59
Figure 2.4 Optimisation of non-toxic concentration of DMSO for BV2 microglia .....	60
Figure 2.5 Evaluation of optimal LPS concentration to activate BV2 microglia .....	61
Figure 2.6 Flowchart of XTT assay and schematics of XTT reduction to XTT formazan...62	
Figure 2.7 Flowchart of sandwich ELISA.....	63
Figure 2.8. Flowchart of Griess assay and chemical representation of nitrite reaction with Griess reagents leading to the azo dye formation .....	64
Figure 2.9 The flowchart of Western blotting experiment. ....	65
Figure 2.10 Flowchart of DPPH assay and chemical reduction of DPPH radical.....	69
Figure 2.11 Flowchart of PGE <sub>2</sub> Enzyme Immunoassay. ....	70
Figure 2.12 Flowchart of immunofluorescence experiment. ....	71
Figure 2.13 Flowchart of InstantOne ELISA.....	72
Figure 2.14 Magnetofection efficiency using different transfection reagent concentrations	75
Figure 2.15 Magnetofection efficiency using different amounts of DNA.....	76

Figure 2.16 Flowchart of reporter gene assay and bioluminescent reactions catalysed by firefly and <i>Renilla</i> luciferases. ....	78
Figure 2.17 The effect of compounds 1 and 2 on the viability of BV2 using XTT.....	79
Figure 2.18 The effects of compounds 1 and 2 on the production of TNF $\alpha$ , IL-6 and IL-1 $\beta$ in LPS activated BV2 cells .....	81
Figure 2.19 The effects of compounds 1 and 2 on nitrite and iNOS production in LPS activated BV2 cells .....	83
Figure 2.20 DPPH scavenging effect of compounds 1 and 2 .....	84
Figure 2.21 Impact of compounds 1 and 2 on PGE <sub>2</sub> and COX-2 expression .....	85
Figure 2.22 Time course of LPS-induced phosphorylation of NF- $\kappa$ B in BV2 cells.....	86
Figure 2.23. Impact of compounds 1 and 2 on phosphorylation of NF- $\kappa$ B in LPS challenged BV2 cells.....	87
Figure 2.24 The effect of compounds 1 and 2 on the nuclear localisation of NF- $\kappa$ B p65 in LPS-stimulated BV2 cells.....	89
Figure 2.25 Time-course of LPS-induced NF- $\kappa$ B luciferase activity in BV2 cells .....	90
Figure 2.26 The effect of compounds 1 and 2 on NF- $\kappa$ B activity in LPS challenged BV2 microglial cells .....	90
Figure 2.27 The effect of compounds 1 and 2 on ERE activity in BV2 cells.....	91
Figure 2.28 Time course experiment for LPS induced p38 phosphorylation in BV2 microglia .....	92
Figure 2.29 The effect of compound 1 on the p-p38 level in LPS challenged BV2 cells ....	92
Figure 2.30 The time point of LPS-induced p-JNK expression in BV2 microglia.....	93
Figure 2.31 The effect of compound 1 on JNK phosphorylation in LPS challenged BV2 cells .....	93
Figure 2.32 Time course experiment of ERK1/2 phosphorylation in LPS activated BV2 cells .....	94
Figure 2.33 The effect of compound 1 on ERK1/2 phosphorylation in LPS stimulated BV2 cells .....	95
Figure 2.34 Schematic representation of anti-inflammatory action of compound 1 and 2.	102
Figure 3.1 The chemical structure of daidzein.....	104
Figure 3.2 The structural formula of daidzein derivatives - compounds 3 and 4.....	105
Figure 3.3 Determination of maximum non-toxic and active concentrations of compounds 3 and 4 for BV2 cells .....	107
Figure 3.4 Flowchart of siRNA-mediated gene knockdown. ....	109

Figure 3.5 The effect of compounds 3 and 4 on the viability of BV2 using XTT.....	110
Figure 3.6 The effects of compounds 3 and 4 on the production of TNF $\alpha$ , IL-6 and IL-1 $\beta$ in LPS-induced BV2 cells.....	112
Figure 3.7 The effects of compounds 3 and 4 on nitrite and iNOS production in LPS activated BV2 cells.....	114
Figure 3.8 DPPH scavenging effect of compounds 3 and 4. ....	115
Figure 3.9 The effects of compounds 3 and 4 on PGE <sub>2</sub> and COX-2 expression in LPS activated BV2 microglia .....	116
Figure 3.10 The effect of compounds 3 and 4 on p-NF- $\kappa$ B p65 level in LPS activated cells .....	117
Figure 3.11 The effect of compounds 3 and 4 on NF- $\kappa$ B activity in LPS stimulated BV2 cells .....	118
Figure 3.12 The effect of compounds 3 and 4 on LPS-induced p-38 phosphorylation in BV2 microglia .....	119
Figure 3.13 The effect of compounds 3 and 4 on the p-JNK level in LPS activated BV2 cells .....	120
Figure 3.14 The effect of compounds 3 and 4 on ERK1/2 phosphorylation in LPS activated BV2 cells.....	121
Figure 3.15 Effects of compound 3 and 4 on the ERE activity at different time points .....	122
Figure 3.16 The effect of compounds 3 and 4 on ERE activity in BV2 microglia.....	122
Figure 3.17 The effect of ICI 182,780 on compounds 3 and 4 ability to reduce LPS-induced TNF $\alpha$ and IL-6 production in BV2 cells.....	123
Figure 3.18 Efficiency of siRNA mediated ER $\beta$ knockdown in BV2 cells.....	124
Figure 3.19 The effect of ER $\beta$ knockdown in BV2 cells on the anti-inflammatory activity of compounds 3 and 4 .....	125
Figure 3.20 The effect of ML385 on compounds 3 and 4 ability to reduce LPS-induced TNF $\alpha$ , IL-6 and nitrite production in BV2 microglia .....	127
Figure 3.21 The effect of EX527 on compounds 3 and 4 ability to reduce LPS-induced TNF $\alpha$ , IL-6 and nitrite production in BV2 cells.....	129
Figure 3.22 Schematic representation of anti-inflammatory actions of compounds 3 and 4 .....	137
Figure 4.1 Diagram of a neuron. ....	138
Figure 4.2 Diagram of the extrinsic and intrinsic apoptotic pathway.....	140



Figure 4.3 Microscopical assessment of undifferentiated and RA-differentiated SH-SY5Y cells .....	144
Figure 4.4 The effect of BV2 conditioned medium on HT22 viability .....	145
Figure 4.5. The effect of HMC3 conditioned medium on HT22 viability .....	145
Figure 4.6 The effect of HMC3 conditioned medium on SH-SY5Y viability.....	146
Figure 4.7 Viability of SH-SY5Y cells after A $\beta$ <sub>25-35</sub> incubation.....	147
Figure 4.8 Determination of the optimal H <sub>2</sub> O <sub>2</sub> concentration to induce SH-SY5Y cell death .....	148
Figure 4.9 Optimisation of non-toxic concentration of DMSO for differentiated SH-SY5Y cells .....	149
Figure 4.10 Schematic representation of annexin V/PI staining of live, early apoptotic and late apoptotic/necrotic cells.....	149
Figure 4.11 Flowchart of Annexin V/PI staining.....	150
Figure 4.12 Flowchart of Caspase-Glo <sup>®</sup> 3/7 and 9 Assay System.....	152
Figure 4.13 The effect of compounds 3 and 4 on the viability of SH-SY5Y cells .....	154
Figure 4.14 The effect of compounds 3 and 4 on H <sub>2</sub> O <sub>2</sub> -induced reduction of SH-SY5Y cell viability .....	155
Figure 4.15 Viability of cells exposed to different concentrations of compounds 3 and 4 followed by H <sub>2</sub> O <sub>2</sub> -induced apoptosis of SH-SY5Y cells.....	157
Figure 4.16 The effect of compounds 3 and 4 on H <sub>2</sub> O <sub>2</sub> -induced caspase 3/7 activity in SH-SY5Y neurons.....	158
Figure 4.17 The effect of compounds 3 and 4 on H <sub>2</sub> O <sub>2</sub> -induced caspase-9 activity in SH-SY5Y neurons.....	159
Figure 4.18 The effect of compounds 3 and 4 on the Bcl-2 level in SH-SY5Y incubated with or without H <sub>2</sub> O <sub>2</sub> .....	160
Figure 4.19 The impact of ER antagonist on neuroprotective properties of compounds 3 and 4 in SH-SY5Y .....	161
Figure 4.20 Schematic representation of neuroprotective actions of compounds 3 and 4. ....	165
Figure 5.1 Flowchart of ROS immunofluorescence .....	171
Figure 5.2 The Iba1 expression in HMC3 cells .....	174
Figure 5.3 CD14 expression in HMC3 cells .....	175
Figure 5.4 ER $\beta$ and ER $\alpha$ expression in HMC3 cells .....	176
Figure 5.5 ER $\beta$ expression in HMC3 cells .....	177
Figure 5.6 The expression of TLR4 and TLR9 in HMC3 cells .....	178

Figure 5.7 ROS production in HMC3 cells .....	179
Figure 5.8 The effect of ODN 2006, IFN $\gamma$ , LPS and TNF $\alpha$ on the production of nitrite, IL-6 and TNF $\alpha$ in HMC3 cells.....	181
Figure 5.9 The effect of LPS on NF- $\kappa$ B p65 nuclear localisation in HMC3 cells.....	182
Figure 5.10 The effect of IFN $\gamma$ on nuclear localisation of NF- $\kappa$ B p65 in HMC3 cells .....	184
Figure 5.11 The effect of IFN $\gamma$ alone and IFN $\gamma$ with BAY 11-7082 on phosphorylation of NF- $\kappa$ B p65 in HMC3 .....	185
Figure 5.12 The effect of TNF $\alpha$ on NF- $\kappa$ B p65 phosphorylation in HMC3 cells .....	186
Figure 5.13 The effect of IFN $\gamma$ on ERK1/2 activation in HMC3 cells .....	187
Figure 5.14 The effect of IFN $\gamma$ on p38 activation in HMC3. ....	188
Figure 5.15 The effect of TNF $\alpha$ on ERK1/2 activation in HMC3 cells .....	189
Figure 5.16 The effect of TNF $\alpha$ on p38 activation in HMC3 cells .....	190
Figure 7.1 The effect of compounds 3 and 4 on the viability of HMC3 using XTT .....	204
Figure 7.2 The effect of compounds 3 and 4 on the production of IL-6 in TNF $\alpha$ activated HMC3 cells .....	205
Figure 7.3 TNF $\alpha$ production in untreated and LPS-activated BV2 microglia.....	206

## LIST OF TABLES

Table 2.1 The list of primary antibodies used in immunoblotting experiments.....	68
Table 5.1 The list of antibodies used for immunofluorescence staining.....	170

## LIST OF ABBREVIATIONS

17 $\beta$ -HSD	17 $\beta$ -hydroxysteroid dehydrogenase
AA	Arachidonic acid
AD	Alzheimer's Disease
ADAM	A disintegrin and metalloproteinases
AMPA	$\alpha$ -amino-3-hydroxy-5-methyl-4-isoxazolepropionic acid receptor
ANOVA	Analysis of variance
AP-1	Activator protein 1
APAF-1	Apoptotic protease activating factor 1
APP	Amyloid precursor protein
ARE	Antioxidant response elements
A $\beta$	Amyloid beta
BAF	B cell-activating factor
BBB	Blood-brain barrier
BCA	Biochanin A
Bcl-2	B-cell lymphoma 2
BDNF	Brain-derived neurotrophic factor
BSA	Bovine serum albumin
BSF	B-cell differentiation factor
bZIP	Basic leucine zipper
cAMP	Cyclic adenosine monophosphate
ChAT	Choline acetyltransferase
CNS	Central nervous system
Compound 1	5-hydroxy-3-(4-methoxyphenyl)-4-oxochromen-7-yl N-undecylcarbamate
Compound 2	5-hydroxy-3-(4-methoxyphenyl)-4-oxochromen-7-yl dodecanoate
Compound 3	Ethyl 2-(4-(7-hydroxy-4-oxo-4H-chromen-3-yl)phenyl)acetate
Compound 4	3-(4-(4-(3-chloropropyl)-1H-1,2,3-triazol-1-yl)phenyl)-7-hydroxy-4H-chromen-4-one
COX-2	Cyclooxygenase 2
cPGES	Cytosolic prostaglandin E synthases
DMSO	Dimethyl sulfoxide

DPPH	2,2-Diphenyl-1-picrylhydrazyl
E1	Estrone
E2	Oestradiol
E3	Estriol
E4	Estetrol
EIA	Enzyme immunoassay
ELISA	Enzyme-linked immunosorbent assay
EP	E-prostanoid
ER	Oestrogen receptor
ERE	Oestrogen response element
ERK	Extracellular signal-regulated kinase
FADD	Fas-associated death domain protein
FBS	Foetal bovine serum
GABA	Gamma-aminobutyric acid
GAP-43	Growth-associated protein 43
GPR30	G protein-coupled oestrogen receptor -1
GPX	Glutathione peroxidase
GWAS	Genome-wide association studies
H <sub>2</sub> O <sub>2</sub>	Hydrogen peroxide
HMC3	Human microglial clone 3 cell line
HO-1	Heme oxygenase-1
ICE	Interleukin-1 converting enzyme
IFN $\gamma$	Interferon gamma
IL	Interleukin
iNOS	Inducible nitric oxide synthases
JAK	Janus kinase
JNK	c-Jun N-terminal-activated protein kinase
kDa	Kilodalton
Keap1	Kelch-like erythroid cell-derived protein
LPS	Lipopolysaccharide
MAPK	Mitogen-activated protein kinase
MHC	Major histocompatibility complex

MOMP	Mitochondrial outer membrane permeabilization
mPGES	Microsomal prostaglandin E synthases
NADPH	Nicotinamide adenine dinucleotide phosphate
NED	N-1-naphthyl ethylenediamine dihydrochloride
NF- $\kappa$ B	Nuclear factor kappa-light-chain-enhancer of activated B cells
NMDAR	N-methyl-D-aspartate receptor
NO	Nitric oxide
NO $\cdot_2$	Nitrogen dioxide
NOS	Nitric oxide synthases
NQO1	Nicotinamide adenine dinucleotide phosphate quinone oxidoreductase 1
Nrf2	Nuclear factor erythroid 2-related factor 2
NSAIDs	Non-steroidal Anti-inflammatory Drugs
O $\cdot^-_2$	Superoxide
OH $\cdot$	Hydroxyl radical
ONOO $^-$	Peroxynitrite
PAMP	Pathogen-associated molecular patterns
PARP	Poly (ADP-ribose) polymerase
PBS	Phosphate buffered saline
PGE2	Prostaglandin E2
PKA	Protein kinase A
PLA $_2$	Phospholipase A2
PMS	Phenazine methosulfate
PMSF	Phenylmethane sulfonyl fluoride
PPAR- $\gamma$	Peroxisome proliferator-activated receptor gamma
PRR	Pathogen recognition receptors
PTGS	Prostaglandin-endoperoxide synthase
RANKL	Receptor activator of NF- $\kappa$ B ligand
ROS	Reactive oxygen species
SEM	Standard error of the mean
SERM	Selective Oestrogen Receptor Modulators
SIRT1	Sirtuin 1
sMaf	Small musculoaponeurotic fibrosarcoma proteins

SNPs	Single nucleotide polymorphisms
SOD	Superoxide dismutase
SP-1	Stimulating protein-1
STAT	signal transducer and activator of transcription
TBST	Mixture of Tris-buffered Saline and Polysorbate 20 (also known as Tween 20)
TLR	Toll-like receptor
TMB	Tetramethylbenzidine
TNF $\alpha$	Tumor necrosis factor alpha
TRADD	Tumour necrosis factor receptor type 1-associated death domain protein
XTT	2,3-bis-(2-methoxy-4-nitro-5-sulfophenyl)-2H-tetrazolium-5-carboxanilide

# 1 Chapter I – General introduction

This thesis explores the anti-inflammatory and neuroprotective properties of novel isoflavones analogues and possible signalling pathways involved in those actions.

Chapter I presents insight into the literature related to neuroinflammation, its mechanisms and consequences. Furthermore, this chapter provides an introduction to the family of compounds used in this study and its biological activity. Chapter II highlights anti-inflammatory properties of biochanin A derivatives and their molecular mechanism at the protein level. Biochanin A is an isoflavone abundantly found in legumes with diverse biological actions, most notably as a phytoestrogen. Chapter III presents the anti-inflammatory actions of daidzein derivatives and possible mechanisms responsible for these activities. Similarly to biochanin A, daidzein also belongs to the isoflavone family with extensive pharmacological properties due to phytoestrogenic properties. Chapter IV gives evidence for neuroprotective properties of daidzein derivatives and insight into its molecular mechanism. The lack of human neuroinflammatory models presents challenges for translation of studies from rodent cell lines to clinical trials due to insufficient correlation with the human genome. Therefore, chapter V presents assessment of human microglial clone 3 cell line (HMC3) as an alternative cellular model to study neuroinflammation and anti-inflammatory activity of compounds. Chapter VI provides concluding remarks and directions for future research.

## 1.1 Neuroinflammation

Neuroinflammation is an organism's defensive mechanism initiated in the Central Nervous System (CNS) by metabolic or traumatic injuries, infections, ageing and neurodegenerative disorders (DiSabato, Quan, & Godbout, 2016). Neuroinflammation is a neuroprotective process involved in the degradation of inflammatory insult followed by restoration of homeostasis and repair of damaged tissue, i.e. promoting neurogenesis and neurite outgrowth (Sochocka, Diniz, & Leszek, 2017). However, prolonged neuroinflammation lacks the resolution of the inflammation phase, which cause chronic and progressive neuronal loss. It is established that the immunological response of the brain is mainly mediated by glial cells. Chronic activation of glial cells has been observed as an accompanying factor of neurodegenerative disorders (Chen, Zhang, & Huang, 2016). Moreover, chronic neuroinflammation is also associated with peripheral immune cells infiltration into CNS.

Although, the CNS is generally considered as an immunologically privileged site due to blood-brain barrier (BBB) which prevents pathogens, peripheral immune cells and various proteins from non-selectively crossing into CNS. BBB is composed of endothelial cells of the capillary wall, astrocyte end-feet, and pericytes embedded in the capillary basement membrane. The BBB is a highly selective semipermeable barrier. However, numerous pathologic states, including trauma, hypoxia, infection, inflammation, dietary components, environmental toxins and genetic factors can cause disturbances in the BBB (Małkiewicz et al., 2019). BBB disruption leads to a reduction in barrier tightness, which consequently compromises the protection of the brain cells. Loss of BBB integrity allows migration of the peripheral immune cells into the CNS, which activates glial cells that cause further damage of BBB and neuroinflammation. BBB impairment may be initiated in periphery or CNS and is associated with neurodegenerative disorders (Erickson, Dohi, & Banks, 2012).

## **1.2 Neuroinflammation in the pathogenesis of neurodegeneration**

Ageing is one of the causes leading to disruption in the communication and balance between the brain and the immune system. Therefore, ageing is the most significant risk factor for neurodegenerative disorders. Franceschi et al., (2007) introduced the term *inflammaging*, which describes the ageing-induced shift of the immune system towards pro-inflammatory status. The ageing process results in alterations of morphological, phenotypical and transcriptional activities of immune brain cells. Morphological changes of aged microglia include decreased processes complexity, de-ramification and shortening of processes which indicate their phenotypic change toward activated state (Sierra, Gottfried-Blackmore, McEwen, & Bulloch, 2007). Furthermore, aged microglia enhance expression of inflammatory-related proteins such as major histocompatibility complex II (MHC II), toll-like receptors (TLRs) (Sierra et al., 2007). This altered inflammatory profile of microglia causes their sensitization which is revealed by increased expression of inflammatory markers and mediators, decreased threshold and time for activation, and exaggerated immune response following activation (DiSabato et al., 2016). Therefore, elevated microglial activation caused by the ageing process contributes to a chronic state of neuroinflammation and consequently neurodegeneration.

Damage to neuronal structure and function is often caused by chronic neuroinflammation, which is not only one of the symptoms but also causes the neurodegeneration (Kanazawa, 2001). Neurodegeneration is characterised by the progressive loss of specific subtype of



neuronal cells leading to functional and mental impairments (Chen, Zhang, & Huang, 2016). Loss of neurons in the cerebral cortex and hippocampus leads to Alzheimer's disease (AD) (Hussain, Zubair, Pursell, & Shahab, 2018). AD is the most common form of dementia and is the most prevalent neurodegenerative disorder of modern society. Globally, 47 million people are living with the AD, and it is estimated that this number will increase to 131.5 million by 2050 (Prince, Wimo, Guerchet, 2015). The AD is an incurable neurodegenerative disease which is accompanied by a prolonged neuroinflammatory process. The AD leads to gradual deterioration of the cognitive functions, and consequently, a patient's loss of independence. The main pathological symptom of the AD is an aggregation of  $\beta$ -amyloid plaques ( $A\beta$ ) and neurofibrillary tangles. Amyloid  $\beta$  plaques are composed of  $A\beta$  peptides formed by 39-42 amino acids.  $A\beta$  is accumulated in the limbic system, mainly in the hippocampus and the associative fields of the cerebral cortex.  $A\beta$  arises as a result of the amyloidogenic proteolytic cleavage of the  $\beta$ -amyloid precursor protein ( $\beta$ APP) by the  $\beta$  and  $\gamma$  secretases. Neurofibrillary tangles are aggregates of the hyperphosphorylated microtubule-associated protein tau which accumulate inside the cells (Galimberti & Scarpini, 2012).

Selkoe and Hardy (2002) presented a theory of AD pathogenesis called *Amyloid Cascade Hypothesis*, which postulates that abnormal accumulation of  $A\beta$  plaques leads to neurodegeneration. This theory is based on numerous studies which show that  $A\beta$  plaques trigger an inflammatory response by the innate immune system of the brain (Meda et al., 1995; Rogers et al., 1992). The exact processes leading to the pathogenesis of neurodegeneration in AD have not been fully understood. However, a growing body of evidence suggests that neuroinflammation is not only a symptom of neurodegeneration but is a substantial factor contributing to the progression of the disease (Perry & Teeling, 2013).

According to neuroinflammation theory, the most critical pathophysiological event for the AD development is chronic activation of the microglial cells (Wojtera, Kłoszewska, Sobów, & Liberski, 2006). This theory was inspired by Haga, Akai & Ishii (1989) study, which described the accumulation of microglial cells in and around  $A\beta$  deposits in human brains. The critical role of neuroinflammation in the progression of AD is also supported by numerous studies demonstrating the highly increased immunological microglial activity in patients with AD (Łabuzek et al., 2015). Moreover, Meda et al. (1995) indicated that the stimulation of microglial cells with  $A\beta$  in combination with  $IFN\gamma$  leads to the production of numerous neurotoxic agents, including cytokines, ROS and NOS. Furthermore, pro-inflammatory factors secreted by activated microglia at high concentrations have cytotoxic

properties causing neuronal deterioration (Brown & Vilalta, 2015). Epidemiological studies suggested that long-term use of non-steroidal anti-inflammatory drugs (NSAIDs) can delay AD development (Wojtera et al., 2006). Therefore, reduction of neuroinflammation may serve as a strategy to slow down the development of neurodegeneration.

Moreover, last decade findings of genome-wide association studies (GWAS) determined that two-thirds of AD-risk single nucleotide polymorphisms (SNPs) are exclusively or most highly expressed in microglia. Therefore, alongside 48 AD-risk SNPs, 29 of which are most highly expressed by microglia (McQuade & Blurton-Jones, 2019). Most of the genetic loci that robustly associate with AD-risk are implicated in immune system functions, including the innate immune response, phagocytosis and lipid metabolism (Gray, Kinghorn, & Woodling, 2020). Consequently, the role of microglia and neuroinflammation in the pathogenesis of AD neurodegeneration seems to be more important than previously assumed. AD is a multifactorial disorder with genetic and epigenetic risk factors. Currently, there is no cure for AD and treatment strategies are focusing on the alleviation of symptoms (Loera-Valencia et al., 2019). Hence, reduction of chronic inflammation which is a disease-escalating factor might slow down the progression of neurodegeneration.

### **1.3 Microglia**

Microglia are immunocompetent brain cells with phagocytic properties which constitute from 10 to 20% of all glial cells in CNS. Microglia were first described in 1932 by Rio-Hortega who based on fixed tissue staining with silver carbonate method in detail described nature, function and structural plasticity of microglia (Figure 1.1) (Tremblay, Lecours, Samson, Sánchez-Zafra, & Sierra, 2015). Microglia originate in the yolk sac and infiltrate the brain during early embryonic stages where they maintain themselves until adulthood via local proliferation (Ginhoux & Prinz, 2015). Microglial cells play a crucial role in maintaining brain homeostasis and facilitate neuroplasticity. During neurogenesis, microglia mediate synaptic pruning and modulate neuronal proliferation and differentiation (Tong & Vidyadaran, 2016). Microglial morphology varies based on their function. In healthy CNS, microglia occur in ramified morphology abbreviated by small cell body and numerous extending protrusions. Ramified state of microglia, also known as M0, indicates resting microglia and occurs during homeostasis. However, even in resting-state microglia are highly active and constantly survey the surrounding environment through the chemotaxis. Microglia express the highest number of receptors among all CNS cells; hence they are extremely

sensitive and responsive to pathogens and molecules secreted by adjacent cells (Helmut, Hanisch, Noda, & Verkhratsky, 2011).

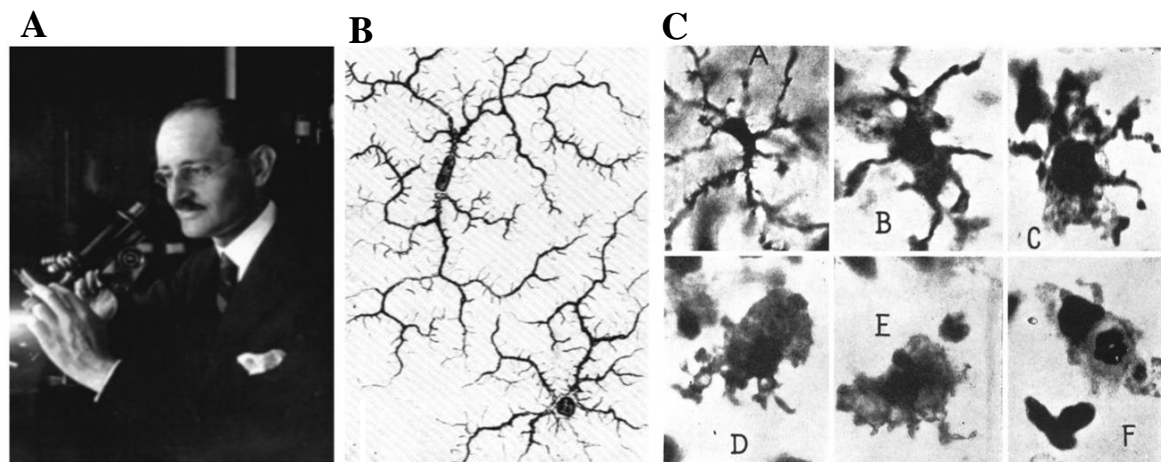


**Figure 1.1 Morphology of microglial cells.** (A) Pio del Rio-Hortega (1882–1945) - Spanish neuroscientist who discovered microglia. (B) Morphology of ramified microglial cells drawn by Pio del Rio-Hortega. (C) Photomicrographs of microglia showing phagocytosis captured by Rio-Hortega: A: ramified microglia with thick, long protrusions; B: microglia with enlarged soma and short protrusions; C: enlarged cell with small protrusions; D and E: hypertrophic cell with small pseudoptotic forms; F: microglial cell phagocytosing leukocyte. Source: (Helmut et al., 2011).

Disturbance of brain homeostasis or invading pathogens are sensed by danger-associated molecular patterns (DAMPs) or pathogen-associated molecular patterns (PAMPs) which cause morphological and immunogenic phenotype changes of microglia resulting in amoeboid shape and alteration of microglial function. Amoeboid morphology indicates activated microglia and is recognized as the hallmark of neuroinflammation. Based on receptor expression, a variety of microglial activation phenotypes has been distinguished. However, to simplify, they can be classified into two main phenotypes M1 and M2. M1 phenotype is also known as classically activated pro-inflammatory activation. In turn, M2 phenotype relates to alternatively activated microglia, which promote immune-resolution and tissue repair. M1 activated microglia conduct phagocytosis of damaged cells, microbes, debris or proteins. Moreover, M1 cells produce an array of pro-inflammatory factors such as cytokines (TNF $\alpha$ , IL-1 $\beta$ , IL-6), chemokines, prostaglandins and ROS/NOS (Łabuzek, Skrudlik, Gabryel, & Okopień, 2015). Biologically active substances secreted by M1 microglia act as autocrine and paracrine signalling molecules, thereby recruiting brain and periphery immune cells to migrate into the lesion site and combat inflammatory stimuli (Helmut et al., 2011).

In normal physiological conditions, M1 phenotype is counterbalanced by M2 phenotype, which induces anti-inflammatory gene expression. M2 alternative activation, reduce

inflammation and restore damaged tissues. Moreover, this alternative microglial activation participates in the mechanisms of neuroplasticity, neuro-regeneration, and remyelination. Therefore, lack of M2 stage leads to chronic inflammation causing over-activation of microglia, which further escalate inflammatory response and mediates neurodegeneration (Arcuri, Mecca, Bianchi, Giambanco, & Donato, 2017).

## **1.4 Mediators of neuroinflammation**

### **1.4.1 Cytokines**

Cytokines are small complex proteins released by several immune cells in various tissues; these proteins control both, the initiation, and following phases of the immune response. Cytokines enable migration of immunocompetent cells into the infection site and upregulate expression of pro-inflammatory genes, thereby modulating the inflammatory response (Becher, Spath, & Goverman, 2017). Currently, there are more than 300 known cytokines which include chemokines, interleukins, interferons, and tumour necrosis factors. An increased level of cytokines such as TNF $\alpha$ , IL-6 and IL-1 $\beta$  has been observed during neurodegenerative disorders. Hence, they can serve as biomarkers to estimate the severity of disease and verify if a potential treatment is effective (Su, Bai, & Zhang, 2016). The following part discusses TNF $\alpha$ , IL-6 and IL-1 $\beta$  and their impact on neuroinflammation and neurodegeneration.

#### **1.4.1.1 Tumour Necrosis Factor $\alpha$**

Tumour Necrosis Factor  $\alpha$  (TNF $\alpha$ ) is a pro-inflammatory cytokine, and it has been established that in CNS it produced in highest abundance by microglia. However, it is also secreted in lower amounts by astrocytes and neurons. TNF $\alpha$  is formed as a 27-kDa precursor composed of 233 amino acids. TNF $\alpha$  occurs in two different forms, as a membrane-related and soluble form. The membrane-related form is a precursor of TNF $\alpha$  and can be released from the membrane in proteolysis process by activation of TNF-alpha converting enzyme (TACE). Released TNF $\alpha$  consists of 157 amino acids weighting 17-kDa (Mubarak, 2019). Soluble forms of TNF $\alpha$  form bioactive homotrimer, which mediates TNF $\alpha$  biological effects through tumour necrosis factor receptor 1 (TNFR1) and tumour necrosis factor receptor 2 (TNFR2). Both TNF receptors are widely expressed in different cell types, and their activation induces various signalling pathways; hence TNF $\alpha$  is a pleiotropic cytokine (Figure

1.2). Activation of TNFR1 and TNFR2 triggers five signalling pathways including apoptotic pathway associated with tumour necrosis factor receptor type 1-associated DEATH domain protein (TRADD), NF- $\kappa$ B pathway, p38 MAPK, c-Jun N-terminal kinase (JNK) and extracellular signal-regulated kinase (ERK) pathway. In physiological conditions, TNF $\alpha$  is produced in low amounts and controls many physiological processes such as neuronal development, synaptic transmission, cell survival and neuronal homeostasis (Sedger & McDermott, 2014).

However, during pathological conditions such as neuroinflammation, TNF $\alpha$  production is highly upregulated, which reinforces inflammatory reaction resulting in increased production of pro-inflammatory factors such as cytokines and ROS/NOS. Additionally, during neuroinflammation TNF $\alpha$  orchestrates microglia-mediated phagocytosis neutralizing pathogens and degrading damaged tissue. Furthermore, excessive TNF $\alpha$  production may induce glutamate excitotoxicity via two mechanisms. Indirectly by inhibition of glutamate transport on astrocytes and directly by upregulation of synapse's surface expression of ionotropic glutamate receptors such as  $\alpha$ -amino-3-hydroxy-5-methyl-4-isoxazolepropionic acid receptor (AMPA) and N-methyl-D-aspartate receptor (NMDAR) simultaneously accompanied by downregulation of gamma-aminobutyric acid (GABA) receptors thereby increasing synaptic excitatory/inhibitory ratio (Olmos & Lladó, 2014). Moreover, during chronic neuroinflammation, TNF $\alpha$  causes a vicious cycle of autoregulation and acceleration of neuroinflammation, leading to neurotoxicity, upregulated phagocytosis and consequently neurodegeneration (Rubio-Perez & Morillas-Ruiz, 2012).

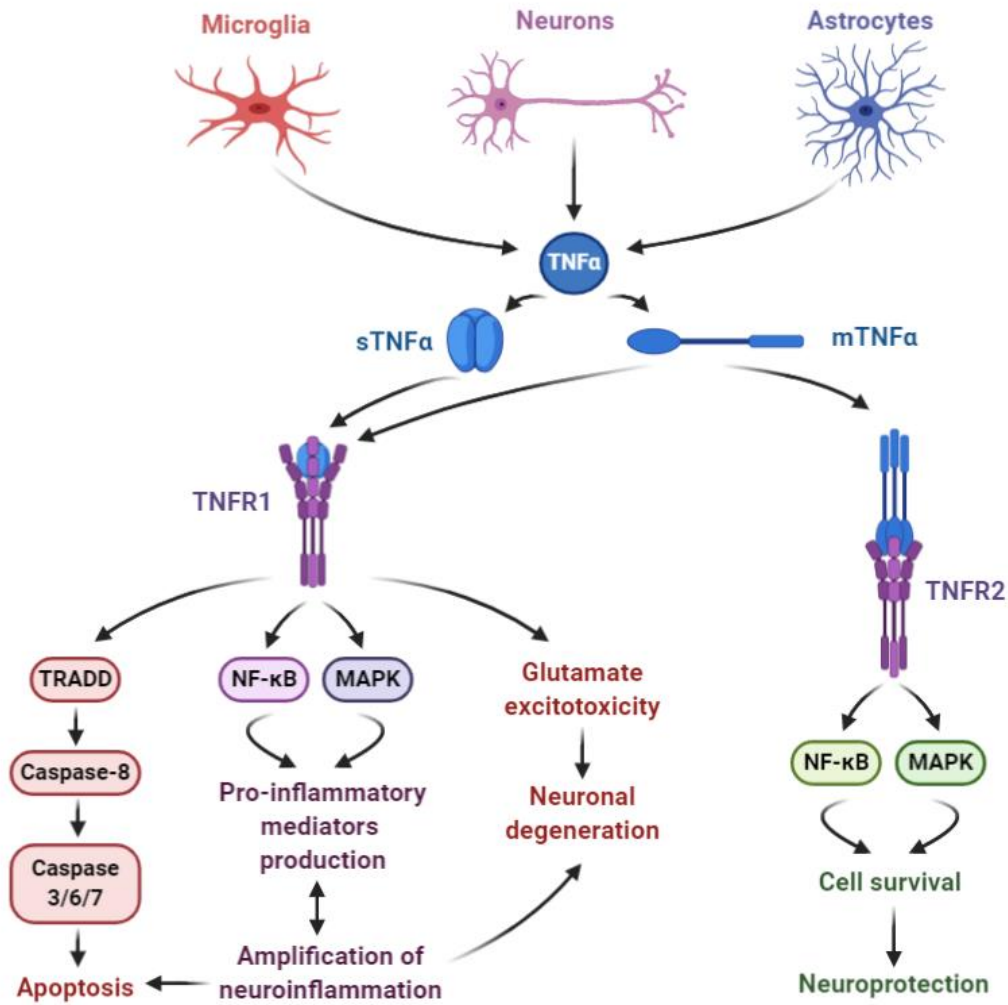


**Figure 1.2 TNF $\alpha$  cytokine production and signalling via TNFR1 and TNFR2.** TNFR1 activation leads to recruitment of TRADD and proteolytic activation of caspase-8 followed by activation of executioner caspases-3/-6/-7 and consequently apoptosis. Active TNFR1 also phosphorylates NF- $\kappa$ B and MAPKs signalling pathways which upregulate expression of pro-inflammatory mediators and thereby amplify inflammatory process and neurodegeneration. Next detrimental effect of TNFR1 activation is glutamate excitotoxicity which causes neuronal degeneration. In turn, TNFR2 activation triggers NF- $\kappa$ B and MAPKs, leading to cell survival and neuroprotection.

### 1.4.1.2 Interleukin-6

Interleukin 6 (IL-6) is a pleiotropic cytokine expressed in high amounts during inflammation. IL-6 is composed of 184 amino acids. IL-6 was initially identified in 1985 as a B-cell differentiation factor type-2 which induce the maturation of B cells into antibody-producing cells (Erta, Quintana, & Hidalgo, 2012). IL-6 cytokine is secreted by immune and non-immune cells including microglia, endothelial cells and neurons. In turn, IL-6 receptor (IL-6R) is expressed less abundantly than its ligand; it is located on a surface of microglia but not oligodendrocytes or astrocytes (Rothaug, Becker-Pauly, & Rose-John, 2016). Moreover, IL-6R also exists as soluble IL-6R (sIL-6R) form, which arises via alternative splicing or by limited proteolysis of a disintegrin and metalloproteinases (ADAM) gene family members ADAM10 and ADAM17. IL-6 induces a cellular response in two different manners: classical and trans-signalling (Figure 1.3). Classical pathway mainly occurs in microglia and involve IL-6 binding to membrane-bound IL-6R, which triggers glycoprotein 130 (gp130) dimerization and phosphorylation of downstream targets JAK/STAT, MAPK and PI3K. Trans-signalling pathway of IL6 takes place in cells which are lacking transmembrane protein IL-6R and express gp130, e.g. neuronal cells, astrocytes, oligodendrocytes and endothelial cells. The IL-6/sIL-6R complex binds to gp130 and triggers the same transduction pathways as classical signalling (Chalaris, Garbers, Rabe, Rose-John, & Scheller, 2011). Both classical and trans-signalling pathway leads to hexamer formation composed of two IL-6, two IL-6R and two gp130. Moreover, like sIL-6R, a soluble form of gp130 (sgp130) also exists and is created by alternative splicing of gp130 mRNA. Sgp130 inhibits trans-signalling but do not affect classical signalling pathway (Erta et al., 2012).

At low physiological concentrations, IL-6 acts as neuromodulator; its actions include induction of the cholinergic phenotype, neurogenesis and promotion of neuronal survival via upregulation of brain-derived neurotrophic factor (BDNF). However, IL-6 expression is highly upregulated during neuroinflammation, e.g. following CNS infection, injury or neurodegeneration such as AD (Rothaug et al., 2016). Moreover, *in vitro* studies showed that IL-6 production could also be induced by various cytokines, inflammatory factors, and neurotransmitters. Campbell et al. (2014) indicated that the detrimental effects of IL-6 in the brain are mediated by trans-signalling. It has been demonstrated that the IL-6 expression is increased around A $\beta$  plaques and in cerebrospinal fluid in AD patients (Scheller, Chalaris, Schmidt-Arras, & Rose-John, 2011). IL-6 is not only a by-product of neuroinflammation in the AD, but it also escalates AD progression by upregulation of APP and

hyperphosphorylation of tau which causes increased extracellular A $\beta$  plaque accumulation and consequently neuronal death (Erta et al., 2012).

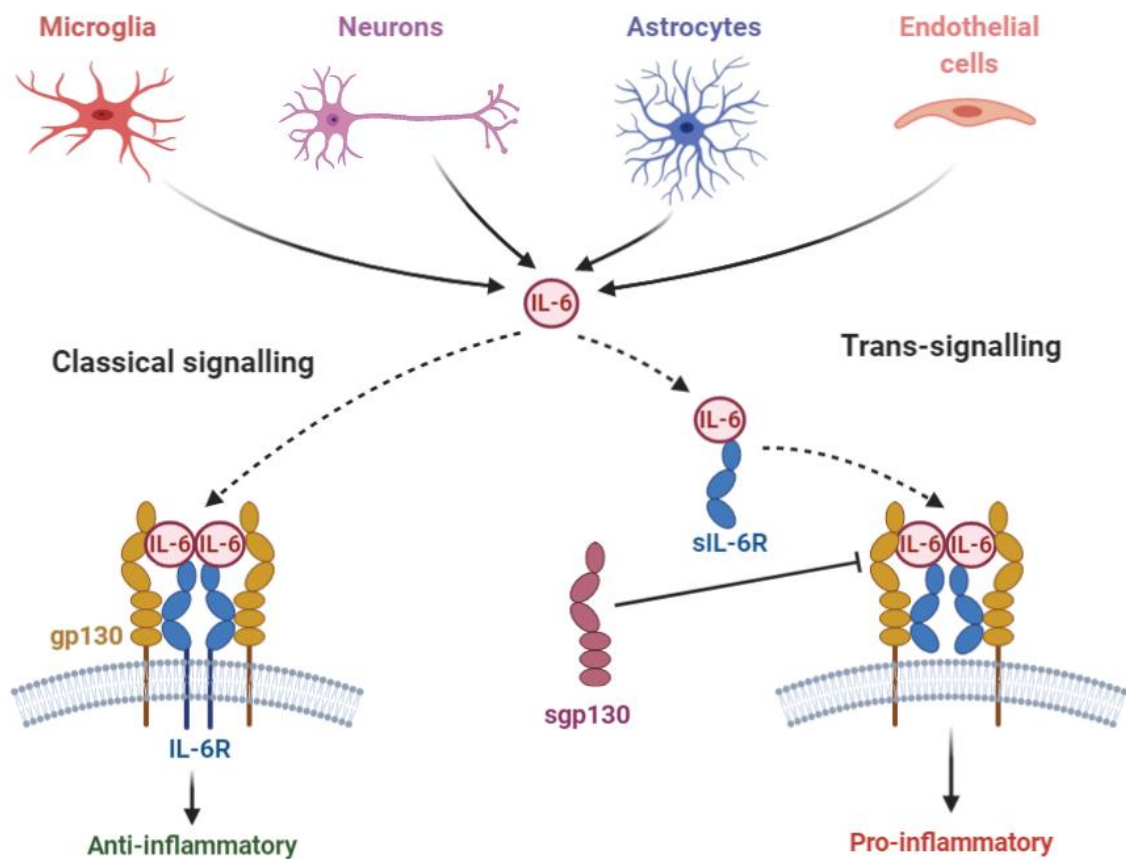


**Figure 1.3 IL-6 cytokine secretion and classical and trans-signalling pathways.** In a CNS IL-6 is secreted by microglia, neurons, astrocytes and endothelial cells. IL-6 cytokine may produce biological actions via two different mechanisms classical and trans-signalling. Classical signalling pathway involves IL-6 cytokine binding to membrane-bound IL-6Rs which triggers dimerization of gp130 and anti-inflammatory signal transduction. Trans-signalling involves the formation of IL-6/sIL-6R complex, which binds to gp130 and activate the immune response. However, sgp130 blocks trans-signalling pathway.

### 1.4.1.3 Interleukin-1 $\beta$

The next crucial cytokine regulating the immunological response in CNS is interleukin 1 $\beta$  (IL-1 $\beta$ ). Moreover, like other cytokines, IL-1 $\beta$  besides being present in the CNS during acute and chronic inflammation is also expressed at relatively low levels under physiological conditions. Therefore, this cytokine regulates many essential biological functions that are not related to immunological activities including metabolism, temperature regulation, sleep, food and water intake, and synaptic transmission (Basu, Krady, & Levison, 2004). The IL-1 $\beta$  cytokine is highly upregulated during inflammation and in a brain is mainly secreted by microglia and in lower amounts by astrocytes, oligodendrocytes, neurons and endothelial cells (Hewett, Jackman, Claycomb, Neuroscience, & Haven, 2012). IL-1 $\beta$  cytokine is



produced as 31-kD pro-peptide termed pro-IL-1 $\beta$ . However, to gain biological activity precursor of IL-1 $\beta$  is cleaved by the cysteine protease caspase-1, also known as an interleukin-1 converting enzyme (ICE). ICE is activated through the formation of a multi-protein complex - the inflammasome. The inflammasome can sense PAMP or DAMP and initiate a pro-inflammatory response through the sequential cleavage and thus, activation of the ICE and IL-1 $\beta$  (Lopez-Castejon & Brough, 2011). IL-1 $\beta$  acts via a group of receptors called IL-1R, which can be distinguished into IL-1R1 and IL-1R2 (Figure 1.4) (Boraschi & Tagliabue, 2013). IL-1 $\beta$  is one of the first cytokines that appear during inflammation; hence it is considered as a master regulator of the immune response. This interleukin induces secretion of a broad range of proinflammatory mediators, such as TNF $\alpha$ , IL-6 and COX-2/PGE<sub>2</sub> and inducible nitric oxide synthase (Basu et al., 2004). In the brain, elevated levels of IL-1 $\beta$  cause disruptions in the blood-brain barrier (BBB) leading to leukocytes infiltration. IL-1 $\beta$  induces activation of microglia and astrocytes, which escalates and sustains pathophysiological process contributing to exacerbation of neurotoxicity (Hewett et al., 2012).

Numerous reports have correlated the increased level of IL-1 $\beta$  with neurological disorders (Rubio-Perez & Morillas-Ruiz, 2012). Moreover, a vast amount of data shows a potential relationship between IL-1 $\beta$  and neuronal apoptosis (Shaftel, Griffin, & Kerry, 2008). Elevated levels of IL-1 $\beta$  were reported in patients with the AD. It has been established that reactive microglia which surround amyloid deposits secrete large amounts of IL-1 $\beta$  (Rubio-Perez & Morillas-Ruiz, 2012). Both *in vivo* and *in vitro* studies indicated that this interleukin escalates  $\beta$ -APP mRNA synthesis, presumably by increased gamma-secretase activity. Additionally, IL-1 $\beta$  plays also a detrimental role in AD development by hyperphosphorylation of tau protein via a p38 mitogen-activated protein kinases (MAPK-p38) pathway which leads to the formation of neurofibrillary tangles (Shaftel et al., 2008). A growing body of evidence indicates that the absence of IL-1 $\beta$  signalling delays neuroinflammation and subsequently neurodegeneration (Basu et al., 2004).

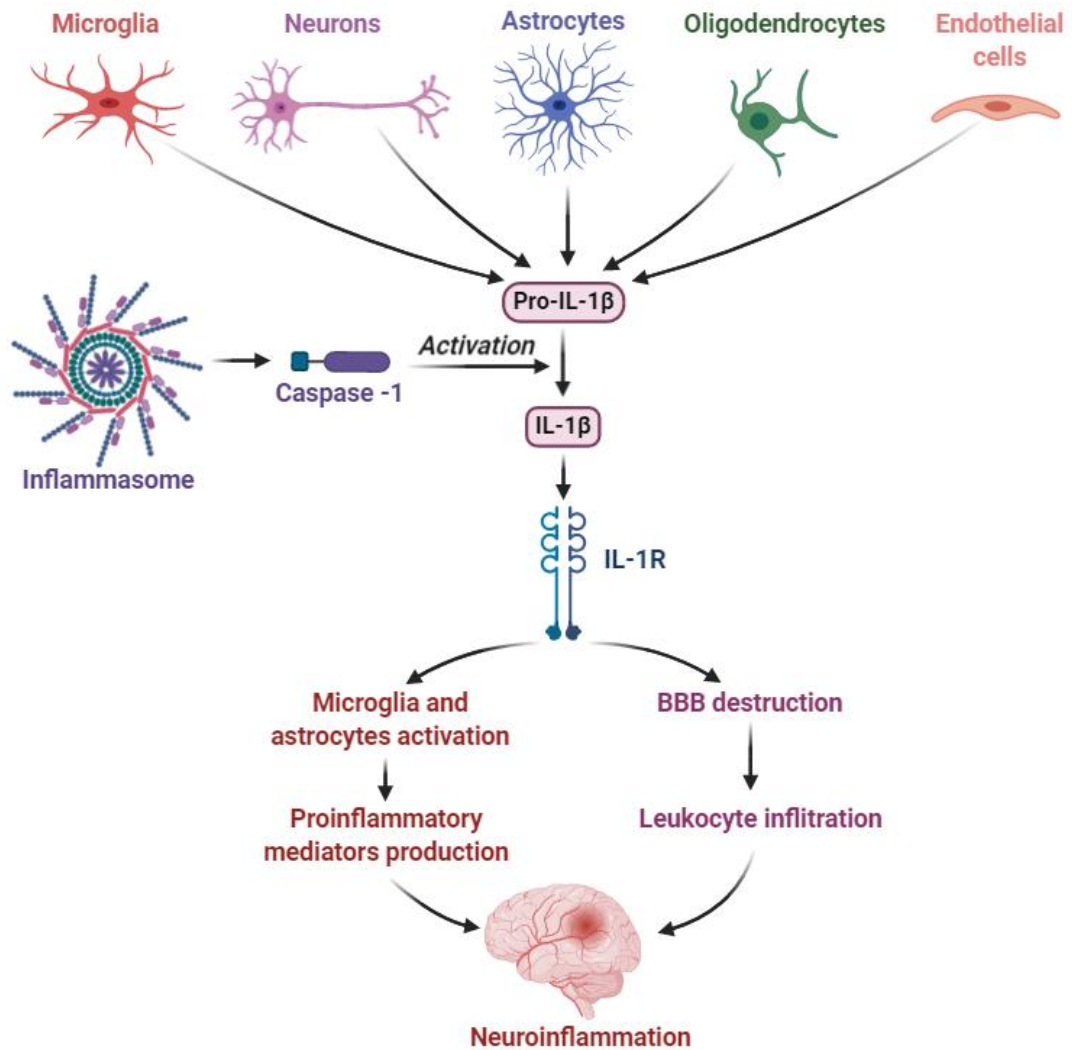


**Figure 1.4 Pro-IL-1 $\beta$  production, activation and its pathological effects.** IL-1 $\beta$  is secreted by microglia, neurons, astrocytes, oligodendrocytes and endothelial cells as inactive precursor protein termed pro-IL-1 $\beta$ . When cell recognises PAMS or DAMP, it activates inflammasome which cleaves pro-caspase-1 to active caspase-1. Caspase-1 proteolytically cleaves the precursor of the IL-1 $\beta$  into active mature peptides which via IL-1R promote and sustain the inflammatory response. Activated IL-1R triggers production of various pro-inflammatory mediators and disturb BBB, causing leukocyte recruitment into the brain which aggravates neuroinflammation.

### 1.4.2 Reactive Oxygen and Nitrogen Species

Reactive Oxygen Species (ROS) and Reactive Nitrogen Species (RNS) is a collective term of chemically reactive molecules containing oxygen or nitrogen atom, respectively. Examples of ROS include superoxide ( $O_2^{\bullet-}$ ), hydrogen peroxide ( $H_2O_2$ ), hydroxyl radical ( $OH^{\bullet}$ ) and singlet oxygen ( $O_2$ ). In turn, RNS include nitric oxide ( $NO^{\bullet}$ ), nitrogen dioxide ( $NO_2^{\bullet}$ ) and peroxynitrite ( $ONOO^-$ ). RONS regulate cellular homeostasis and act as prime modulators of cellular dysfunction contributing to disease pathophysiology (Forrester, Kikuchi, Hernandez, Xu, & Griending, 2018). ROS production takes place in various cellular compartments including mitochondria, cell membrane, peroxisome, cytoplasm and endoplasmic reticulum. In mitochondria, the electron transport chain located on the inner mitochondrial membrane generate the  $O_2^{\bullet-}$  radical during the process of oxidative phosphorylation. Additionally, mitochondrial membrane enzymes – oxidoreductases such as monoamine oxidase, dihydroorotate dehydrogenase and  $\alpha$ -glycerophosphate dehydrogenase produce  $H_2O_2$ . Peroxisome contributes to  $O_2^{\bullet-}$  and  $NO^{\bullet}$  generation via xanthine oxidase and the inducible form of nitric oxide synthase, respectively. The cytoplasm contains xanthine oxidase enzyme required to produce uric acid by the breakdown of purine nucleotides which create  $O_2^{\bullet-}$  and  $H_2O_2$  as a by-product (Di Meo, Reed, Venditti, & Victor, 2016).

Furthermore, RONS are generated during various biochemical reactions of the cell, and at low concentrations, they are crucial for the proper course of many physiological processes. However, at high concentrations, they transform from regulatory molecules into toxic products of cellular metabolism. Therefore, to avoid high levels of RONS cells employ antioxidant system activity which neutralizes the oxidative and nitrosative effects of ROS and NOS (Di Meo et al., 2016). The antioxidant defence of cell might be distinguished into enzymatic systems, e.g. superoxide dismutase (SOD), glutathione peroxidase (GPX), catalase and non-enzymatic endogenous systems including glutathione. However, when antioxidative mechanisms are not efficient enough to neutralize the oxidizing agents and repair cellular damage, then the oxidative stress occurs (Nimse & Pal, 2015).

Pathological conditions such as chronic neuroinflammation are accompanied by oxidative stress. During neuroinflammation high amounts of ROS are produced by microglia via the nicotinamide adenine dinucleotide phosphate (NADPH) oxidase. NADPH oxidase is dormant under during homeostasis. However, this membrane-bound protein complex can be easily activated by cytokines, including  $TNF\alpha$  or bacterial fragments such as

lipopolysaccharide. NADPH is responsible for “respiratory burst” of phagocytes (Sarniak, Lipińska, Tytman, & Lipińska, 2016). Phagocytic NADPH oxidase is composed of two transmembrane glycoproteins gp91phox and p22phox which make up flavocytochrome b558. NADPH oxidase also contains the cytosolic components p47phox, p67phox, p40phox and the small G-protein Rac1 or Rac2 which upon activation translocate to the membrane, docking with flavocytochrome b558. NADPH oxidase products are superoxide and hydrogen peroxide (Ma et al., 2017).

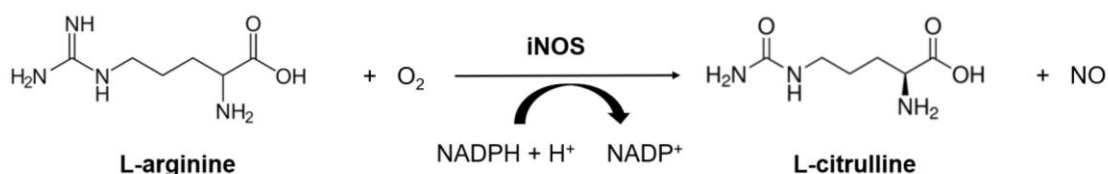


**Figure 1.5 Enzymatic synthesis of nitric oxide.** Amino acid L-arginine is a precursor of nitric oxide which is produced by iNOS enzyme with the use of oxygen and NADPH as co-factors. Adapted from: (Abán et al., 2018)

Alongside NADPH activation, neuroinflammation also activates nitric oxide synthase (NOS), which generates RNS. NOSs can be divided into two constitutive isoforms: neuronal (nNOS) and endothelial (eNOS) which are calcium-dependent, and one non-calcium dependent - inducible isoform (iNOS) involved in the immune response. NOS produces nitric oxide (NO) from L-arginine, oxygen, and NADPH (Figure 1.5). NO act as intercellular messenger modulating blood flow and neural activity (Peixoto, Nunes, & Rapôso, 2017). NO readily penetrate the cell membrane, hence works as a non-conventional neurotransmitter because it directly alters its targets instead of working on a receptor level. However, at high levels NO transform its function from neuromodulator to neurotoxic agent which induce nitrosative and oxidative stress by activation of the MAP kinase pathways, and induction of endoplasmic reticulum stress and stimulation of mitochondrial permeability thereby leading to apoptosis (Yuste, Tarragon, Campuzano, & Ros-Bernal, 2015). NO is free radical with unpaired valence electron. Therefore, this molecule is highly chemically reactive with the half-life of a few seconds in oxygenated aqueous solutions. Hence, NO may spontaneously react with superoxide (O<sub>2</sub><sup>•-</sup>), which is generated by NADPH to form highly reactive peroxynitrite (ONOO<sup>-</sup>). Peroxynitrite is more reactive than its parental molecules. Hence it causes more damage than NO and O<sub>2</sub><sup>•-</sup> by interactions with most critical cellular biomolecules. Peroxynitrite can readily react with proteins, lipids and nucleic acids (figure 1.6). On a protein level ONOO<sup>-</sup> can react with transition metal centres inactivating enzymes

involved in critical metabolic processes including haemoglobin or cytochrome c. Moreover  $\text{ONOO}^-$  can affect protein structure and function by reaction with amino acids which include oxidation of cysteine residues or tyrosine nitration which affects mitochondrial respiratory chain contributing to neurodegeneration (Pacher, Beckman, & Liaudet, 2007). Peroxidation of membrane lipids is known to substantially alter the assembly, composition, structure, and dynamics of lipid membranes causing degradation of cellular membranes integrity and consequently cell death (Gaschler & Stockwell, 2017). Peroxynitrite also induces significant DNA damage via damage-causing DNA breaks and activation of the nuclear enzyme poly(ADP-ribose) polymerase (PARP), a pathway related to the upregulation of inflammatory processes and induction of cell death (Pacher et al., 2007).

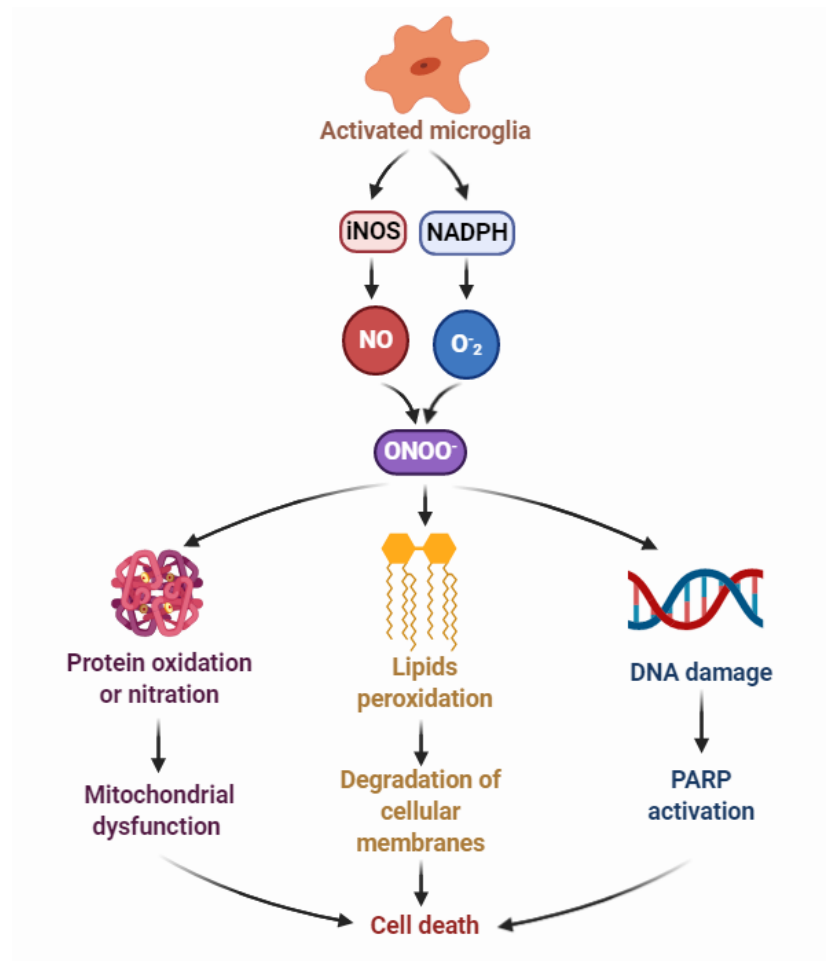


**Figure 1.6 Oxidative/nitrosative damage caused to cells by peroxynitrite.** Activated microglia express iNOS, which upregulate nitric oxide level. Additionally, activated microglia activate NADPH oxidase, which produces a high amount of superoxide. Nitric oxide may spontaneously react with superoxide ( $\text{O}_2^{\bullet-}$ ) and form highly reactive peroxynitrite ( $\text{ONOO}^-$ ). Peroxynitrite is powerful oxidant exhibiting a wide array of cell-damaging effects which include protein oxidation or nitration, lipid peroxidation and DNA damage.

### 1.4.3 Prostaglandins

Prostaglandins are autocrine and paracrine signalling molecules which belong to a group of physiologically active lipid compounds called eicosanoids. Prostaglandins are biosynthesized nearly by all nucleated cells. Hence, they are found in most tissues. Prostaglandins are derived by the enzymatic oxidation of the polyunsaturated fatty acid called arachidonic acid (AA) released from membrane phospholipids by a phospholipase A<sub>2</sub> (PLA<sub>2</sub>) (Aïd & Bosetti, 2011). Formation of prostaglandins is conducted by cyclooxygenase (COX) isoenzymes, also known as prostaglandin-endoperoxide synthase (PTGS) enzyme and terminal prostaglandin E synthases (PGES). COX isoforms transform AA into prostaglandin H<sub>2</sub> (PGH<sub>2</sub>) which is further converted by PGES to PGE<sub>2</sub>. PGES are distinguished into microsomal PGES-1 and -2 (mPGES-1/-2), and cytosolic PGES (cPGES). mPGES-1 production is markedly induced by pro-inflammatory stimuli and is functionally coupled with COX-2. mPGES-2 is constitutively expressed and released into the cytoplasm in various cells and can be coupled with both COX-1 and COX-2. cPGES is constitutively expressed in various cells and can regulate COX-1-dependent immediate PGE<sub>2</sub> generation (Park, Pillinger, & Abramson, 2006). COX occurs in two distinct isoforms COX-1 and COX-2. COX-1 is constitutively expressed in cells and is responsible for housekeeping functions in various tissues such as kidney and gastrointestinal tract, e.g., mucosal protection. COX-2 is nearly undetectable in most peripheral cells, but its synthesis is highly upregulated upon inflammatory stimulation. Hence, COX-2 is a crucial mediator of inflammatory pathways (Ricciotti, Emanuela and FitzGerald, 2012). However, in the brain, both COX-1 and COX-2 are constitutively expressed. Several studies demonstrated that COX-2 contributes to fundamental brain functions, such as synaptic activity, memory consolidation, and functional hyperemia (Minghetti, 2004). Moreover, COX-2 deletion was shown to exacerbate neuroinflammation, increase neuronal damage and BBB permeability (Aïd & Bosetti, 2011). Therefore, in contrast to the periphery, in CNS, COX-2 contributes to normal physiological functions. However, similarly to the periphery, level of COX-2 in a brain is also upregulated by inflammatory factors. Therefore, increased expression of COX-2 is a hallmark of neurodegenerative disorders, including Alzheimer's disease.

Prostaglandin E<sub>2</sub> (PGE<sub>2</sub>) is the most abundant prostaglandin produced in the body. PGE<sub>2</sub> exhibits versatile biological activities which are mediated by a family of four G protein-coupled receptors, E-prostanoid (EP) receptors - EP1 to EP4 (Figure 1.7). Activation of EP1 receptor results in increased intracellular calcium ion influx which in turn enhances glutamate

presynaptic release. Receptor EP2 and EP4 increase cyclic adenosine monophosphate (cAMP) whereas EP3 decrease cAMP (Woodling & Andreasson, 2016). EP3 and EP4 have the highest affinity for PGE<sub>2</sub> and are most abundantly expressed in contrast to EP1 found only in restricted tissues and the least abundant EP2 (Famitafreshi & Karimian, 2020). Direct effects of EP1-mediated neurotoxicity have been demonstrated in models of neurodegeneration, examining the survival of cultured dopaminergic neurons. EP2 receptor activation participates in the generation of reactive oxygen species (ROS) and increased NOS activity, thereby accelerating inflammatory oxidative response and secondary neurotoxicity. Function of the EP3 receptor so far is not firmly defined. Activation of EP4 receptor suppress microglial activation as well as microglia-induced neuroinflammation. Current literature suggests dichotomy of PGE<sub>2</sub> action mediating toxic or pro-survival effects in models of neurological disease, depending on cell type and the specific injury context (Andreasson, 2010).

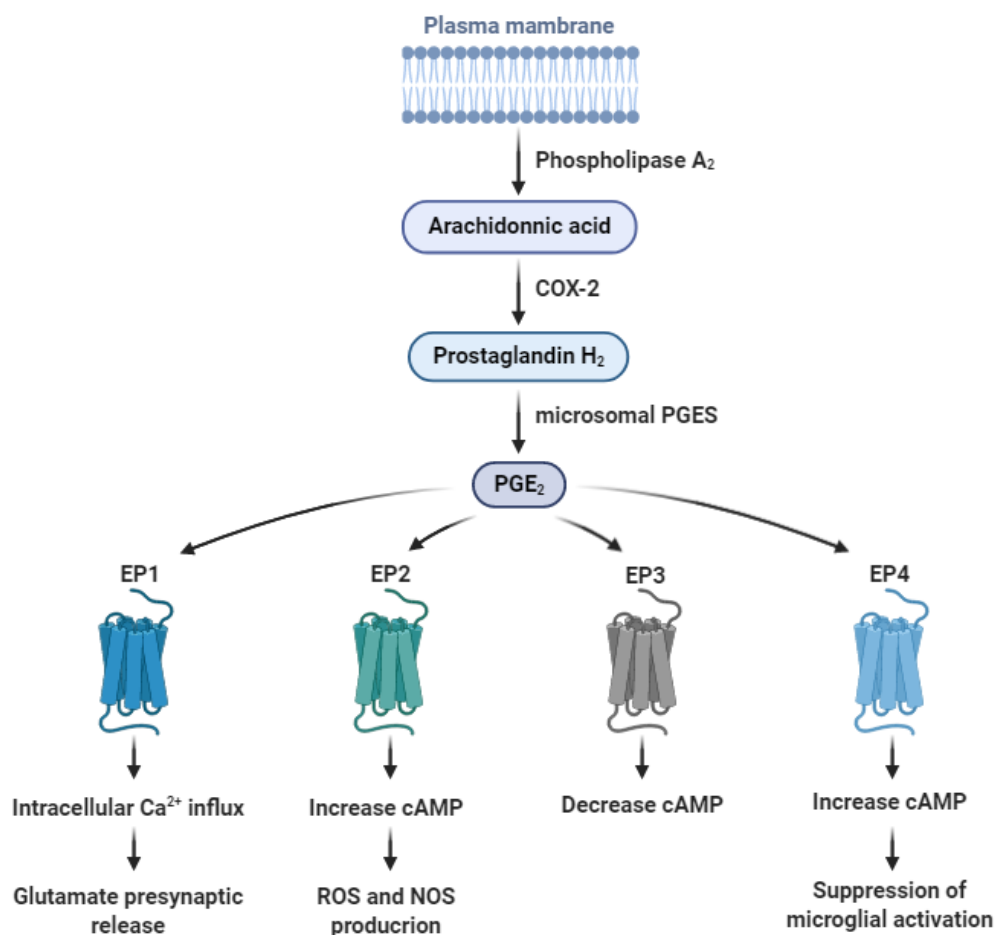


**Figure 1.7 The biosynthesis of PGE<sub>2</sub> and its signalling.** Phospholipase A<sub>2</sub> release from the membrane arachidonic acid, which is transformed by COX-2 enzyme to prostaglandin H<sub>2</sub>. Prostaglandin H<sub>2</sub> serve as a substrate for microsomal PGES to form active prostaglandins such as PGE<sub>2</sub>. PGE<sub>2</sub> mediates its action via EP1-4 receptors.

## **1.5 Signalling pathways modulating neuroinflammation**

The activity of various intracellular pathways coordinates neuroinflammation. Those pathways ensure an appropriate signal transmission which enables cellular response to external stimuli. In a healthy organism, the processes of cellular responses are tightly controlled, but in the pathological state such as chronic neuroinflammation constant activation of pro-inflammatory signalling pathways may result in damage-causing signals (Chen et al., 2016; Haegeman, 2003). Moreover, alongside pro-inflammatory signalling mechanisms cells possess endogenous defence pathways which alleviate inflammation and restore physiological functions (Dinkova-Kostova & Talalay, 2008). Therefore, neuroinflammation might be reduced by inhibition of pro-inflammatory signalling or upregulation of anti-inflammatory pathways.

### **1.5.1 NF- $\kappa$ B transcription factor**

Nuclear factor kappa-light-chain-enhancer of activated B cells (NF- $\kappa$ B) is an important transcription factor which controls the expression of more than 400 genes, including many pro-inflammatory cytokines, chemokines and enzymes including TNF $\alpha$ , IL-6, IL-1, iNOS and COX-2 (Figure 1.8). NF- $\kappa$ B is present in almost all animal cells and is responsible for the regulation of inflammatory responses of the organism (Jones & Kounatidis, 2017). However, chronic activation of the NF- $\kappa$ B pathway has been linked to inflammation-induced neurodegeneration (Shih, Wang, & Yang, 2015). Therefore, inhibition of NF- $\kappa$ B activity is considered as a therapeutic potential for the treatment of inflammation and neurodegeneration (Gupta, Sundaram, Reuter, & Aggarwal, 2010; Yamamoto & Gaynor, 2001).

NF- $\kappa$ B signalling pathway can be distinguished into a canonical and non-canonical pathway, also known as an alternative pathway. These pathways have been divided into two separate routes because they differ in a signalling mechanism. The canonical pathway is triggered by ligands of various cytokine receptors, pattern recognition receptors (PRRs). Whereas the non-canonical NF- $\kappa$ B pathway is activated by TNF family cytokines (except TNF $\alpha$ ), CD40 ligand, B cell-activating factor (BAFF) and receptor activator of NF- $\kappa$ B ligand (RANKL) (Lawrence, 2009). In canonical pathway activation of PRR such as TLR leads to phosphorylation of the I $\kappa$ B kinase complex (IKK) which is composed of the IKK $\alpha$  and IKK $\beta$  subunits and a main regulatory subunit NF- $\kappa$ B essential modulator (NEMO) also known as an inhibitor of nuclear factor kappa-B kinase subunit gamma (IKK $\gamma$ ). Phosphorylated IKK



activates I $\kappa$ B which allows to I $\kappa$ B ubiquitous modification and degradation by the proteasome. Degradation of inhibitory I $\kappa$ B leads to rapid and transient nuclear translocation of p50 (NF- $\kappa$ B1) and RelA, also known as nuclear factor NF- $\kappa$ B p65 subunit (Liu, Zhang, Joo, & Sun, 2017). In contrast to the canonical pathway, the alternative pathway is independent of IKK $\beta$  and IKK $\gamma$  and requires only IKK $\alpha$ , which is regulated by NF- $\kappa$ B inducing kinase (NIK). Alternative pathway does not involve I $\kappa$ B $\alpha$  degradation, but it relies on the processing of the p52 (NF- $\kappa$ B2) precursor protein, p100 which is phosphorylated and ubiquitously degraded. This allows dimerization and nuclear translocation of RelB and p52 (Figure 1.8). Alternative NF- $\kappa$ B pathway regulates processes of adaptive immunity such as B-cell activation (Lawrence, 2009).

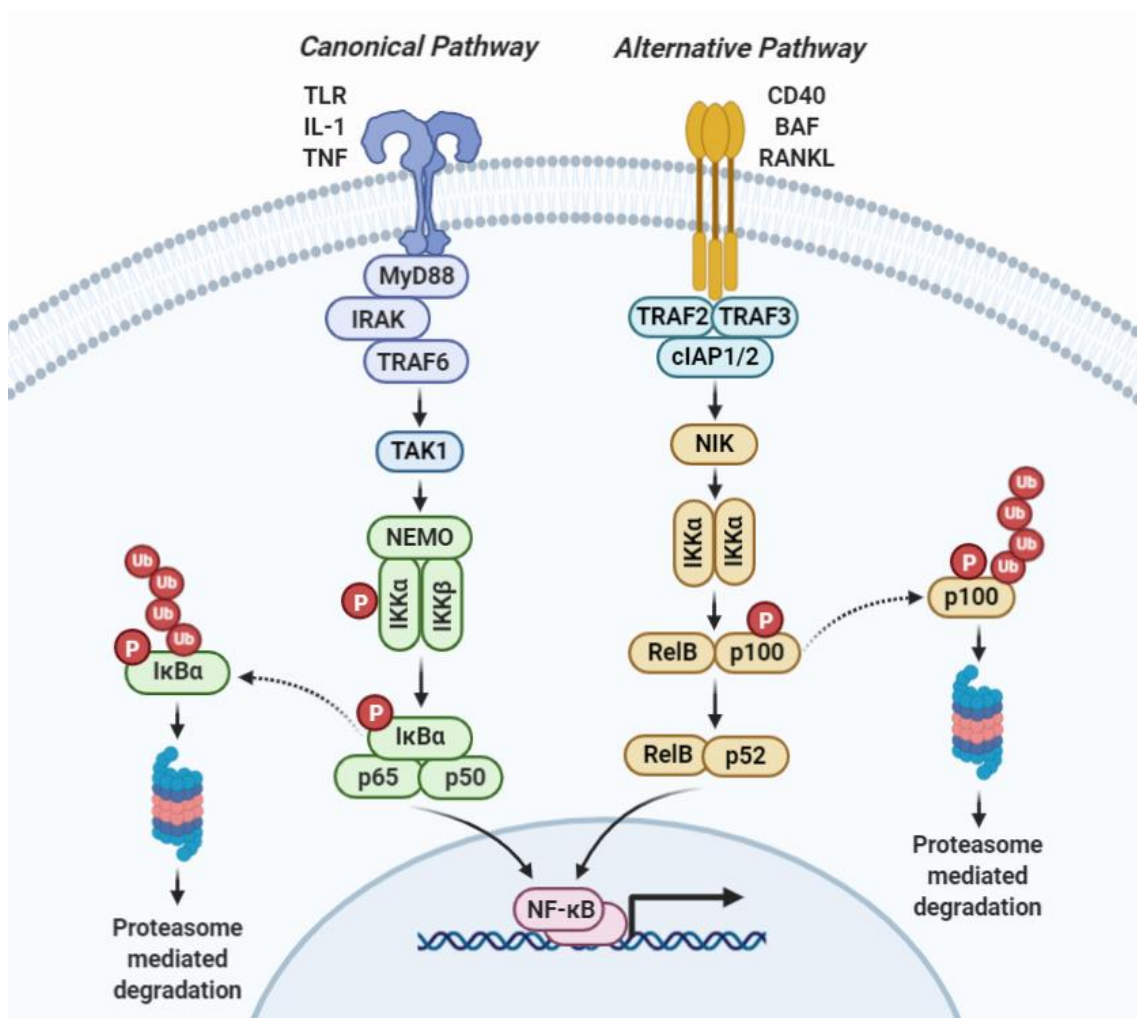


**Figure 1.8 Canonical and alternative NF- $\kappa$ B signalling pathway.** Canonical pathway is triggered by pro-inflammatory cytokines (TNF $\alpha$ , IL-1 $\beta$ , and TLR which recognize PRR). In contrast, the non-canonical pathway is activated by TNF family cytokines including CD40L, BAF and RANKL. In the canonical pathway, IKK activation leads to phosphorylation and degradation of I $\kappa$ B, and consequently, nuclear translocation of p65/p50. While in alternative pathway activation of NIK and IKK $\alpha$  cause processing of p100 to p52, which allows dimerization and nuclear translocation of RelB/p52.

## 1.5.2 MAPKs

Apart from NF- $\kappa$ B, another signalling pathway which plays a crucial role in the regulation of inflammation are the pathways involving the activation of the MAPKs. Mitogen-activated kinases (MAPKs) are a highly conserved class of serine/threonine protein kinases. Based on the effector kinases, three main families of MAPKs have been distinguished: extracellular signal-regulated kinase (ERK), JNK/SAPK (c-Jun N-terminal-activated protein kinase) and p38 (Ronkina et al., 2010). In each signalling pathway, the effector kinase is controlled by a "higher-order" kinase. Together they form an enzymatic cascade, i.e., a system in which proteins are sequentially activated as a result of phosphorylation. MAP kinases participate in signalling pathways triggered by a three-level cascade of kinases. These cascades start with MAPKKK (MAP3K or MKKK) which activates MAPKK (MAP2K or MKK), subsequently phosphorylating effector MAP kinases (MAPK). Stimulus  $\rightarrow$  MAPKKK  $\rightarrow$  MAPKK  $\rightarrow$  MAPK  $\rightarrow$  answer (Figure 1.9). MAP kinases are activated by the double phosphorylation of threonine and tyrosine in the Thr-X-Tyr motif found in the activation loop, where X is Glu, Pro, and Gly in ERK, JNK, and p38 MAPK, respectively (Kaminska, 2005). The consequence of MAPK activation is inflammation, apoptosis, differentiation, and proliferation. Several studies indicated the involvement of MAPK-dependent signalling pathways in the pathophysiology of neurodegenerative diseases (Lee & Kim, 2017; Munoz & Ammit, 2010; J. Sun & Nan, 2017; Wojda, 2012).

### 1.5.2.1 p38 MAPK

p38 MAPK pathway is activated under stress conditions. Protein p38 is distinguished into four isoforms  $\alpha$ ,  $\beta$ ,  $\gamma$  and  $\delta$ . In the brain, highly expressed genes are those encoding p38 $\alpha$  and  $\beta$ . Among four isoforms only p38 $\alpha$  is involved in the production of pro-inflammatory cytokines and enzymes. Activation of p38 $\alpha$  MAPK can be triggered by PAMP, DAMP and cytokines. This signalling pathway is directly activated by MKK 3 and 6 (Yang et al., 2014). Upregulation of this signalling cascade initiate activation of transcription factors such as ATF2 (activating transcription factor 2) and NF- $\kappa$ B, which leads to upregulation of pro-inflammatory genes and consequently the production of inflammatory cytokines such as TNF $\alpha$ , IL-1 $\beta$ , IL-6 and enzymes including iNOS (Krzyzowska et al., 2010). Moreover, p38 increase cytokine expression not only by induction of transcription but also by increasing mRNA stability (Cargnello & Roux, 2011). mRNAs coding for inflammatory response genes are unstable and increased p-p38 was shown to induce stabilisation of adenylate-uridylylate-

rich containing endogenous mRNAs and reporter mRNAs, including those of IL-6, TNF $\alpha$  and cyclooxygenase-2 (Kaminska, 2005). Upregulated p38 MAPK pathway has been identified in the post-mortem brains of AD patients and animal models (Lee & Kim, 2017). Accumulating evidence suggests that p38 MAPK inhibitors could slow down the progression of neurodegeneration by alleviation of neuroinflammation (Munoz & Ammit, 2010). Furthermore, p38 triggers expression of  $\beta$ -secretase, which is the enzyme processing APP into amyloidogenic fragments A $\beta$ 42. Therefore, inhibition of p38 signalling alongside alleviating neuroinflammation might reduce A $\beta$  synthesis (Lee & Kim, 2017).

### **1.5.2.2 ERK1/2**

First identified MAPK kinase was extracellular signal-regulated kinase (ERK). It occurs in the form of two isoforms: ERK1 (p44) and ERK2 (p42), commonly referred to as ERK1/2. ERK is activated by Raf/MEK/ERK. This cascade is triggered by various mitogens, endotoxins, or stress, which leads to activation of transcription factors. A functional consequence of the ERK1/2 kinase cascade activation is the regulation of the cell cycle, proliferation, differentiation, and transformation (Sun & Nan, 2017). In a brain, ERK plays a crucial role in learning, the formation of memory and synaptic plasticity. Moreover, it also mediates cell death in several neuronal systems. Neuronal death induced by H<sub>2</sub>O<sub>2</sub>, glutamate, nitric oxide and  $\beta$ -amyloid has been prevented by pharmacological blockade of the ERK1/2 pathway (Subramaniam & Unsicker, 2010). Additionally, a growing body of evidence indicates that ERK1/2 is involved in neuroinflammation. In microglia, ERK1/2 can be induced by LPS and controls the regulation of inflammatory cytokine production and iNOS expression (Sun & Nan, 2017). ERK1/2 signalling pathway has been implicated in the pathogenesis of various neurological disorders, including AD. ERK1/2 is demonstrated to phosphorylate tau contributing to neurofibrillary tangles (NFTs) formation. Additionally, ERK1/2 inhibition has been shown to be associated with a reduction of  $\beta$ -amyloid neurotoxicity (Liu, Su, Li, & Ni, 2003; Sun & Nan, 2017). Furthermore, activated ERK1/2 signalling pathway contributes to neurodegeneration progression through inflammatory genes expression. Numerous reports indicate that various pharmaceutical-based therapies used to reduce neuroinflammation suppressed ERK1/2 signalling cascade (Shao et al., 2013; Wang et al., 2010; Xia et al., 2015).

### 1.5.2.3 JNK

C-Jun N-terminal kinases (JNK) is also known as stress-activated protein kinase (SAPK). The JNK family consists of three isoforms: the commonly present JNK 1 and JNK 2 and only existing in the brain and heart - JNK 3. In the brain, JNK3 is neuronal specific and is essential for neurite formation and plasticity (Yarza, Vela, Solas, & Ramirez, 2016). JNK 1/2 play a vital role in the modulation of immune cell function. The JNK kinase cascade is activated by stressors such as UV irradiation, oxidative stress, LPS, and cytokines such as TNF $\alpha$  or IL-1. JNK activation is directly triggered by MKK 4 and 7, which in turn are activated by MKKK, such as apoptosis signal-regulating kinase 1 (ASK1), MEKK1-4, TAK1 or mixed-lineage kinase 1-3 (MLK1-3). JAK signalling pathway regulates inflammatory mechanisms and cell death via intrinsic/extrinsic apoptotic pathways (Dong, Davis, & Flavell, 2002). In microglia, JNK activation was shown to modulate AP-1 target genes, including cyclooxygenase-2, TNF $\alpha$ , and IL-6 (Waetzig et al., 2005). Moreover, specific JNK antagonists have been demonstrated to act as potent anti-inflammatory agents (Kaminska, 2005). Increased expression of phosphorylated JNK has been observed during neurodegenerative disorders. JNK activation may be triggered by aggregated proteins, including A $\beta$ . Furthermore, JNK plays also a direct role in the formation of neurofibrillary tangles by phosphorylation of tau (Yarza et al., 2016).

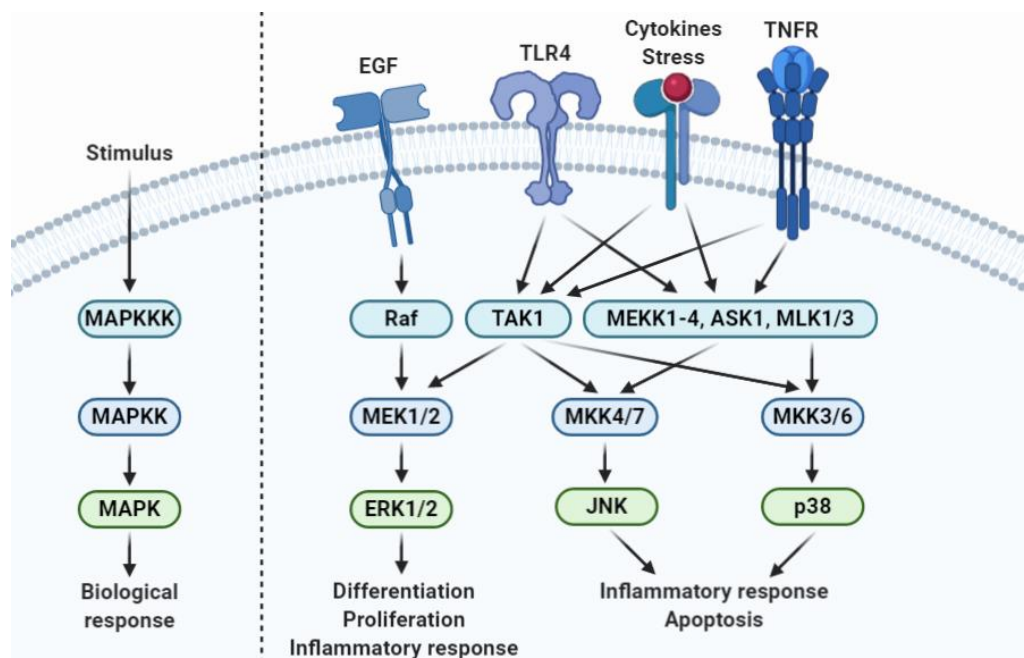


**Figure 1.9 MAPK signalling pathways.** MAPKs are activated by various stress signals including cytokines, PAMP, DAMP and growth factors. Stress signal activate MAPKKK such as TAK1, MEKK1-4, ASK1 and MLK1/3, then signal is transduced to MAPKK and consequently MAPK such as ERK1/2, JNK and p38. Activated p38 and JNK upregulate inflammatory response and induce apoptosis. In turn, ERK1/2 mainly modulates cellular differentiation and proliferation and to a lesser extent inflammation.

### 1.5.3 Nrf2 antioxidant transcription factor

Nuclear factor erythroid 2-related factor 2 (Nrf2) is a crucial regulator of endogenous defence systems. Nrf2 is a member of the “cap 'n' collar” (CNC) family of a basic leucine zipper (bZIP) transcription factors. Nrf2 controls expression of genes involved cellular protection against oxidative damage triggered by injury and inflammation (Dinkova-Kostova, Kostov, & Kazantsev, 2018). Nrf2 contains seven highly conserved regions known as Nrf2-ECH homology (Neh) 1–7 domains vital for their self-regulation and activity. The Neh1 domain comprises the CNC-bZIP region which heterodimerizes with small musculoaponeurotic fibrosarcoma proteins (sMaf) and other transcription partners to recognize and bind to antioxidant response elements (ARE) for activation of gene transcription (Figure 1.10) (F. He, Ru, & Wen, 2020). The Neh2 domain mediates the interaction with Nrf2 negative regulator Kelch-like erythroid cell-derived protein with CNC homology-associated protein 1 (Keap1). Keap1 inhibits Nrf2 transcriptional activity by its ubiquitination and proteasomal degradation. However, oxidative stress conditions lead to modification of critical cysteine thiols of Keap1 and Nrf2, Nrf2 dissociates from Keap1 binding and translocate into the nucleus. In the nucleus, Nrf2 heterodimerizes with small Maf proteins and initiate expression of an array of antioxidant genes including NAD(P)H dehydrogenase [quinone] 1 (NQO1), glutathione peroxidase (GPx) and heme oxygenase-1 (HO-1). Neh 3-5 act as transactivation domains facilitating interaction with other transcription co-activators. Neh 4-5 recruit cAMP response element-binding protein (CREB)-binding protein. The Neh7 and Neh 6 domains mediate binding to negative regulators of Nrf2:  $\beta$ -transducin repeat-containing protein ( $\beta$ -TrCP) and retinoid X receptor-alpha (RXR $\alpha$ ), respectively (Dinkova-Kostova et al., 2018).

Oxidative stress results in the overproduction of cytokines which further intensifies oxidative stress and inflammation. Nrf2 activation prevents transcriptional upregulation of pro-inflammatory cytokines, e.g. IL-6 and IL-1 $\beta$  and enzymes such as iNOS and COX-2 (Ahmed, Luo, Namani, Wang, & Tang, 2017). Therefore, Nrf2 signalling plays a crucial role in the downregulation of neuroinflammation. Those positive biological effects might slow progression and ameliorate symptoms of neurodegenerative disorders, including Alzheimer's disease.

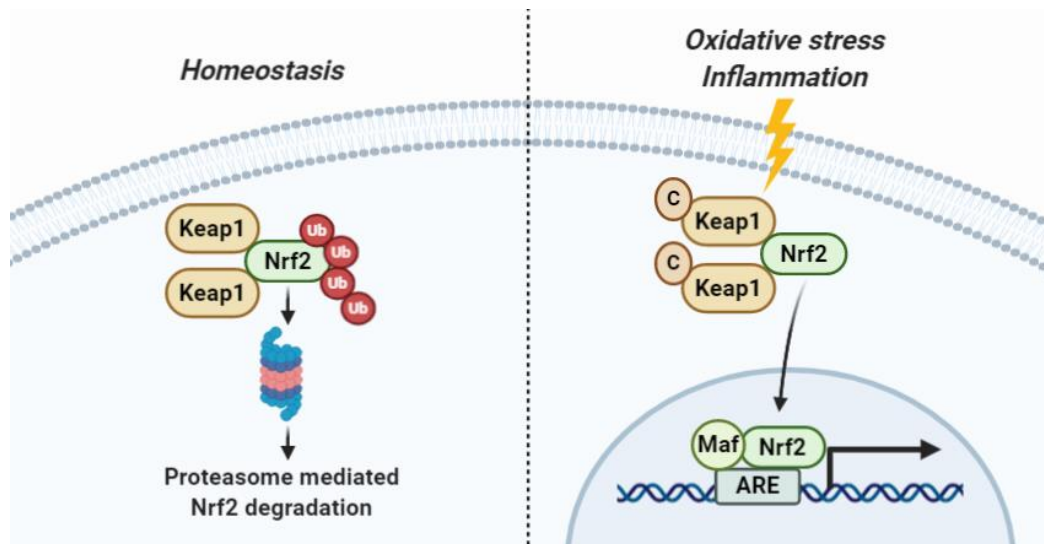


**Figure 1.10 Nrf2 signalling in homeostasis and stress conditions.** During homeostasis, Nrf2 is negatively regulated by a cytosolic protein called Keap1, which constitutively ubiquitinates Nrf2 leading to proteasomal degradation. However, during stress conditions, Nrf2 detach from Keap1 and translocates to the nucleus where it heterodimerizes with Maf proteins and other transcription partners to recognize and bind to ARE for activation of gene transcription.

#### 1.5.4 SIRT1 in the regulation of inflammatory responses

Sirtuins are a family of proteins that regulate cellular homeostasis. Sirtuins possess either mono-ADP-ribosyltransferase or NAD<sup>+</sup>-dependent deacetylase activity. In mammals, seven forms of sirtuins are distinguished (SIRT1-7). SIRT1, SIRT6 and SIRT7 are predominantly found in the nucleus, and SIRT3, SIRT4 and SIRT5 in the mitochondria, and SIRT2 in the cytoplasm. Distinct subcellular compartment localization of sirtuins indicate their divergent biological functions within the cell. The best-characterized protein of the sirtuin family is SIRT1. Sirtuin 1 (SIRT1) is a nicotinamide adenosine dinucleotide (NAD)-dependent deacetylase which removes acetyl groups from various proteins. SIRT1 deacetylates and thereby deactivate proteins that contribute to cellular regulation of metabolic and physiological processes. SIRT1 cleaves the nicotinamide ribosyl bond of NAD<sup>+</sup> and transfers the acetyl group from proteins to NAD<sup>+</sup>, generating the metabolite O-acetyl-ADP ribose, deacetylated substrate and nicotinamide (Xie, Zhang, & Zhang, 2013).

A large body of evidence indicates that SIRT1 plays a vital role in the modulation of the development and progression of inflammation through inhibition of critical inflammatory transcription factors (Singh et al., 2018). SIRT1 has been demonstrated to deacetylate NF- $\kappa$ B, which is acetylated at multiple lysine residues. Acetylation of various lysines regulates the activity of protein with each lysine acetylation side-specific biological outcomes. Acetylation at Lys218 and Lys221 of p65 impair binding with its inhibitory protein I $\kappa$ B.

Acetylation of p65 at Lys310 is required for transactivation of NF- $\kappa$ B genes. SIRT1 deacetylates p65 at Lys310, thereby repressing NF- $\kappa$ B transcription of various inflammation-related genes (Xie et al., 2013). Another important transcriptional regulator targeted by SIRT1 is activator protein 1 (AP-1) responsible for the inducible expression of many inflammatory mediators. AP-1 is composed of proteins belonging to the Fos, Jun families. Post-translational acetylation regulates transcriptional activity of AP-1. SIRT1 may decrease acetylation of subunits of AP-1 and inhibit its transcriptional activity of inflammatory mediators such as COX-2 (Xie et al., 2013).

Moreover, SIRT1 inhibits gene expression not only by deacetylation of transcription factors but also by deacetylation of histones. Histones are proteins that condense and structure the DNA. Hence, they play a crucial role in the transition between active and inactive chromatin states silencing and triggering gene expression. Histone acetylation at the lysine residue at the N terminus weakens the DNA-histone binding allowing RNA polymerase II and transcription complexes to bind the naked DNA and initiate transcription (Rahman & Islam, 2011). High levels of SIRT1 expression has been demonstrated to serve as a protective mechanism against inflammation (Xie et al., 2013). Therefore, SIRT1 overexpression may prevent or damp the progression of neurodegeneration.

## **1.6 Oestrogens in neuroinflammation and neurodegeneration**

Oestrogens are the primary female sex hormones responsible for the development and regulation of the female reproductive system and secondary sex characteristics. However, oestrogens are also found in significantly lower levels in men. Therefore, this indicates that oestrogen is implicated in the broader spectrum of physiological functions. Oestrogen has been shown to play a vital role in the maintenance of homeostasis in the skeletal system, cardiovascular system and CNS (Vrtačnik, Ostanek, Mencej-Bedrač, & Marc, 2014). Chemically, oestrogens belong to the family of organic compounds known as steroids. The steroid core structure is composed of 17 carbon atoms arranged as four fused rings: three six-member cyclohexane rings and one five-member cyclopentane ring. Endogenous oestrogens can be distinguished into estrone (E1), oestradiol (E2), estriol (E3) and estetrol (E4) (Figure 1.11). Oestrogens core structure is composed of 18 carbons bonded together in four rings. They consist of one benzene ring, a phenolic hydroxyl group, and a ketone group (E1), or one (E2), two (E3), or three (E4) hydroxyl groups (Fuentes & Silveyra, 2019).

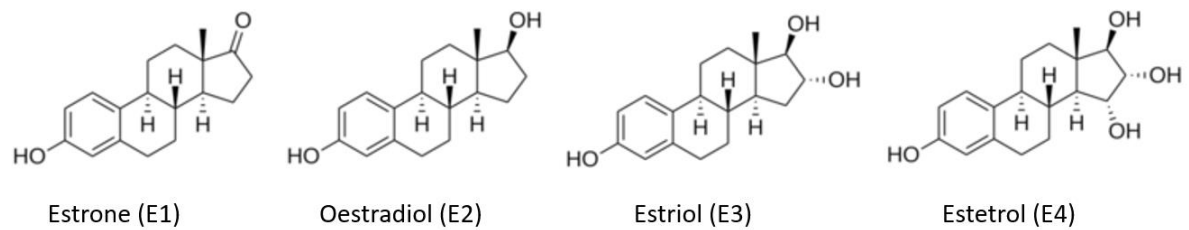


**Figure 1.11** The structural representation of oestrogens.

Oestradiol is the most potent and prevalent oestrogen in the human body. Oestradiol is mainly synthesized in ovaries from cholesterol. However, smaller amounts are also produced by the liver, pancreas, bone, breasts, skin, adrenal glands, and adipose tissue. Moreover, the biosynthesis of oestradiol is not only limited to periphery, but it also occurs in the brain. Biosynthesis of oestradiol in the brain is conducted by neurons and astrocytes, which express all necessary enzymes required to synthesize oestradiol from cholesterol. Microglial cells and oligodendrocytes fail to produce oestradiol from cholesterol (Figure 1.12). However, they can convert less potent estrone to highly active oestradiol using  $17\beta$ -hydroxysteroid dehydrogenase ( $17\beta$ -HSD), which catalyse this reaction (Cui, Shen, & Li, 2013). Besides being produced in the brain, oestradiol can also easily pass BBB, which is attributable to its low molecular weight and lipophilic properties (Samii, Bickel, Stroth & Pardridge, 1994). Therefore, oestradiol levels in the female brain qualitatively mirror levels of circulating oestradiol with sharp reduction observed in the brains of postmenopausal women compared to premenopausal women (Cholerton, Gleason, Baker, & Asthana, 2002, Cui et al., 2013). Postmenopausal women often experience a decline in cognitive abilities, including memory and thinking skills. Furthermore, AD, which is the most common form of dementia has a higher incidence rate in women than men. AD main risk factor is age, and it mainly affects people over 65, which is linked to age-related changes in oestrogen production. Thus, oestrogen seems to play a crucial function in maintaining brain homeostasis (Zárate, Stevnsner, & Gredilla, 2017).



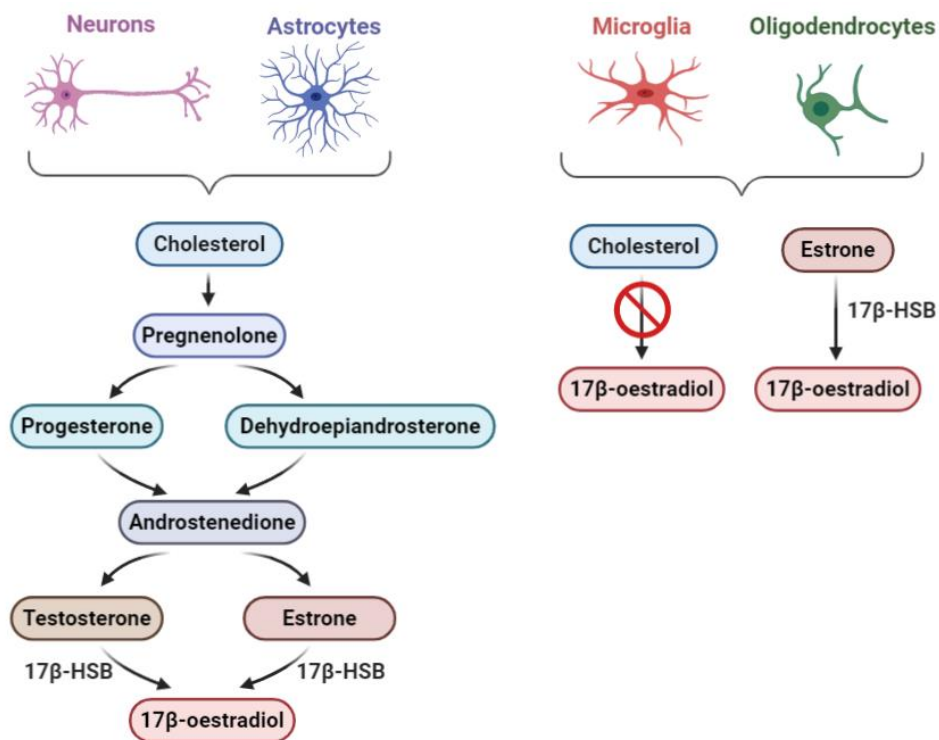


**Figure 1.12 Cell-specific 17 $\beta$ -oestradiol production in a brain.** Neurons and astrocytes have all necessary enzymes to synthesize 17 $\beta$ -oestradiol from cholesterol. In turn, microglia and oligodendrocytes are not able to produce 17 $\beta$ -oestradiol from cholesterol. However, they can transform less potent estrone to 17 $\beta$ -oestradiol using 17 $\beta$ -HSB oxidoreductase. Created based on Cui et al., (2013).

### 1.6.1 Oestrogen signalling pathways

The actions of oestrogen are mediated by the oestrogen receptors (ERs). ERs can be classified into two main groups: nuclear ERs including ER $\alpha$  and ER $\beta$  and membrane-bound ER such as mER $\alpha$ , mER $\beta$ , ER-X and G protein-coupled oestrogen receptor 1 - GPER (GPR30). Both families of ERs are expressed in the periphery, and brain with cell and tissue-specific distributions (Cholerton, Gleason, Baker, & Asthana, 2002). Oestrogen signalling pathways are distinguished into ER-dependent or ER-independent signal transduction (Figure 1.13). ER-dependent signalling is initiated by ligand-ER binding and can be further divided into direct, also known as nuclear-initiated and indirect, also called membrane-initiated ER-induced gene transcription. Direct ER-induced gene expression is triggered by the ligand-activated nuclear ER, which subsequently translocates into the nucleus and binds into a specific DNA sequence called oestrogen response element (ERE). Moreover, nuclear-translocated ER may also interact with, and consequently modulate the activity of other transcription factors, including stimulating protein-1 (SP-1), activator protein 1 (AP-1), NF- $\kappa$ B, and c-jun (Cui et al., 2013).

Indirect ER-induced gene transcription is initiated by activation of membrane-bound ERs which transduce signal via second messengers leading to activation of gene promoters. Furthermore, ER-dependent signalling pathway may also induce non-transcriptional activities via crosstalk with other membrane receptors such as neurotransmitter receptors, tyrosine kinase receptors, and insulin-like growth hormone receptors. In contrast to transcriptional activation, effects of non-transcriptional ER signalling are very rapid, occurring within a few seconds or minutes. For example, activated ion channels modify intracellular calcium or potassium level (Kelly & Levin, 2001). ER-independent signalling pathway may block oxidative stress via limitation of ROS release from damaged mitochondria. Moreover, oestrogens have been shown to act as antioxidants also via free radical scavenging. Another ER-independent signalling pathway is initiated by ligand-independent activation of ERs, leading to ERE-dependent gene transcription. Ligand-independent activation of ERs can be triggered by protein kinase cascades such as protein kinase C (PKC), protein kinase A (PKA), MAPK, EGF, insulin, IGF1, and transforming growth factor-beta (TGF $\beta$ ) (Fuentes & Silveyra, 2019).

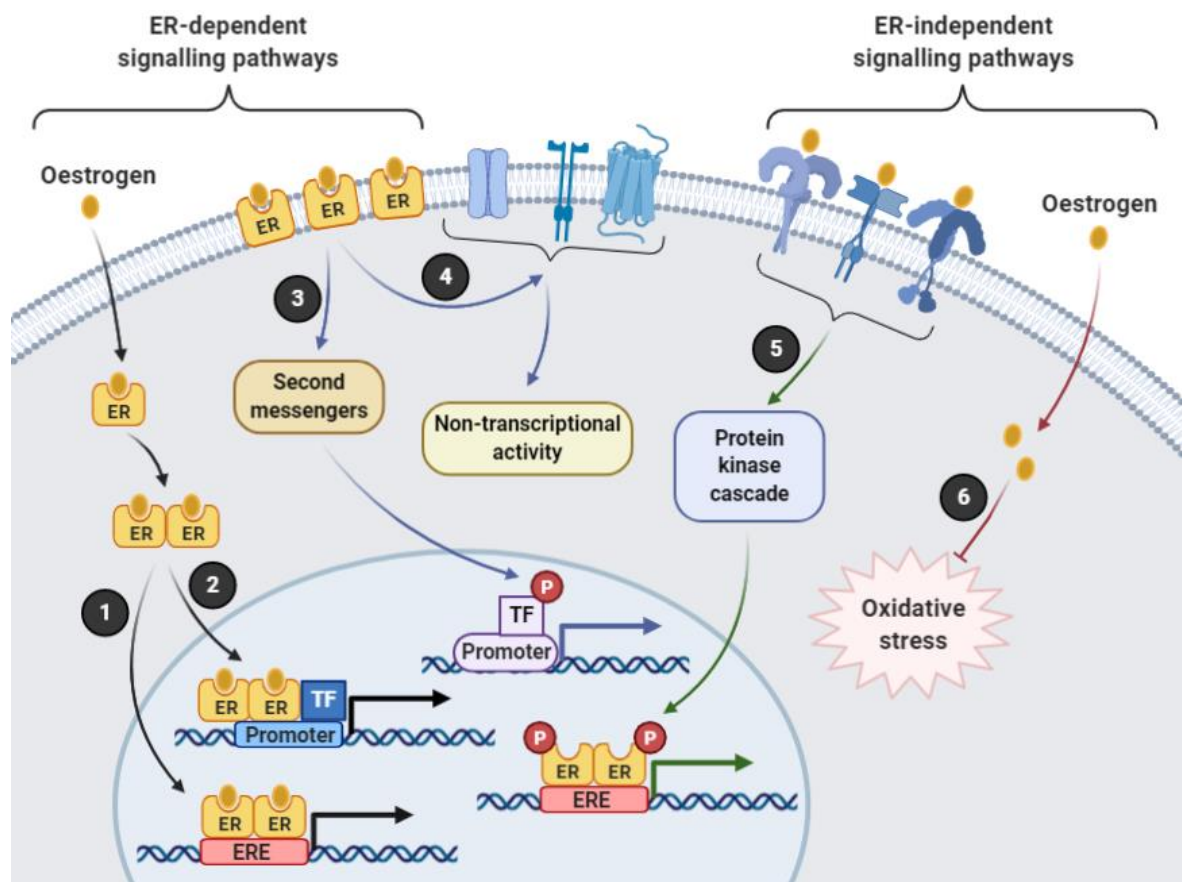


**Figure 1.13 Oestrogenic signalling pathways.** Estrogenic signalling can be divided into the ER-dependent and ER-independent pathway. The ER-dependent pathway may be further distinguished into nuclear-initiated and membrane-initiated. The ER-dependent nuclear-initiated pathway may lead to ERE promoter activation (1)

or interaction of ER with different promoters (2). Membrane ER-dependent pathway may trigger activation of gene expression via second messengers (3) or interact with other membrane receptors (4). ER-independent signalling activates membrane receptors which trigger protein kinase cascade and phosphorylate ER leading to ERE gene expression (5). Another ER-independent signalling pathway relies on antioxidant effects of oestrogens (6).

### **1.6.2 Beneficial effects of oestrogens in the brain**

A large body of evidence demonstrates the positive effects of oestrogens on cognitive functions, thereby indicating their potent neuroprotective activity (Villa, Vegeto, Poletti, & Maggi, 2016). Neuroprotective actions of oestrogens are mediated by modulation of neuronal and glial gene expression. Oestrogens reduce neuronal sensitivity to neurodegenerative factors, propagating their survival. Moreover, oestrogens also increase neuronal regeneration. Oestrogens inhibit apoptosis which is the principle of neurodegeneration. Apoptosis requires the synthesis of many proteins from B-cell lymphoma 2 (Bcl-2) family which control this process. Bcl-2 family includes both anti-apoptotic proteins such as Bcl-2, Bcl-XL, and pro-apoptotic proteins – Bax and Bad. *In vitro* and *in vivo* studies showed that estradiol increases the expression of anti-apoptotic proteins protecting neurons from apoptosis (Singer, Rogers, & Dorsa, 1998; Fan, Pandey, & Cohen, 2008). Oestrogen influence synthesis of these proteins directly by binding of activated ER to ERE in Bcl-2 gene promotor or indirectly by inhibition of expression of Bcl-2 and Bcl-XL inhibitory proteins such as Nip-2 (Vegeto, Pollio, Pellicciari & Maggi, 1999). Both of those mechanisms lead to an increased level of anti-apoptotic proteins promoting cell survival. Another mechanism promoting neuronal survival is ER interaction with the N-methyl-D-aspartate (NMDA) receptor. Oestradiol serves as an antagonist of NMDA receptors. Hence it blocks receptor activation and  $Ca^{2+}$  flux into the cell, thereby protecting neurons from overactivation, which is implicated in excitotoxicity (Ciesielska, Joniec & Czlonkowska, 2002). Moreover, Singer, Pang, Dobie, & Dorsa, (1996) demonstrated that oestrogens alongside the promotion of neuronal survival also increase expression of proteins enhancing neuronal regeneration such as growth-associated protein 43 (GAP-43) which is responsible for axon elongation and is expressed in high levels during neuronal growth.

The beneficial effect of oestrogen on neurodegeneration is also attributed to its anti-inflammatory action on microglia. Neurodegeneration is abbreviated by microglial activation, which leads to alleviated expression of pro-inflammatory factors which in turn further aggravate neuroinflammation contributing to the progression of neurodegeneration. Previous studies evaluating the anti-inflammatory activity of oestradiol demonstrated its

ability to modulate the phenotype of microglia from M1 – pro-inflammatory to M2 – neuroprotective, which stops vicious cycle of neuroinflammation (Zárate et al., 2017). Numerous studies showed ER ability to interact with the NF- $\kappa$ B complex, preventing NF- $\kappa$ B from binding to cytokine genes promoters and thereby suppressing the production of neurotoxic factors (Fuentes & Silveyra, 2019). Additionally, oestrogen presented the ability to reduce oxidative stress through the restoration of mitochondrial functions and potentiation of reductive enzymatic systems (Villa et al., 2016).

## **1.7 Isoflavones**

Isoflavones are polyphenolic compounds which belong to the group of phytoestrogens. Phytoestrogens are plant-derived molecules with structural and functional similarities to mammalian oestrogens. Phytoestrogens can be distinguished into flavonoid and non-flavonoid sub-classes. Flavonoids are typically composed of a 15-carbon skeleton, which consists of two phenyl rings (A and B) and a heterocyclic ring (C). Flavonoids can be subdivided into different groups based on the attachment of carbon of the C ring which the B ring. Flavonoids in which the B ring is linked in position 3 of the C ring are called isoflavones (Panche, Diwan, & Chandra, 2016). Isoflavones are predominantly found in the members of the bean family, Fabaceae (Leguminosae). The family Fabaceae includes various economically significant plants such as soybean, green bean, chickpeas, alfalfa sprout, peanut, and red clover. Moreover, isoflavones are also abundant in highly processed food created from legumes such as tofu, tempeh, and miso. In certain regions of the world where consumption of soy products is high such as Asia, the incidence of breast and gynaecological cancer is much lower when compared to the western population. Those positive biological effects have been attributed to a soy-rich diet. Additionally, various studies indicated that soy isoflavones improve cognitive functions such as verbal fluency, planning and cognitive flexibility in older people (Casini et al., 2006; Gleason et al., 2009; Veldman, Cantorna, & DeLuca, 2001). Furthermore, isoflavones also have been demonstrated to have positive effects in patients with cardiovascular diseases, cancer, osteoporosis. Chen, Lin, & Liu (2015) and Munro et al., (2003) studies showed that increased consumption of isoflavones has no side effects. Therefore, isoflavones seem to have promising therapeutic potential in various spectrum of disorders.

Isoflavones belong to selective oestrogen receptor modulators (SERMs) which act as agonist or antagonist of ER depending on a tissue type. Therefore, in contrast to oestradiol which

binds equally well to both receptors, isoflavones have a greater binding affinity for ER $\beta$  than ER $\alpha$  (Bao, Han, Shim, Wen, & Jiang, 2006; Cos et al., 2003). Therefore, the beneficial health effects of isoflavones are attributed to their higher affinity for ER $\beta$ . Both ERs are widely distributed throughout the human organism. ER $\alpha$  plays a critical role in pathogenesis and proliferation of breast cancer, promoting oncogenic protein expression and inhibition of cell cycle inhibitors such as p21 (Xue et al., 2019). In contrast, ER $\beta$  is a potent tumour suppressor with anti-proliferative effects. Therefore, ER $\beta$  opposes the actions of ER $\alpha$  in reproductive tissue (Kyriakidis & Papaioannidou, 2016).

Beneficial effects of isoflavones on neurodegeneration are demonstrated by a large body of evidence. Those properties can be attributed to isoflavones high affinity to ER $\beta$ , which is abundantly expressed in the brain including hippocampus and prefrontal cortex - areas key for learning, memory and higher-order cognitive function (Soni et al., 2014). Numerous studies demonstrate anti-inflammatory, antioxidant and neuroprotective properties of various isoflavones. The most studied isoflavones are genistein (7,4'-dihydroxy-6-methoxyisoflavone), daidzein (7,4'-dihydroxyisoflavone), biochanin A (5,7-dihydroxy-4'-methoxyisoflavone), and formononetin (7-hydroxy-4'-methoxyisoflavone) (Figure 1.14) (Ahmed et al., 2017; Liang et al., 2019; Subedi et al., 2017; Wang et al., 2015; Yu, Bi, Yu, & Chen, 2016).

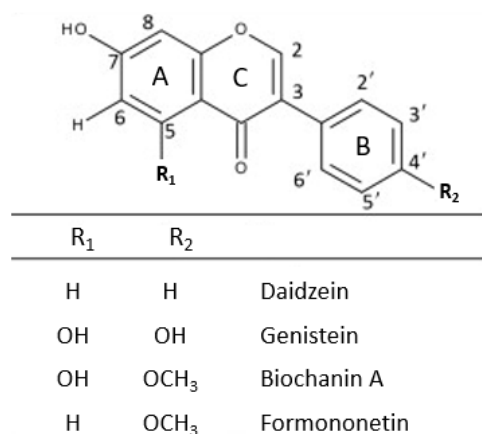


**Figure 1.14** The structural representation of isoflavones. Adapted from: Mahesha, Singh, & Rao, (2007)

## **1.8 Aims and objectives of this study**

AD is the most prevalent neurodegenerative disorder of modern society. It is known that the most prominent risk factor of the AD is age. Moreover, epidemiological studies show a higher incidence of AD in women than in men (Prince et al., 2015). Therefore, it has been proposed that the decrease of oestrogen during menopause may contribute to the intensification of neurodegenerative processes (Ciesielska, Joniec & Czlonkowska, 2002). This hypothesis indicates that oestrogen is an important neuroprotective factor which counteracts AD development. However, oestrogens may cause detrimental side effects, such as gynaecological and breast cancers. Hence, selective activation of ER generated by isoflavones may serve as a potential therapy aiming to reduce neuroinflammation and restore normal physiological brain functions. Furthermore, the failure to translate neuroprotective activities of agents from animals to humans has been linked to species-specific differences. Hence development of immortalized human microglia to study anti-inflammatory properties of compounds might provide an opportunity to access more accurate and robust data which will have profound meaning in assessing the therapeutic potential of studied compounds.

The project aimed to investigate anti-inflammatory properties and the mechanism of action of novel isoflavones analogues. Moreover, this study also aimed to establish neuroprotective properties of tested compounds and molecular mechanisms accountable for those effects. Additionally, this project aimed to develop human microglial cells (HMC3) as a cellular model to study neuroinflammation, which could be an alternative to commonly used murine cell lines models. Human microglial cell model provides the opportunity to overcome species-specific differences and would reveal more accurate information about the therapeutic potential of compounds.

### **Research questions:**

Do the compounds inhibit neuroinflammation? What is their mechanism of action? Are these compounds neuroprotective? What cellular mechanisms lead to neuroprotective effects? Can HMC3 cells serve as a cellular model for neuroinflammation?

### **The gap in the knowledge:**

Currently, there is no cure for neurodegeneration. Hence, this study assessed anti-inflammatory and neuroprotective properties of compounds which could slow down the progression of neurodegeneration. Until now no studies investigated the pharmacological activity and molecular mechanisms of novel carbamate and dodecenoyl ester derivatives of biochanin A, and ethyl ester and chloropropyl triazole daidzein analogues. Therefore, this study, for the first time presents the anti-inflammatory and neuroprotective activities and potential mechanisms of novel isoflavones. The HMC3 cell line has been recently authenticated by American Type Culture Collection (ATCC®) and current literature lacks studies investigating inflammation-inducing ligands in HMC3 cells. Hence this study presents the effect of TNF $\alpha$ , LPS, IFN $\gamma$  and ODN 2006 on pro-inflammatory markers and signalling pathways in HMC3 microglia.

### **Objectives:**

1. Determine the effects of compounds on the levels of pro-inflammatory mediators in LPS-activated BV2 microglia
2. Evaluate the mechanism of anti-neuroinflammatory action of compounds
3. Determine the neuroprotective actions of compounds against H<sub>2</sub>O<sub>2</sub>-induced cell death in SH-SY5Y neuroblastoma
4. Establish molecular mechanisms responsible for neuroprotective properties of compounds
5. Assess the role of oestrogen signalling in anti-inflammatory and neuroprotective actions of compounds
6. Determine the ligand which will induce an inflammatory response in HMC3 leading to the production of pro-inflammatory mediators
7. Determine signalling pathways involved in the increased production of pro-inflammatory mediators in activated HMC3

## 2 Chapter II - Anti-inflammatory Properties and Mechanism of Action of Biochanin A Derivatives

### 2.1 Introduction

#### 2.1.1 Biochanin A

Biochanin A - 5,7-dihydroxy-4'-methoxy-isoflavone (Figure 2.1) is an isoflavone abundantly found in legumes, including red clover, soybeans, alfalfa sprouts, peanuts and chickpea (Sundaresan, Radhiga, & Deivasigamani, 2018). Biochanin A belongs to phytoestrogen family, which is well known for anti-inflammatory and antioxidant, neuroprotective and anti-carcinogenic properties established *in vivo* and *in vitro* studies (Tham, Gardner, & Haskell, 2011). Anti-inflammatory properties of biochanin A were also determined using LPS-activated BV2 microglia. Wu et al., (2015) and Zhang & Chen, (2014) demonstrated that biochanin A reduced inflammatory cytokines and mediators. Wu et al., (2015) indicated the involvement of MAPKs in the above-described effects. Moreover, Zhang & Chen, (2014) demonstrated that inhibition of peroxisome proliferator-activated receptor-gamma (PPAR- $\gamma$ ) attenuates biochanin A anti-inflammatory properties, including reduction of p-NF- $\kappa$ B suggesting the involvement of multiple molecular mechanisms. Due to chemical structure similarity to oestrogen, another molecular target of biochanin A include ER. Nynca et al., (2013) demonstrated biochanin A ability to upregulate ER $\beta$  expression without altering ER $\beta$  and ER $\alpha$  mRNA level and steroidogenesis in porcine granulosa cells. Overk et al., (2005) indicated that biochanin A induced ERE-luciferase expression in MCF-7 cells. A large body of evidence describes biochanin A as neuroprotective (Raheja, Girdhar, Lather, & Pandita, 2018; Sundaresan et al., 2018; Yu, Zhang, Lou, & Wang, 2019). Although biochanin A has many beneficial pharmacological activities, it is not widely used as therapeutic agent due to limited bioavailability (<4%) caused by extensive first-pass metabolism, and biliary elimination (Moon et al., 2006; Raheja et al., 2018). Digested biochanin A undergoes demethylation under hepatic microsomal enzymes and gut microflora, followed by glucuronidation in the liver (Moon et al., 2006). Therefore, synthesis of biochanin A analogues with increased bioavailability could enhance positive effects seen during biochanin A administration and expand its clinical applications.



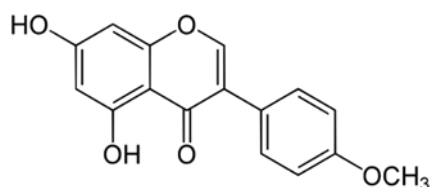


**Figure 2.1** The chemical structure of biochanin A.

### 2.1.2 Biochanin A derivatives

Considering the positive biological effects of biochanin A and limitations of physical properties, this study investigates two biochanin A analogues (Table 2.1): 5-hydroxy-3-(4-methoxyphenyl)-4-oxochromen-7-yl N-undecylcarbamate (Compound 1) and 5-hydroxy-3-(4-methoxyphenyl)-4-oxochromen-7-yl dodecanoate (Compound 2). Compound 1 was created by insertion of carbamate moiety to biochanin A at position 7'. Compound 2 has a similar structure to compound 1 however, instead of carbamate group at position 7' this compound was created by insertion dodecenoyl ester group.

Biochanin A derivatives at position 7'	
<p><b>Compound 1</b></p> <p>5-hydroxy-3-(4-methoxyphenyl)-4-oxochromen-7-yl N-undecylcarbamate</p> <p>Formula: C<sub>28</sub>H<sub>35</sub>NO<sub>6</sub></p> <p>Molecular weight: 481.589</p>	<p><b>Compound 2</b></p> <p>5-hydroxy-3-(4-methoxyphenyl)-4-oxochromen-7-yl dodecanoate</p> <p>Formula: C<sub>28</sub>H<sub>34</sub>O<sub>6</sub></p> <p>Molecular weight: 466.574</p>

**Figure 2.2** The structural formula of biochanin A derivatives – compounds 1 and 2.

## 2.2 Methodology

### 2.2.1 BV2 cell culture

BV2 cells are mouse microglia which have been generated by infecting primary microglial cell cultures with a v-raf/v-myc oncogene carrying retrovirus (J2) (Timmerman, Burm, & Bajramovic, 2018). Bocchini et al., (1992) established that BV2 microglia have morphological, phenotypical, and functional properties of macrophages. Moreover, authors also indicated that BV2 cells express microglial specific markers which distinguish them from body macrophages. Therefore, BV2 cell model is widely used to study neuroinflammation, neurodegeneration, and to test pharmacological activity and molecular mechanisms of potent anti-inflammatory compounds (Stansley, Post, & Hensley, 2012). In this study, BV2 microglial activation was induced by lipopolysaccharide (LPS), which can easily change the phenotype of BV2 microglia from resting to activated - M1 phenotype (Dai et al., 2015). Therefore, BV2 cell line was considered as suitable *in vitro* model to study microglia.

BV2 mouse brain microglial cells (ICLC ATL03001) were purchased from Interlab Cell Line Collection, Banca Biological Cell Factory, Italy. Cells were cultured in Gibco™ Roswell Park Memorial Institute medium 1640 (RPMI, Fisher Scientific) already supplemented with 2 mM glutamine and additionally enriched with 10% Gibco™ Fetal Bovine Serum (FBS, Fisher Scientific), and 100 mM Gibco™ Sodium Pyruvate (Fisher Scientific) in a tissue culture flask T-75 (Sarstedt) with standard surface modification for adherent cells. Cells were incubated in a humid atmosphere of 5% CO<sub>2</sub> and 95% air at 37°C. When cells reached approximately 80% confluence, they were washed with Gibco™ Phosphate Buffered Saline (Fisher Scientific) and then adherent cells were dissociated from the vessel using Gibco™ TrypLE™ Express Enzyme (Fisher Scientific) which allowed cell counting and subsequent subculture.

### **2.2.2 Treatment of BV2 cells with compounds 1 and 2**

Both compounds 5-hydroxy-3-(4-methoxyphenyl)-4-oxochromen-7-yl N-undecylcarbamate (compound 1) and 5-hydroxy-3-(4-methoxyphenyl)-4-oxochromen-7-yl dodecanoate (compound 2) were kindly provided by Gabriel Mengheres (PhD Researcher supervised by Dr Karl Hemming, Department of Chemical Sciences, The University of Huddersfield). Compounds were dissolved in dimethyl sulfoxide (DMSO, Fisher Scientific) and stored in -80°C. BV2 cells were seeded in 96-well, 24-well and 6-well plates with flat base and adherent surface (Sarstedt) at a density of  $5 \times 10^4$  cells/ml in 200  $\mu$ l for 96-well, 1 ml for 24-well and 2 ml for 6-well plate. When cells reached approximately 80% confluence, the culture medium has been changed to serum-free RPMI to reduce the variability of experiments caused by lot to lot variation of serum composition. Subsequently, cells were incubated for 1 – 2 hours at 37°C. Subsequently, BV2 cells were pre-incubated with or without 5, 10, 15 and 20  $\mu$ M of compounds 1 and 2. The final concentration of DMSO in the cell culture medium was kept constant at 0.2% v/v for all concentrations of compounds and untreated control. After pre-treatment with compounds, cells were incubated for 30 minutes at 37°C and then activated using 100 ng/ml of lipopolysaccharide - LPS derived from Salmonella typhimurium, S-form for 1 hour or 24 hours (Innaxon Biosciences).

### 2.2.2.1 Determination of non-toxic and active concentrations of compounds 1 and 2 for BV2 cells

Non-toxic and active concentrations of compounds 1 and 2 for BV2 cells were established during preliminary pilot experiments such as XTT and Griess assay. For preliminary pilot experiments, BV2 cells were pre-incubated with a wide range of concentrations 1 nM – 100  $\mu$ M of the compounds 1 and 2 for 30 minutes followed by LPS (100 ng/ml) activation for 24 hours. Compound 1 at 40  $\mu$ M significantly ( $p < 0.033$ ) reduced BV2 viability compared to untreated control (Figure 2.3 A). In turn compound 2 at any of tested concentrations did not affect BV2 viability (Figure 2.3 C). Compounds 1 and 2 significantly ( $p < 0.033$ ,  $p < 0.002$ ) reduced LPS-induced nitric oxide level starting at concentration 0.1 and 15  $\mu$ M, respectively (Figure 2.3 B and D). Based on the XTT and Griess assay results four non-toxic and active concentrations of compounds 1 and 2 were selected for further experiments - 5, 10, 15 and 20  $\mu$ M.

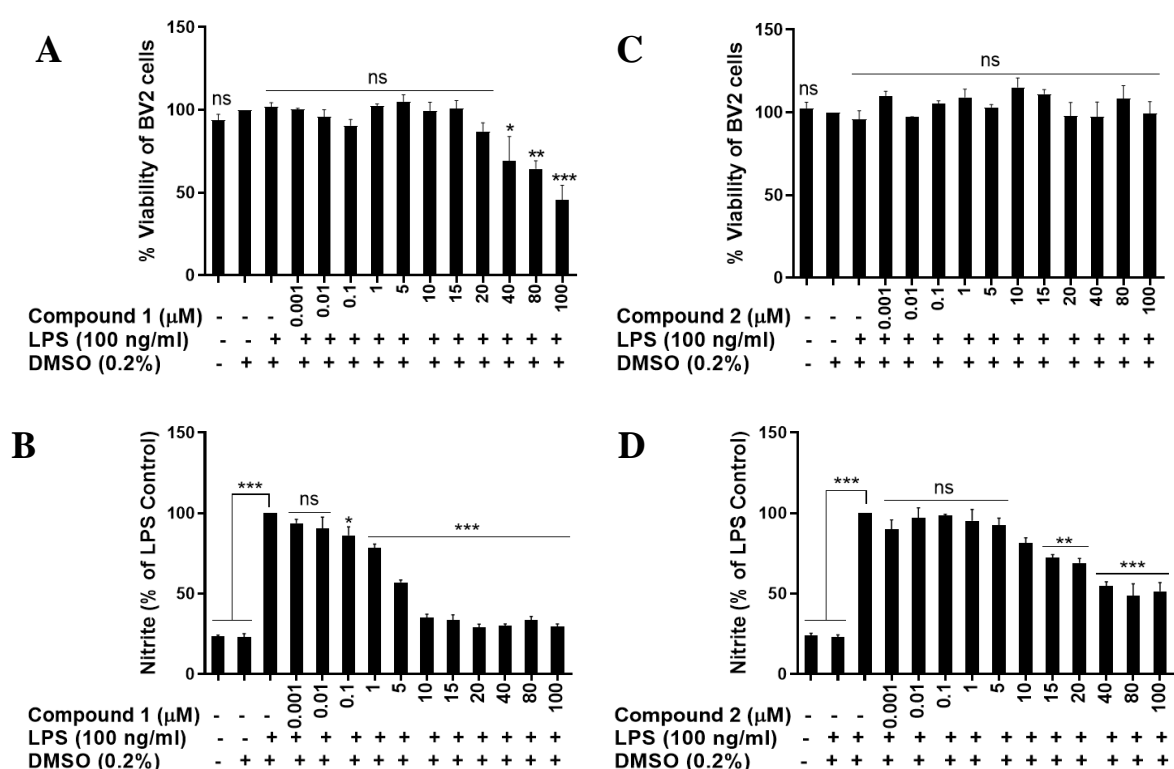


**Figure 2.3 Determination of maximum non-toxic and active concentrations of compounds 1 and 2 for BV2 cells.** BV2 microglia were treated with or without a broad range of concentrations of compounds 1 and 2 (0.001 – 100  $\mu$ M) for 30 minutes and then activated with LPS (100 ng/ml). Subsequently, BV2 cells were incubated for 24 hours, and XTT assay and Griess assay were performed. The maximum non-toxic concentration of compound 1 in BV2 cells was 20  $\mu$ M (A). Compound 1 significantly reduced nitrite production from 0.1  $\mu$ M (B). Compound 2 was not toxic to cells at any of tested concentration 0.001 – 100  $\mu$ M (C). Compound 2 significantly inhibited nitrite production from 15  $\mu$ M (D). All values are expressed as a mean  $\pm$  SEM for three independent experiments. Data were analysed using one-way ANOVA for multiple comparisons with post hoc Student Newman-Keuls test. \* $p < 0.033$ , \*\* $p < 0.002$ , \*\*\* $p < 0.001$  in comparison with untreated control or LPS control.

### 2.2.2.2 Optimisation of non-toxic concentration of DMSO for BV2 microglia

Compounds were dissolved in DMSO; hence viability assay was conducted to establish the non-toxic concentration of DMSO for BV2 microglia. Incubation of cells with DMSO at concentrations 0.2% and 0.4% (v/v) did not reduce BV2 microglia viability. DMSO at 0.8% and 1% (v/v) significantly ( $p < 0.002$ ) reduced BV2 viability compared to untreated cells (Figure 2.4).

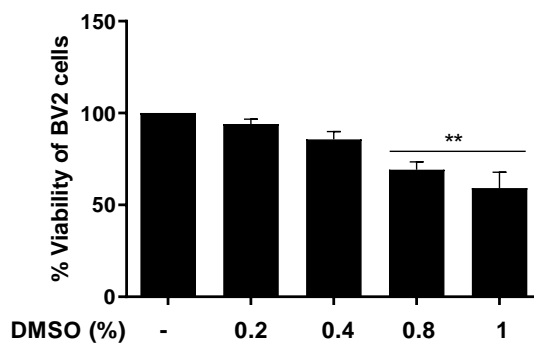


**Figure 2.4 Optimisation of non-toxic concentration of DMSO for BV2 microglia.** BV2 microglia were pre-incubated with various concentrations of DMSO 0.2% - 1% (v/v) for 24 hours, then XTT assay was performed. DMSO was not toxic to cells up to 0.4% final concentration (v/v). All values are expressed as a mean  $\pm$  SEM for three independent experiments. Data were analysed using one-way ANOVA for multiple comparisons with post hoc Student Newman-Keuls test. \*\* $p < 0.002$  in comparison with untreated control.

### 2.2.2.3 Evaluation of optimal LPS concentration to activate BV2 microglia

BV2 microglia were activated with LPS which is a ligand of toll-like receptor 4 (TLR4). TLR4 is an integral membrane glycoprotein specialized in recognizing structurally conserved molecules of bacteria to initiate the inflammatory response. TLR4 belongs to PAMPs, and its activation is coupled to complex signalling pathways, including NF- $\kappa$ B and MAPKs, which orchestrate an inflammatory response (Jack et al., 2005). Therefore, numerous reports indicated activation of TLR4 as a gold standard to trigger the microglial inflammatory response (Baker, Brautigam, & Watters, 2004; Lund et al., 2006; Tao et al., 2018). Evaluation of optimal LPS concentration for BV2 activation was based on nitric oxide production. BV2 cells were stimulated with 25 – 1000 ng/ml of LPS for 24 hours, followed by the assessment of nitrite level. As optimal LPS concentration for BV2 activation was considered 100 ng/ml because it was the lowest concentration of LPS which induced the maximum release of nitrite in BV2 cells (Figure 2.5).

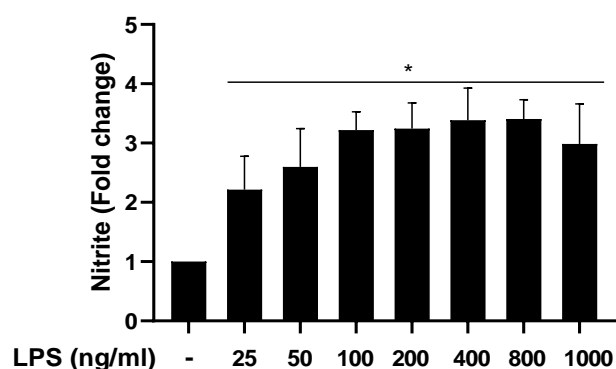


**Figure 2.5 Evaluation of optimal LPS concentration to activate BV2 microglia.** BV2 cells were stimulated with different concentrations of LPS (25 – 1000 ng/ml) for 24 hours. After incubation, cell culture supernatants were collected, and the level of nitrite was evaluated using Griess assay. All concentrations of LPS were significantly upregulating nitrite production. The lowest concentration of LPS which induced maximum nitrite release was obtained with 100 ng/ml. Therefore, this concentration was used for further studies. All values are expressed as a mean  $\pm$  SEM for three independent experiments. Data were analysed using one-way ANOVA for multiple comparisons with post hoc Student Newman-Keuls test. \* $p < 0.033$  in comparison with untreated control.

### 2.2.3 XTT cell viability assay

XTT cell proliferation assay has been used as an indirect measurement of cells metabolic activity in order to establish cells sensitivity to various concentrations of compounds. XTT assay was described more than three decades ago by Scudiero et al., (1988) as an effective assessment of drug effects on cell growth. This assay is based on the metabolic reduction of 2,3-bis(2-methoxy-4-nitro-5-sulfophenyl)-5-[(phenylamino)carbonyl]-2H-tetrazolium hydroxide (XTT) to a water-soluble, brightly orange, formazan product. This bio-reduction of XTT occurs only in viable cells; hence, formazan production is proportional to the number of metabolically active cells. Unlike MTT, XTT dye is not able to cross the cell membrane due to its negative charge. Therefore, plasma membrane electron transporters cleave XTT at the cell surface. To enhance the sensitivity of this assay, phenazine methosulfate (PMS) was used as the intermediate electron acceptor (Scudiero et al., 1988).

To perform XTT assay, BV2 microglia were seeded in 96-well plate with a flat bottom at a density of  $5 \times 10^4$  cells/ml in 200  $\mu$ l of culture medium. Then cells were treated and stimulated as indicated in 2.2.2. Subsequently, cells were incubated 24 hours in CO<sub>2</sub> incubator at 37°C, then 100  $\mu$ l of cell culture medium was removed, and 25  $\mu$ l of XTT/PMS solution was added to each well containing 100  $\mu$ l of cell culture. XTT/PMS solution was composed of 1 mg/ml of Invitrogen™ Molecular Probes™ XTT (Fisher Scientific) and 10 mM PMS (Sigma-Aldrich). This was followed by 2 hours incubation at 37°C, and subsequently, measurement of absorbance at 450 nm using microplate reader (Infinite F50, Tecan).

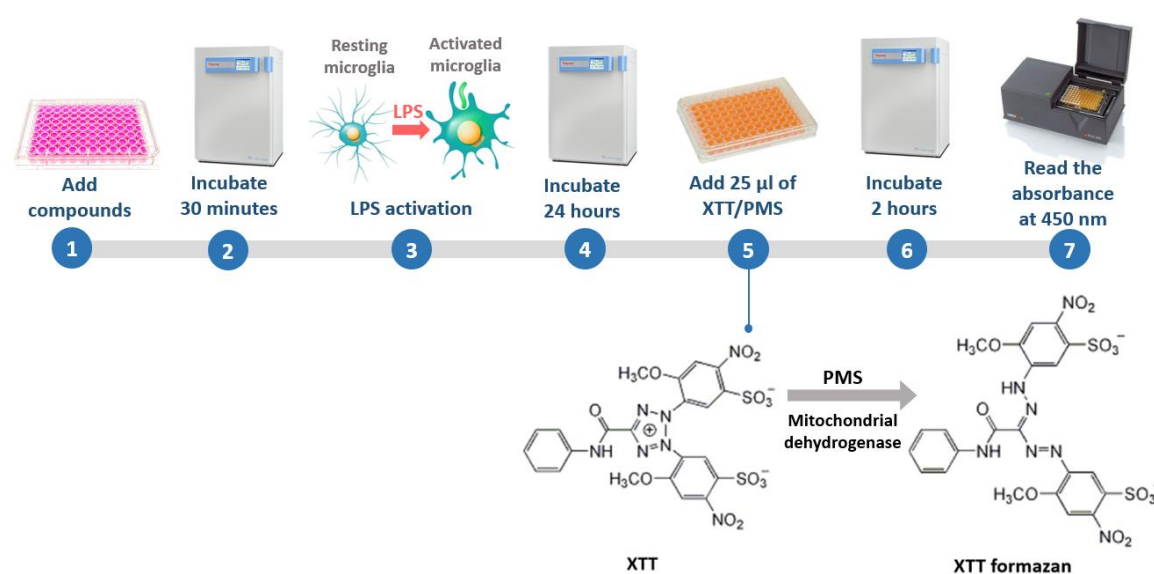


**Figure 2.6** Flowchart of XTT assay and schematics of XTT reduction to XTT formazan. Adapted from (Sidorova et al., 2009).

## 2.2.4 TNF- $\alpha$ , IL-1 $\beta$ and IL-6 ELISA

Enzyme-linked Immunosorbent Assay (ELISA) is a plate-based immunological assay used to detect and quantify antibodies, antigens, and proteins in biological samples. This technique was developed in the 70s of the 20th Century by two independent research groups: Peter Perlmann and Eva Engvall from Sweden and Bauke van Weeman and Anton Schuurs from Holland (Engvall & Perlmann, 1971; Weemen & Schuurs, 1971). In this study sandwich ELISA has been employed as it quantifies antigen between capture and detection antibody, which allows to amplify a signal and leads to the highest sensitivity.

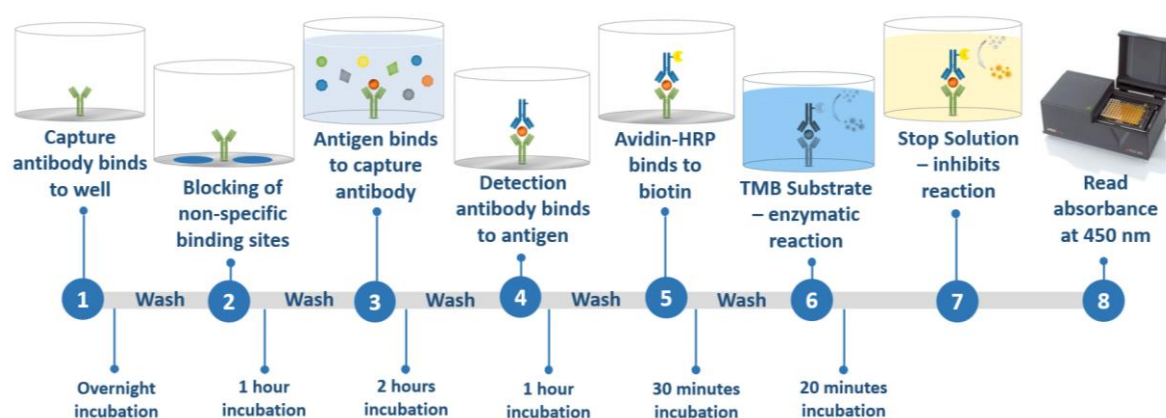


**Figure 2.7** Flowchart of sandwich ELISA.

In this study TNF- $\alpha$ , IL-1 $\beta$ , IL-6 cytokines were measured using Mouse TNF- $\alpha$  ELISA MAX<sup>TM</sup> Deluxe, Mouse IL-1 $\beta$  ELISA MAX<sup>TM</sup> Deluxe and Mouse IL-6 ELISA MAX<sup>TM</sup> Deluxe (BioLegend), respectively. Before conducting ELISA, BV2 microglia were seeded in 24-well plates at a density of  $5 \times 10^4$  cells/ml in 1 ml of culture medium. Then cells were treated and activated as described in [2.2.2](#). After 24 hours of incubation, culture supernatants were collected by centrifugation at  $806 \times g$  for 5 minutes and stored in  $-80^\circ\text{C}$  until needed. One day before conducting ELISA, 96-well plate was pre-coated with 100  $\mu\text{l}$  of coating antibody diluted 1:200 in coating buffer and stored in  $4^\circ\text{C}$  overnight. Next day the plate was washed 4 times with 200  $\mu\text{l}$  of Wash Buffer comprising of phosphate-buffered saline (PBS, Sigma-Aldrich) and 0.05% TWEEN<sup>®</sup> 20 (Sigma-Aldrich). Subsequently, 200  $\mu\text{l}$  of Assay Diluent 1X was added, and the plate was incubated 1 hour shaking 200 rpm at room temperature. After that, the plate was washed with Wash Buffer as indicated above, and 100  $\mu\text{l}$  of diluted standards and cell culture supernatants were added (cell culture supernatants for TNF $\alpha$  ELISA were diluted 1:10 with assay diluent). After 2 hours of incubation, the plate was re-washed as indicated above, and 100  $\mu\text{l}$  of detection antibody diluted 1:200 in Assay



Diluent was added and incubated 1 hour shaking 200 rpm at room temperature. This was followed by a plate wash with Wash Buffer and 30 minutes of incubation with 100  $\mu$ l of Avidin-HRP diluted 1:1000 with Assay Diluent. Afterwards, the plate was washed again with Wash Buffer, and 100  $\mu$ l of tetramethylbenzidine (TMB) substrate solution was added and incubated in the dark for 20 minutes. TMB reaction was stopped by adding 100  $\mu$ l of Stop Solution (0.16 M Sulphuric Acid), resulting in a colour change from blue to yellow. This allowed to measure absorbance at 450nm using a microplate reader (Infinite F50, Tecan) which was directly proportional to the concentration of specific cytokines.

### 2.2.5 Griess assay

The levels of nitric oxide (NO) in tested samples were detected using the Griess Reagent System from Promega. This assay is based on the diazotization reaction and uses sulfanilamide and N-1-naphthyl ethylenediamine dihydrochloride (NED) under phosphoric acid conditions. Above described reaction results in a colour change to pink, which allows to measure the absorbance. Griess primarily developed this technique in 1879. Nitric oxide (NO) is non-stable molecule hence to determine its level Griess Reagent System detects nitrite ( $\text{NO}_2^-$ ) which is stable biodegradation product of nitric oxide (Coneski & Schoenfisch, 2012).

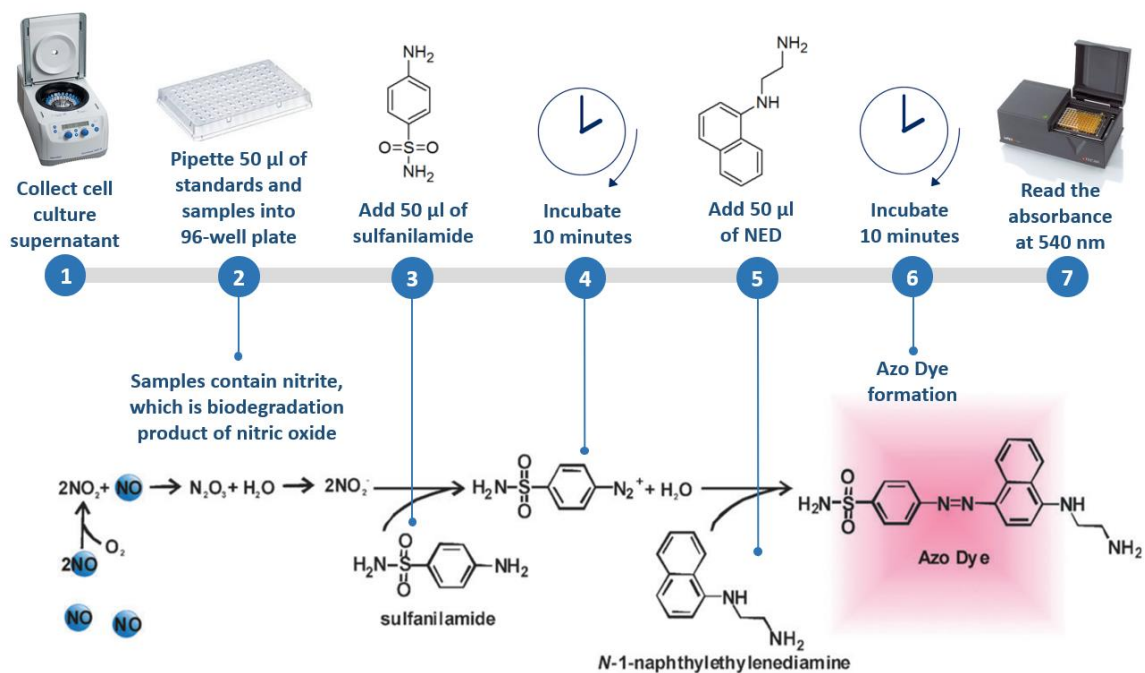


**Figure 2.8. Flowchart of Griess assay and chemical representation of nitrite reaction with Griess reagents leading to the azo dye formation.** Adapted from (Coneski & Schoenfisch, 2012)

For Griess assay, cells were seeded in 24-well plates at a density of  $5 \times 10^4$  cells/ml in 1 ml of culture medium then treated and stimulated as described in 2.2.2. Then BV2 microglia were incubated 24 hours at 37°C in CO<sub>2</sub> incubator. Subsequently, supernatants were collected, and 50 µl was pipetted in triplicate into 96-well plate. Next 50 µl of sulphanilamide was added to the plate which was incubated for 10 minutes in the dark at room temperature. Thereafter 50 µl of NED was added and incubated as indicated above. After 10 minutes of incubation, absorbance was measured at 540 nm using a microplate reader (Infinite F50, Tecan).

### 2.2.6 Western blotting

The Western blot experiments allow to detect and relatively quantify target proteins. This technique involves three main elements: first is the separation of proteins according to their size, second is the transfer of proteins from the gel into solid support, e.g., polyvinylidene difluoride (PVDF) membrane, and final step is to mark specific protein using a primary and secondary antibody (Mahmood & Yang, 2012).

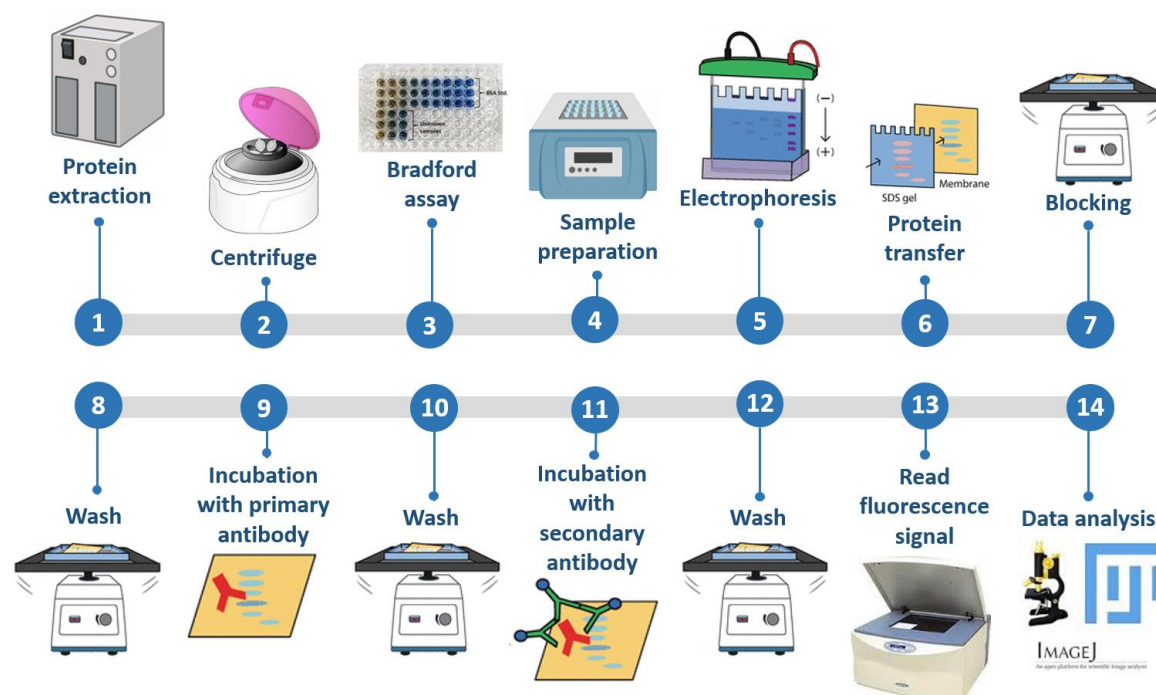


Figure 2.9 The flowchart of Western blotting experiment.

### **2.2.6.1 Whole-cell lysate preparation**

To perform Western blotting, cells were seeded in 6-well plates at a density of  $5 \times 10^4$  cells/ml in 2 ml of culture medium, at approximately 80% confluence cells were treated as indicated in [2.2.2](#) and incubated. At the end of incubation, the cell pellet was collected by centrifugation of cell culture medium and scraping adherent cells from a culture plate. Then cell pellet was washed with Gibco™ Phosphate Buffered Saline (Fisher Scientific). Next cell membrane was disrupted using 1X Cell Lysis Buffer (Cell Signalling) containing 1 mM phenylmethane sulfonyl fluoride (PMSF, Sigma-Aldrich) and 1:100 Thermo Scientific™ Halt™ Phosphatase Inhibitor Single-Use Cocktail (Fisher Scientific). After 15 minutes of incubation on ice, cells were briefly sonicated four times for 10 seconds with a 10 seconds interval between each sonication and centrifuged for 15 minutes at  $17,135 \times g$  in a 4°C microcentrifuge (Labnet Prism™ R Refrigerated Microcentrifuge).

### **2.2.6.2 Bradford assay**

Protein concentrations were quantified using Thermo Scientific™ Pierce™ Coomassie (Bradford) Protein Assay Kit (Fisher Scientific). Bradford (1976) described this assay as a rapid and sensitive colourimetric method for protein quantitation. This technique is based on Coomassie G-250 dye reaction with basic and aromatic side chains of proteins leading to colour change from reddish/brown to blue. Bovine serum albumin (BSA) has been employed as a standard in concentrations from 125 to 2000 µg/ml. For this assay, 5 µl of standards and diluted protein samples were pipetted in duplicate into 96-well plate (Sarstedt), and 250 µl of Coomassie reagent was added and incubated 10 minutes. Subsequently, absorbance was measured at 595 nm using a microplate reader (Infinite F50, Tecan) and protein concentrations were calculated based on the standard curve.

### **2.2.6.3 Immunoblotting**

Equal concentrations of samples were prepared, and then 5 µl of Invitrogen™ NuPAGE™ LDS Sample Buffer (4X) and 2 µl of Invitrogen™ Novex™ NuPAGE™ Sample Reducing Agent (10X) (Fisher Scientific) were added and denatured by heating for 10 minutes in 70°C. To separate proteins, gel electrophoresis was conducted using Invitrogen™ NuPAGE™ 4 to 12%, Bis-Tris Mini Protein Gels (Fisher Scientific). Electrophoresis was carried in Invitrogen™ Mini Gel Tank (Fisher Scientific) using Invitrogen™ NuPAGE™ MES SDS Running Buffer and Invitrogen™ NuPAGE™ Antioxidant (Fisher Scientific) at a constant

voltage of 200 V and starting current of 160 mA for 35 minutes. Subsequently, proteins from the gel were transferred onto polyvinylidene fluoride (PVDF) membrane (Millipore) using Invitrogen™ NuPAGE® Transfer Buffer 1x (Fisher Scientific). The transfer was performed using the Invitrogen™ Mini Blot Module for Mini Gel Tank (Fisher Scientific) at a constant voltage of 20 V and starting current of 390 mA for 60 minutes. Then, membranes were washed for 5 minutes with Tris Buffered Saline with Tween 20 (TBST) (Santa Cruz Biotechnology). Afterwards, membranes were blocked for 60 minutes at room temperature using Odyssey® Blocking Buffer TBS (LI-COR Biosciences) diluted 1:1 with TBS. Then, membranes were washed three times with TBST for 5 minutes and incubated overnight with primary antibody at 4°C on rocking shaker (Table 2.2). The next day, membranes were washed again as described above and incubated in the dark with anti-rabbit Alexa Fluor 680 goat secondary antibody (Fisher Scientific) or anti-mouse Alexa Fluor 680 goat antibody (Abcam) (diluted 1:10000 in TBST) for 60 minutes at room temperature. After incubation membranes were washed, and proteins were detected using LI-COR 9120 Odyssey infrared system. Precision Plus Protein™ Dual Color Standards (Bio-Rad) were used to determine the molecular weight of detected bands. Later, the density of specific proteins was analyzed by Image J (National Institutes of Health, USA) and normalized to  $\beta$ -actin (Sigma-Aldrich). Densitometric analysis of antibody responses on Western blot was quantified based on software's conversion of protein bands to histograms which are proportional to protein density. Subsequently area under the histogram was quantified and normalized to area under the histogram of control band.

Antibodies	Supplier	Product no.	Dilution	Antibody Type
<b>Anti-actin (20-33)</b>	Sigma-Aldrich	A5060	1:1000	Rabbit polyclonal
<b>Anti-Human ER<math>\beta</math> (MC10)</b>	eBioscience	14-9336-80	1:1000	Mouse monoclonal
<b>ER<math>\alpha</math> (D12)</b>	Santa Cruz Biotechnology	8005	1:500	Mouse monoclonal
<b>ER<math>\beta</math> (1531)</b>	Santa Cruz Biotechnology	53494	1:500	Mouse monoclonal
<b>COX-2</b>	Abcam	15191	1:1000	Rabbit polyclonal
<b>iNOS (D6B65S)</b>	Cell Signalling Technology	13120S	1:1000	Rabbit monoclonal
<b>Phospho-p44/42 MAPK (ERK1/2) (Thr202/Tyr204)</b>	Cell Signalling Technology	4370	1:1000	Rabbit monoclonal
<b>Phospho-SAPK/JNK (Thr183/Tyr185) (81E11)</b>	Cell Signalling Technology	4668	1:1000	Rabbit monoclonal
<b>Total p44/42 MAPK (ERK1/2) (137F5)</b>	Cell Signalling Technology	4695	1:1000	Rabbit monoclonal
<b>Total SAPK/JNK</b>	Cell Signalling Technology	9252	1:1000	Rabbit polyclonal
<b>Phospho-NF-<math>\kappa</math>B p65 (S536) (93H1)</b>	Cell Signalling Technology	3033S	1:1000	Rabbit monoclonal
<b>p38<math>\alpha</math> (C-20)</b>	Santa Cruz Biotechnology	535	1:500	Rabbit polyclonal
<b>Phospho-p38 MAPK (T180/Y182)</b>	Cell Signalling Technology	9215S	1:1000	Rabbit monoclonal

**Table 2.1 The list of primary antibodies used in immunoblotting experiments.**

### 2.2.7 DPPH assay

DPPH assay evaluates the antioxidant potential of compounds. This method was first described more than a half-century ago by Blois in 1958. This technique assesses free radical scavenging properties of antioxidants on stable free radical DPPH. DPPH is reduced by accepting hydrogen atom from antioxidants which cause a colour change from violet to yellow, allowing colourimetric detection of the antioxidant activity (Kedare & Singh, 2011).

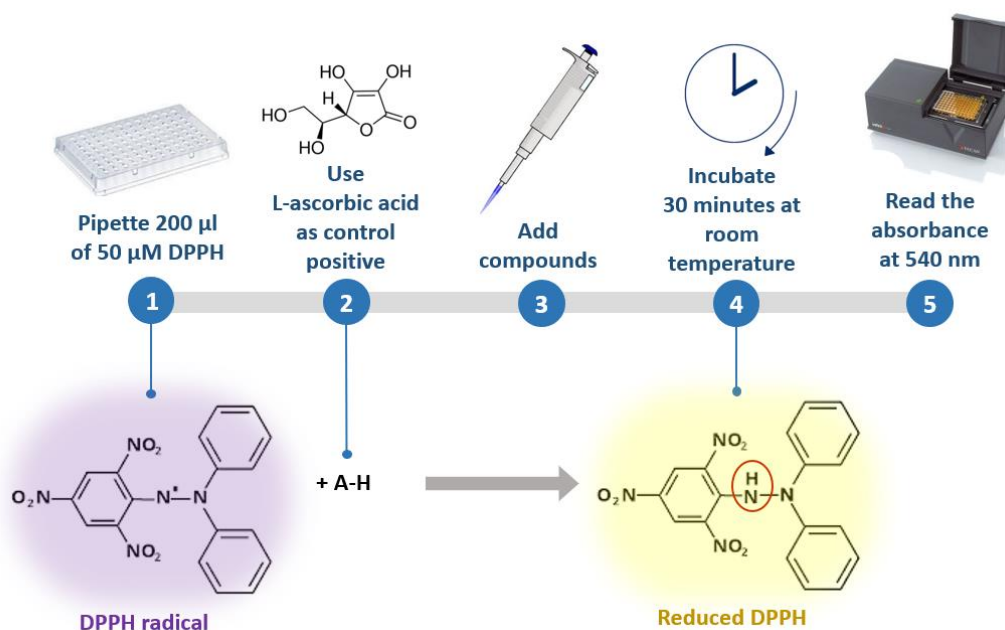


Figure 2.10 Flowchart of DPPH assay and chemical reduction of DPPH radical.

2,2-Diphenyl-1-picrylhydrazyl (DPPH) by Alfa Aesar™ (Fisher Scientific) was prepared in methanol to final concentration 50 µM. Then 200 µl of DPPH solution was added into 96-well plate. Next, different concentrations (1.25 – 40 µM) of L-(+)-Ascorbic acid by Alfa Aesar™ (Fisher Scientific) were pipetted into the DPPH solution to serve as an antioxidant standard. Afterwards, compounds 1 and 2 (at final concentrations 5 – 20 µM) were added into DPPH solution. Then, the plate was incubated in the dark at room temperature for 30 minutes, and absorbance was measured at 540 nm using a microplate reader (Infinite F50, Tecan). DPPH scavenging effect (% inhibition) was calculated using the below formula.

$$\text{DPPH scavenging effect (\% inhibition)} = \frac{(A_0 - A_1)}{A_0} * 100$$

Where:

A1 indicates the absorbance of the sample

A0 indicates the absorbance of the control (methanol solution of DPPH)

## 2.2.8 PGE<sub>2</sub> enzyme immunoassay

Enzyme immunoassay (EIA) like ELISA relies on antigen-antibody specificity to detect and quantify protein of interest. EIA uses enzyme-conjugated antibodies which bind to the protein of interest, allowing to the enzymatic conversion of substrate into an observable end-product.

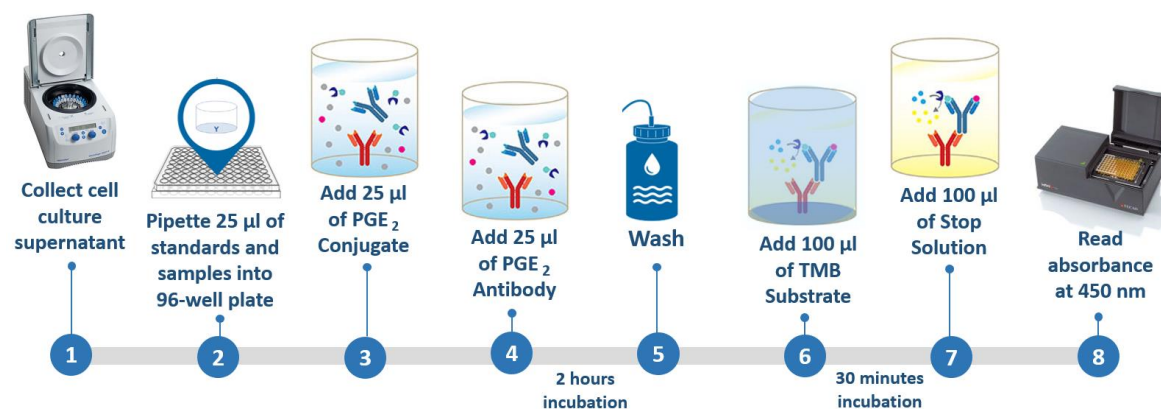


Figure 2.11 Flowchart of PGE<sub>2</sub> Enzyme Immunoassay.

PGE<sub>2</sub> was detected using PGE<sub>2</sub> Multi-Format EIA Kit (Arbor Assays). Before the experiment, BV2 microglia were seeded in 24-well plates at a density of  $5 \times 10^4$  cells/ml in 1 ml of culture medium then treated and stimulated as described in [2.2.2](#). After 24 hours of incubation, cell culture supernatants were collected by centrifugation at  $806 \times g$  for 5 minutes. Next 25 µl of standards and samples were pipetted into 96-well plate already pre-coated and provided by the manufacturer. This was followed by pipetting 25 µl of DetectX<sup>®</sup> Prostaglandin E<sub>2</sub> Conjugate and 25 µl of the DetectX<sup>®</sup> Prostaglandin E<sub>2</sub> Antibody, except blank. Subsequently, the plate was sealed and incubated 2 hours at room temperature, shaking 200 rpm. After incubation content of the plate was discarded, and wells were washed four times with 300 µl of Wash Buffer. Then 100 µl of the TMB substrate was added into each well, and the plate was incubated 30 minutes at room temperature without shaking. At the end of incubation reaction of the substrate with the bound PGE<sub>2</sub>-peroxidase conjugate was stopped by adding 100 µl of the Stop Solution. Afterwards, absorbance was measured at 450 nm using a microplate reader (Infinite F50, Tecan) and PGE<sub>2</sub> concentrations were calculated based on standards (3.906-1000 pg/ml).

## 2.2.9 Immunofluorescence

Immunofluorescence technique relies on the specificity of antibodies for their antigens in order to mark specific targets within a cell with fluorescent dyes. This allows visualizing distribution and quantity of marked biomolecule within the cell.

For immunofluorescence staining, BV2 cells were seeded in 8-well cell culture chambers (Sarstedt) at a density of  $5 \times 10^4$  cells/ml in 500  $\mu$ l of culture medium. Then cells were and treated and stimulated as indicated in [2.2.2](#). After 60 minutes of incubation with (LPS 100 ng/ml) cells were washed with 200  $\mu$ l of Dulbecco's Phosphate-Buffered Saline (DPBS; Thermo Scientific) and fixed with 100  $\mu$ l of 100% ice-cold methanol for 10 minutes in  $-20^\circ\text{C}$ . This was followed by DPBS wash and blocking of non-specific binding sites with 200  $\mu$ l of 5% Bovine Serum Albumins (BSA; Sigma-Aldrich) and 10% of Horse Serum (Santa Cruz) dissolved in DPBS. Following 60 minutes incubation at room temperature, cells were incubated overnight at  $4^\circ\text{C}$  with 200  $\mu$ l of NF- $\kappa$ B p65 primary antibody (C-20; Santa Cruz) diluted in blocking solution to 1:100. The next day, cells were washed with DPBS and incubated for 2 hours in the dark with 200  $\mu$ l of Alexa Fluor<sup>®</sup> 488-conjugated donkey anti-rabbit IgG (Thermo Scientific) secondary antibody diluted 1:500. Thereafter, cells were washed with DPBS and stained with 200  $\mu$ l of 50 nM of 4', 6 diamidino-2-phenylindole dihydrochloride (DAPI; Invitrogen) for 2 - 5 minutes. Subsequently, cells were washed, and images were captured using EVOS<sup>®</sup> FLoid<sup>®</sup> Cell Imaging Station and then processed using ImageJ software.

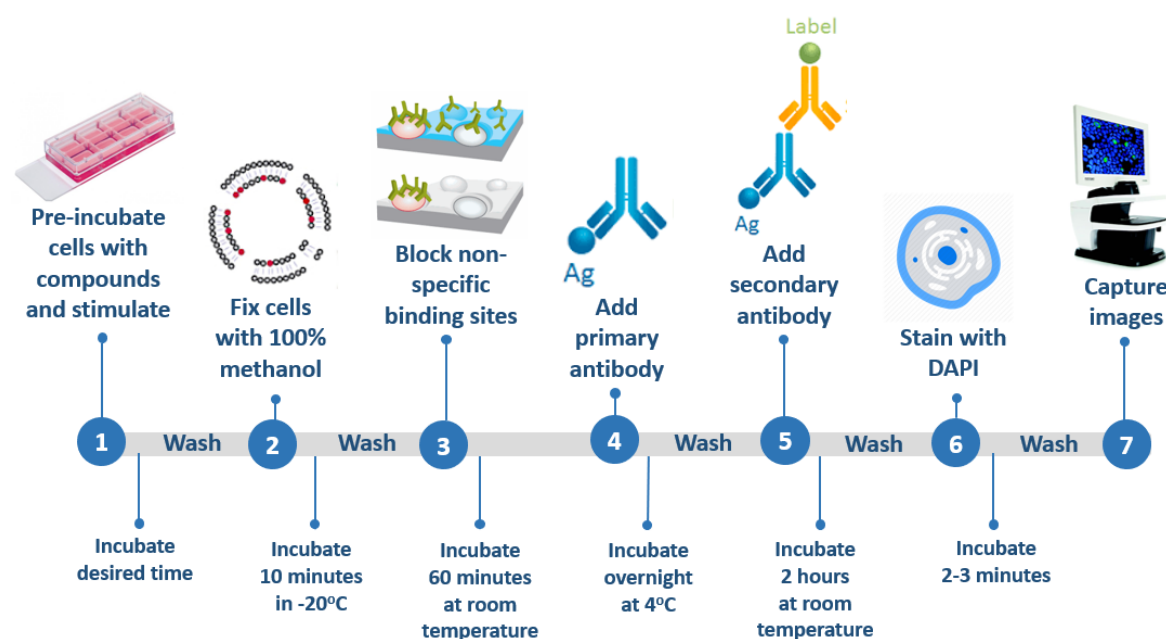


Figure 2.12 Flowchart of immunofluorescence experiment.



### 2.2.10 InstantOne™ ELISA for p-NF-κB and p-p38

The InstantOne™ ELISA combines the specificity of sandwich ELISA with next generation ready to use pre-coated ELISA kits which require only one incubation step. In this assay antibody/analyte sandwich complex formation is obtained during one incubation for the rapid detection of desired proteins. Level of p-NF-κB and p-p38 were investigated using Invitrogen™ NF-κB p65 (Phospho) [pS536] Human InstantOne™ ELISA Kit and p38 MAPK (Phospho) [pT180/pY182] Multispecies InstantOne™ ELISA Kit (Fisher Scientific).

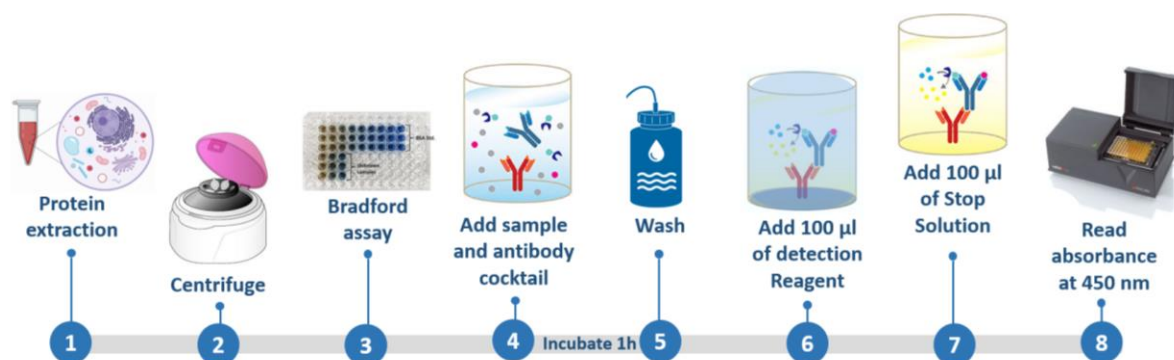


Figure 2.13 Flowchart of InstantOne ELISA.

For InstantOne ELISA, BV2 cells were seeded in 6-well plates for adherent cells at a density of  $5 \times 10^4$  cells/ml in 2 ml of culture medium. At approximately 80% confluence, cells were treated and stimulated as described in [2.2.2](#). This was followed by 60 minutes incubation in 37°C and collection of whole-cell lysates as indicated in [2.2.6.1](#). Next, to ensure equal loading of protein extract into the ELISA plate, Bradford assay was conducted as described in [2.2.6.2](#). Before the experiment, pre-coated wells of 96-well plate provided by the manufacturer were washed twice with sterile water to remove preservatives. Subsequently, InstantOne ELISA Microplate Wells were loaded with 50 µg of sample lysate and 50 µl of Antibody Cocktail (Capture Antibody Reagent and Detection Antibody Reagent in 1:1 ratio) and incubated for 1 hour on a microplate shaker at room temperature. After incubation, wells were washed three times with 200 µl/well of Wash Buffer (1X). Then, 100 µl of the Detection Reagent was added to each of the assay's wells and incubated for a further 20 minutes. In the next step, the reaction was stopped by adding 100 µl/well of Stop Solution and absorbance was measured at 450 nm using a microplate reader (Infinite F50, Tecan) which was directly proportional to the concentration of protein of interest.

### **2.2.11 Reporter gene assay**

Reporter gene assays are widely used to study promoters of the gene of interest, such as regulation of its expression. Reporter assays consist of a regulatory element of interest cloned into a vector with the reporter gene. Reporter gene encodes for proteins, which activity can be easily detected and quantified using luminescence, e.g., luciferase.

This study employed dual-luciferase format, where transcription factor activity was assessed using firefly luciferase and normalized to reporter gene constitutively expressing *Renilla* luciferase. BV2 cells are difficult to transfect; hence, instead of chemical transfection, magnetofection has been used. Smolders et al., (2018) described this method as highly efficient and superior to other transfection systems in microglia. This technique exploits magnetic force to concentrate magnetic nanoparticles / DNA complexes into the target cells. Glial-Mag transfection reagents and magnetic plate were purchased from OZ Biosciences.

#### **2.2.11.1 Optimisation of magnetofection**

In order to optimize magnetofection method Monster Green Fluorescent Protein Vector (Qiagen) has been used to control transfection efficiency. Firstly, the optimal volume of Glial-Mag was assessed, where a fixed amount of DNA and various amounts of Glial-Mag were introduced to cells. For optimisation of magnetofection BV2 cells were seeded in 24-well plate (Sarstedt) at a density of  $4 \times 10^4$  cells/ml in 1 ml of culture medium and incubated until approximately 60% confluent. Then cell's medium was changed to Opti-MEM (450  $\mu$ l), and cells were incubated 2 hours at 37°C. After incubation four microcentrifuge tubes containing Glial-Mag / DNA at ratio 2:1, 3:1, 3.5:1 and 4:1 were prepared. Subsequently, microcentrifuge tubes were incubated 25 minutes at room temperature to allow the formation of DNA / magnetic nanoparticles complexes. After incubation 50  $\mu$ l of DNA solution and 5  $\mu$ l of Glial-Boost was added dropwise to cells, and this was followed by 30 minutes incubation on a magnetic plate. Two hours after transfection 500  $\mu$ l of Opti-MEM medium was added to each well, and cells were further incubated 24 hours. After incubation immunofluorescent images were captured using EVOS® FLoid® Cell Imaging Station and then processed using ImageJ software. Then, BV2 cells were harvested using 200  $\mu$ l of TrypLE Express (Fisher Scientific), and magnetofection efficiency was also monitored by flow cytometry analysis of GFP using Guava® easyCyte 5 Benchtop Flow Cytometer. Immunofluorescence and flow cytometry data demonstrated the highest transfection rate of Glial-Mag / DNA at ratio 3:1 (Figure 2.14). This was followed by optimisation of DNA

amount using a constant volume of Glial-Mag 0.6  $\mu$ l/well and different amounts of DNA 0.2  $\mu$ g/well and 0.4  $\mu$ g/well. BV2 cells were prepared as described above. Glial-Mag/DNA mixture was prepared in microcentrifuge tubes at ratio 3:1 and 3:2 and incubated for 25 minutes at room temperature. Then, 50  $\mu$ l of Glial-Mag/DNA complexes were added to the cells, followed by the addition of 5  $\mu$ l of Glial-Boost into each well. Afterwards, cells were incubated 30 minutes on the magnetic plate and then, 2 hours without the magnetic plate. After 2 hours elapsed medium was changed to Opti-MEM medium for two wells, and 500  $\mu$ l of Opti-MEM medium was added to another two wells to determine if that will affect transfection efficiency. Subsequently, cells were incubated for 24 hours and GFP expression was measured using immunofluorescence (EVOS<sup>®</sup> FLoid<sup>®</sup> Cell Imaging Station) and flow cytometry (Guava<sup>®</sup> easyCyte 5 Benchtop Flow Cytometer). Results indicated that optimal Glial-Mag/DNA ratio for BV2 magnetofection is 3:1 and medium change 2 hours after incubation on magnetic plate reduced transfection efficiency, suggesting that instead of medium change, 500  $\mu$ l of the medium should be added to cells (Figure 2.15).

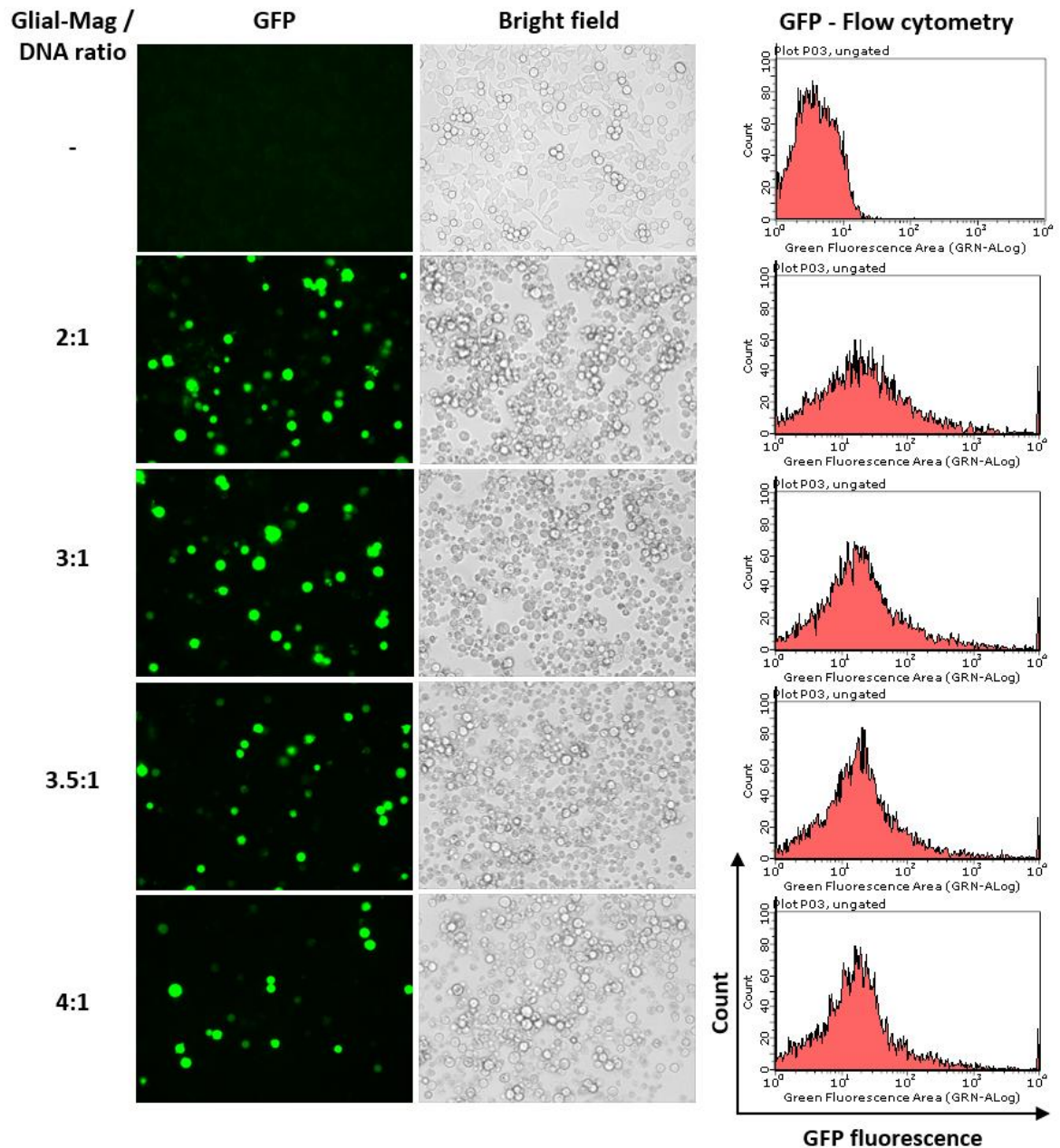


**Figure 2.14 Magnetofection efficiency using different transfection reagent concentrations.** BV2 cells have been transfected with GFP vector using Glial-Mag in various ratios and then incubated for 24 hours. Immunofluorescent images show GFP expression. Immunofluorescent images were captured using the EVOS<sup>®</sup> FLoid<sup>®</sup> Cell Imaging Station and then processed using ImageJ software. Additionally, GFP expression was also monitored using flow cytometry. Flow cytometry plots represent GFP fluorescence in log scale vs count. The highest expression of GFP was obtained with 3:1 Glial-Mag to DNA ratio.

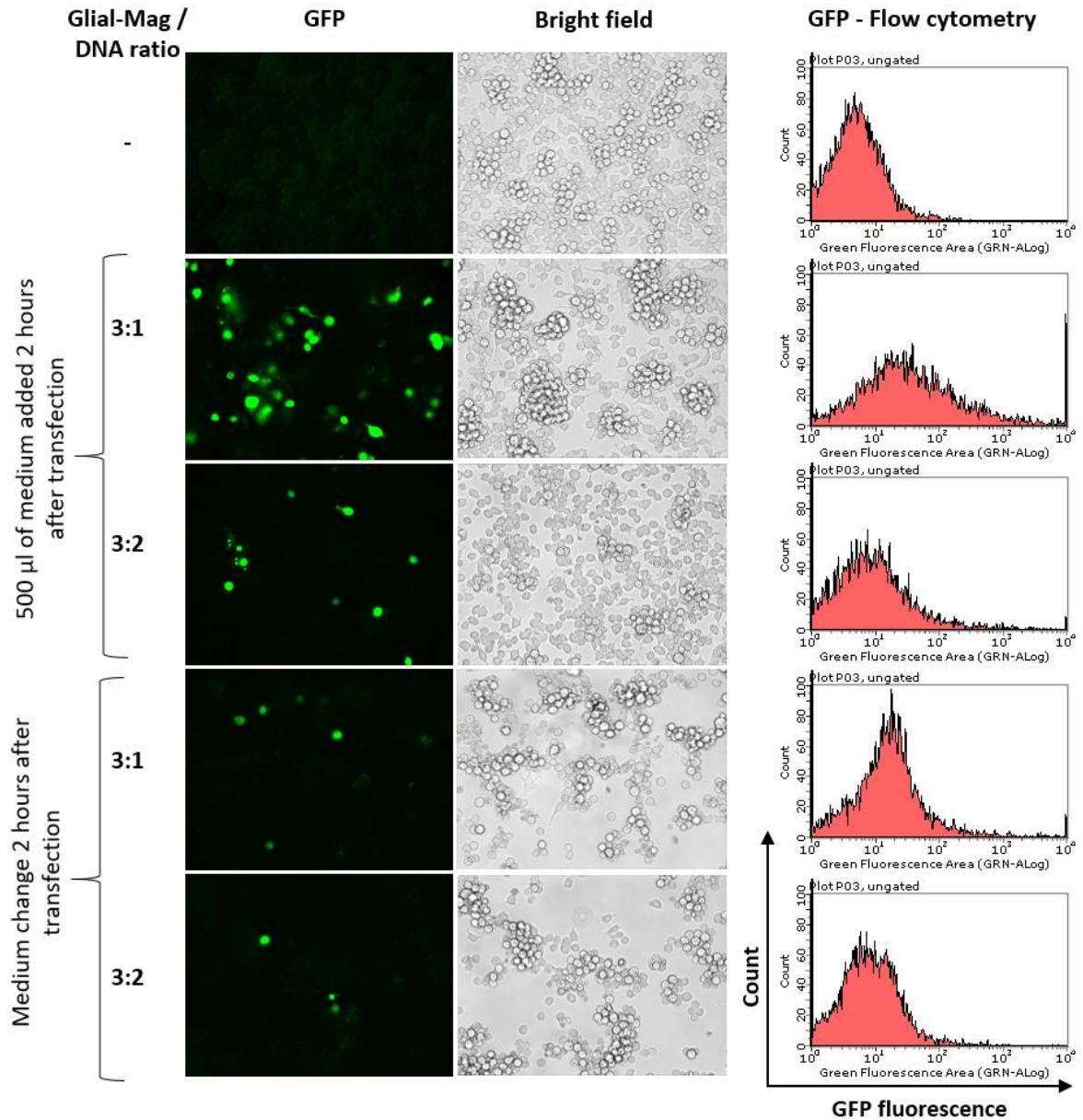


**Figure 2.15 Magnetofection efficiency using different amounts of DNA.** BV2 cells have been transfected with varying amounts of GFP vector using a constant volume of Glial-Mag and then incubated for 24 hours. Immunofluorescent images show GFP expression. Immunofluorescent images were captured using the EVOS® FLoid® Cell Imaging Station and then processed using ImageJ software. Additionally, GFP expression was also monitored using flow cytometry. Flow cytometry plots represent GFP fluorescence in log scale vs count. The highest expression of GFP was obtained with 3:1 Glial-Mag to DNA ratio.

### 2.2.11.2 NF- $\kappa$ B and ERE reporter gene assay

BV2 cells were seeded in 24-well plate (Sarstedt) at density  $4 \times 10^4$  cells/ml in 1 ml of culture medium and incubated until approximately 60% confluent. Then cell's medium was changed to Opti-MEM (450  $\mu$ l), and cells were incubated 2 hours at 37°C. After incubation, Glial-Mag/DNA complexes were prepared at ratio 3:1 in 50  $\mu$ l Opti-MEM medium (Gibco™) using Glial-Mag (OZ Biosciences) and Cignal NF- $\kappa$ B Reporter Assay Kit (LUC; CCS-013L) or Cignal ERE Reporter Assay Kit (LUC; CCS-005L) by Qiagen. Prepared Glial-Mag/DNA complexes were incubated for 25 minutes at room temperature, and then they were added dropwise to the cells. This was followed by the addition of 5  $\mu$ l of Glial-Boost to each well. Then cells were placed on a magnetic plate for 30 minutes and incubated 2 hours without a plate in 37°C. After incubation 500  $\mu$ l of Opti-MEM medium was added to each well, and cells were further incubated for 24 hours. Then the medium was changed to serum-free RPMI, and cells were treated with compounds only for ERE reporter gene assay and with compounds followed by LPS (100 ng/ml) stimulation for NF- $\kappa$ B reporter gene assay. For ERE reporter gene assay BV2 cells were incubated with compounds for 24 hours, and for NF- $\kappa$ B reporter gene assay cells were incubated for 8 hours after LPS activation. After the appropriate incubation time, the Dual-Glo® Luciferase Assay System (Promega) was performed. This assay enables to quantify luminescent signal from firefly and *Renilla* luciferase. Firefly and *Renilla* luciferase are generated by transcriptional activation of genetic elements to fully functional enzymes. The activity of experimental reporter is measured as firefly luminescence which is activated by firefly luciferase is the presence of beetle luciferin, ATP, magnesium and molecular oxygen. In turn, the activity of control reporter is proportional to *Renilla* luminescence which is created by mono-oxygenation of coelenterazine catalysed by *Renilla* luciferase in the presence of molecular oxygen (Figure 2.15). Before commencing the assay 925  $\mu$ l of cell culture medium was removed from each well, then 75  $\mu$ l of Dual-Glo® Luciferase Reagent was added, and the plate was exposed to shaking 100 rpm for 15 minutes at room temperature. After shaking liquid containing lysed cells was transferred into a white 96-well plate, and firefly luminescence was measured in a luminometer (FLUOstar OPTIMA Plate Reader by BMG Labtech). Afterwards, Dual-Glo® Stop & Glo® reagent was prepared by diluting the Dual-Glo® Stop & Glo® Substrate 1:100 into Dual-Glo® Stop & Glo® Buffer, and 75  $\mu$ l of this reagent was added into each well. Then, the plate was incubated for a further 10 minutes at room temperature, and *Renilla*

luminescence was measured using the same plate reader as above. Experimental reporter values were normalized to control reporter to obtain optimal and consistent results.

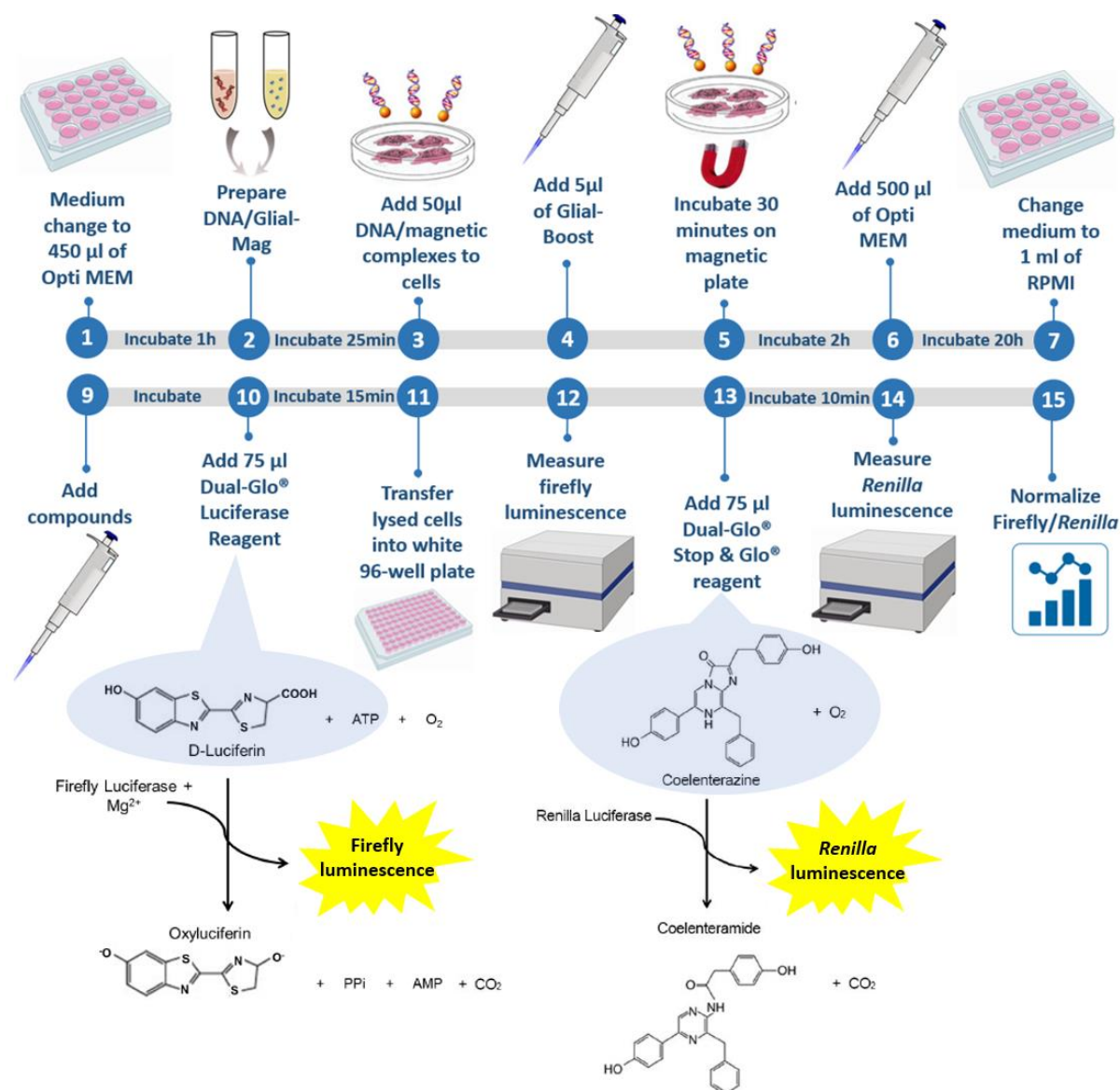


Figure 2.16 Flowchart of reporter gene assay and bioluminescent reactions catalysed by firefly and *Renilla* luciferases.

### 2.2.12 Statistical analysis

Data were analysed using one-way analysis of variance (ANOVA) or two-way ANOVA with post hoc Student-Newman-Keuls test (with multiple comparisons) and are expressed as mean  $\pm$  SEM of at least three independent samples and experiments repetitions (N=3) unless otherwise stated. As statistically significant considered are values \* $p < 0.033$ , \*\* $p < 0.002$ , \*\*\* $p < 0.001$  compared with untreated control or LPS-stimulated control. Statistical analysis was executed using Graph Pad Prism software version 8.

## 2.3 Results

### 2.3.1 The effect of compounds 1 and 2 on the viability of BV2 cells using XTT

Viability of BV2 cells was measured 24 hours after pre-incubation with compounds 1 and 2 in order to confirm that reduced production of pro-inflammatory mediators was not caused by decreased cell viability but by pharmacological actions of compounds. Results show that pre-incubation with compounds 1 and 2 at 5, 10, 15 and 20  $\mu\text{M}$  did not affect the viability of BV2 microglial cells (Figure 2.17). There was no significant difference in the viability of BV2 cells between control untreated and compounds 1 and 2 pre-incubated BV2 cells.

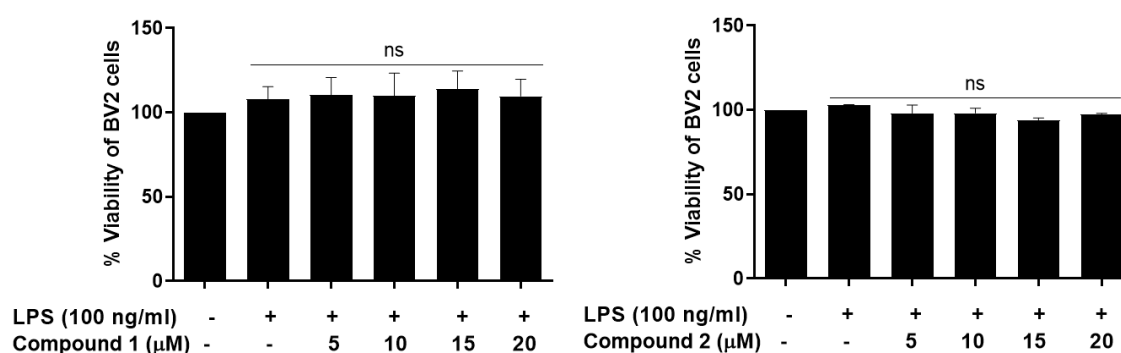


**Figure 2.17 The effect of compounds 1 and 2 on the viability of BV2 using XTT.** BV2 cells were incubated with or without compounds 1 and 2 (5 - 20  $\mu\text{M}$ ) for 30 minutes and then activated with LPS (100 ng/ml). Subsequently, BV2 cells were incubated for 24 hours, and XTT assay was performed. Compounds 1 and 2 (5-20  $\mu\text{M}$ ) did not affect the viability of BV2 microglia. All values are expressed as mean  $\pm$  SEM for N=3. Data were analysed using one-way ANOVA for multiple comparisons with post hoc Student Newman-Keuls test. \* $p < 0.033$  in comparison to untreated control.



### **2.3.2 The effects of compounds 1 and 2 on the production of TNF $\alpha$ , IL-6, and IL-1 $\beta$ in LPS-activated BV2 microglia**

The neuroinflammatory process is accompanied by the microglial production of various pro-inflammatory cytokines. Hence, the cytokines level serves as a biomarker for neuroinflammation and shows the effectiveness of potential treatment. To establish anti-inflammatory properties of compounds 1 and 2, the levels of TNF $\alpha$ , IL-6, and IL-1 $\beta$  were measured after pre-incubation of BV2 cells with different concentrations of compounds followed by 24 hours LPS (100 ng/ml) activation.

Untreated cells produced low amounts of pro-inflammatory cytokines (TNF $\alpha$ , IL-6, and IL-1 $\beta$ ), which were significantly ( $p < 0.001$ ) increased by LPS stimulation. Compound 1 at 15 and 20  $\mu\text{M}$  significantly ( $p < 0.033$ ) inhibited TNF $\alpha$  expression to  $67 \pm 12\%$  and  $65 \pm 4\%$ , respectively when compared to LPS control value of 100% (Figure 2.18 A). Whereas at a concentration of 5 and 10  $\mu\text{M}$  of compound 1, TNF $\alpha$  production was not significantly reduced to  $81 \pm 2\%$  and  $77 \pm 9\%$ , respectively, compared to LPS control value of 100%. Compound 1 at 10, 15 and 20  $\mu\text{M}$  significantly ( $p < 0.033$ ) reduced the level of IL-6 to  $64 \pm 5\%$ ,  $61 \pm 7\%$ , and  $69 \pm 10\%$ , respectively, compared to LPS control value of 100%. However, compound 1 at 5  $\mu\text{M}$  did not induce a significant decrease in the level of IL-6 production when compared to LPS control – 100% (Figure 2.18 B). The production of IL-1 $\beta$  was significantly reduced by compound 1 at 10, 15 and 20  $\mu\text{M}$  to  $79 \pm 6\%$ ,  $71 \pm 5\%$ , and  $70 \pm 3\%$ , respectively, compared to LPS control value of 100% (Figure 2.18 C).

Compound 2 significantly ( $p < 0.033$ ) decreased the TNF $\alpha$  production only at the highest tested concentration - 20  $\mu\text{M}$  to  $77 \pm 4\%$  compared to LPS control of 100% (Figure 2.18 D). However, at 5, 10 and 15  $\mu\text{M}$ , the inhibitory effect of compound 2 on TNF $\alpha$  production was not significant. Compound 2 at 15 and 20  $\mu\text{M}$  significantly ( $p < 0.033$ ) inhibited IL-6 release to  $52 \pm 11\%$  and  $61 \pm 11\%$ , respectively, compared to LPS control value of 100% (Figure 2.18 E). Compound 2 significantly ( $p < 0.001$ ) suppressed production of IL-1 $\beta$  to  $70 \pm 3\%$ ,  $48 \pm 5\%$ ,  $53 \pm 2\%$  and  $49 \pm 3\%$  from control value of 100% when used at 5, 10, 15 and 20  $\mu\text{M}$ , respectively (Figure 2.18 F).

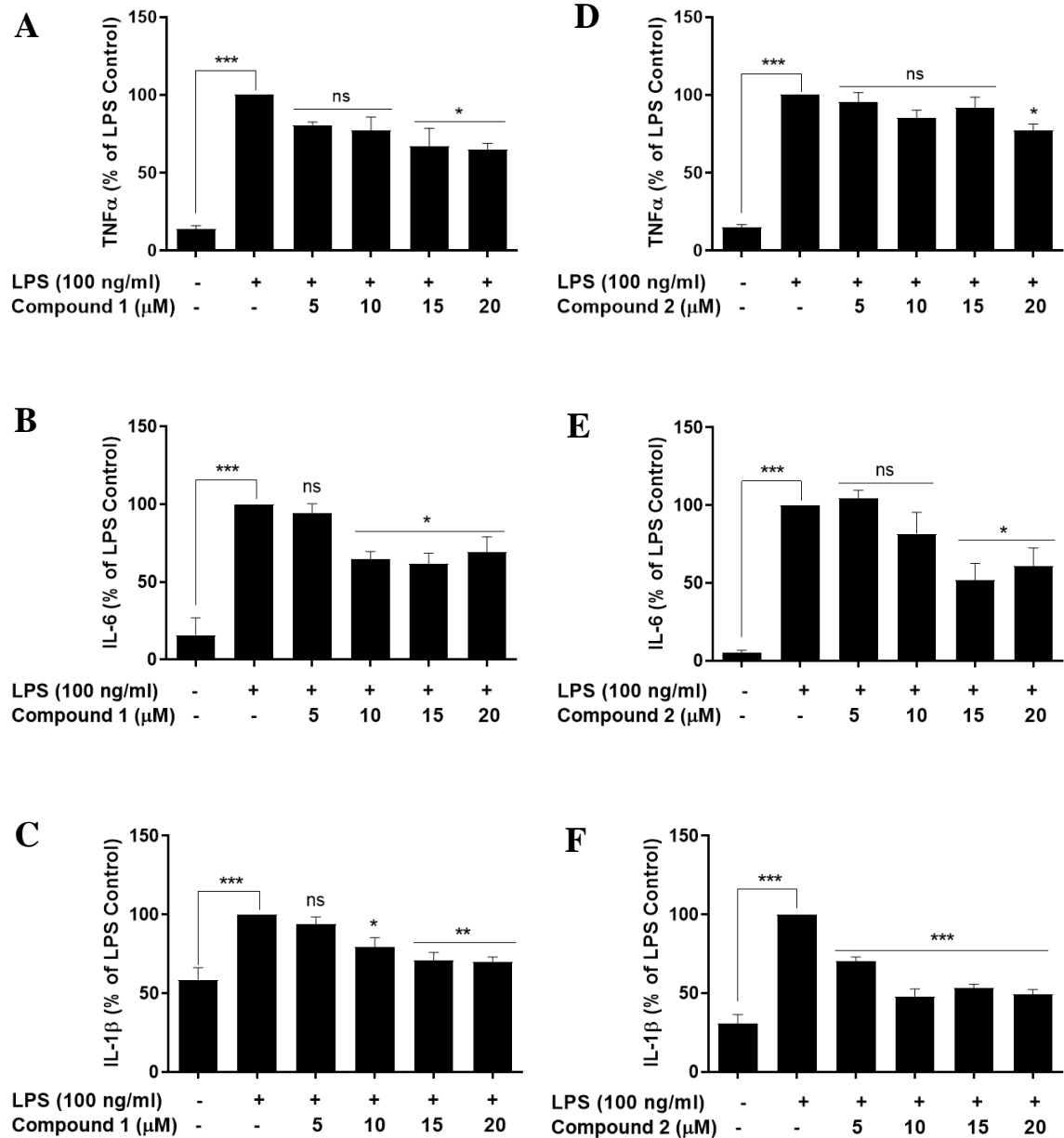


**Figure 2.18** The effects of compounds 1 and 2 on the production of TNF $\alpha$ , IL-6 and IL-1 $\beta$  in LPS-activated BV2 cells. BV2 were pre-incubated for 30 minutes with compounds 1 and 2 (5 – 20  $\mu$ M) and then activated with LPS (100 ng/ml) for 24h. After incubation, supernatants were collected, and ELISAs were performed. Compound 1 significantly inhibited TNF $\alpha$  expression at 15  $\mu$ M and 20  $\mu$ M, whereas compound 2 only at 20  $\mu$ M, when compared to LPS control. IL-6 production was significantly decreased by compound 1 at 10, 15 and 20  $\mu$ M and by compound 2 at 15 and 20  $\mu$ M, when compared to LPS control. IL-1 $\beta$  release in LPS activated microglia was significantly blocked by compound 1 (except the lowest concentration – 5  $\mu$ M) and by compound 2 when compared to LPS control. All values are expressed as a mean  $\pm$  SEM for N=3. Data were analysed using one-way ANOVA for multiple comparisons with post hoc Student Newman-Keuls test. \* $p$ <0.033, \*\* $p$ <0.002, \*\*\* $p$ <0.001 in comparison with LPS control.

### **2.3.3 The effects of compounds 1 and 2 on iNOS and nitrite expression in LPS-activated BV2 cells**

Nitric oxide (NO) is a free radical largely involved in inflammation and neurodegeneration. NO is non-stable hence to determine its level Griess Reagent System was employed to measure nitrite (NO<sub>2</sub><sup>-</sup>) which is stable biodegradation product of NO. Inducible nitric oxide synthase enzyme catalyses NO production from L-arginine (Tripathi, Tripathi, Kashyap, & Singh, 2007).

BV2 cells were stimulated with 100 ng/ml of LPS in the presence and absence of compounds 1 and 2 for 24 hours. After incubation, Griess assay and iNOS Western blot were performed. Untreated samples contained low physiological amounts of nitrite and lack of iNOS protein, which were significantly ( $p < 0.001$ ) upregulated after 24-hour LPS stimulation.

Compound 1 at 5, 10, 15 and 20  $\mu\text{M}$  in a concentration-dependent manner significantly ( $p < 0.002$  and  $p < 0.001$ ) decreased the level of nitrite from control value of 100% to  $74 \pm 4\%$ ,  $64 \pm 5\%$ ,  $53 \pm 8\%$ , and  $39 \pm 5\%$ , respectively (Figure 2.19 A). Compound 1 at 5, 10, 15 and 20  $\mu\text{M}$  in a concentration-dependent manner significantly ( $p < 0.001$ ) reduced iNOS protein level to  $42 \pm 15\%$ ,  $35 \pm 12\%$ ,  $18 \pm 9\%$  and  $6 \pm 1\%$ , respectively, compared to LPS control value of 100% (Figure 2.19 B).

Compound 2 at 5, 10, 15 and 20  $\mu\text{M}$  significantly ( $p < 0.001$ ) decreased the level of nitrite from control value of 100% to  $83 \pm 3\%$ ,  $75 \pm 3\%$ ,  $74 \pm 1\%$ , and  $63 \pm 4\%$ , respectively (Figure 2.19 C). Compound 2 at 5, 10, 15 and 20  $\mu\text{M}$  also significantly ( $p < 0.002$ ) reduced iNOS protein level to  $83 \pm 3\%$ ,  $75 \pm 3\%$ ,  $74 \pm 1\%$  and  $63 \pm 4\%$ , respectively, compared to LPS control value of 100% (Figure 2.19 D).

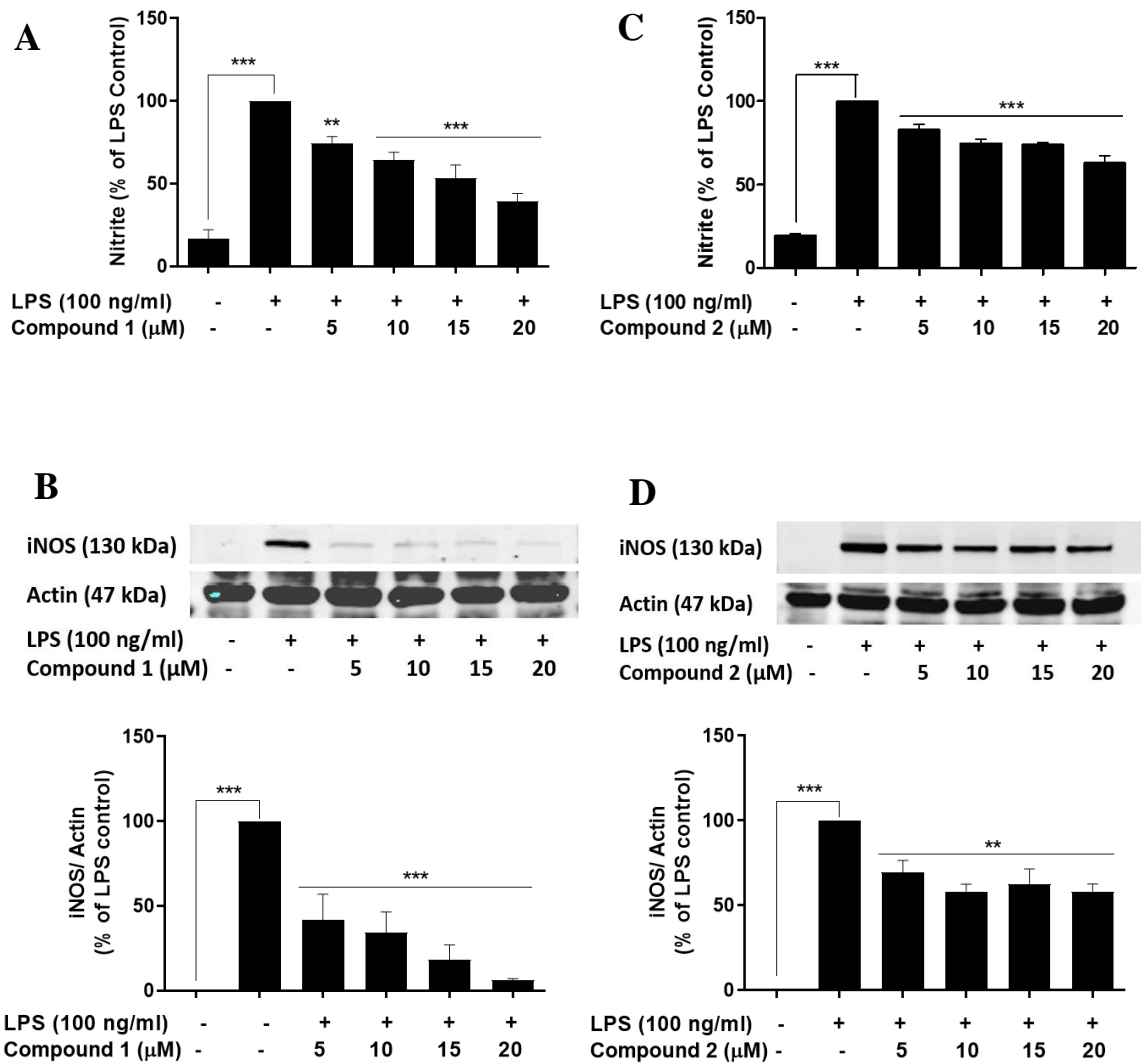


**Figure 2.19** The effects of compounds 1 and 2 on nitrite and iNOS production in LPS activated BV2 cells. Cells were treated with compounds 1 and 2 for 30 minutes and then stimulated with LPS (100 ng/ml) for 24 hours. After incubation medium supernatants and cell lysates were collected and Griess assay and immunoblotting were performed. Compound 1 (A) and compound 2 (B) significantly in concentration-dependent manner reduced level of nitrite. Compound 1 (C) and 2 (D) significantly inhibited expression of iNOS. Actin has been used as a loading control. All values are expressed as a mean  $\pm$  SEM for N=3. Data were analysed using one-way ANOVA for multiple comparisons with post hoc Student Newman-Keuls test. \*\* $p < 0.002$ , \*\*\* $p < 0.001$  in comparison with LPS control.

### 2.3.4 Evaluation of the free-radical scavenging properties of compounds 1 and 2

Free radicals are both result and cause of inflammation. Reduction of free radicals alleviates protein, lipids and DNA destruction, which in turn reduce inflammation. It has been shown that isoflavones act as antioxidants through the mechanisms which include direct and indirect antioxidant systems (Pallauf, Duckstein, Hasler, Klotz, & Rimbach, 2017; Rimbach et al., 2003). DPPH assay has been employed to examine free radical scavenging properties of compound 1 and 2. Neither compounds 1 nor 2 did scavenge DPPH free radical at any of the tested concentrations (Figure 2.20).

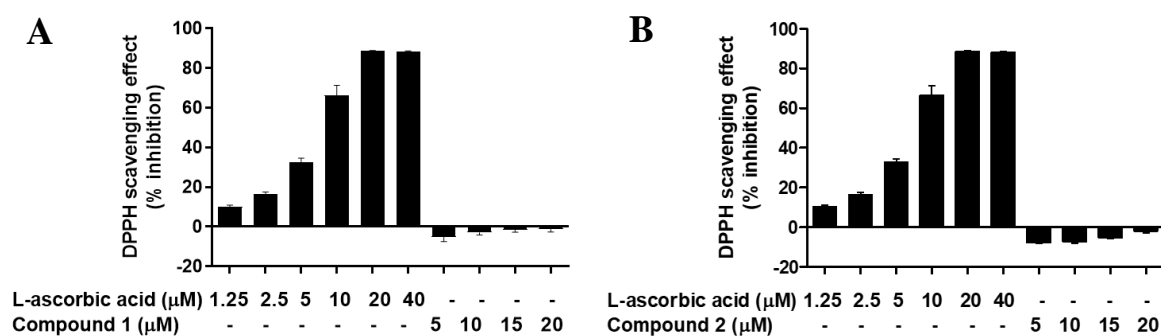


**Figure 2.20** DPPH scavenging effect of compounds 1 and 2. Different concentrations (5 – 20 μM) of compounds 1 and 2 were added to 50 μM of DPPH and incubated for 30 minutes. L-(+)-Ascorbic acid (1.25 – 40 μM) was used as control positive. Compounds 1 and 2 do not possess free radical scavenging properties. DPPH scavenging effect (% inhibition) was calculated using formula:  $\text{DPPH scavenging effect (\% inhibition)} = \frac{(A_0 - A_1)}{A_0} \times 100$ . Where: A1 indicates the absorbance of the sample and A0 indicates the absorbance of the control (methanol solution of DPPH). All values are expressed as a mean  $\pm$  SEM for N=3.

### 2.3.5 The effects of compounds 1 and 2 on PGE<sub>2</sub> production and COX-2 expression in LPS-activated BV2 cells

Prostaglandin-endoperoxide synthase, also known as cyclooxygenase (COX-2) is an enzyme responsible for the production of prostaglandins such as PGE<sub>2</sub> from arachidonic acid. Therefore, COX-2 is a key inflammatory enzyme which inhibition has been shown to reduce inflammation. To determine if compounds 1 and 2 can reduce COX-2 production, Western blot analysis was carried out. BV2 cells were incubated with or without compound 1 and 2 (5 – 20 μM) for 30 minutes and then activated by LPS (100 ng/ml). After 24 hours incubation, medium supernatants and cell lysates were collected, and PGE<sub>2</sub> ELISA and Western blot for COX-2 were performed.

Untreated BV2 cells contained a low amount of PGE<sub>2</sub> and COX-2, whereas LPS-activated BV2 cells upregulated approximately 3.4-fold PGE<sub>2</sub> and approximately 1.9-fold COX-2 production. Pre-treatment with compound 1 did not significantly decrease the production of

PGE<sub>2</sub> at any of the tested concentrations when compared to LPS control (Figure 2.21 A). Similarly, compound 1 also did not significantly inhibit the COX-2 protein level compared to LPS control (Figure 2.21 B).

Pre-treatment with compound 2 did not significantly reduce the LPS-induced PGE<sub>2</sub> and COX-2 level in LPS-stimulated BV2 cells (Figure 2.21 C and D).

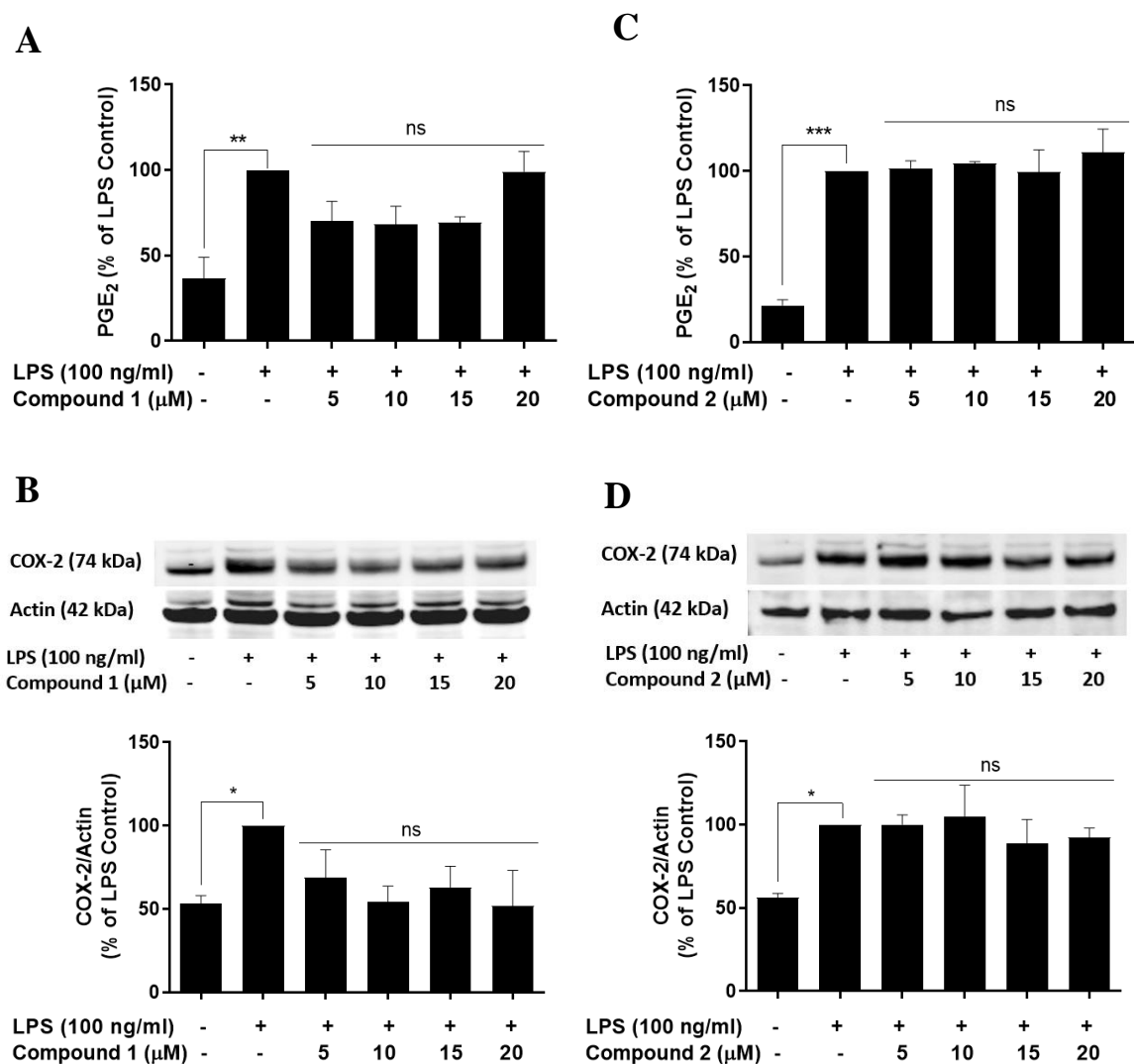


**Figure 2.21 Impact of compounds 1 and 2 on PGE<sub>2</sub> and COX-2 expression in LPS-activated BV2 cells.** Cells were treated with compounds 1 and 2 for 30 minutes and then stimulated with LPS (100 ng/ml) for 24 hours. After incubation medium supernatants and cell lysates were collected for PGE<sub>2</sub> EIA and COX-2 immunoblotting were performed. Compound 1 did not significantly reduce PGE<sub>2</sub> production (A) and COX-2 expression (B) at all tested concentrations in LPS-activated BV2 cells. Compound 2 did not decrease the level of PGE<sub>2</sub> (C) and did not significantly reduce COX-2 expression (D). Actin has been used as a loading control. All values are expressed as a mean ± SEM for N=3. Data were analysed using one-way ANOVA for multiple comparisons with post hoc Student Newman-Keuls test. \*p<0.033, \*\*p<0.002, \*\*\*p<0.001 in comparison with LPS control.

### 2.3.6 The effects of compounds 1 and 2 on NF- $\kappa$ B signalling pathway in LPS-activated BV2 microglia

NF- $\kappa$ B is a transcription factor regulating the expression of more than 400 proteins, including various pro-inflammatory signalling molecules (Liu et al., 2017). Therefore, inhibition of that signalling pathway has been shown to reduce inflammation. Hence, to determine if compounds 1 and 2 anti-inflammatory properties are NF- $\kappa$ B dependent, phosphorylation of NF- $\kappa$ B p65 has been measured using ELISA, nuclear localisation of NF- $\kappa$ B p65 was assessed using immunofluorescence. Furthermore, NF- $\kappa$ B reporter gene assay has been conducted to establish NF- $\kappa$ B promoter activity.

#### 2.3.6.1 The effect of compounds 1 and 2 on phosphorylation of NF- $\kappa$ B p65

Unstimulated BV2 cells contained low amounts of p-NF- $\kappa$ B, and LPS stimulation caused approximately 2.4-fold increase of p-NF- $\kappa$ B protein. Time course experiment indicated that the highest phosphorylation of NF- $\kappa$ B p65 occurs 60 minutes after LPS stimulation (Figure 2.22).

Therefore, BV2 microglia were incubated with or without compounds 1 and 2 (5 – 20  $\mu$ M) for 30 minutes, followed by LPS (100 ng/ml) stimulation for 60 minutes. Then, the whole-cell lysates were collected, and p-NF- $\kappa$ B ELISA was conducted. Data presented in Figure 2.23 indicate that pre-treatment with compounds 1 and 2 did not decrease the phosphorylation of NF- $\kappa$ B in LPS-activated BV2 cells.

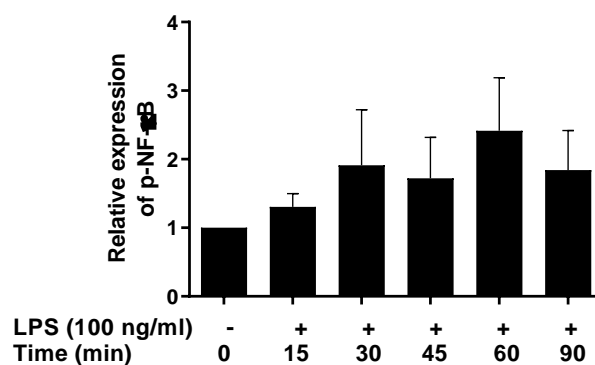


**Figure 2.22 Time course of LPS-induced phosphorylation of NF- $\kappa$ B in BV2 cells.** Cells were incubated with LPS (100 ng/ml) for 15, 30, 45, 60 and 90 minutes. Then cell lysates were collected and p-NF- $\kappa$ B ELISA was performed. The highest level of p-NF- $\kappa$ B was observed 60 minutes after LPS activation. All values are expressed as a mean  $\pm$  SEM for N=2.

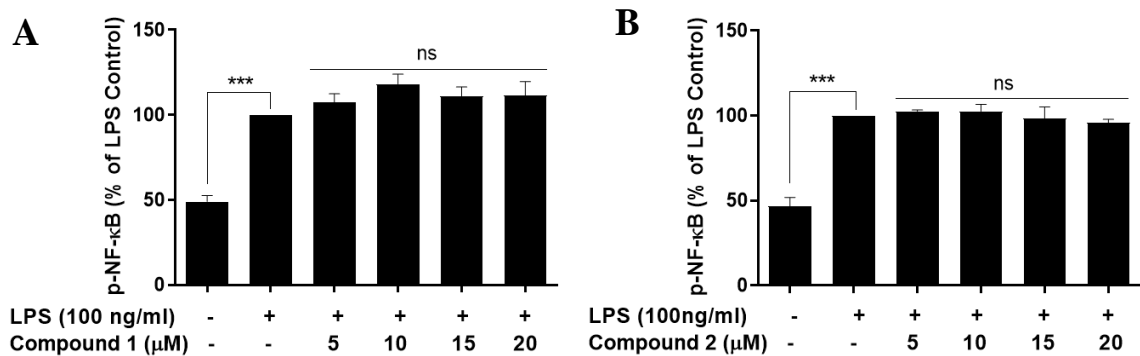
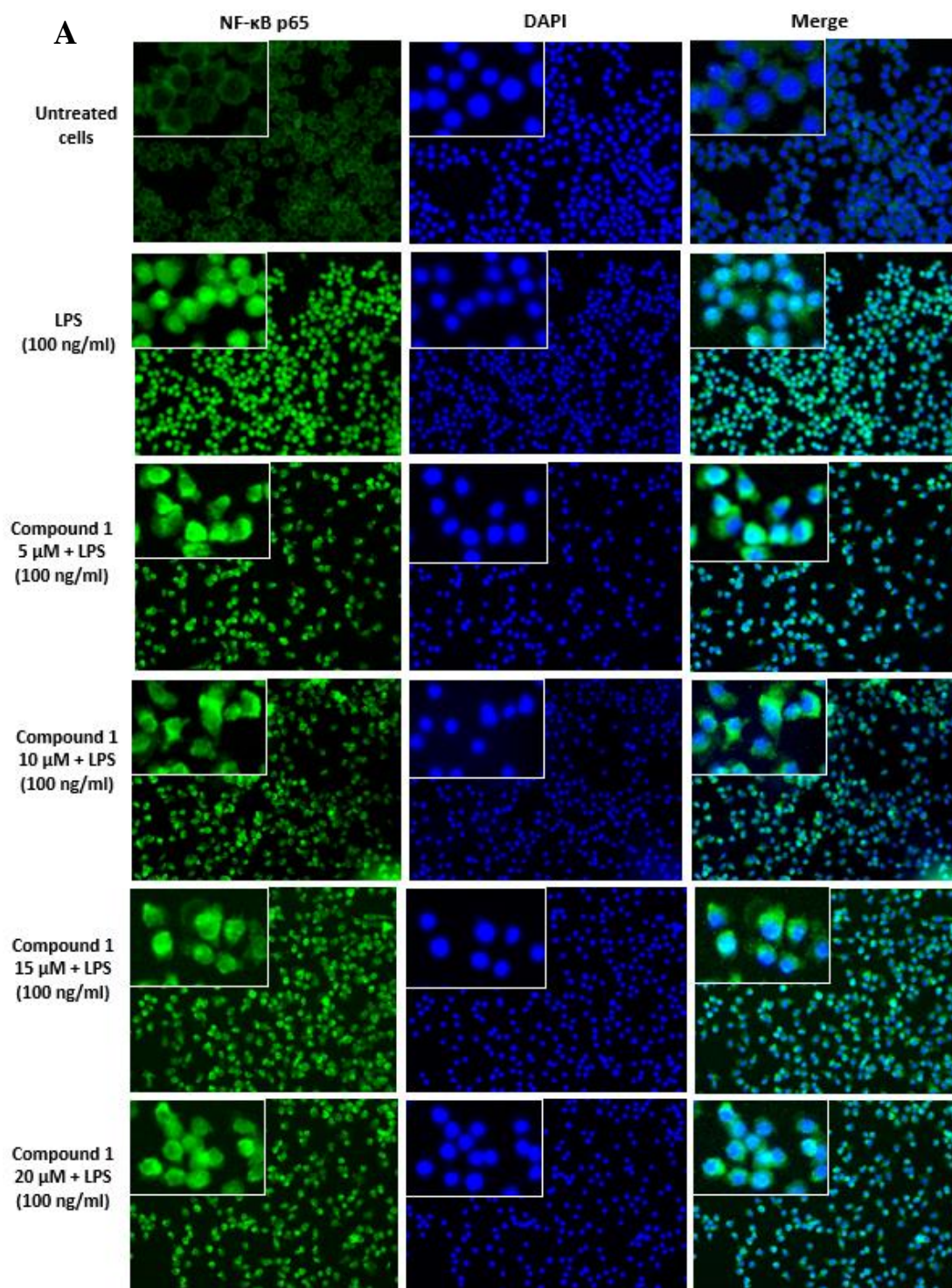


**Figure 2.23. Impact of compounds 1 and 2 on phosphorylation of NF-κB in LPS activated BV2 cells.** Cells were pre-incubated with compounds 1 and 2 (5 – 20 μM) for 30 minutes and then stimulated with LPS (100 ng/ml) for 60 minutes. After incubation cell lysates were collected, and p-NF-κB ELISA was conducted. Compounds 1 and 2 did not decrease the level of p-NF-κB p65 in LPS-activated BV2 cells. All values are expressed as a mean ± SEM for N=3. Data were analysed using one-way ANOVA for multiple comparisons with post hoc Student Newman-Keuls test. \*\*\*p<0.001 in comparison with LPS control.



### 2.3.6.2 The effect of compounds 1 and 2 on the nuclear localisation of NF- $\kappa$ B p65 in LPS-activated BV2 cells

In resting microglia (untreated control), NF- $\kappa$ B p65 subunit is located in the cytoplasm, while microglial activation causes nuclear translocation of NF- $\kappa$ B p65. Data presented in Figure 2.24 illustrate that compounds 1 (A) and 2 (B) did not inhibit nuclear localisation of NF- $\kappa$ B p65 at any of the tested concentrations (5 – 20  $\mu$ M).



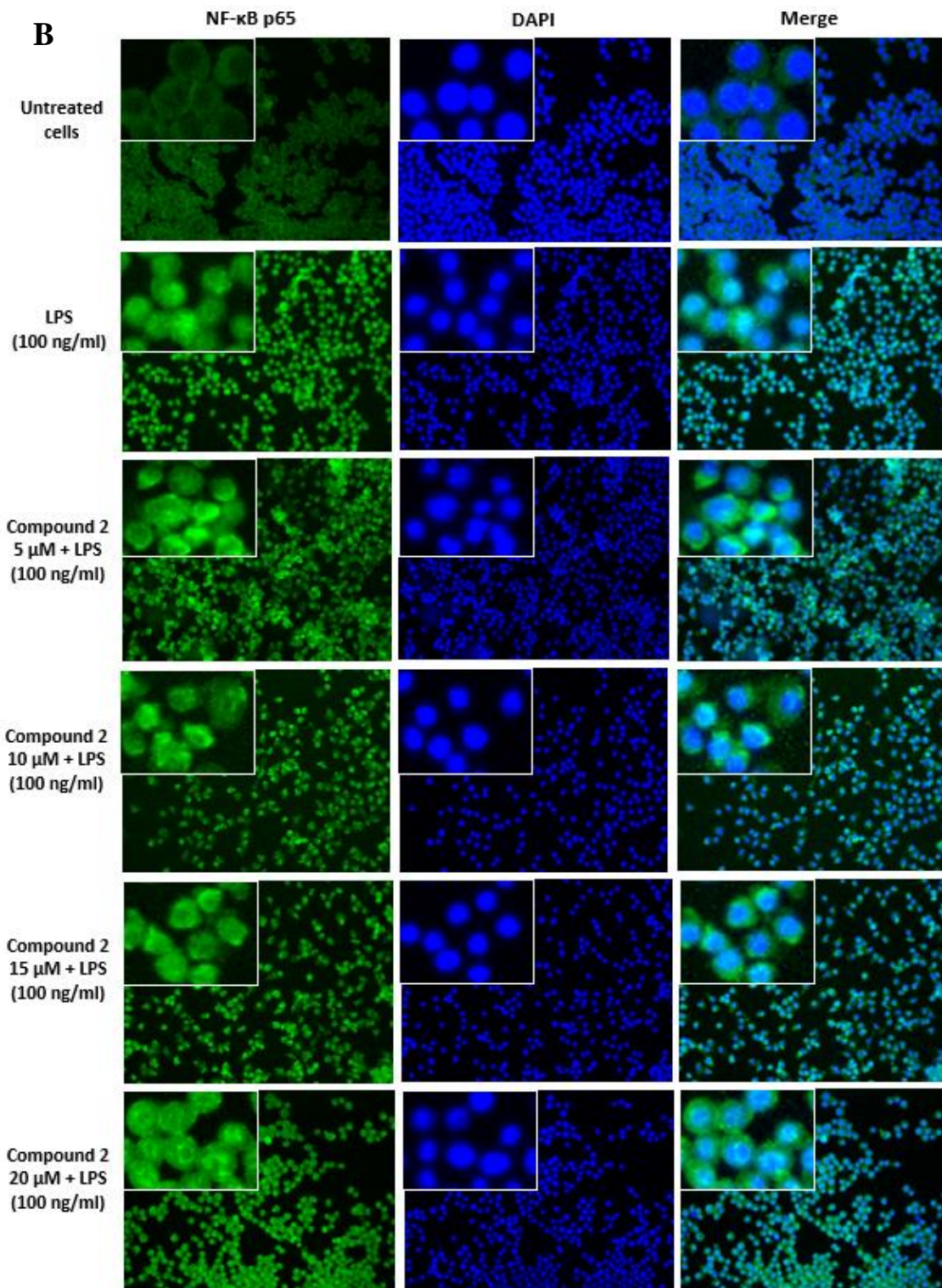


**Figure 2.24** The effect of compounds 1 and 2 on the nuclear localisation of NF-κB p65 in LPS-stimulated BV2 cells. Cells were pre-incubated with compounds 1 and 2 (5 – 20 μM) for 30 minutes and then stimulated with LPS (100 ng/ml) for 60 minutes. After incubation NF-κB immunofluorescence was performed. Compounds 1 (A) and 2 (B) did not inhibit nuclear localisation of NF-κB p65 in LPS-activated BV2 microglia. Green indicates NF-κB p65, blue shows DAPI staining. Images were captured with the EVOS® FLoid® Cell Imaging Station and then processed using ImageJ software.

### 2.3.6.3 The effect of compounds 1 and 2 on NF-κB activity in LPS challenged BV2 cells

To further determine if the NF-κB signalling pathway is involved in observed anti-inflammatory properties of compounds, reporter gene assay has been employed. To determine optimal incubation time for LPS-induced NF-κB luciferase activity time-course experiment was conducted at 3, 6, 8 and 24 hours. Data presented in Figure 2.25 show that LPS (100 ng/ml) induced the highest NF-κB luciferase activity 8 hours after stimulation. Therefore, the effect of compounds 1 and 2 on LPS-induced NF-κB activation was measured after 8 hours. LPS stimulation induced approximately 14.4-fold increase of NF-κB activity when compared to unstimulated control. Pre-treatment with compounds 1 and 2 (5 – 20 μM) did not inhibit LPS-induced NF-κB activity (Figure 2.26 A and B).

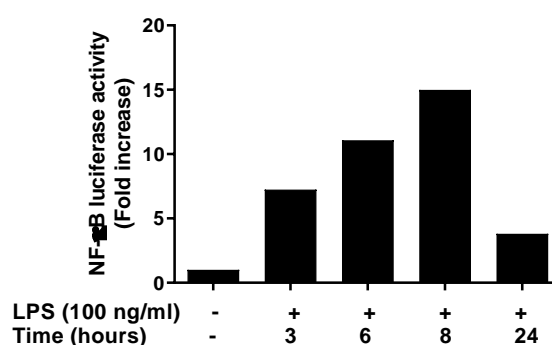


**Figure 2.25 Time-course of LPS-induced NF-κB luciferase activity in BV2 cells.** BV2 cells were transfected with NF-κB reporter and incubated for 20 hours. After incubation medium was changed and cells were incubated with 100 ng/ml of LPS for 3, 6, 8 and 24 hours. After incubation, The Dual-Glo Luciferase assay was performed. Data are presented as a ratio of experimental / control reporter for N=1. The highest NF-κB activity was observed 8 hours after LPS stimulation.

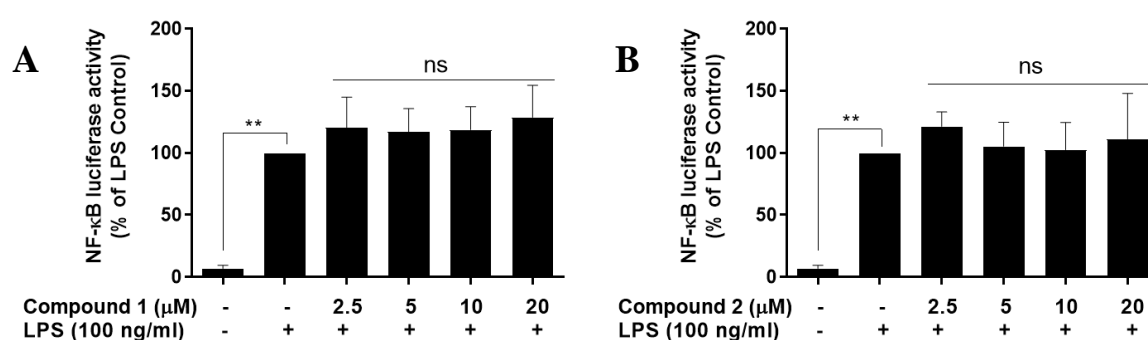


**Figure 2.26 The effect of compounds 1 and 2 on NF-κB activity in LPS challenged BV2 microglial cells.** BV2 cells were transfected with NF-κB transcription reporter encoding firefly luciferase and a constitutively active reporter vector encoding *Renilla* luciferase. After 20-hour incubation medium was changed and cells were treated with compounds 1 and 2 (5 – 20 μM) for 30 minutes followed by LPS stimulation for 8 hours. After incubation, The Dual-Glo Luciferase assay used to quantify NF-κB firefly luciferase and control reporter *Renilla* luciferase activities in transfected cells. Compounds 1 and 2 did not significantly decrease NF-κB activity. Data are presented as a ratio of experimental / control reporter. All values are expressed as a mean ± SEM for N=3. Data were analysed using one-way ANOVA for multiple comparisons with post hoc Student Newman-Keuls test. \*\*p<0.002 in comparison with LPS control.

### 2.3.7 The effect of compounds 1 and 2 on ERE activity in BV2 microglial cells

Biochanin A belongs to isoflavone family which are known to act as phytoestrogens in mammals. Phytoestrogens mimic oestrogen by binding to ER and then activating ERE leading to gene transcription. Therefore, to assess if compounds 1 and 2 reflect these characteristics, ERE-promoter luciferase-based reporter gene assay has been carried out in BV2 microglia cells.

Data presented in Figure 2.27 A show that compound 1 at concentrations of 5 – 20  $\mu\text{M}$  significantly ( $p < 0.033$ ) increased ERE activity approximately 4.1-fold compared to untreated cells. Compound 2 significantly ( $p < 0.033$ ,  $p < 0.002$  and  $p < 0.001$ ) in a concentration-dependent manner increased ERE activity approximately 2.8-fold, 4-fold, 5-fold and 5.5-fold when incubated with 5, 10, 15 and 20  $\mu\text{M}$ , respectively, compared to untreated control (Figure 2.27 B).

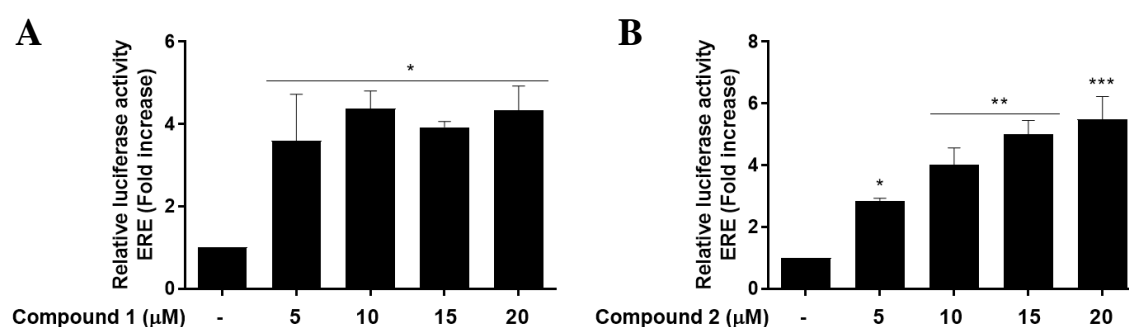


**Figure 2.27 The effect of compounds 1 and 2 on ERE activity in BV2 cells.** BV2 cells were transfected with ERE reporter and then incubated with compounds 1 and 2 (5 – 20  $\mu\text{M}$ ) for 24 hours. After incubation, The Dual-Glo Luciferase assay used to quantify firefly and *Renilla* luciferase activities in transfected cells. Compounds 1 and 2 significantly increased ERE activity. ERE reporter activity was normalized to *Renilla* co-reporter. Data are presented as a ratio of experimental/control reporter. All values are expressed as a mean  $\pm$  SEM for N=3. Data were analysed using one-way ANOVA for multiple comparisons with post hoc Student Newman-Keuls test. \* $p < 0.033$ , \*\* $p < 0.002$ , \*\*\* $p < 0.001$  in comparison with untreated control.

### 2.3.8 The effect of compounds 1 on LPS-induced MAPKs phosphorylation in BV2 microglial cells

Compound 1 was more effective in inhibiting key inflammatory mediators such as TNF- $\alpha$ , IL-6 and NO than compound 2. Therefore, only the effect of compound 1 on MAPKs LPS-induced phosphorylation was investigated.

#### 2.3.8.1 The effect of compound 1 on p38 phosphorylation induced by LPS in BV2 microglial cells

The p38 kinase is known to control the production of key inflammatory mediators, hence the effect of compound 1 on p38 phosphorylation was investigated using ELISA. Time-course experiment showed that the highest level of p-p38 occurred 60 minutes after LPS (100 ng/ml) activation (Figure 2.28). Pre-incubation of BV2 microglia with compound 1 (5 – 20  $\mu$ M) did not reduce LPS-induced p-p38 level (Figure 2.29).

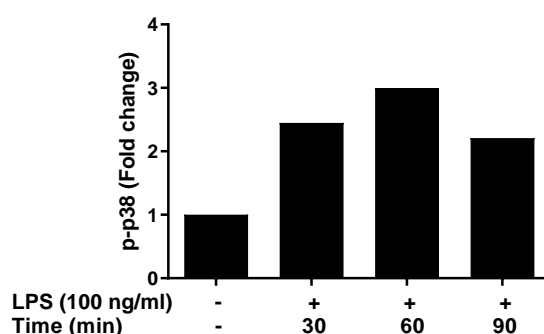


**Figure 2.28** Time-course experiment for LPS induced p38 phosphorylation in BV2 microglia. BV2 cells were incubated with LPS 100 ng/ml for 30, 60 and 90 minutes. After incubation level of p-p38 was analysed in whole-cell lysates using ELISA. The highest p-p38 level occurred 60 minutes following LPS activation.

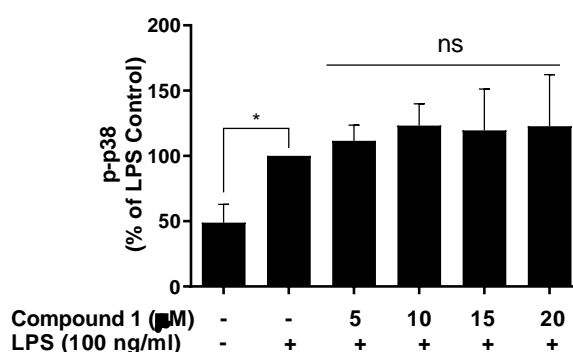


**Figure 2.29** The effect of compound 1 on the p-p38 level in LPS challenged BV2 cells. BV2 microglia were pre-incubated with compound 1 (5 – 20  $\mu$ M) for 30 minutes followed by 60 minutes LPS activation. After incubation whole cell lysates were collected, and protein level was quantified using Bradford assay and p-p38 ELISA was conducted. Compound 1 did not decrease p-p38 level in LPS stimulated cells. All values are expressed as a mean  $\pm$  SEM for N=3. Data were analysed using one-way ANOVA for multiple comparisons with post hoc Student Newman-Keuls test. \* $p < 0.033$  in comparison with LPS control.

### 2.3.8.2 The effect of compound 1 on JNK phosphorylation in LPS challenged BV2 cells

JNK pathway controls the transcription of numerous pro-inflammatory signalling molecules. Hence, to determine if anti-inflammatory properties of compound 1 were JNK dependent Western blot analysis was performed to measure the p-JNK level. Figure 2.30 shows the time point expression of LPS-induced p-JNK level. The highest level of p-JNK occurred 60 minutes after LPS activation. Non-stimulated cells expressed low levels of p-JNK; approximately 2.6-fold increase was induced after LPS activation. Compound 1 did not attenuate the phosphorylation of JNK in LPS-stimulated BV2 cells (Figure 2.31).

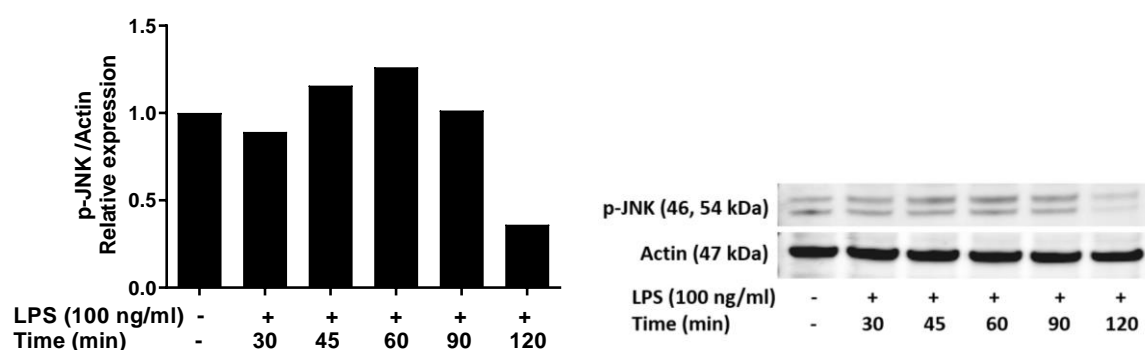


**Figure 2.30** The time-course of LPS-induced p-JNK expression in BV2 microglia. Cells were activated with LPS (100 ng/ml) at a different time point (30 – 120 min). At the end of incubation, the lysate was collected, and Western blot was performed. The highest production of p-JNK occurred at 60 minutes. N=1

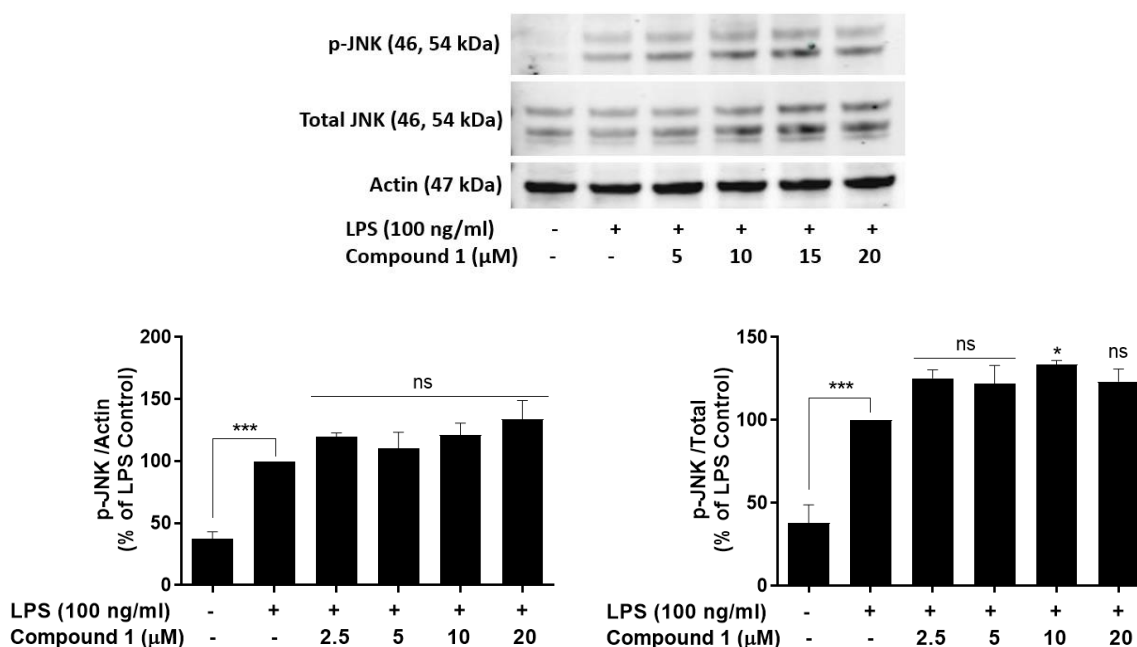


**Figure 2.31** The effect of compound 1 on JNK phosphorylation in LPS challenged BV2 cells. Cells were pre-treated with compound 1 and then stimulated with LPS (100 ng/ml) for 1h. After incubation cell lysates were collected, and Western blotting was performed. BV2 challenged with LPS increased JNK phosphorylation. Pre-incubation with compound 1 (2.5 – 20 μM) did not decrease JNK phosphorylation. Actin and total JNK has been used as a loading control. All values are expressed as a mean ± SEM for N=3. Data were analysed using one-way ANOVA for multiple comparisons with post hoc Student Newman-Keuls test. \*p<0.033, \*\*\*p<0.001 in comparison with LPS control.

### 2.3.8.3 The effect of compound 1 on LPS-induced ERK1/2 phosphorylation in BV2 microglial cells

ERK1/2 belongs to the signal transduction proteins involved in the regulation of inflammation, differentiation, and apoptosis. Therefore, to establish if the ERK1/2 signalling pathway was responsible for observed anti-inflammatory properties of compound 1 level of p-ERK1/2 was measured using Western blotting. To determine the optimal incubation time for the detection of p-ERK1/2 level, time-course experiment was conducted at 30, 45, 60, 90, and 120 minutes after LPS stimulation. Figure 2.33 shows that the highest production of p-ERK1/2 occurred at 60 minutes. Therefore, the effect of compound 1 on p-ERK1/2 level was monitored at 60 minutes after exposure to LPS. LPS activation caused approximately 1.2-fold increase of p-ERK1/2 protein level compared to untreated cells. Experiments showed that compound 1 did not inhibit the LPS-induced phosphorylation of ERK1/2 at none of the examined concentrations (Figure 2.33).

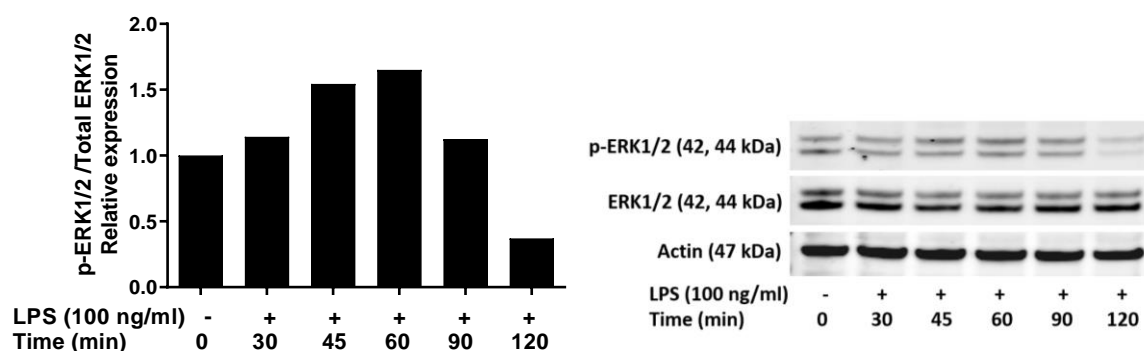


**Figure 2.32 Time-course experiment of ERK1/2 phosphorylation in LPS activated BV2 cells.** Cells were activated with LPS (100 ng/ml) at a different time point (30 – 120 min). At the end of incubation, lysates were collected, and Western blot was performed. The highest production of p-ERK1/2 occurred at 60 minutes. N=1.

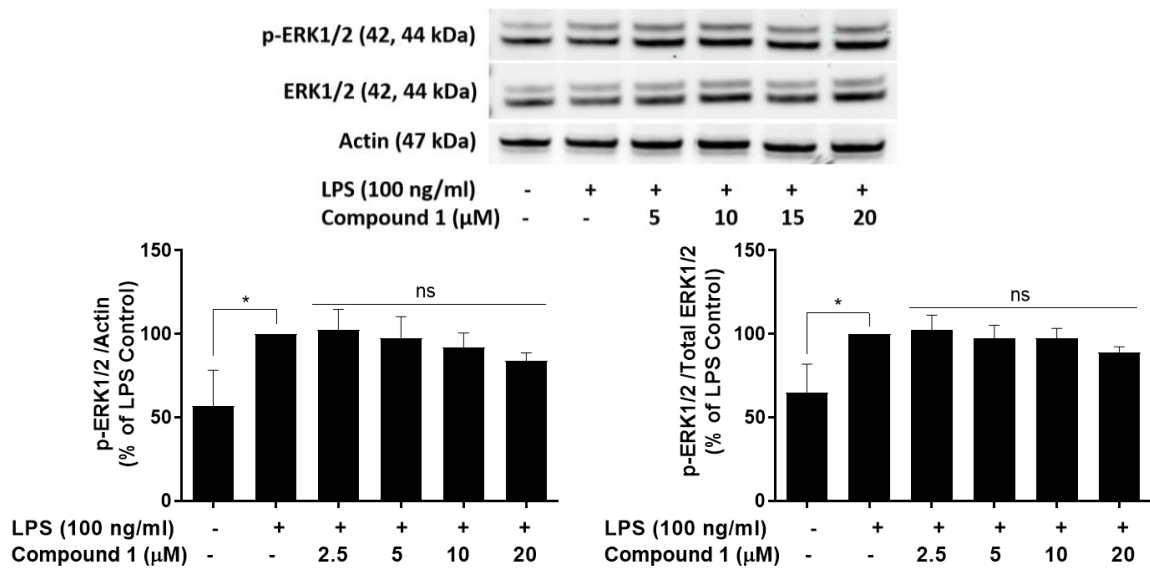


**Figure 2.33** The effect of compound 1 on ERK1/2 phosphorylation in LPS stimulated BV2 cells. Cells were pre-treated with compound 1 and then stimulated with LPS (100 ng/ml) for 1h. After incubation cell lysates were collected, and Western blotting was performed. BV2 challenged with LPS increased phosphorylation of ERK1/2. Pre-incubation with compound 1 (2.5 – 20 μM) did not decrease ERK1/2 phosphorylation. Actin and total ERK1/2 have been used as a loading control. All values are expressed as a mean ± SEM for N=3. Data were analysed using one-way ANOVA for multiple comparisons with post hoc Student Newman-Keuls test. \*p<0.033 in comparison with LPS control.



## 2.4 Discussion

Inflammation is usually a defensive mechanism of the organism; however, crossing the physiological limits of this process can turn this reaction into a harmful one. Chronic neuroinflammation is closely associated with neurodegeneration, hence compounds which inhibit inflammatory response may serve as a potential therapy to slow down neurodegeneration (Rubio-Perez & Morillas-Ruiz, 2012). Beneficial biological effects of phytochemicals have been widely established, and those include anti-inflammatory, antioxidant, neuroprotective and anti-cancerous activities (Cos et al., 2003; Sirotkin, 2014; Soni et al., 2014). Biochanin A is a member of phytochemicals family, and it is known to express positive anti-inflammatory, antioxidant, neuroprotective and anti-cancerous properties (Sundaresan et al., 2018). However, despite many pharmacological activities, its broader utility is limited by low aqueous solubility and poor bioavailability (Raheja et al., 2018).

Therefore, concluding upon proven knowledge of benefits of biochanin A, this chapter investigated two novel biochanin A analogues – compounds 1 and 2. The main aim of this chapter was to evaluate anti-inflammatory properties and molecular mechanisms of compounds 1 and 2. To obtain compound 1, core structure of biochanin A was modified in position 7' by insertion of carbamate group which is broadly used in medicinal chemistry to enhance chemical stability and permeability across cellular membranes (Ghosh & Brindisi, 2015). In turn compound 2 was created by insertion of dodecenoyl ester moiety also at position 7' resulting in increased lipid solubility. As compounds 1 and 2 inserted functional groups contain large alkyl chain, they both enhance lipid solubility (Harrold & Zavod, 2014). Moreover, Fokialakis et al., (2012) indicated that biochanin A derivatives containing long aliphatic chains suppressed proliferation of cancerous cell lines and displayed higher stability than original compound and other analogues, suggesting them as safer alternatives. Consequently, introduced chemical modifications to biochanin A in the form of large alkyl chain enhanced its lipophilicity and stability, which should increase their bioavailability. Therefore, to assess if structural changes implemented to biochanin A had an effect on its anti-inflammatory properties, novel compounds were examined using LPS-activated BV2 microglia.

During an inflammatory response, microglia produce large amounts of pro-inflammatory mediators, which are cytotoxic to neurons. Therefore, the reduction of those factors could

alleviate neurodegeneration. The level of pro-inflammatory cytokines serves as a biomarker and helps to estimate the severity of the disease leading to the verification of the effectiveness of potential treatments. However, before the evaluation of possible anti-inflammatory activities of compounds viability assay was performed to establish if the compounds at tested concentrations are cytotoxic to the cells. Both biochanin A derivatives - compounds 1 and 2 did not reduce the viability of the BV2 cells, indicating that all observed reductions of pro-inflammatory mediators are caused by pharmacological reactions, and not by a decrease in the cell viability. Anti-inflammatory properties of biochanin A analogues were assessed based on the ability to reduce LPS-induced production of pro-inflammatory cytokines. Compound 1 significantly reduced the level of TNF $\alpha$  when tested at two highest concentrations of 15 and 20  $\mu$ M, whereas compound 2 significantly inhibited TNF $\alpha$  only when tested at 20  $\mu$ M. Pre-treatment with compound 1 significantly reduced IL-6 at when used at 10  $\mu$ M, 15  $\mu$ M, and 20  $\mu$ M, while compound 2 reduced IL-6 levels when used at 15  $\mu$ M and 20  $\mu$ M. However, compound 2 was more active than compound 1 in decreasing IL-1 $\beta$  production. These data suggest that both compounds mitigate neuroinflammation. The next biomarker, which was used to assess the anti-inflammatory properties of compounds was nitric oxide. Nitric oxide is produced by NOS from L-arginine. Hence, expression of iNOS is directly proportional to nitric oxide and inhibition of iNOS will block nitric oxide production (Knowles & Moncada, 1994). Nitric oxide can readily react with various substances such as lipids, DNA and proteins. Thus, when nitric oxide production is elevated by neuroinflammation, this causes tissue damage, which in turn leads to neurodegeneration (Asiimwe et al., 2016). Griess assay was used to investigate the levels of nitric oxide by measuring its stable biodegradation product – nitrite. Additionally, Western Blotting was used to detect iNOS expression. Results show that compounds 1 and 2 significantly reduced the level of nitrite and iNOS in LPS-activated BV2 microglia cells. Pre-treatment with compound 1 at 20  $\mu$ M reduced the level of nitrite to 39%, and pre-treatment with compound 2 at the same concentration decreased the nitrite level to 63% when compared to LPS control as 100%. There was also a difference between the efficacy of compounds 1 and 2 in inhibiting iNOS expression. At 20  $\mu$ M compound 1 inhibited iNOS expression to 6%, compound 2 to 54% when compared to LPS control as 100%. Chabrier, Demerlé-Pallardy, & Auguet, (1999) described that blocking of iNOS and consequently nitric oxide could alleviate pathogenesis of neurological diseases. Therefore, according to this theory, compound 1 and 2 can be considered as a potential treatment alleviating neuroinflammation-mediated neurodegeneration. Moreover, it was evident that compound 1 was more efficient than

compound 2 in the inhibition of pro-inflammatory mediators. Pre-treatment with compound 1 more effectively reduced level of TNF $\alpha$ , IL-6, iNOS and NO than pre-treatment with compound 2. Chemical structure of compounds 1 and 2 are very similar; the only difference between the two compounds is one amine group in compound 1. Therefore, the amine may have a significant impact on the affinity of the compound for the receptors and finally its potency. Furthermore, another factor which can enhance compound 1 activity is the higher polarity of the compound caused by the electronegativity of the N atom. Studies of anti-inflammatory properties of biochanin A showed similar reduction pattern of cytokines, iNOS and NO, hence functional groups inserted to precursor compound did not inhibit those positive biological effects (Wu et al., 2015; Zhang & Chen, 2014). Nevertheless, detailed analysis of % inhibition cannot be directly compared to this study due to different LPS concentrations used to stimulate BV2 cells. Wu (2015) and Zhang (2014) studies used LPS at 10  $\mu$ g/ml and 0.5  $\mu$ g/ml, respectively, however, in this study, LPS was used at 100 ng/ml.

Antioxidant activities of polyphenolic compounds have been widely reported (Kładna, Berczyński, Kruk, Piechowska, & Aboul-Enein, 2016). Antioxidants can act directly by scavenging free radicals or by interaction with a network of antioxidant enzymes. (Dizhbite, Telysheva, Jurkjane, & Uldis, 2004; Guo, Rimbach, Moini, Weber, & Packer, 2002; Himamura et al., 2014; Kedare & Singh, 2011; Sharma & Bhat, 2009). Free radical scavenging properties of phytoestrogens has been attributed to hydroxyl groups present in their aromatic rings (Romera-Castillo & Jafféab, 2015). Compound 1 and 2 have one hydroxyl group in A-ring at position 5'. To assess if biochanin analogues have radical scavenging proprieties DPPH assay was performed. Results indicated that both compounds do not possess DPPH radical scavenging activity. This is in line with the data presented by Sherif & Gebreyohannes, (2018) where biochanin A exhibited no significant radical scavenging activity. Moreover, the authors investigated also biochanin A analogues with various substituents in B-ring at position 4'. They observed an enhanced free radical-scavenging activity in biochanin A analogues with hydrogen and hydroxyl group at position 4' in B-ring. Biochanin A and compounds 1 and 2 do not have a hydroxyl group in this position and thus exhibit weak DPPH scavenging activity. Consequently, their antioxidant properties might not be attributed to free radical-scavenging activity, but other mechanisms such as membrane stabilisation or increase in the level of antioxidant enzymes such as superoxide dismutase (SOD), catalase (CAT) glutathione peroxidase (GPx) and decrease of pro-oxidant enzymes including NAD(P)H and xanthine oxidase (XO) might play a role.

Therefore, future experiments should investigate indirect prevention of the formation of free radicals.

Another biomarker which plays a role in the inflammatory process is PGE<sub>2</sub>, a potent inflammatory mediator generated by COX-2 enzyme. Accumulating evidence suggests that COX-2/PGE<sub>2</sub> signalling may play a role in neuroinflammation (Aid & Bosetti, 2011; Combrinck et al., 2006; Johansson et al., 2015). However, Minghetti, (2004) argued that a direct role of COX-2 in neurodegenerative events is controversial due to its constitutive expression in the healthy brain in contrast to only inflammation-induced production in the periphery. COX-2 enzyme participates in fundamental brain functions, including synaptic plasticity, memory consolidation, and functional hyperaemia (Minghetti, 2004). Moreover, Combrinck et al., (2006) indicated that COX-2/PGE<sub>2</sub> levels vary with the severity of Alzheimer's disease (AD) where low levels are observed with mild memory impairment, and high in advanced AD stage. Additionally, the authors reported a longer median age of death of patients with higher PGE<sub>2</sub> levels. Those data suggest that alleviated COX-2 might be adaptive reaction aiming to restore physiological functions and homeostasis disrupted by neuroinflammation. On the contrary, epidemiological studies indicated that NSAIDs are protective against neurodegeneration. However, those effects might be mediated by COX-2-independent mechanisms which induce downregulation of NF- $\kappa$ B, AP-1 and MAPK (Ajmone-Cat, Bernardo, Greco, & Minghetti, 2010). Phytochemicals, including biochanin A are known to reduce PGE<sub>2</sub> (Y. Zhang & Chen, 2014). Therefore, the effect of compounds 1 and 2 were examined on COX-2/PGE<sub>2</sub>, and results indicated that compounds did not affect LPS-induced expression of COX-2 and PGE<sub>2</sub>. Thus, this study showed that functional moieties inserted to biochanin A influenced pharmacological properties of compounds suggesting that altered chemical structure of novel derivatives unbalances activation or repression of proteins which regulate biochanin A properties. Funk & FitzGerald, (2007) demonstrated that selective COX-2 inhibition leads to cardiovascular malfunction due to the increase of platelet aggregation. Therefore, compounds 1 and 2 might serve as an interesting substitute for anti-inflammatory compounds, with a potential for patients with a predisposition to cardiovascular diseases.

Compounds 1 and 2 share structural similarities with 17 $\beta$ -oestradiol and its precursor biochanin A. Biochanin A belongs to phytoestrogen family, known to activate ERs. Activation of those receptors has been shown to produce anti-inflammatory and neuroprotective properties (Ishihara, Itoh, Ishida, & Yamazaki, 2015; Villa et al., 2016).

Reporter gene assay demonstrated that biochanin A analogues upregulated the ERE activity, suggesting that the compounds' anti-inflammatory actions are mediated via ERE-dependent regulation of transcriptional activation. This activation might be classical ER-dependent or ER ligand-independent. The ER-dependent response is induced by ER $\alpha$  or ER $\beta$  where activated ER migrate to the nucleus, binds to ERE and regulate gene expression. ER expression is tissue-specific; nevertheless, both receptors are expressed in the human brain with varied expression in different brain regions. Moreover, Weiser, Foradori, & Handa, (2008) indicated that ER $\beta$  is more prevalent in the hippocampus, which is responsible for memory. Additionally, numerous studies suggest that among ERs, ER $\beta$  is particularly crucial in the cognitive process. BV2 microglial cells have been demonstrated to express mainly ER $\beta$ ; hence this cell model provides a unique system for the study of the functions of ER $\beta$  (Baker, Brautigam, & Watters, 2004; El-Bakoush & Olajide, 2018). This suggests that observed activation of ERE is occurring via ER $\beta$ , rather than ER $\alpha$ . Alternative signalling pathway, which might lead to ERE activation is ligand-independent ER activation. Chen et al., (2013) demonstrated that phytoestrogen ginsenoside Rg1 activates ERE in ER ligand-independent manner. Moreover, Gao et al., (2019) presented that this ER-ligand independent activation might be induced by GPER and IGFR signalling. Activation of the above receptors leads to MEK activation and phosphorylation of ER leading to ERE transcriptional activation. Additionally, ER activation might lead to activation of the non-classical genomic pathway where ER can interact or influence the activity of other transcription factors such as stimulating protein-1 (SP-1), AP-1, NF- $\kappa$ B, and c-jun (Cui et al., 2013).

The observed anti-inflammatory properties of compounds triggered the investigation of potential signalling pathways involved in this activity. As NF- $\kappa$ B is the key regulator of genes coding for cytokines, and iNOS, hence the effect of compounds on this signalling pathway was examined. ELISA experiments revealed that both biochanin A analogues did not decrease LPS-induced p-NF- $\kappa$ B level. Additionally, immunofluorescence experiment also indicated the lack of compounds effect on nuclear localisation of NF- $\kappa$ B protein, which indicates that compounds did not affect upstream NF- $\kappa$ B signalling steps. Nonetheless, several more mechanisms may block signal transduction downstream of NF- $\kappa$ B phosphorylation and its nuclear translocation (Kalaitzidis & Gilmore, 2005). Several groups reported that ER agonists did not inhibit nuclear translocation of NF- $\kappa$ B, but still were able to reduce NF- $\kappa$ B activity by affecting NF- $\kappa$ B–DNA binding (Speir, Yu, Takeda, Ferrans, & Cannon, 2000b), decreasing histone acetyltransferase activity (Harnish, Scicchitano,

Adelman, Lyttle, & Karathanasis, 2000) or NF- $\kappa$ B dependent transactivation (Tzagarakis-Foster, Geleziunas, Lomri, An, & Leitman, 2002), competition or interference with transcriptional coactivators (Speir, Yu, Takeda, Ferrans, & Cannon, 2000) Therefore, to exclude the effects of compounds on transcriptional level including DNA/NF- $\kappa$ B binding, interfering with co-activators, or inhibiting DNA-bound NF- $\kappa$ B transcriptional activation, reporter gene assay was performed. Both biochanin A analogues did not inhibit LPS-induced NF- $\kappa$ B activity; thus, anti-inflammatory properties of compounds seem to be NF- $\kappa$ B independent. On the contrary, Zhang & Chen, (2014) indicated that biochanin A reduced phosphorylation of I $\kappa$ B and NF- $\kappa$ B. Authors also suggested that anti-inflammatory properties of biochanin A are regulated by activation of PPAR- $\gamma$ , which blocks NF- $\kappa$ B and subsequently inhibits the release of pro-inflammatory mediators.

ER ligands have also been shown to act via ER to operate via a variety of cytoplasmic signalling cascades, including MAPKs (Schwartz, Verma, Bivens, Schwartz, & Boyan, 2016). A large body of evidence suggests that the reduction of MAPKs might inhibit the production of iNOS, TNF $\alpha$ , IL-6 and IL-1 $\beta$  (Bhat, Zhang, Lee, & Hogan, 1998; Y. Choi, Lee, Lim, Sung, & Kim, 2009; Cobb, 2016; Kaminska, 2005; Krzyzowska et al., 2010). However, Baker et al., (2004) argued, that ERK1/2 activation by 17 $\beta$ -oestradiol might be responsible for its ability to reduce iNOS/NO. MAPK activation has been shown to induce ligand-independent ERE transcriptional activity (Cui et al., 2013). Therefore, the action of ERE-activators might differ from non-estrogenic compounds due to ER properties to interfere with other transcription factors. The ability of compound 1 to reduce iNOS/NO, TNF $\alpha$  and IL-6 was more prominent than compound 2; hence only the effects of compound 1 on MAPKs were examined. Pre-treatment with compound 1 did not attenuate LPS-induced phosphorylation of p38, JNK and ERK1/2, suggesting that anti-inflammatory properties of the compound 1 are MAPKs independent. In contrary, Wu et al., (2015) reported that biochanin A inhibits the activation of the MAPKs pathway in BV2 microglial cells. Therefore, the functional group inserted into biochanin A changed not only its physical, but also the pharmacological properties.

In summary, biochanin A analogues – compound 1 and 2 reduced the production of TNF $\alpha$ , IL-6, IL- $\beta$ , iNOS and NO in LPS-activated BV2 microglia cells. Pre-treatment with both compounds did not inhibit COX-2/PGE<sub>2</sub> LPS-induced signalling and did not scavenge DPPH radical. Moreover, compounds were more effective in decreasing the levels of iNOS and nitrite than other pro-inflammatory mediators. The expression of iNOS and nitrite was

significantly reduced at all tested concentrations (5 – 20  $\mu$ M) whereas expression of pro-inflammatory cytokines was not significantly reduced at the lowest tested concentration (5  $\mu$ M) by both compounds. Additionally, compounds upregulated ERE activity and did not affect NF- $\kappa$ B activity in LPS-stimulated BV2 microglia cells. Therefore, both compounds presented NF- $\kappa$ B-independent weak anti-inflammatory properties, suggesting that the observed effects could be ER-mediated via direct ERE activation or ER transactivation or inhibition of other transcription factors or by compounds interference with post-transcriptional or post-translational mechanisms. Figure 2.34 summarises the possible pathways by which compounds 1 and 2 induce their anti-inflammatory actions.

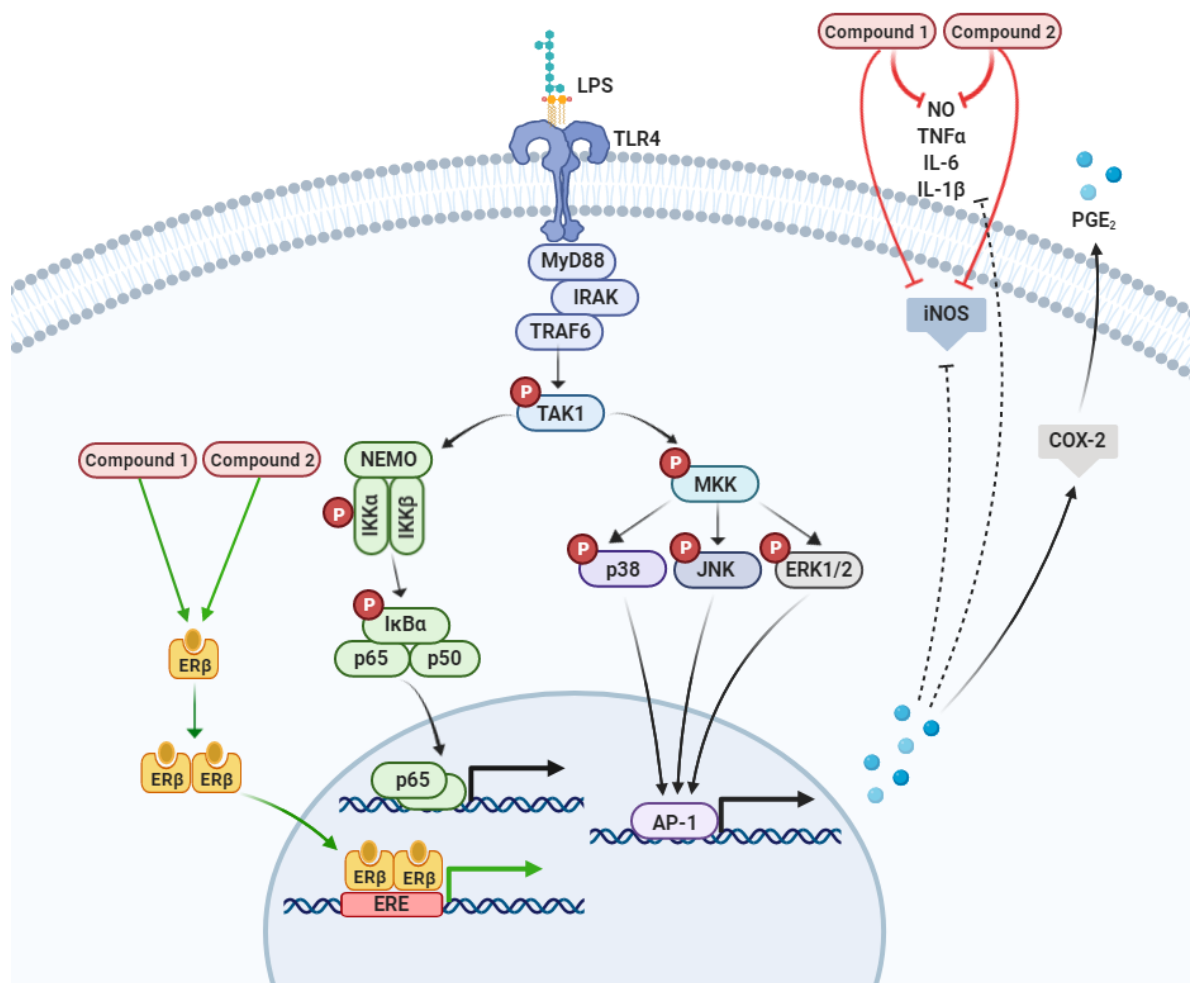


**Figure 2.34** Schematic representation of anti-inflammatory action of compound 1 and 2.

## 3 Chapter III - Anti-inflammatory Properties and Mechanism of Action of Daidzein Derivatives

### 3.1 Introduction

#### 3.1.1 Daidzein

Daidzein (7-hydroxy-3-(4-hydroxyphenyl)-4H-chromen-4-one) is an isoflavone naturally occurring in dietary products such as soybeans and other legumes which belong to the Fabaceae family (Figure 3.1). Daidzein is also classified as phytoestrogen due to oestrogen-like structure and properties (Ahmed et al., 2017). The literature on daidzein has highlighted several beneficial pharmacological activities, including anti-cancer (Choi & Kim, 2008), cardioprotective (Kim et al., 2009), anti-inflammatory (Choi et al., 2012), antioxidant (Kampkötter et al., 2008; J. Liang et al., 2008) and neuroprotective (Kajta et al., 2013b; J. M. Stout, Knapp, Banz, Wallace, & Cheatwood, 2013) properties. The anti-inflammatory properties of daidzein have been widely tested *in vivo* and *in vitro* systems (Sun et al., 2016). Studies which focused on peripheral inflammation indicated anti-inflammatory activities of daidzein in Caco-2 - human epithelial colorectal carcinoma (Peng, Shi, Zhang, Mine, & Tsao, 2017), J7774 macrophages (Hämäläinen, Nieminen, Vuorela, Heinonen, & Moilanen, 2007), RAW264.7 macrophages (Choi et al., 2012; Jin, Son, Min, Jung, & Choi, 2012). Moreover, daidzein has been demonstrated to penetrate BBB; hence its anti-inflammatory properties can also be utilized in the brain during neurological disorders (Xiao et al., 2016). A large body of literature recognised daidzein potential to reduce neuroinflammation using mice primary astrocytes (Liu, Lin, Sheu, & Sun, 2009), HAPI microglia (Jantaratnotai, Utaisincharoen, Sanvarinda, Thampithak, & Sanvarinda, 2013), BV2 microglia and C6 astrocytes (Subedi et al., 2017). Common anti-inflammatory actions of daidzein across different cell lines include reduction of nitric oxide, iNOS and IL-6 production. It has been proposed that NF- $\kappa$ B and STAT1 pathways are responsible for the anti-inflammatory actions (Choi et al., 2012). Furthermore, contradictory data concerning daidzein effect on MAPKs indicates that daidzein did not decrease LPS-induced phosphorylation of JNK and p38 (Choi et al., 2012), whereas Tomar et al., (2019) reported that daidzein reduced JNK, p38 and ERK activation. However, Choi's (2012) study was conducted using murine macrophages, and Tomar's (2019) employed adult male rats; thus, the differences in daidzein activities may be due to species differences or cell type.



Alongside anti-inflammatory actions, daidzein has demonstrated to act as an antioxidant. In a study which aimed to determine antioxidant properties of daidzein, Liang et al., (2008) found that daidzein possesses radical scavenging activities and can change membrane fluidity through incorporation to it, thereby hampering free radical migration. However, Kampkötter et al., (2008) argued that daidzein does not have prominent antioxidant effects in cell-free assay systems. Hence, its antioxidant properties are not due to free radical scavenging. Therefore, to better understand daidzein's antioxidant mechanisms, authors analysed indirect antioxidant actions and discovered significant induction of catalase promoter activity. This indicates that daidzein act as an antioxidant via up-regulation of antioxidative enzymes. Moreover, Froyen & Steinberg (2010), further confirmed that daidzein upregulated antioxidant genes. Additionally, the authors linked this activity to ER $\beta$  and Nrf2 activation.

Therapeutic properties of natural products are widely recognised. Hence, they serve as an inspiration for many currently used drugs. However, natural compounds mainly consist of carbon, hydrogen and oxygen atoms with limited nitrogen and halogen atoms. Therefore, insertion of nitrogen or halogen atoms may lead to the compound's optimisation (Z. Guo, 2017). Moreover, the incorporation of functional groups allows assessing the structure-activity relationship. Therefore, this chapter presents the anti-inflammatory activity of two novel daidzein analogues.

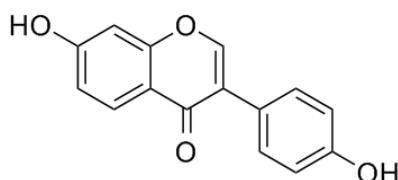


**Figure 3.1** The chemical structure of daidzein.

### 3.1.2 Daidzein derivatives

Chapter three presents the anti-inflammatory properties of two daidzein derivatives: ethyl 2-(4-(7-hydroxy-4-oxo-4H-chromen-3-yl)phenyl)acetate (Compound 3) and 3-(4-(4-(3-chloropropyl)-1H-1,2,3-triazol-1-yl)phenyl)-7-hydroxy-4H-chromen-4-one (Compound 4) (Table 3.1). Compound 3 was created by insertion of an ethyl ester moiety into daidzein B-ring at position 4'. To create compound 4, a functional group-containing chloropropyl triazole was also added to daidzein B-ring at position 4'.

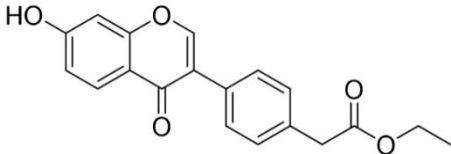
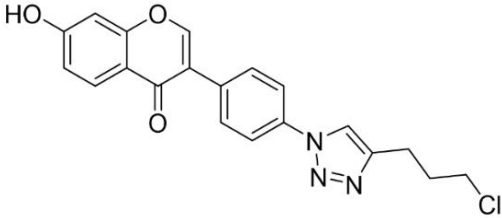
Daidzein derivatives at position 4'	
<p style="text-align: center;"><b>Compound 3</b></p> <p style="text-align: center;">Ethyl 2-(4-(7-hydroxy-4-oxo-4H-chromen-3-yl)phenyl)acetate</p> <p style="text-align: center;">Formula: C<sub>19</sub>H<sub>16</sub>O<sub>5</sub></p> <p style="text-align: center;">Molecular weight: 324.33</p> 	<p style="text-align: center;"><b>Compound 4</b></p> <p style="text-align: center;">3-(4-(4-(3-chloropropyl)-1H-1,2,3-triazol-1-yl)phenyl)-7-hydroxy-4H-chromen-4-one</p> <p style="text-align: center;">Formula: C<sub>20</sub>H<sub>16</sub>ClN<sub>3</sub>O<sub>3</sub></p> <p style="text-align: center;">Molecular weight: 381.82</p> 

Figure 3.2 The structural formula of daidzein derivatives - compounds 3 and 4.

## 3.2 Methodology

### 3.2.1 BV2 cell culture

BV2 cell culture was conducted as indicated in chapter two, section [2.2.1](#)

### 3.2.2 Treatment of BV2 microglia with ICI 182,780, ML385 and EX527

BV2 cells were seeded in 24-well plates at a density of  $5 \times 10^4$  cells/ml in 1 ml of culture medium per well and incubated until reached approximately 80% confluence. Then, the cell culture medium was changed to serum-free RPMI medium followed by 1 – 2-hour incubation. Subsequently, cells were pre-incubated with 10 nM of ICI 182,780 (Fulvestrant; Sigma-Aldrich), or 10  $\mu$ M of ML385 (Sigma-Aldrich) or 1  $\mu$ M of EX527 (Sigma-Aldrich) for 30 minutes followed by compounds 3 and 4 treatment and further incubation. After 30 minutes-incubation cells were activated for 24 hours with 100 ng/ml of LPS derived from *Salmonella typhimurium*, S-form (Innaxon Biosciences).

### 3.2.3 Treatment of BV2 cells with compounds 3 and 4

Daidzein derivatives: ethyl 2-(4-(7-hydroxy-4-oxo-4H-chromen-3-yl)phenyl)acetate (Compound 3) and 3-(4-(4-(3-chloropropyl)-1H-1,2,3-triazol-1-yl)phenyl)-7-hydroxy-4H-chromen-4-one (Compound 4) were kindly provided by Gabriel Mengheres (PhD Researcher supervised by Dr Karl Hemming, Department of Chemical Sciences, The University of Huddersfield). Compounds were dissolved in DMSO and stored in  $-80^{\circ}\text{C}$ . BV2 cells were seeded in 96-well, 24-well and 6-well plates with flat base and adherent surface (Sarstedt) at a density of  $5 \times 10^4$  cells/ml in 200  $\mu$ l/well for 96-well, 1 ml/well for 24-well and 2 ml/well for 6-well plate. When cells reached approximately 80% confluence, the culture medium was changed to serum-free RPMI to reduce the variability of experiments caused by lot to lot variation of serum composition. Subsequently, cells were incubated for 1 – 2 hours at  $37^{\circ}\text{C}$ , and then treatment of BV2 microglia with compounds was performed. Preliminary pilot experiments such as XTT and Griess assay were carried out using a wider range of concentrations 0.6  $\mu$ M – 20  $\mu$ M of the compounds (Figure 3.3). These experiments allowed for the establishment of optimal compound concentrations used for further experiments (compound 3 – 2.5, 5, and 10  $\mu$ M; compound 4 – 5, 10 and 20  $\mu$ M). The final concentration of DMSO in the cell culture medium was kept constant at 0.2% v/v for all concentrations of compounds and untreated control. After treatment with compounds, cells were incubated for

30 minutes at 37°C followed by 100 ng/ml lipopolysaccharide (LPS) derived from *Salmonella typhimurium*, S-form (Innaxon Biosciences) activation.

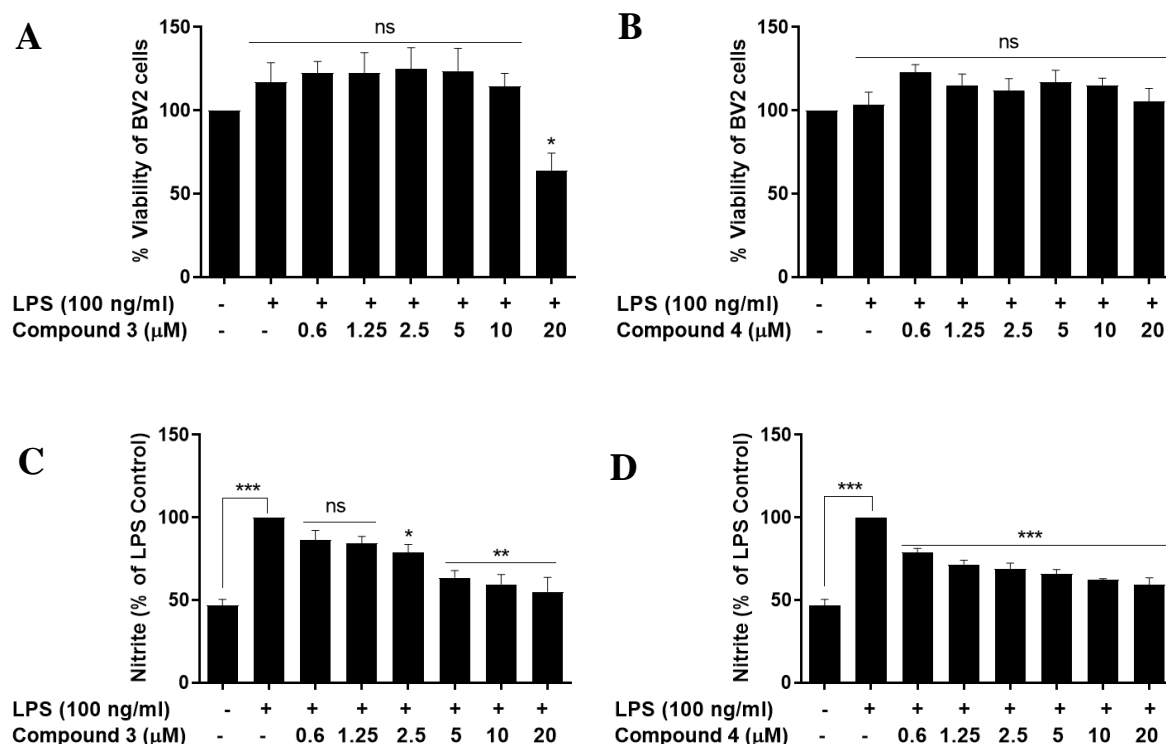


**Figure 3.3 Determination of maximum non-toxic and active concentrations of compounds 3 and 4 for BV2 cells.** BV2 microglia were treated with or without a range of concentrations of compounds 3 and 4 (0.6 – 20 μM) for 30 minutes and then activated with LPS (100 ng/ml). Subsequently, BV2 cells were incubated for 24 hours, and XTT assay and Griess assay were performed. (A) The maximum non-toxic concentration of compound 3 in BV2 cells was 10 μM, at 20 μM compound 3 significantly ( $p < 0.033$ ) reduced BV2 cell viability. (B) Compound 3 was able to significantly ( $p < 0.033$ ) reduce nitrite production from 2.5 μM. (C) Compound 4 did not reduce cells viability at any of tested concentrations 0.6 – 20 μM. (D) Compound 4 significantly ( $p < 0.001$ ) inhibited nitrite production from 0.6 μM. All values are expressed as a mean  $\pm$  SEM for  $N=3$ . Data were analysed using one-way ANOVA for multiple comparisons with post hoc Student Newman-Keuls test. \* $p < 0.033$ , \*\* $p < 0.002$ , \*\*\* $p < 0.001$  in comparison with untreated control or LPS control.

### 3.2.4 XTT cell viability assay

XTT cell viability assay was performed as described in chapter two, section [2.2.3](#)

### 3.2.5 TNF $\alpha$ , IL-6 and IL-1 $\beta$ ELISAs

ELISAs were conducted as indicated in chapter two, section [2.2.4](#)

### 3.2.6 Griess assay

Griess assay was performed as described in chapter two, section [2.2.5](#)

### **3.2.7 Western blotting**

Western blotting was conducted as described in chapter two, section [2.2.6](#)

### **3.2.8 DPPH assay**

DPPH assay was carried out as indicated in chapter two, section [2.2.7](#)

### **3.2.9 PGE<sub>2</sub> enzyme immunoassay**

PGE<sub>2</sub> enzyme immunoassay was performed as described in chapter two, section [2.2.8](#)

### **3.2.10 InstantOne™ ELISA for p-NF-κB and p-p38**

InstantOne™ ELISAs were conducted as indicated in chapter two, section [2.2.9](#)

### **3.2.11 Reporter gene assay**

Reporter gene assay was performed as described in chapter two, section [2.2.11.2](#)

### **3.2.12 siRNA mediated knockdown of ERβ in BV2 cells**

Gene knockdown is an experimental technique by which the individual gene expression is temporary decreased. This technique allows studying effects of loss-of-function of a specific gene. Temporary change in gene expression that does not modify the chromosomal DNA, but it affects post-transcriptionally gene expression. One of the post-transcriptional gene silencing methods is mRNA degradation known as RNA interference (RNAi). This technique uses small double-stranded interfering RNAs (siRNA), which are complementary to the target mRNA to be silenced. siRNAs are introduced into cytoplasm using transfection, which is followed by their processing using an RNA-induced silencing complex (RISC). RISC consists of Dicer and Argonaute protein which plays a central role in RNA silencing processes. RISC guides the system to bind and cleave the target mRNA, resulting in gene knockdown (Joshua-Tor, 2004).

To perform ERβ knockdown, BV2 microglia were seeded in 6-well plates at a density of  $4 \times 10^4$  cells/ml in 2 ml of culture medium per well and incubated until reached approximately 60% confluence. Then, the cell culture medium was changed to 1 ml of Gibco™ Opti-MEM (Fisher Scientific), and cells were incubated 2 hours at 37°C. Subsequently, Glial-Mag/siRNA complexes were prepared using 1.8 μl of Glial-Mag (OZ Biosciences) and 2 μl of control siRNA (sc-37007; Santa Cruz Biotechnology) or ERβ siRNA (sc-35326; Santa

Cruz Biotechnology) diluted in 200  $\mu$ l Opti-MEM medium. Prepared Glial-Mag/siRNA complexes were incubated for 30 minutes at room temperature, and then they were added dropwise to the cells. Afterwards, 20  $\mu$ l of Glial-Boost was added to each well. Then cells were placed on a magnetic plate for 30 minutes. This was followed by 2 hours incubation at 37°C and addition of 800  $\mu$ l of Opti-MEM medium to each well. Subsequently, cells were incubated for 24 hours in 37°C. Then whole-cell lysates were collected, and Western blot analysis was conducted as described in [2.2.6](#). Western blot analysis of ER $\beta$  protein level allowed to establish knockdown efficiency ([Figure 3.17](#)).

In this study, the siRNA-mediated gene knockdown technique was used to study the loss-of-function of ER $\beta$  on anti-inflammatory properties of compounds 3 and 4. Therefore, 24 hours after knockdown experiments, the Opti-MEM medium was changed to serum-free RPMI followed by 2 hours incubation in 37°C. Subsequently, cells were treated with compounds 3 and 4 and stimulated with 100 ng/ml of LPS as described in [3.2.1](#). After 24-hour incubation cell supernatants were collected, and TNF $\alpha$  and IL-6 ELISAs were conducted as indicated in [2.2.4](#).

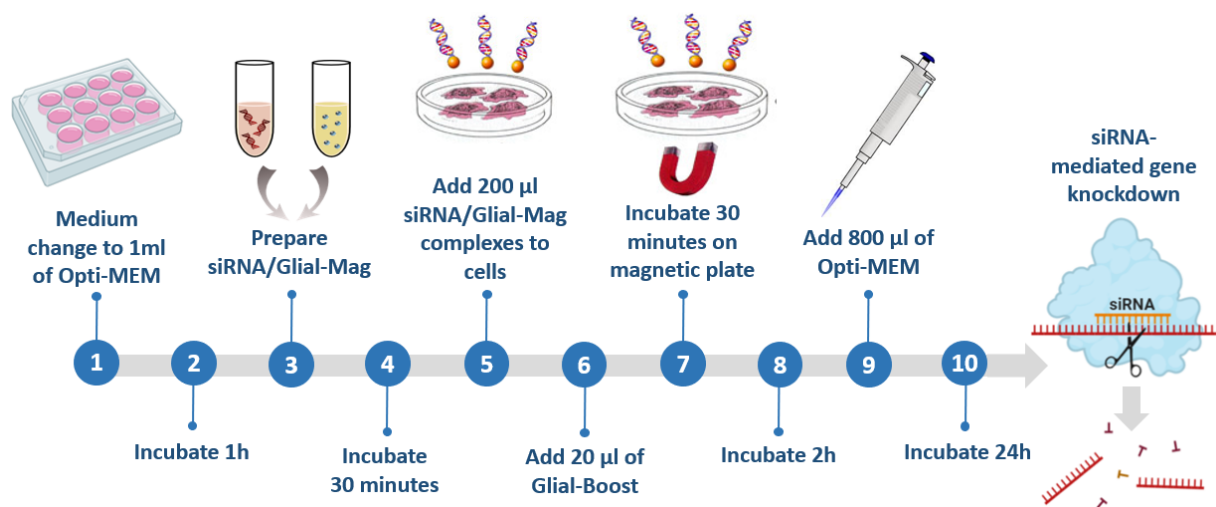


Figure 3.4 Flowchart of siRNA-mediated gene knockdown.

### 3.2.13 Statistical analysis

Statistical analysis was performed as described in chapter two, section [2.2.12](#).

### 3.3 Results

#### 3.3.1 The effect of compounds 3 and 4 on BV2 cell viability using XTT

XTT assay was performed to examine if compounds show direct cytotoxic effects in BV2 microglia. Cells were incubated with compounds 3 (2.5, 5 and 10  $\mu\text{M}$ ) and 4 (5, 10 and 20  $\mu\text{M}$ ) for 30 minutes followed by 24-hour stimulation with 100 ng/ml of LPS. XTT assay demonstrated that compounds 3 and 4 did not affect the viability of BV2 cells at any of the tested concentrations (Figure 3.5). There was no significant difference in the viability of BV2 cells between control untreated cells and compound 3 and 4 pre-incubated BV2 cells.

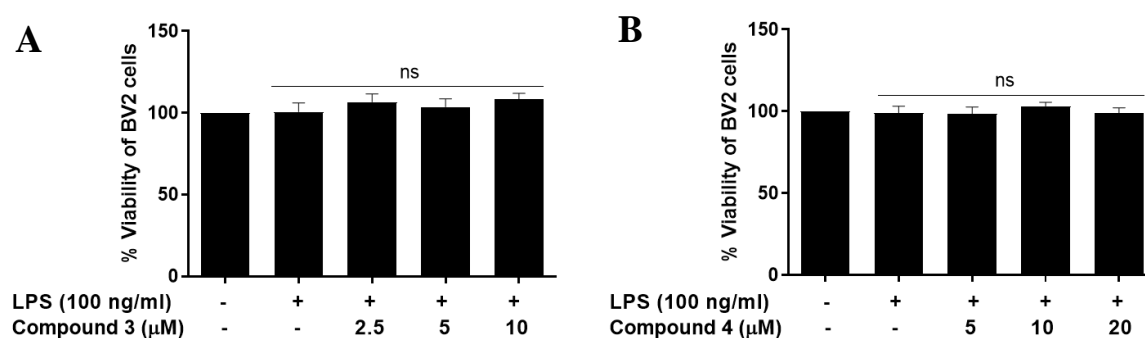


**Figure 3.5** The effect of compounds 3 and 4 on the viability of BV2 using XTT. BV2 cells were incubated with or without compounds 3 (2.5, 5 and 10  $\mu\text{M}$ ) and 4 (5,10 and 20  $\mu\text{M}$ ) for 30 minutes and then activated with LPS (100 ng/ml). Subsequently, BV2 cells were incubated for 24 hours, and XTT assay was performed. Compounds 3 (A) and 4 (B) did not significantly reduce the viability of BV2 microglia. All values are expressed as mean  $\pm$  SEM for N=3. Data were analysed using one-way ANOVA for multiple comparisons with post hoc Student Newman-Keuls test. \* $p < 0.033$  in comparison to untreated control.

### 3.3.2 The effects of compounds 3 and 4 on TNF $\alpha$ , IL-6 and IL-1 $\beta$ production in LPS activated BV2 cells

Increased production of pro-inflammatory cytokines is the central characteristic of neuroinflammation and neurodegeneration (Mrak & Griffin, 2005). Hence cytokines level is often used as an indicator of the severity of inflammation and helps estimate biological response to treatment. Therefore, to determine anti-inflammatory properties of compounds 3 and 4, BV2 cells were treated with compounds 3 (2.5, 5 and 10  $\mu$ M) and 4 (5, 10 and 20  $\mu$ M) for 30 minutes. Then cell inflammation was induced with 100 ng/ml of LPS followed by 24-hour incubation and detection of cytokines using ELISAs.

Untreated cells produced low amounts of pro-inflammatory cytokines TNF $\alpha$ , IL-6, and IL-1 $\beta$ , which were significantly ( $p < 0.001$ ) increased by 24-hour LPS stimulation. Compound 3 at 2.5, 5 and 10  $\mu$ M significantly ( $p < 0.001$ ) inhibited production of TNF $\alpha$  in LPS-activated microglia to  $59.4 \pm 5.6\%$ ,  $47.9 \pm 10.5\%$ ,  $44 \pm 13.5\%$ , respectively, compared to LPS control value of 100% (Figure 3.6 A). Compound 4 also significantly ( $p < 0.001$ ) suppressed TNF $\alpha$  level to  $32.1 \pm 4.1\%$ ,  $29.4 \pm 2.2\%$  and  $27.1 \pm 2.4\%$  from control value of 100% when used at 5, 10, and 20  $\mu$ M, respectively (Figure 3.6 B).

Compound 3 at 2.5, 5 and 10  $\mu$ M in a concentration-dependent manner significantly ( $p < 0.01$ ,  $p < 0.001$ ) decreased IL-6 production to  $63.1 \pm 10\%$ ,  $44.3 \pm 3.7\%$ , and  $32.6 \pm 8.2\%$ , respectively compared to LPS control value of 100% (Figure 3.6 C). Compound 4 at 5, 10 and 20  $\mu$ M significantly ( $p < 0.001$ ) reduced the level of IL-6 to  $17.4 \pm 3.1\%$ ,  $15.8 \pm 2.4\%$ , and  $15.9 \pm 1.6\%$ , respectively, when compared to LPS control value of 100% (Figure 3.6 D).

Compound 3 at 5, 10, and 20  $\mu$ M in a concentration-dependent manner significantly ( $p < 0.033$ ) suppressed the production of IL-1 $\beta$  to  $68.2 \pm 7.8\%$ ,  $61.9 \pm 5.4\%$ , and  $57.7 \pm 9\%$ , respectively, compared to LPS control value of 100% (Figure 3.6 E). The effect of compound 4 followed a similar pattern with the significant ( $p < 0.001$ ) inhibition of LPS-induced production of IL-1 $\beta$  to  $43 \pm 7.2\%$ ,  $46.9 \pm 5.6\%$  and  $47.5 \pm 3.3\%$  from control value of 100% when used at 5, 10, 15 and 20  $\mu$ M, respectively (Figure 3.6 F).



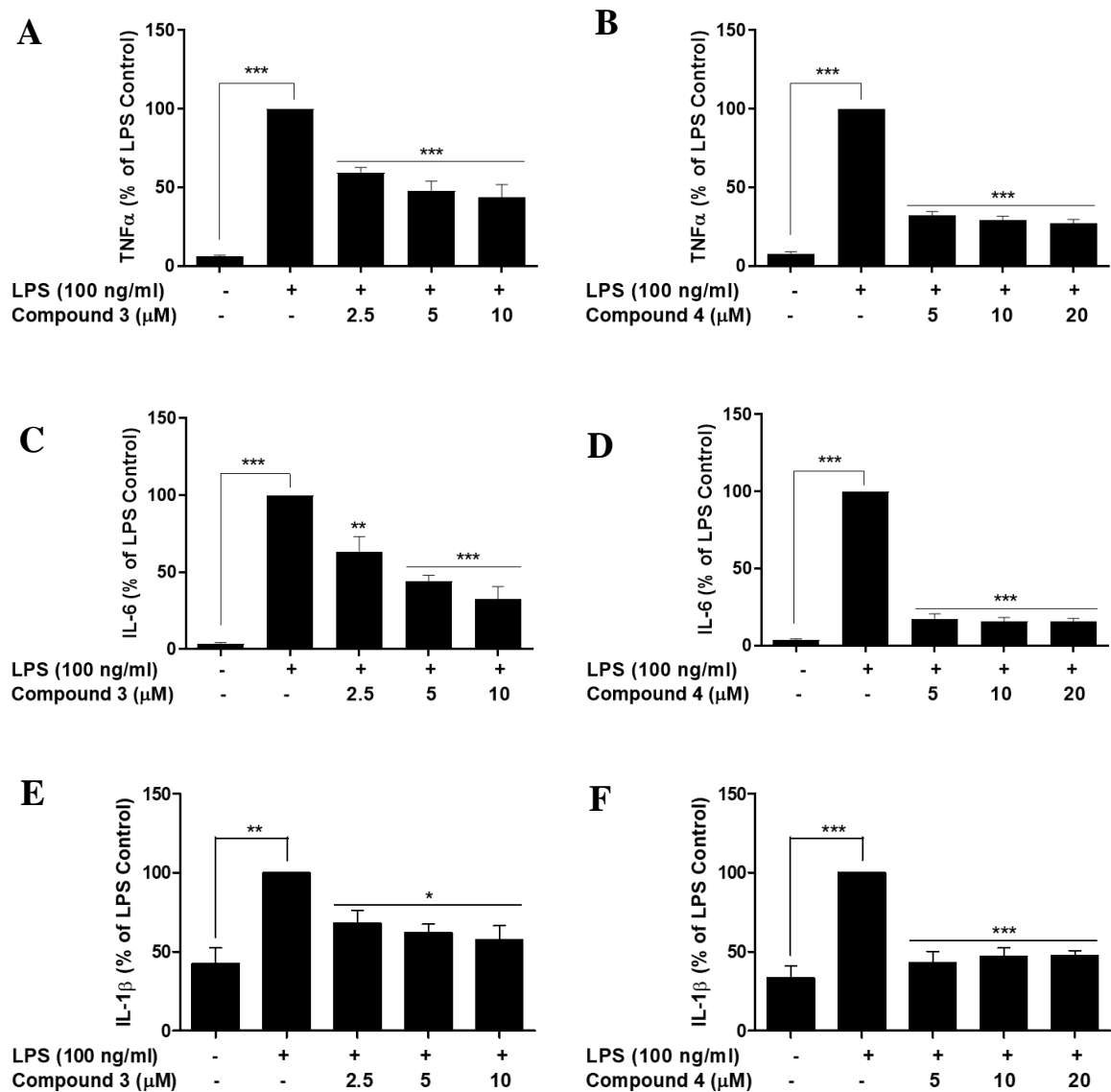


**Figure 3.6** The effects of compounds 3 and 4 on the production of TNF $\alpha$ , IL-6 and IL-1 $\beta$  in LPS-induced BV2 cells. BV2 microglia were pre-incubated for 30 minutes with compounds 3 (2.5 – 10  $\mu$ M) and 4 (5 – 20  $\mu$ M) and then activated with LPS (100 ng/ml) for 24h. After incubation, supernatants were collected, and ELISAs were performed. Compound 3 and 4 significantly at all tested concentrations reduced production of TNF $\alpha$  (A and B), IL-6 (C and D), and IL-1 $\beta$  (E and F) in LPS-activated microglia. All values are expressed as a mean  $\pm$  SEM for N=3. Data were analysed using one-way ANOVA for multiple comparisons with post hoc Student Newman-Keuls test. \* $p$ <0.033, \*\* $p$ <0.002, \*\*\* $p$ <0.001 in comparison with LPS control.

### **3.3.3 The effects of compounds 3 and 4 on nitrite and iNOS production in LPS-activated BV2 microglia**

Nitrite is stable biodegradation product of nitric oxide; production of which is catalysed by iNOS during neuroinflammation (Yuste et al., 2015). To determine if compounds 3 and 4 have the ability to alleviate inflammation, BV2 cells were stimulated with 100 ng/ml of LPS in the presence or absence of compound 3 (2.5, 5 and 10  $\mu$ M) or 4 (5, 10 and 20  $\mu$ M) for 24 hours. After incubation, Griess assay and immunoblotting were performed. Untreated microglia produced low physiological amounts of nitrite and iNOS. Whereas LPS stimulation significantly ( $p < 0.001$ ) increased the level of nitrite approximately 3.6-fold and iNOS approximately 27.7-fold compared to untreated cells.

Compound 3 at 2.5, 5 and 10  $\mu$ M in a concentration-dependent manner significantly ( $p < 0.001$ ) suppressed LPS-induced nitrite production to  $75.5 \pm 3.2\%$ ,  $68.2 \pm 1.5\%$ ,  $48.5 \pm 0.4\%$ , respectively, when compared to LPS control value of 100% (Figure 3.7 A). Similarly compound 3 significantly ( $p < 0.001$ ) inhibited LPS-induced iNOS level to  $27.1 \pm 4.9\%$ ,  $23.2 \pm 14\%$  and  $14.3 \pm 11.5\%$  from control value of 100% when used at 2.5, 5 and 10  $\mu$ M, respectively (Figure 3.7 B).

Compound 4 at 5, 10 and 20  $\mu$ M in a concentration-dependent manner significantly ( $p < 0.001$ ) reduced LPS-induced nitrite production to  $68.8 \pm 5.3\%$ ,  $63 \pm 5.1\%$ ,  $58.2 \pm 1.2\%$ , respectively, compared to LPS control value of 100% (Figure 3.7 C). Similarly, compound 4 significantly ( $p < 0.001$ ) suppressed iNOS level to  $8.2 \pm 2.8\%$ ,  $6 \pm 2.4\%$  and  $4.8 \pm 2\%$  from control value of 100% when used at 5, 10 and 20  $\mu$ M, respectively (Figure 3.7 D).

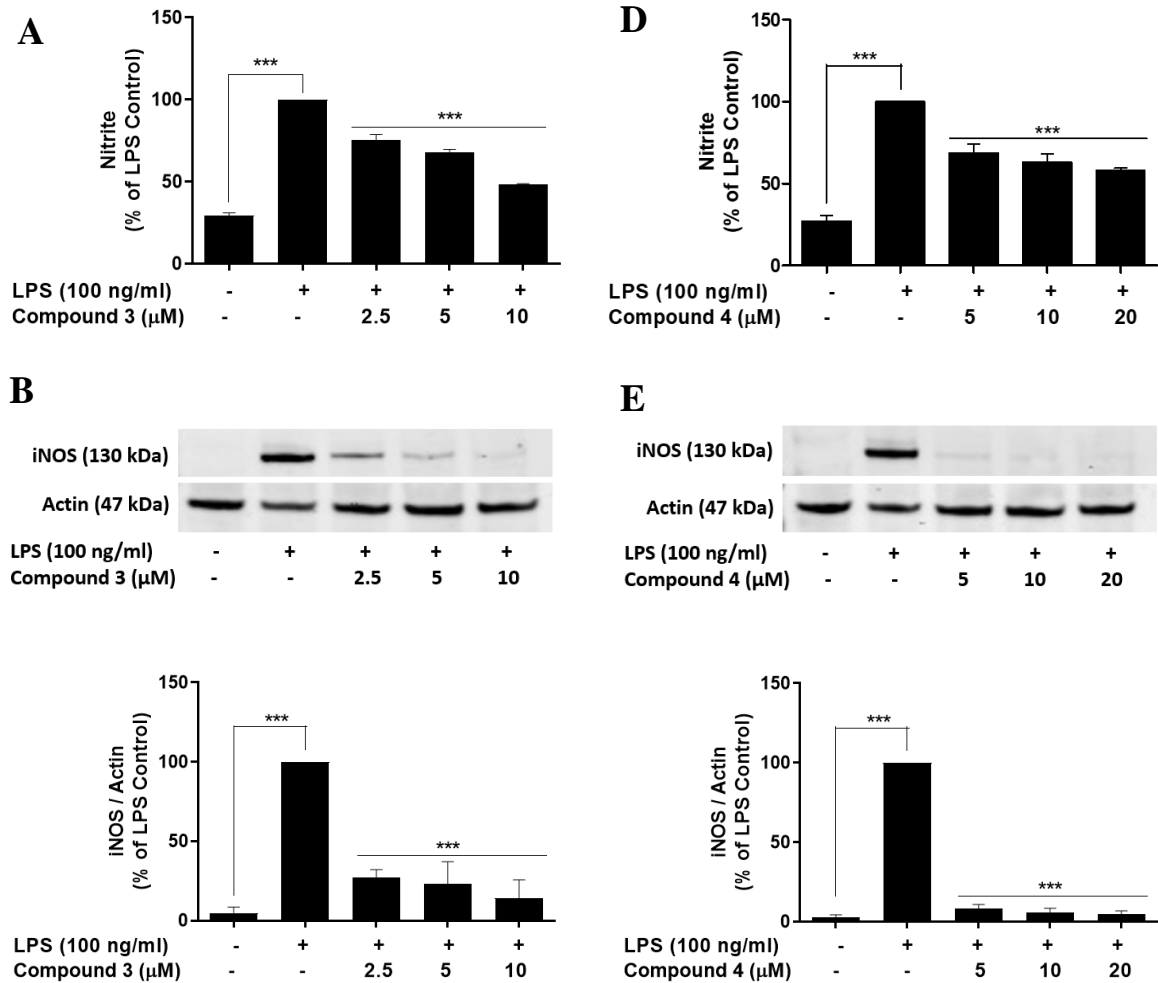


**Figure 3.7** The effects of compounds 3 and 4 on nitrite and iNOS production in LPS activated BV2 cells. Cells were treated with compounds 3 (2.5 – 10  $\mu$ M) and 4 (5 – 20  $\mu$ M) for 30 minutes and then activated with LPS (100 ng/ml) for 24 hours after incubation supernatants, and cell lysates were collected for Griess assay and immunoblotting experiments. Compound 3 (A and B) significantly ( $p < 0.001$ ) in a concentration-dependent manner reduced level of nitrite and iNOS. Compound 4 (C and D) significantly ( $p < 0.001$ ) inhibited LPS-induced production of nitrite and iNOS. Actin has been used as a loading control. All values are expressed as a mean  $\pm$  SEM for N=3. Data were analysed using one-way ANOVA for multiple comparisons with post hoc Student Newman-Keuls test. \*\*\* $p < 0.001$  in comparison with LPS control.

### 3.3.4 Evaluation of free-radical scavenging properties of compounds 3 and 4

Neuroinflammation induces oxidative stress leading to the production of free radical molecules which are highly reactive with cellular structures. Hence, compounds which directly neutralise free radicals inhibit the oxidation process, a chemical reaction that can cause cell damage (Arulselvan et al., 2016). Free radical scavenging properties of compounds 3 (2.5, 5 and 10  $\mu\text{M}$ ) and 4 (5, 10 and 20  $\mu\text{M}$ ) were assessed using DPPH assay. Figure 3.8 indicates that compounds 3 and 4 did not scavenge DPPH free radical at any of the tested concentrations, whereas L-ascorbic acid in a concentration-dependent manner neutralised DPPH radical.

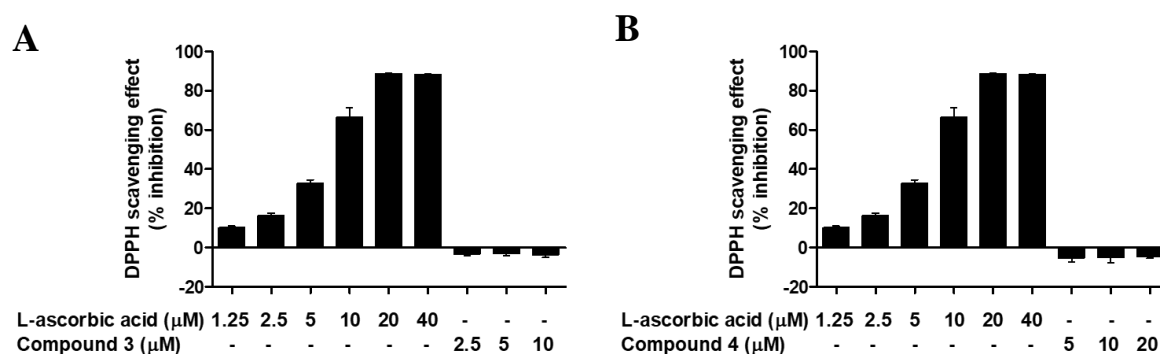


**Figure 3.8 DPPH scavenging effect of compounds 3 and 4.** Compounds 3 (2.5, 5 and 10  $\mu\text{M}$ ) and 4 (5, 10 and 20  $\mu\text{M}$ ) were added to 50  $\mu\text{M}$  of DPPH solution followed by 30 minutes incubation and absorbance reading. L-(+)-Ascorbic acid (1.25 – 40  $\mu\text{M}$ ) was used as control positive. Compounds 3 (A) and 4 (B) did not neutralise free DPPH radical at any of the tested concentrations. DPPH scavenging effect (% inhibition) was calculated using formula:  $\text{DPPH scavenging effect (\% inhibition)} = ((A_0 - A_1) / A_0) * 100$ . Where:  $A_1$  indicates the absorbance of the sample and  $A_0$  indicates the absorbance of the control (methanol solution of DPPH). All values are expressed as a mean  $\pm$  SEM for  $N=3$ .

### 3.3.5 The effects of compounds 3 and 4 on PGE<sub>2</sub> and COX-2 expression in LPS-induced BV2 microglia

PGE<sub>2</sub> is a principal inflammatory mediator generated by COX-2 from arachidonic acid. Nonsteroidal anti-inflammatory drugs (NSAIDs) directly target COX-2, reducing PGE<sub>2</sub> and mitigating inflammation (Johansson et al., 2015). To assess the effects of compounds 3 and 4 on PGE<sub>2</sub> and COX-2, BV2 cells were incubated with compounds for 30 minutes. Then cells were activated with 100 ng/ml of LPS for 24 hours, followed by PGE<sub>2</sub> enzyme immunoassay and COX-2 immunoblotting. Untreated cells produced low levels of PGE<sub>2</sub> and COX-2 which were significantly ( $p < 0.001$ ;  $p < 0.002$ ) increased after LPS-induced activation.

Compound 3 did not significantly alter LPS-induced PGE<sub>2</sub> and COX-2 production in BV2 cells (Figure 3.9 A and B). After incubation of cells with compound 3 at 2.5, 5 and 10  $\mu\text{M}$

PGE<sub>2</sub> level was 123 ± 17%, 130 ± 14% and 126 ± 11%, respectively. Similarly, COX-2 level was not significantly affected by compound 3; its level was 95 ± 9%, 110 ± 11% and 131 ± 10%, after pre-treatment with 2.5, 5 and 10 μM of compound 3, respectively, compared to LPS control value of 100%.

Data presented in Figure 3.9 C show that compound 4 at 5, 10 and 20 μM not significantly decreased PGE<sub>2</sub> level to 89 ± 12%, 82 ± 5% and 75 ± 4%, respectively, compared to LPS control value of 100%. Compound 4 not significantly increased LPS-induced COX-2 protein level, after treatment with 5, 10 and 20 μM of compound 4 COX-2 level was 107 ± 12%, 114 ± 11%, and 105 ± 7%, respectively, compared to LPS control value of 100% (Figure 3.9 D).

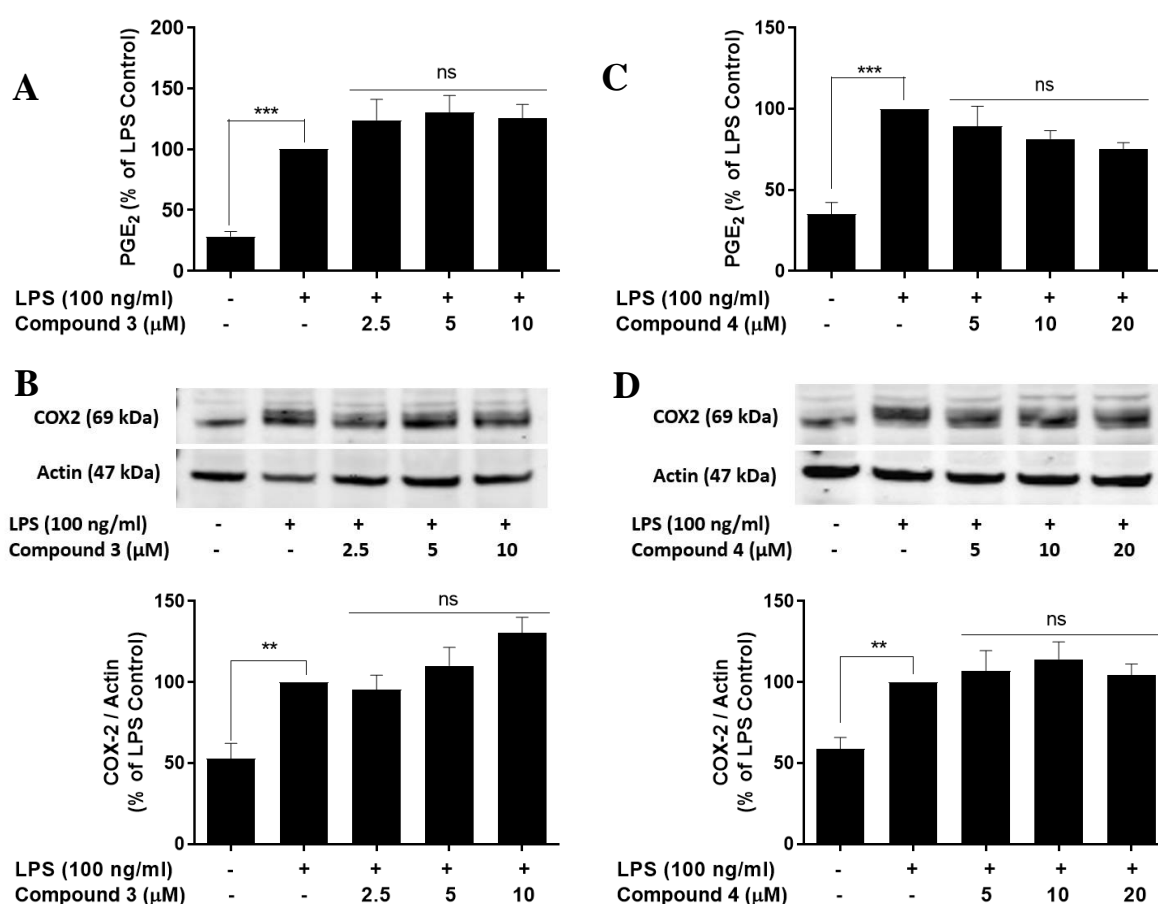


**Figure 3.9** The effects of compounds 3 and 4 on PGE<sub>2</sub> and COX-2 expression in LPS activated BV2 microglia. BV2 were incubated for 30 minutes with or without compounds 3 (2.5, 5 and 10 μM) and 4 (5, 10 and 20 μM) followed by 24-hour incubation with LPS (100 ng/ml). Next day cell culture supernatants and cell lysates were collected for PGE<sub>2</sub> enzyme immunoassay and Western blotting. Actin used as a loading control. Compound 3 did not significantly inhibit PGE<sub>2</sub> and COX-2 production at all tested concentrations in LPS activated BV2 cells. Incubation with compound 4 also did not significantly decrease PGE<sub>2</sub> and COX-2 protein level in LPS-activated BV2 microglia. Actin has been used as a loading control. All values are expressed as a mean ± SEM for a minimum of N=3. Data were analysed using one-way ANOVA for multiple comparisons with post hoc Student Newman-Keuls test. \*p<0.033, \*\*p<0.002, \*\*\*p<0.001 in comparison with LPS control.

### 3.3.6 The effect of compounds 3 and 4 on LPS-induced NF- $\kappa$ B activation in BV2 cells

An NF- $\kappa$ B signalling pathway is considered a crucial regulator of inflammatory response. This pathway regulates the transcription of many inflammatory-related proteins (Shih et al., 2015). Therefore, encouraged by the ability of compounds 3 and 4 to reduce pro-inflammatory mediators, the effect of compounds on NF- $\kappa$ B activation in BV2 cells was investigated. The ability of compounds to inhibit the NF- $\kappa$ B pathway was assessed by the impact of compounds on phosphorylation of NF- $\kappa$ B p65 followed by the investigation of the NF- $\kappa$ B promoter activity in LPS-activated BV2 cells.

#### 3.3.6.1 The effect of compounds 3 and 4 on LPS-induced phosphorylation of NF- $\kappa$ B p65 in BV2 cells

To determine effect of compounds on LPS-induced phosphorylation of NF- $\kappa$ B p65, BV2 cells were pre-incubated with or without compound 3 (2.5, 5 and 10  $\mu$ M) or 4 (5, 10 and 20  $\mu$ M) for 30 minutes followed by LPS (100 ng/ml) stimulation for 60 minutes. Sixty-minutes incubation was selected based on time-course experiment showing the highest LPS-induced p-NF- $\kappa$ B level at this time point (Figure 2.22). ELISA experiment indicated that LPS activated cells significantly ( $p < 0.002$ ) increased p-NF- $\kappa$ B p65 level compared to untreated cells. Data presented in Figure 3.10 A show that compound 3 did not significantly inhibit the phosphorylation of NF- $\kappa$ B p65 in LPS activated BV2 cells when compared to LPS control. In turn, cells incubated with 5, 10 and 20  $\mu$ M of compound 4 significantly ( $p < 0.002$ ) decreased LPS-induced phosphorylation of NF- $\kappa$ B p65 to  $71 \pm 6\%$ ,  $66 \pm 6\%$  and  $59 \pm 8\%$ , respectively, when compared to LPS control value of 100% (Figure 3.10 B).

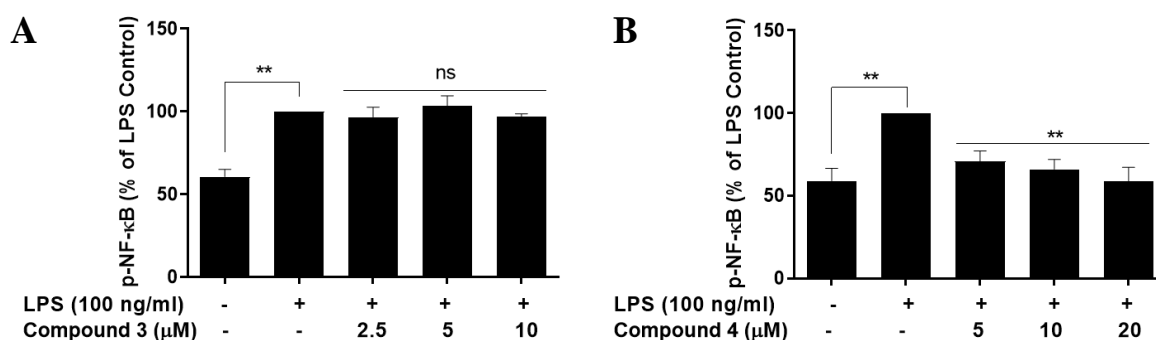


**Figure 3.10** The effect of compounds 3 and 4 on p-NF- $\kappa$ B p65 level in LPS activated cells. Cells were treated with or without compounds 3 (2.5, 5 and 10  $\mu$ M) and 4 (5, 10 and 20  $\mu$ M) and then stimulated with LPS (100 ng/ml) for 60 minutes. After incubation cell lysates were collected, and p-NF- $\kappa$ B ELISA was conducted. Compound 3 did not significantly decrease the level of p-NF- $\kappa$ B p65 in LPS-activated BV2 cells, whereas compound 4 ( $p < 0.002$ ) inhibited phosphorylation of NF- $\kappa$ B p65 at all tested concentrations. All values are

expressed as a mean  $\pm$  SEM for N=3. Data were analysed using one-way ANOVA for multiple comparisons with post hoc Student Newman-Keuls test. \*\*p<0.002 in comparison with LPS control.

### 3.3.6.2 The effect of compounds 3 and 4 on NF- $\kappa$ B LPS-induced activity in BV2 microglia

The impact of compounds 3 and 4 on NF- $\kappa$ B promoter activity was examined using LPS activated BV2 microglia. BV2 cells were transfected with NF- $\kappa$ B transcription reporter vector encoding firefly luciferase with constitutively active reporter encoding *Renilla* luciferase. Transfected cells were incubated with or without compounds 3 (2.5, 5 and 10  $\mu$ M) and 4 (5, 10 and 20  $\mu$ M) for 30 minutes followed by LPS (100 ng/ml) stimulation for eight hours. Eight-hour incubation was selected based on time-course experiment showing the highest NF- $\kappa$ B luciferase activity eight hours after LPS stimulation (Figure 2.25). Pre-incubation of BV2 cells with compound 3 did not significantly reduce LPS-induced NF- $\kappa$ B luciferase activity at any tested concentration (Figure 3.11 A). In turn, pre-incubation of BV2 microglia with 10 and 20  $\mu$ M of compound 4 significantly (p<0.002) inhibited NF- $\kappa$ B luciferase activity to  $79 \pm 5\%$  and  $73 \pm 4\%$ , respectively, compared to LPS control value of 100% (Figure 3.11 B).

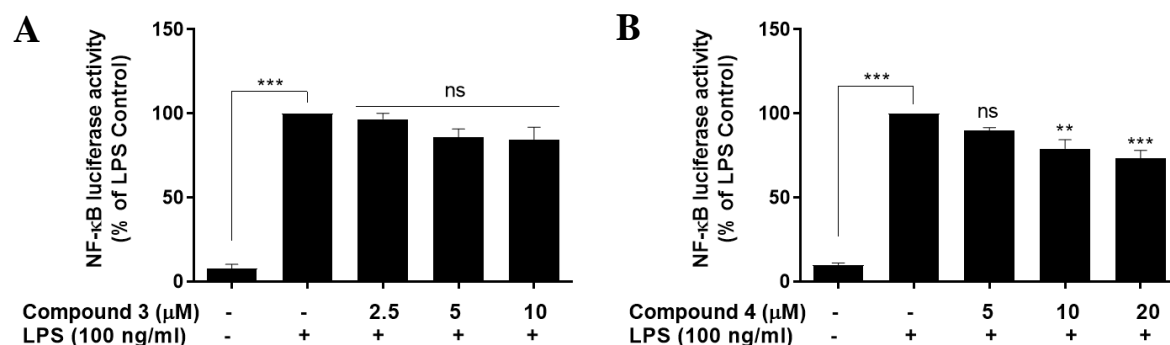


**Figure 3.11 The effect of compounds 3 and 4 on NF- $\kappa$ B activity in LPS stimulated BV2 cells.** BV2 cells were transfected with NF- $\kappa$ B transcription reporter encoding firefly luciferase and a constitutively active reporter encoding *Renilla* luciferase. After 20-hour incubation medium was changed and cells were treated with compounds 3 (2.5, 5 and 10  $\mu$ M) and 4 (5, 10 and 20  $\mu$ M) for 30 minutes followed by LPS stimulation for 8 hours. After incubation, The Dual-Glo Luciferase assay used to quantify NF- $\kappa$ B firefly luciferase and control reporter *Renilla* luciferase activities in transfected cells. Pre-incubation with compounds 3 (5 and 10  $\mu$ M) did not reduce NF- $\kappa$ B luciferase activity. In turn, pre-incubation with 4 (10 and 20  $\mu$ M) significantly reduced LPS-induced NF- $\kappa$ B promoter activity. Data are presented as a ratio of experimental / control reporter. All values are expressed as a mean  $\pm$  SEM for N=3. Data were analysed using one-way ANOVA for multiple comparisons with post hoc Student Newman-Keuls test. \*p<0.033, \*\*p<0.002, \*\*\*p<0.001 in comparison with LPS control.

### 3.3.7 The effect of compounds 3 and 4 on LPS-induced MAPKs activation in BV2 microglia

Besides NF- $\kappa$ B, another pathway which plays a crucial role in directing cellular responses to neuroinflammation is MAPKs. MAPKs can be distinguished into p38, JNK and ERK1/2. Inhibition of MAPKs has been attributed to the reduction of cytokines (Kaminska, Gozdz, Zawadzka, Ellert-Miklaszewska, & Lipko, 2009; Malgorzata, Weronika, Beata, Marek, & Ada, 2009). Therefore, to investigate the effect of compounds 3 and 4 on activation of MAPKs, BV2 cells were treated with compounds 3 and 4 for 30 minutes followed by 60 minutes activation with 100 ng/ml of LPS and p-p38, p-JNK and p-ERK1/2 detection. Sixty-minutes incubation was selected based on time-course experiments showing the highest LPS-induced p-38, p-JNK and p-ERK1/2 level at this time point (Figure 2.28, Figure 2.30 and Figure 2.32).

#### 3.3.7.1 The effect of compounds 3 and 4 on LPS-induced p-38 phosphorylation

ELISA experiment demonstrates that untreated cells contained a low level of p-p38 which were significantly ( $p < 0.002$ ) unregulated after 60-minutes LPS (100 ng/ml) stimulation. Pre-incubation of BV2 microglia with compound 3 at 2.5, 5 and 10  $\mu$ M not significantly decreased LPS-induced p-p38 level to  $109 \pm 3\%$ ,  $99 \pm 4\%$  and  $81 \pm 7\%$ , respectively, compared to LPS control value of 100% (Figure 3.12 A). Similarly, pre-incubation with compound 4 at 5, 10 and 20  $\mu$ M also not significantly reduced p-p38 protein level, to  $94 \pm 5.8\%$ ,  $90 \pm 3\%$  and  $89 \pm 5.6\%$ , respectively, compared to LPS control value of 100% (Figure 3.12 B).

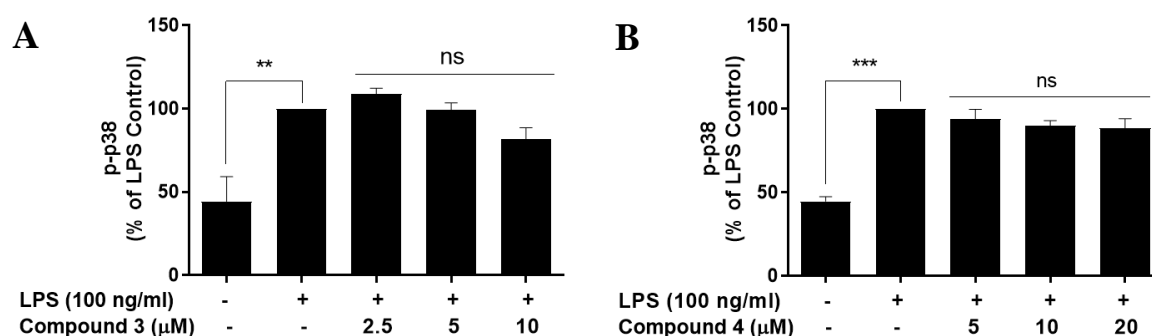


**Figure 3.12** The effect of compounds 3 and 4 on LPS-induced p-38 phosphorylation in BV2 microglia. BV2 cells were treated with or without compounds 3 (2.5, 5 and 10  $\mu$ M) and 4 (5, 10 and 20  $\mu$ M) and then stimulated with LPS (100 ng/ml) for 60 minutes. After incubation, cell lysates were collected for p-p38 ELISA. Compound 3 did not significantly reduce LPS-induced p38 phosphorylation at any of the tested concentrations. Similarly, compound 4 also did not significantly inhibit p38 phosphorylation in LPS activated BV2 cells. All values are expressed as a mean  $\pm$  SEM for N=3. Data were analysed using one-way ANOVA for multiple comparisons with post hoc Student Newman-Keuls test. \* $p < 0.033$ , \*\* $p < 0.002$ , \*\*\* $p < 0.001$  in comparison with LPS control.



### 3.3.7.2 The effect of compounds 3 and 4 on LPS-induced JNK phosphorylation

Immunoblotting for p-JNK shows that BV2 untreated cells produced a low level of p-JNK which was significantly ( $p < 0.002$ ) increased by 60 LPS (100 ng/ml) activation. Pre-incubation of BV2 cells with compound 3 did not significantly alter p-JNK level; after incubation with 2.5, 5 and 10  $\mu\text{M}$  of compound 3 p-JNK was  $134 \pm 6\%$ ,  $135 \pm 19\%$  and  $132 \pm 21\%$ , respectively, compared to LPS control value of 100% (Figure 3.13 A). Similarly, cells pre-incubated with 5, 10 and 20  $\mu\text{M}$  of compound 4 did not significantly decrease LPS-induced phosphorylation of JNK; p-JNK protein level was  $111 \pm 5\%$ ,  $109 \pm 8\%$  and  $105 \pm 8\%$ , respectively, compared to LPS control value of 100% (Figure 3.13 B).

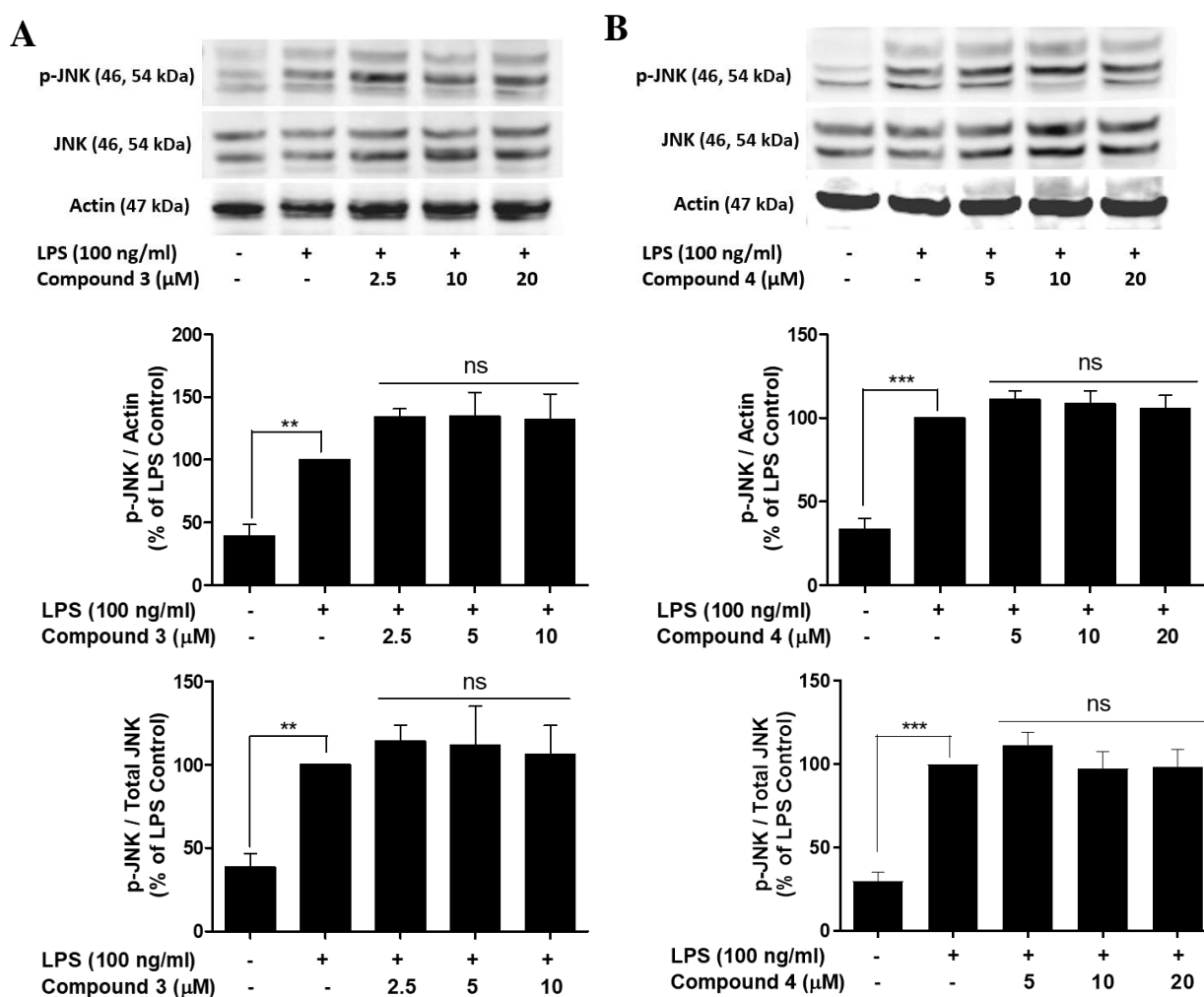


**Figure 3.13** The effect of compounds 3 and 4 on the p-JNK level in LPS activated BV2 cells. Cells were treated with or without compounds 3 (2.5, 5 and 10  $\mu\text{M}$ ) and 4 (5, 10 and 20  $\mu\text{M}$ ) and then stimulated with LPS (100 ng/ml). After 60 minutes incubation with LPS cell lysates were collected and for immunoblotting experiments. Compound 3 and 4 did not significantly decrease the level of p-JNK in LPS-activated BV2 cells. Actin and total JNK was used as a loading control. All values are expressed as a mean  $\pm$  SEM for  $N=3$ . Data were analysed using one-way ANOVA for multiple comparisons with post hoc Student Newman-Keuls test. \*\* $p < 0.002$ , \*\*\* $p < 0.001$  in comparison with LPS control.

### 3.3.7.3 The effect of compounds 3 and 4 on LPS-induced ERK1/2 phosphorylation

LPS-activated BV2 cells significantly ( $p < 0.033$ ) upregulated p-ERK1/2 protein level compared to untreated cells. Pre-incubation of BV2 microglia with compound 3 at 2.5, 5 and 10  $\mu\text{M}$  not significantly increased p-ERK1/2 level to  $120 \pm 5\%$ ,  $117 \pm 11\%$  and  $117 \pm 10\%$ , respectively, compared to LPS control value of 100% (Figure 3.14 A). Whereas pre-incubation of cells with compound 4 at 5, 10 and 20  $\mu\text{M}$  not significantly decreased LPS-induced p-ERK1/2 level to  $93 \pm 13\%$ ,  $98 \pm 10\%$  and  $75 \pm 4\%$ , respectively, compared to LPS control value of 100% (Figure 3.14 B).

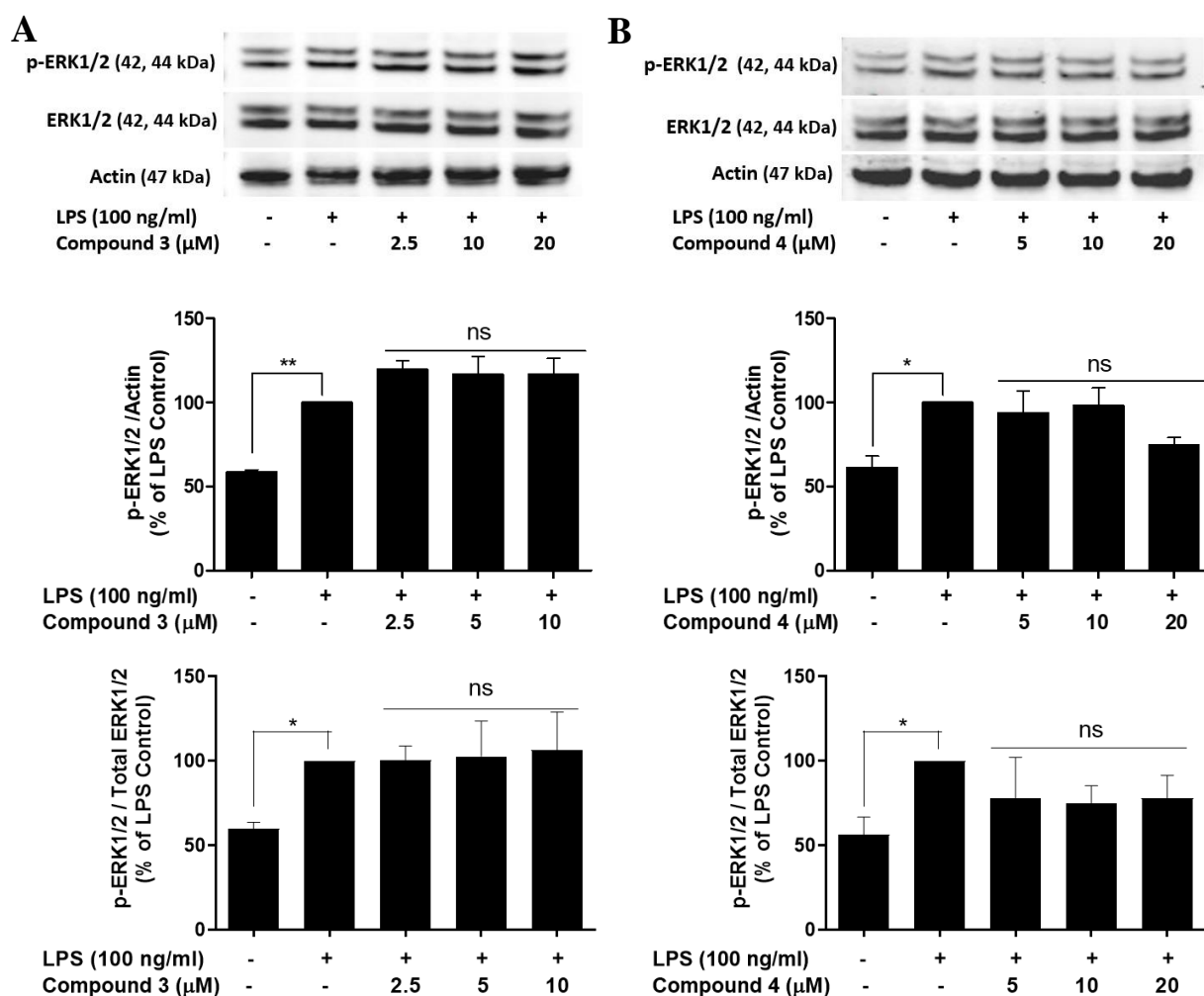


**Figure 3.14** The effect of compounds 3 and 4 on ERK1/2 phosphorylation in LPS activated BV2 cells. Cells were pre-treated with compounds 3 (2.5, 5 and 10  $\mu\text{M}$ ) and 4 (5, 10 and 20  $\mu\text{M}$ ) and then stimulated with LPS (100 ng/ml) for 60 minutes. After incubation cell lysates were collected, and Western blotting was performed. BV2 activated with LPS increased ERK1/2 phosphorylation when compared to untreated cells. Pre-incubation with compounds 3 (A) and 4 (B) did not significantly alter LPS-induced ERK1/2 phosphorylation. Actin and total ERK1/2 was used as a loading control. All values are expressed as a mean  $\pm$  SEM for N=3. Data were analysed using one-way ANOVA for multiple comparisons with post hoc Student Newman-Keuls test. \* $p < 0.033$ , \*\* $p < 0.002$  in comparison with LPS control.

### 3.3.8 The effect of compounds 3 and 4 on ERE activity in BV2 microglia

This study is investigating daidzein analogues, which parental compound - daidzein has shown to activate ERE. Moreover, ERE activation is considered to produce anti-inflammatory actions. Therefore, to establish if compounds 3 and 4 upregulate ERE promoter, BV2 cells were transfected with ERE reporter vector encoding firefly luciferase and a constitutively active reporter encoding *Renilla* luciferase. Time-course experiment showed that compounds 3 and 4 induced the highest ERE activity after 24-hour exposure - approximately 3.8-fold and 3.6-fold increase, respectively. Therefore, further experiments assessing ERE activity were conducted after 24-hour incubation. Figure 3.16 A indicates that compound 3 at 5 and 10  $\mu\text{M}$  significantly ( $p < 0.033$ ) increased (~2.3-fold) ERE activity when compared to untreated cells. Compound 4 at 5, 10 and 20  $\mu\text{M}$  also significantly ( $p < 0.033$ ) upregulated (~2.7-fold) ERE promoter activity compared to untreated cells (Figure 3.16 B).

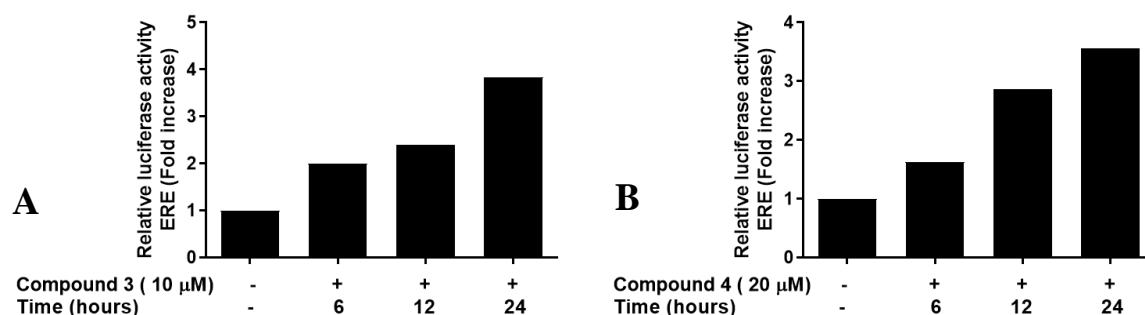


**Figure 3.15 Effects of compound 3 and 4 on the ERE activity at different time points.** Transfected BV2 with ERE and *Renilla* reporter were treated with compounds 3 – 10  $\mu\text{M}$  (A) or compound 4 – 20  $\mu\text{M}$  (B) for different time periods and firefly, and *Renilla* luminescence was quantified. Compounds 3 and 4 increased ERE activity in a time-dependent manner with the highest activity at 24 hours. ERE reporter activity was normalized to *Renilla* co-reporter.

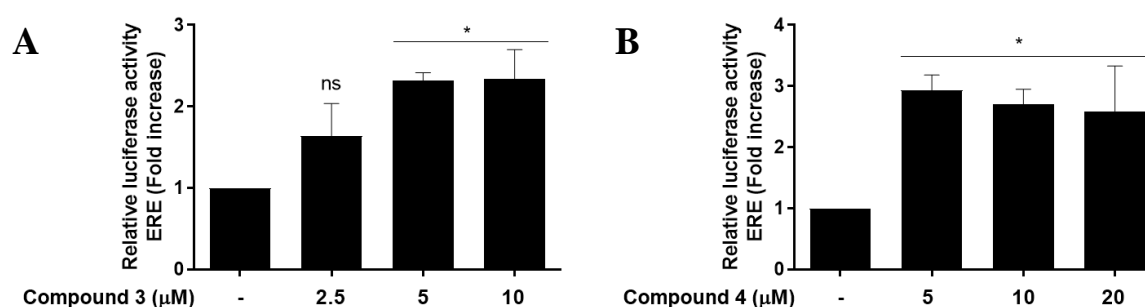


**Figure 3.16 The effect of compounds 3 and 4 on ERE activity in BV2 microglia.** BV2 cells were transfected with ERE reporter and then incubated with compounds 3 (2.5, 5 and 10  $\mu\text{M}$ ) and 4 (5, 10 and 20  $\mu\text{M}$ ) for 24 hours. After incubation, The Dual-Glo Luciferase assay used to quantify firefly and *Renilla* luciferase activities in transfected cells. Compounds 3 significantly in a concentration-dependent manner for concentrations 2.5 – 5  $\mu\text{M}$  increased ERE activity. Compound 4 also significantly ( $p < 0.033$ ) upregulated ERE activity. ERE reporter activity was normalized to *Renilla* co-reporter. Data are presented as a ratio of experimental/control reporter. All values are expressed as a mean  $\pm$  SEM for N=3. Data were analysed using one-way ANOVA for multiple comparisons with post hoc Student Newman-Keuls test. \* $p < 0.033$  in comparison with untreated control.

### 3.3.9 The impact of ER antagonism on anti-inflammatory properties of compounds 3 and 4 in BV2 microglia

Compounds 3 and 4 showed the ability to reduce pro-inflammatory cytokines in LPS-activated BV2 cells. Hence, to examine if those properties are ER-dependent, cells were pre-incubated with ER antagonist - ICI 182,780 (10 nM) for 30 minutes followed by treatment with compounds 3 and 4 and LPS (100 ng/ml) stimulation and TNF $\alpha$  and IL-6 ELISAs. Untreated cells produced low physiological amounts of TNF $\alpha$  and IL-6, which were significantly increased in LPS-activated cells incubated with or without ICI 182,789. Compound 3 in cells pre-incubated with ICI 182,780 did not lose the ability to reduce TNF $\alpha$ , and IL-6 production in LPS activated cells (Figure 3.17 A and B). Similarly, compound 4 in the presence or absence of ICI 182,780 significantly ( $p < 0.001$ ) diminished LPS-induced TNF $\alpha$  and IL-6 production (Figure 3.17 C and D). ER antagonist did not affect compounds 3 and 4 ability to reduce LPS-induced TNF $\alpha$  and IL-6 production.

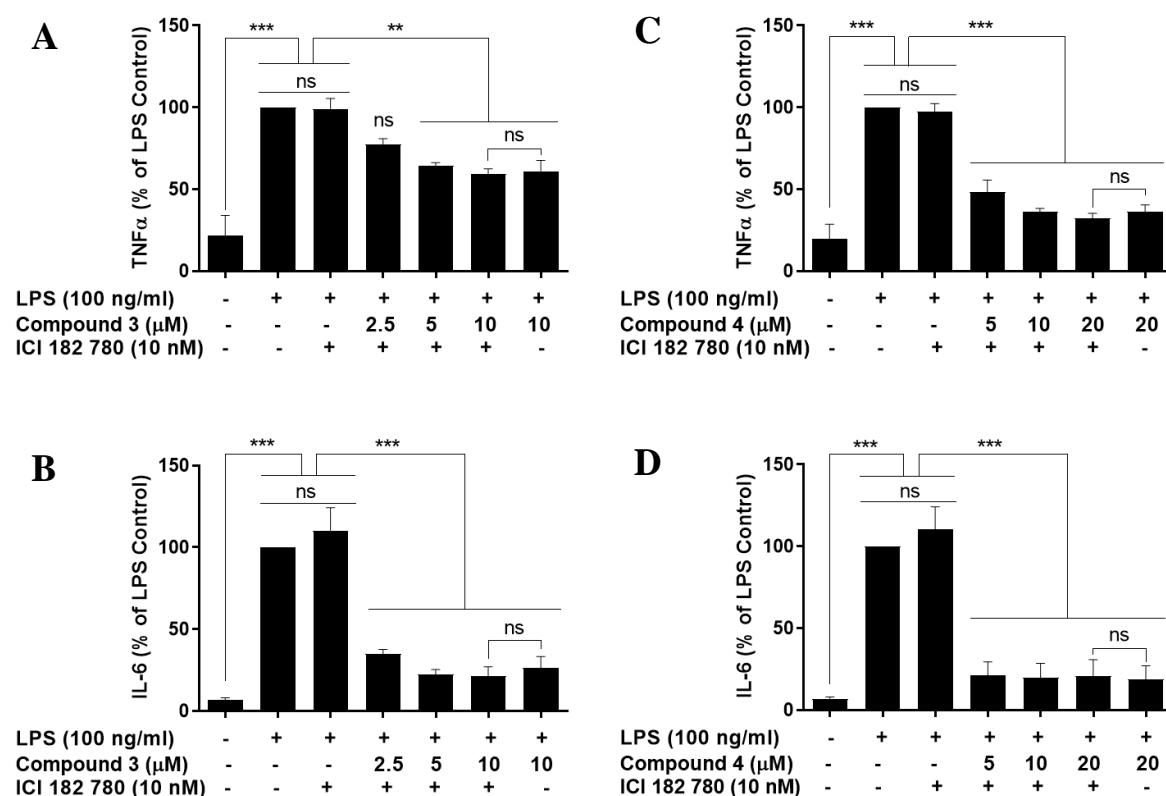


**Figure 3.17** The effect of ICI 182,780 on compounds 3 and 4 ability to reduce LPS-induced TNF $\alpha$  and IL-6 production in BV2 cells. BV2 microglia were pre-incubated with or without ICI 182,780 (10 nM) for 30 minutes followed by compounds 3 (2.5, 5 and 10  $\mu$ M) and 4 (5, 10 and 20  $\mu$ M) treatment for 30 minutes and LPS (100 ng/ml) activation for 24 hours. Next day cell culture supernatants were collected for TNF $\alpha$  and IL-6 ELISAs experiments. Compounds 3 and 4 in presence or absence of ICI 182,780 significantly diminished LPS-induced TNF $\alpha$  and IL-6 production in BV2 cells. All values are expressed as a mean  $\pm$  SEM for N=3. Data were analysed using one-way ANOVA for multiple comparisons with post hoc Student Newman-Keuls test. \*\* $p < 0.002$  and \*\*\* $p < 0.001$ .

### 3.3.10 The effect of ER $\beta$ knockdown on anti-inflammatory activity of compounds 3 and 4 in BV2 microglia

Previous results indicated that ER $\beta$  antagonism did not affect the anti-inflammatory properties of compounds 3 and 4. Therefore, siRNA-mediated knockdown of ER $\beta$  was carried out in BV2 cells to confirm further the lack of effect of ER $\beta$  activation on anti-inflammatory actions of compounds. siRNA-mediated knock-down efficiency of ER $\beta$  was assessed using Western blotting. Figure 3.18 shows that BV2 cells transfected with ER $\beta$  siRNA significantly ( $p < 0.033$ ) reduced ER $\beta$  protein level to  $47 \pm 6\%$  compared to control siRNA value of 100%.

BV2 cells were transfected with ER $\beta$  siRNA or control siRNA for 24 hours followed by 30-minutes pre-treatment with compounds 3 (10  $\mu$ M) or 4 (20  $\mu$ M) and LPS (100 ng/ml) stimulation for 24 hours. Data presented in Figure 3.19 A and B show that ER $\beta$  knockdown did not affect compound 3 ability to significantly ( $p < 0.001$ ) reduce LPS-induced TNF $\alpha$  and IL-6 production. Similarly, the inhibitory effect of compound 4 on LPS-induced TNF $\alpha$  and IL-6 production BV2 microglia was not affected in ER $\beta$  knockdown BV2 cells (Figure 3.19 C and D).

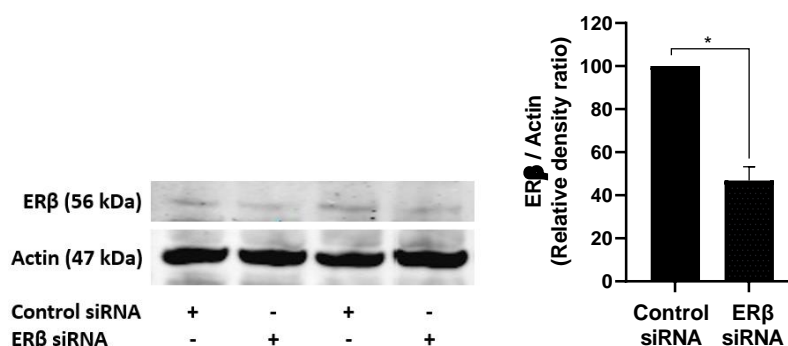


**Figure 3.18 Efficiency of siRNA mediated ER $\beta$  knockdown in BV2 cells.** The BV2 cells were transfected with control siRNA or ER $\beta$  siRNA for 24 hours. Then cell lysates were collected for Western blot analysis. BV2 microglia transfected with ER $\beta$  siRNA reduced ER $\beta$  protein level to  $47 \pm 6\%$  compared to control siRNA value of 100%. Actin has been used as a loading control. All values are expressed as a mean  $\pm$  SEM for N=2. Data were analysed using unpaired t-test. \* $p < 0.033$  in comparison with control siRNA transfected cells.

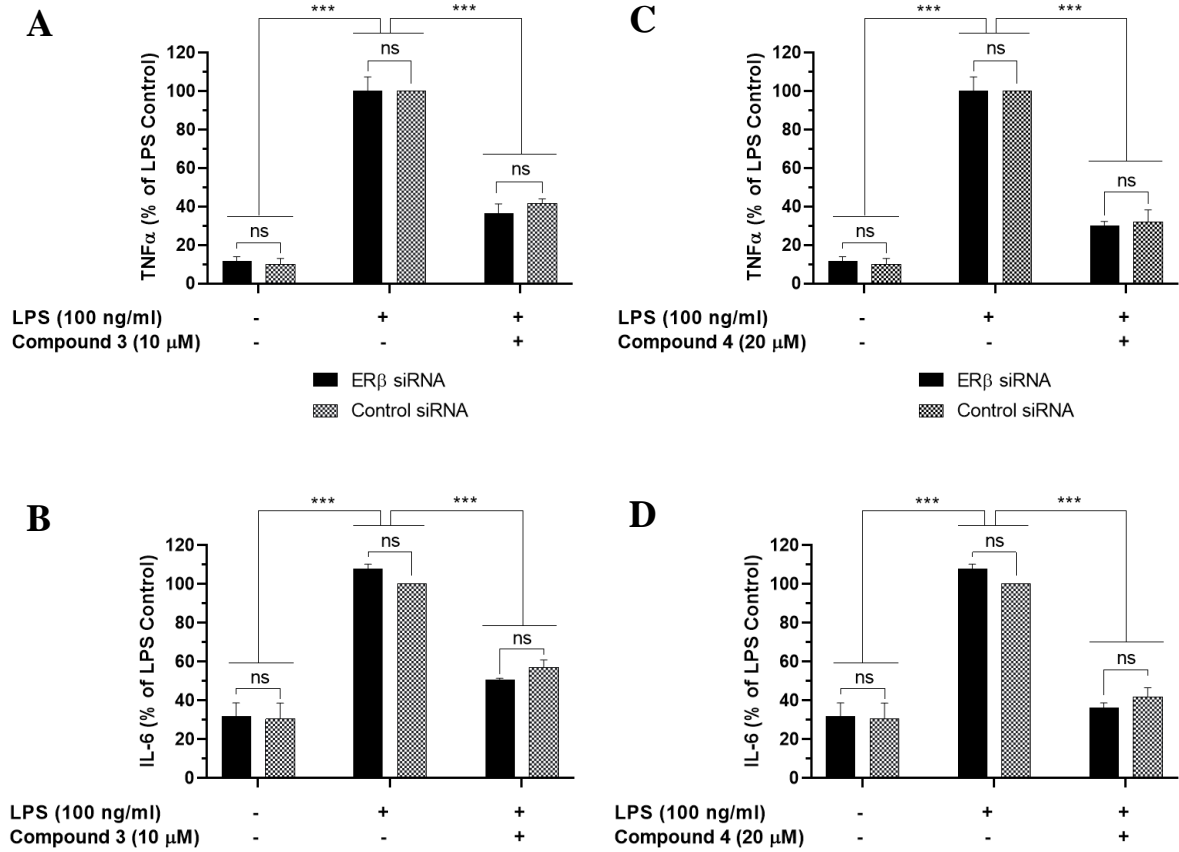


**Figure 3.19 The effect of ERβ knockdown in BV2 cells on the anti-inflammatory activity of compounds 3 and 4.** BV2 microglia were transfected with ERβ siRNA or controlsiRNA for 24 hours. Then cells were pre-treated with compounds 3 (10 μM) and 4 (20 μM) for 30 minutes followed by stimulation with LPS (100 ng/ml). After 24-hour incubation with LPS, cell supernatants were collected for TNFα and IL-6 ELISAs experiments. Pre-incubation with compound 3 significantly ( $p < 0.001$ ) reduced LPS-induced TNFα (A) and IL-6 (B) production in cells transfected with ERβ siRNA or control siRNA. Moreover, not significant difference was observed in compound ability to reduce both cytokines between ERβ siRNA or control siRNA transfected cells. Similarly, pre-incubation with compound 4 also significantly ( $p < 0.001$ ) reduced LPS-induced TNFα (C) and IL-6 (D) production in cells transfected with ERβ siRNA or control siRNA. All values are expressed as a mean  $\pm$  SEM for N=3. Data were analysed using two-way ANOVA for multiple comparisons with post hoc Student Newman-Keuls test. \* $p < 0.033$ , \*\* $p < 0.002$  and \*\*\* $p < 0.001$ .

### **3.3.11 The impact of Nrf2 antagonism on anti-inflammatory properties of compounds 3 and 4 in LPS-activated BV2 cells**

Nrf2 is a key transcription factor that regulates an array of antioxidant gene expressions that protect against oxidative damage triggered by inflammation (Ahmed, Luo, Namani, Wang, & Tang, 2017). Therefore, the effect of compounds 3 (10  $\mu$ M) and 4 (20  $\mu$ M) was investigated on their ability to reduce LPS-induced pro-inflammatory mediators in cells pre-incubated with or without ML385, which is an Nrf2 antagonist. ML385 inhibits the Nrf2 transcription factor's activity by binding to Neh1, a CNC-bZIP domain (Singh et al., 2016).

Data presented in Figure 3.20 show that untreated cells produced low physiological amounts of TNF $\alpha$  and IL-6 which significantly ( $p < 0.001$ ) increased in LPS-activated cells pre-incubated with or without 10  $\mu$ M of ML385. Pre-incubation of cells with ML385 not significantly increased TNF $\alpha$  and IL-6 level to  $108 \pm 5.7\%$  and  $119 \pm 16.5\%$ , respectively, compared to LPS-treated cells as 100%. Surprisingly pre-incubation with ML385 significantly ( $p < 0.001$ ) reduced LPS-induced nitrite production, compared to LPS control. Pre-incubation with compound 3 in the presence or absence of ML385 significantly ( $p < 0.001$ ) decreased LPS upregulated level of TNF $\alpha$  and IL-6 (Figure 3.20 A and B). Additionally, there was no significant difference between cells incubated with or without ML385 followed by compound 3 treatment and LPS-stimulation. Similar effects of TNF $\alpha$  and IL-6 reduction were observed in LPS-activated cells incubated with compound 4 in the presence or absence of ML385 comparing to LPS control (Figure 3.20 D and E). Additionally, not significant difference of TNF $\alpha$  reduction was observed between compound 4 treated cells in the presence or absence of ML385 followed by LPS activation. Whereas significant ( $p < 0.033$ ) difference was detected in compound 4 ability to reduce LPS-induced IL-6 level by compound 4 in cells with or without ML385 pre-treatment (Figure 3.19 E). Due to ML385 ability to inhibit LPS-induced nitrite production, the effect of Nrf2 inhibition on compounds 3 and 4 nitrite reduction cannot be determined (Figure 3.20 C and F).

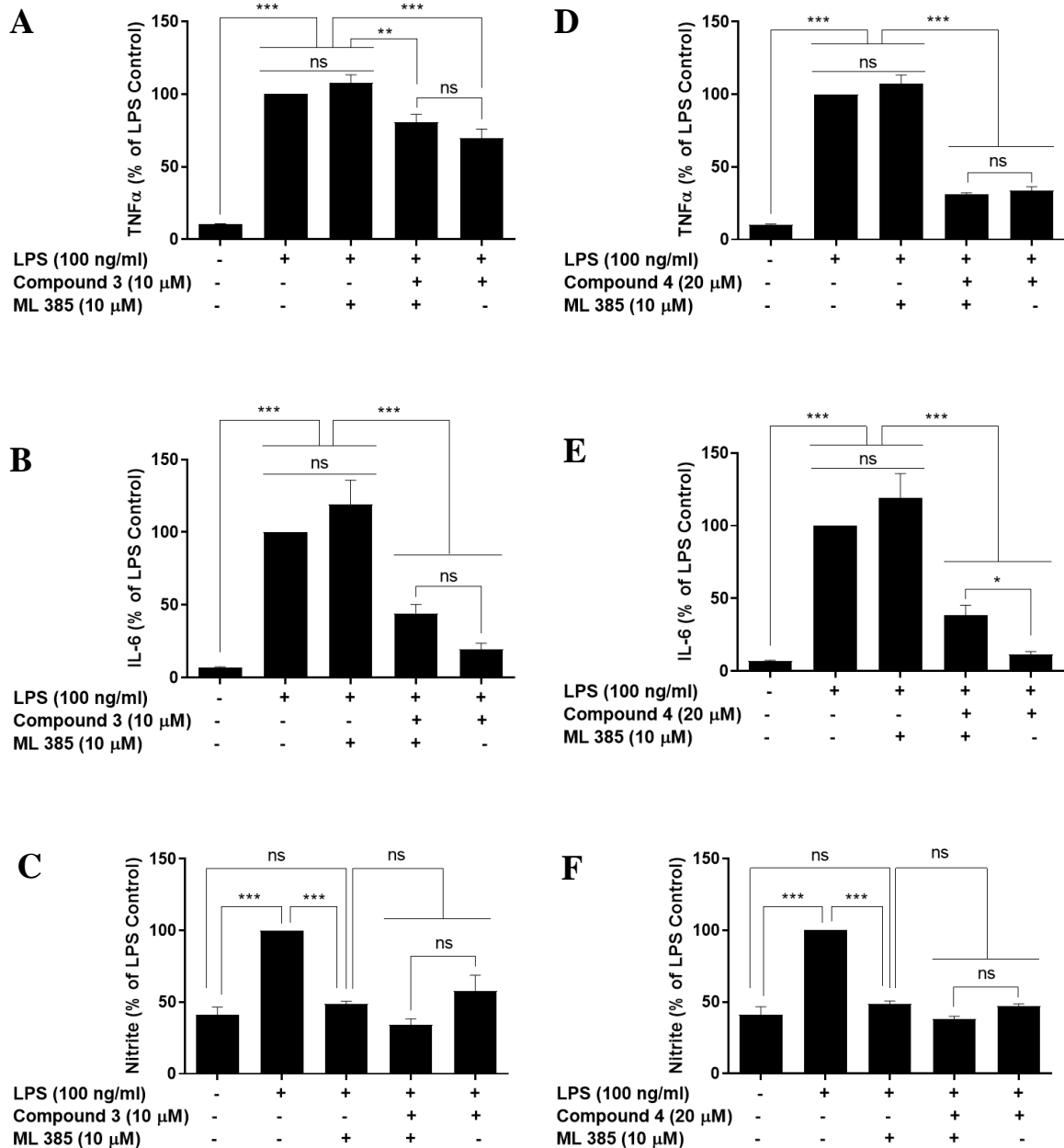


**Figure 3.20** The effect of ML385 on compounds 3 and 4 ability to reduce LPS-induced TNF $\alpha$ , IL-6 and nitrite production in BV2 microglia. BV2 cells were pre-incubated with or without ML385 (10  $\mu$ M) for 30 minutes followed by compounds 3 (10  $\mu$ M) and 4 (20  $\mu$ M) treatment and 24-hour LPS (100 ng/ml) activation. Next day cell culture supernatants were collected for TNF $\alpha$ , IL-6 ELISAs and Griess assay. Treatment with compounds 3 and 4 in the presence or absence of ML385 significantly ( $p < 0.001$ ) diminished LPS-induced TNF $\alpha$  and IL-6 production in BV2 cells. ML385 significantly ( $p < 0.001$ ) downregulated LPS-induced nitrite production; hence ML385 effect on inhibitory effects of compounds 3 and 4 on nitrite level cannot be assessed. All values are expressed as a mean  $\pm$  SEM for N=3. Data were analysed using one-way ANOVA for multiple comparisons with post hoc Student Newman-Keuls test. \* $p < 0.033$ , \*\* $p < 0.002$  and \*\*\* $p < 0.001$ .



### **3.3.12 The impact of SIRT1 antagonism on anti-inflammatory properties of compounds 3 and 4 in LPS-activated BV2 microglia**

SIRT1 has been shown to negatively regulate neuroinflammation through histones deacetylation of critical transcription factors such as NF- $\kappa$ B or AP-1, consequently repressing transcription of various inflammation-related genes (Xie et al., 2013). Zhao et al., (2013) indicated that EX527 is highly selective and potent SIRT1 inhibitor. To determine if compounds 3 and 4 anti-inflammatory properties are SIRT1-dependent, BV2 cells were pre-incubated with or without EX527 (1  $\mu$ M) for 30 minutes followed by compounds 3 (10  $\mu$ M) and 4 (20  $\mu$ M) treatment and 24-hour LPS-activation, and measurement of pro-inflammatory mediators.

Untreated cells produced low physiological amounts of TNF $\alpha$ , IL-6 and nitrite, which were significantly upregulated in LPS-activated cells with or without EX527 pre-treatment. Pre-incubation of cells with EX527 not significantly increased TNF $\alpha$  and nitrite level to  $124 \pm 23.9\%$  and  $101 \pm 18.1\%$ , respectively, compared to LPS-treated cells as 100%. In turn, pre-treatment with EX527 followed by LPS-activation significantly ( $p < 0.033$ ) upregulated IL-6 production to  $141 \pm 16.3\%$  compared to LPS treated. Treatment of cells with compound 3 in the presence or absence of EX527 significantly ( $p < 0.033$ ) reduced LPS-induced TNF $\alpha$ , IL-6 and nitrite level (Figure 3.21 A, B and C). Additionally, there was not significant difference between cells pre-incubated with or without EX527, followed by compound 3 treatment and LPS-stimulation. Similarly, compound 4 in the presence or absence of EX527 significantly ( $p < 0.001$ ) diminished LPS-induced TNF $\alpha$ , IL-6 and nitrite production (Figure 3.21 D, E and F). Not significant difference was observed between cells incubated with or without EX527, followed by treatment with compound 4 and LPS-activation.

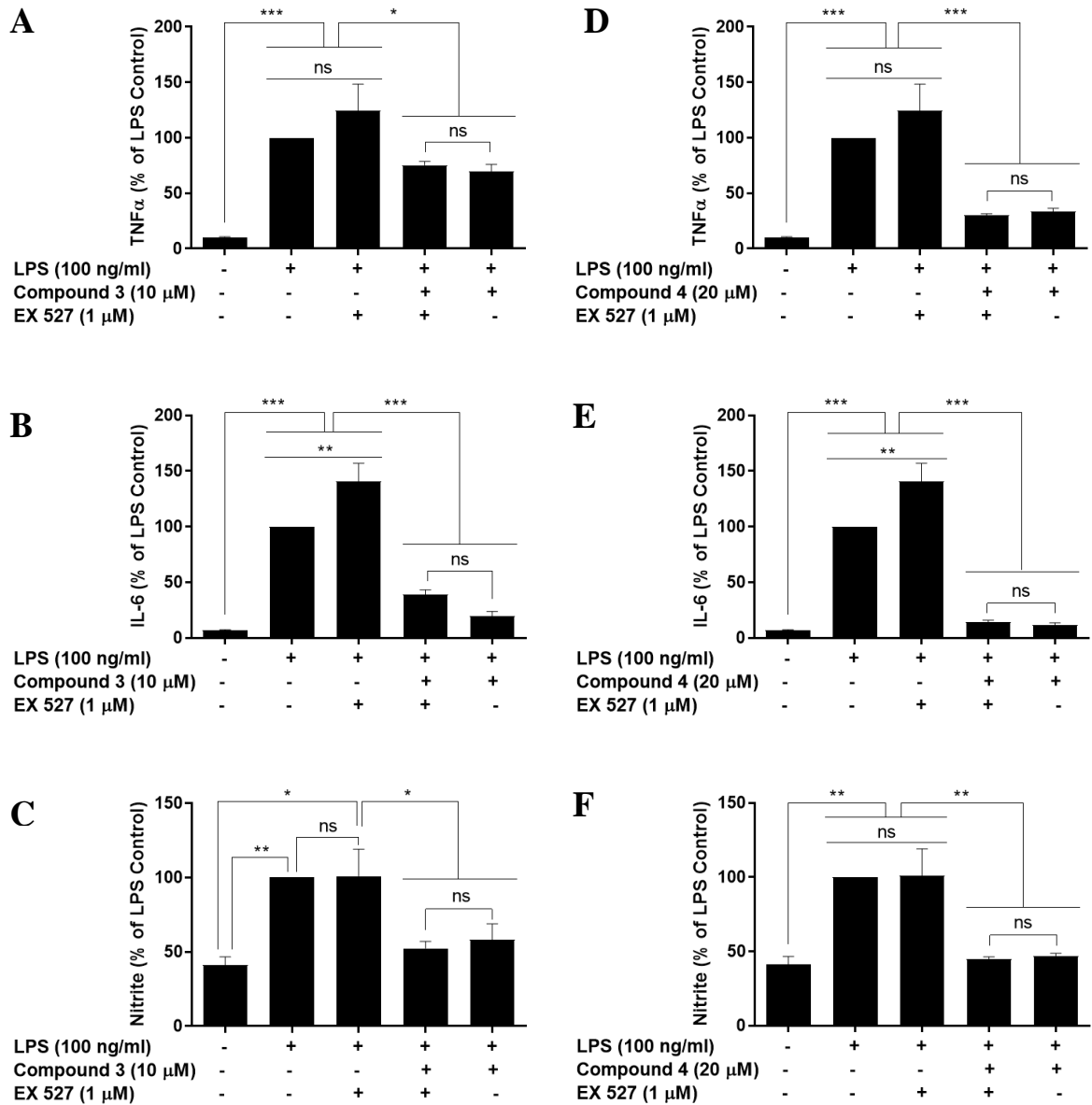


**Figure 3.21** The effect of EX527 on compounds 3 and 4 ability to reduce LPS-induced TNF $\alpha$ , IL-6 and nitrite production in BV2 cells. BV2 microglia were pre-incubated with or without EX527 (1  $\mu$ M) for 30 minutes followed by compounds 3 (10  $\mu$ M) and 4 (20  $\mu$ M) treatment and 30 minutes incubation. After incubation cells were activated for 24 hours with LPS (100 ng/ml) and cell culture supernatants were collected and analysed for TNF $\alpha$ , IL-6 and nitrite levels. Compounds 3 and 4 with or without EX527 significantly ( $p < 0.001$ ) diminished LPS-induced TNF $\alpha$ , IL-6 and nitrite production in BV2 cells. All values are expressed as a mean  $\pm$  SEM for N=3. Data were analysed using one-way ANOVA for multiple comparisons with post hoc Student Newman-Keuls test. \* $p < 0.033$ , \*\* $p < 0.002$  and \*\*\* $p < 0.001$ .

### 3.4 Discussion

Prolonged neuroinflammation is closely associated with neurodegeneration. Chronically activated microglia produce a large quantity of pro-inflammatory mediators, which at high concentrations are neurotoxic. Therefore, the alleviation of neuroinflammation may mitigate neurodegenerative disorders (Chen et al., 2016). Epidemiological studies indicated that the Asian population had a lower incidence of neurodegenerative disorders and cancers (Zhao, Mao, & Diaz Brinton, 2009). Further research associated those health benefits to consumption of soy-containing food. Consequently, the extraction of compounds from soy identified daidzein as one of the most active chemicals with anti-inflammatory, antioxidant, anti-cancerous and neuroprotective properties (Sun et al., 2016). Therefore, encouraged by daidzein positive pharmacological effects, this study elucidates anti-inflammatory properties and molecular mechanism of two daidzein analogues – compounds 3 and 4.

Modification of the functional group can change compound electronics, solubility, and steric dimensions (Harrold & Zavod, 2014). Consequently, those modifications can affect bioavailability, specificity, and potency of the molecule. The compounds tested in this study were created by insertion of the functional group into daidzein B-ring at position 4'. Compound 3 contains ethyl ester moiety, which is known to increase lipid solubility and stability of molecule (Harrold & Zavod, 2014). By contrast, compound 4 was created by insertion of the chloropropyl triazole functional group. Introduction of a chlorine atom to compounds has been shown to improve intrinsic biological activity by increasing reactivity and electrophilicity of molecule (Turnbull, 2000). Furthermore, the use of triazole scaffold in medicinal chemistry gained broad interest in recent years due to its broad pharmacological activities (Zhou & Wang, 2012). This unique five-membered heterocycle with three nitrogen atoms is electron rich system which allows binding with a variety of enzymes and receptors. Moreover, triazoles are remarkably stable towards hydrolysis, oxidative and reductive conditions, and enzymatic degradation (Dheer, Singh, & Shankar, 2017). Therefore, they are present as a structural component of the broad spectrum of drugs including antimicrobial, anti-inflammatory, analgesic, antihypertensive, antimalarial, antidepressant, antihistaminic, antioxidant, antidiabetic et cetera (Kharb, Sharma, & Yar, 2011). Therefore, this study provides insight into the effect of ethyl ester and chloropropyl triazole moiety on anti-inflammatory properties and mechanism of action of daidzein derivatives.

An initial objective of the project was to identify anti-inflammatory properties of daidzein derivatives. The critical element to achieve that objective is the fact that the inflammation process results in the release of pro-inflammatory mediators; therefore, their levels can serve as biomarkers. The monitoring of pro-inflammatory cytokines level provides information about the severity of inflammation and effectiveness of performed treatment. LPS is the most commonly used pro-inflammatory stimulus for microglia. LPS associates with TLR4 which activates signalling cascades involving NF- $\kappa$ B and MAPKs. Those signalling pathways activate transcription factors leading to upregulation of pro-inflammatory genes such as cytokines. BV2 activated with LPS produced large amounts of TNF $\alpha$ , IL-6 and IL-1 $\beta$ . A recent study by Lepennetier et al., (2019) demonstrated that cerebrospinal fluid of patients with neuroinflammatory diseases contains increased levels of multiple cytokines such as TNF $\alpha$  and IL-6 when compared to healthy patients. Hence response of BV2 microglia to LPS imitate neuroinflammation observed in human. Compounds 3 and 4 significantly attenuated LPS-induced TNF $\alpha$ , IL-6 and IL-1 $\beta$  secretion without affecting cell viability. Therefore, observed reductions of pro-inflammatory mediators are triggered by pharmacological actions of compounds. Similarly, Jantaratnotai et al., (2013) also reported daidzein ability to inhibit LPS-induced IL-6 in HAPI microglia. Liu et al., (2009) indicated lack of daidzein effect on IL-6 but showed a reduction of IL-1 and TNF $\alpha$  in mice primary astrocytes. In turn, studies of daidzein in murine RAW264.7 showed its ability to inhibit IL-6, whereas TNF $\alpha$  reduction was not observed (Choi et al., 2012). All above-mentioned studies used LPS as an inflammation-inducing agent, hence small differences in daidzein properties to decrease cytokines may be attributed to cell type. Accumulating evidence indicates that the reduction of pro-inflammatory cytokines diminishes neurotoxicity (Wang, Tan, Yu, & Tan, 2015). Therefore, daidzein derivatives possess anti-inflammatory properties which could alleviate neurodegeneration.

Next pro-inflammatory mediator which is highly upregulated during neuroinflammation is nitric oxide. During inflammation, large amounts of nitric oxide are produced from L-arginine by iNOS. Overproduction of nitric oxide leads to cytotoxicity through damage of proteins and DNA. Therefore it has been reported that iNOS inhibition ameliorates inflammation and neurodegeneration (Chabrier et al., 1999). Unstimulated cells produced low physiological amount of nitric oxide with barely detectable iNOS expression. However, LPS stimulation significantly enhanced NO/iNOS production. Daidzein derivatives diminished nitric oxide production through inhibition of iNOS protein in LPS stimulated

BV2 cells. These results reflect those of Subedi et al., (2017) who reported daidzein inhibitory effect on NO/iNOS in LPS-activated BV2 microglia. Therefore, daidzein analogues did not lose NO/iNOS inhibitory properties due to the insertion of functional groups into B-ring at position 4'.

The next inflammatory biomarker is prostaglandin E2 (PGE<sub>2</sub>) generated by cyclooxygenase 2 (COX-2) conversion of arachidonic acid. PGE<sub>2</sub> role in the augmentation of inflammation has been widely described (Johansson et al., 2015; Nakanishi & Rosenberg, 2013; Nicholas Dias, Yung Peng, 2017). PGE<sub>2</sub> reduction is a common mechanism of action of NSAIDs. However, Minghetti, (2004) indicates that PGE<sub>2</sub> activity in the brain might differ from periphery due to its constitutive expression in the healthy brain in contrast to only inflammation-induced production in the periphery. Therefore, the exact effect of PGE<sub>2</sub> during neuroinflammation remains to be fully elucidated. Daidzein was shown to reduce the expression of COX-2 in LPS-activated BV2 microglia (Subedi et al., 2017). Compound 3 at 5 µM and 10 µM not significantly increased PGE<sub>2</sub> and COX-2 protein level to 126% and 131%, respectively, compared to LPS control. Therefore, insertion of the ethyl ester group to daidzein resulted in modification of properties. However, Hermenegildo, Oviedo, García-Pérez, Tarín, & Cano, (2005) compared to Subedi et al., (2017) demonstrated the opposite effect of daidzein on COX-2 production. In line with the results presented in this study, the authors indicated that daidzein enhanced COX-2 mRNA expression and protein content without affecting COX-1 levels in human endothelial cells. Interestingly, those effects were abolished by oestrogen receptor antagonist - ICI 182,780, suggesting ER involvement. Similar results indicating daidzein induction of COX-2 expression were also presented by Bevilacqua, Iovine, Iannella, Gasparri, & Monfrecola (2011). In contrast to compound 3, compound 4 at 20 µM not significantly reduced PGE<sub>2</sub> production to 75% compared to LPS control. Moreover, compound 3 did not affect LPS-induced COX-2 level. Thus, a slight decrease of PGE<sub>2</sub> might be caused by modulation of microsomal prostaglandin E synthase (mPGES-1). The mPGES-1 is an enzyme that alongside COX-2 regulates PGE<sub>2</sub> expression (Martin & Jones, 2017). Therefore, inhibition of mPGES-1 will block PGE<sub>2</sub> expression without affecting COX-2. The discrepancy between the effect of compound 3 and 4 on PGE<sub>2</sub> is attributed to introduced daidzein modifications. This suggests that ethyl ester and chloropropyl triazole functional group had an opposite impact on PGE<sub>2</sub>/mPGES-1/COX-2 signalling. However, their effects on TNFα, IL-6, IL-1β and nitric oxide remained similar.

Therefore, introduced chemical modifications to compounds 3 and 4 affected only their specificity to proteins involved in PGE<sub>2</sub> signalling.

Prior studies have noted the importance of antioxidant activities of phytoestrogens. However, those studies evaluating daidzein observed inconsistent results on its ability to quench free radicals. Liang et al., (2008) reported that daidzein possesses radical scavenging activities. Nevertheless, Kampkötter et al., (2008) argued that daidzein does not have prominent antioxidant effects in cell-free assay systems; hence its antioxidant properties observed might not be due to free radical scavenging. Daidzein derivatives did not scavenge DPPH radical, whereas control positive – L-ascorbic acid showed prominent DPPH reduction properties. Daidzein derivatives do not possess free radical scavenging activities. Thus, as Kampkötter et al., (2008) indicated, compounds might express their antioxidant properties via inhibition of expression of free radicals or promoting the expression of antioxidant enzymes. Daidzein has been shown to induce nuclear factor erythroid 2-related factor 2 (Nrf2) activation (Froyen & Steinberg, 2010; Pallauf et al., 2017). Nrf2 is a master transcription factor regulating the antioxidant stress response. Nrf2 is located in the cytoplasm with its inhibitory protein Kelch-like ECH-associated protein 1 (Keap1). However, conformational change in Keap1 leads to Nrf2 nuclear translocation where it heterodimerizes with small Maf proteins and binds to antioxidant response elements (AREs) initiating expression of antioxidant proteins. Moreover, Nrf2 activation has been demonstrated to inhibit other transcription factors such as NF- $\kappa$ B resulting in repression of proinflammatory genes. Activated Nrf2 reduces NF- $\kappa$ B and AP-1 activity via competition for transcriptional co-activator CBP (CREB-binding protein)–p300 complex (Wardyn, Ponsford, & Sanderson, 2015). Kim, Lee, Shin, & Lee, (2013) demonstrated in BV2 cells that activation of Nrf2 by ethyl pyruvate inhibited p65-p300 interaction. To determine, whether daidzein derivatives inhibitory effect on pro-inflammatory mediators was due to Nrf2 activation, Nrf2 was inhibited using ML385 and TNF $\alpha$ , IL-6 and nitrite were measured. ML385 inhibits Nrf2 activity via binding to one of its domains – Neh1 which unbalance DNA recognition and dimerization with small Maf proteins. ELISAs experiments demonstrated that Nrf2 inhibition slightly in not significant manner upregulated expression of TNF $\alpha$  and IL-6 to 106% and 119%, respectively, compared to LPS control. Similar pattern of increased TNF $\alpha$ , IL-1 $\beta$  and IL-6 cytokines expression was observed in Nrf2 knockout mice astrocytes (Pan, Wang, Wang, Zhu, & Mao, 2012). Nrf2 deletion deprives cell antioxidant response leading to amplification of oxidative environment which upregulates NF- $\kappa$ B and pro-inflammatory mediators (Wardyn et al., 2015). Inhibition

of Nrf2 had no effect on compounds 3 and 4 reduction of TNF $\alpha$  and IL-6. These findings suggest that anti-inflammatory properties of daidzein derivatives in LPS-activated BV2 are Nrf2-independent. Surprisingly, ML385 inhibited LPS-induced NO production in BV2. Therefore, effect of Nrf2 inhibition on compounds 3 and 4 NO reduction cannot be evaluated. ML385 is relatively new Nrf2 inhibitor developed by Singh et al., in 2016 as treatment for advanced non-small cell lung cancer. Therefore, its effect on NO/iNOS remains to be elucidated.

Presented results supported the hypothesis that daidzein derivatives exert anti-inflammatory properties on activated microglia. Therefore, to evaluate molecular mechanisms of those actions, the effects of compounds were tested on main inflammation regulatory pathways such as NF- $\kappa$ B and MAPKs. NF- $\kappa$ B is a master regulator of pro-inflammatory genes, including those encoding for TNF $\alpha$ , IL-1 $\beta$  and IL-6 (Liu et al., 2017). Compound 3 did not reduce LPS-induced phosphorylation of NF- $\kappa$ B p65. In contrast, compound 4 inhibited LPS-induced activation of NF- $\kappa$ B p65. Similar effects to compound 4 were attributed to daidzein. Choi et al., (2012) and Hämäläinen et al., (2007) reported daidzein ability to reduce NF- $\kappa$ B activation. Therefore, administration of chloropropyl triazole moiety to daidzein did not amend specificity of the compound to inhibit NF- $\kappa$ B signalling. In turn, ethyl ester functional group inserted to daidzein abolished its property to inhibit NF- $\kappa$ B activity upstream of the cell nucleus. However, the complexity of NF- $\kappa$ B signal transduction enables to target this pathway at multiple stages downstream of NF- $\kappa$ B p65 phosphorylation. Potential downstream mechanisms leading to NF- $\kappa$ B inhibition could interfere with its nuclear translocation, histone acetylation, NF- $\kappa$ B–DNA binding, recruitment of cofactors or inhibition of transcriptional activity. Consequently, to assess, if compound 3 was able to target mechanisms mentioned above to inhibit NF- $\kappa$ B downstream of phosphorylation of NF- $\kappa$ B p65, reporter gene assay was conducted. As expected, compound 4 reduced NF- $\kappa$ B transcriptional activity. Additionally, reporter gene assays also showed a lack of negative regulation of NF- $\kappa$ B transcriptional activity by compound 3. Therefore, the anti-inflammatory activity of compound 3 is NF- $\kappa$ B-independent.

Inhibition of this transduction pathway may be caused by the direct action of the compound or its ability to target other signalling pathways which participate in crosstalk with pro-inflammatory transcription factors, thereby leading to its inhibition. As described earlier interplay of Nrf2 with NF- $\kappa$ B or AP-1 was excluded because Nrf2 inhibition had no effect on compounds anti-inflammatory properties. Next possible transcription factor which could

modulate anti-inflammatory activity was ERE. Daidzein belongs to phytoestrogen family known to mimic the action of oestrogen due to structural similarities. Moreover, daidzein has been demonstrated to have high specificity for ER $\beta$  which is expressed by BV2 (Baker, Brautigam, & Watters, 2004; El-Bakoush & Olajide, 2018; Kuiper et al., 1998). Reporter gene assays confirmed compounds ability to activate ERE in BV2 cells. Activation of ERs has been shown to inhibit NF- $\kappa$ B signal transduction at multiple stages which can be divided into indirect modulation occurring in the cytoplasm or direct interference in a nucleus. Cytoplasmic mechanisms include suppression of IKK phosphorylation and I $\kappa$ B degradation (Huang et al., 2013). Nuclear mechanisms may interfere with NF- $\kappa$ B-DNA binding (Pelzer, Neumann, De Jager, Jazbutyte, & Neyses, 2001), recruitment of coactivators (Speir et al., 2000b) or transcriptional inactivation of DNA bound NF- $\kappa$ B (Kalaitzidis & Gilmore, 2005). Moreover, oestrogen receptor activation has been described to not only inhibit the activity of NF- $\kappa$ B or AP-1 thereby reducing expression of many inflammatory-related proteins but also may affect promoters of specific genes such as IL-6 (Galien & Garcia, 1997; Stein & Yang, 1995). Therefore, to determine if oestrogen activation was controlling anti-inflammatory properties of compounds such as TNF $\alpha$  and IL-6 reduction, ERs were blocked using ICI 182,780 and levels of cytokines were measured. ICI 182,780 is antioestrogen which promote ER degradation and prevent ER interaction with coactivators (Smith & O'Malley, 2004). ELISAs experiments revealed that daidzein derivatives retained their anti-inflammatory properties during ER inhibition. Therefore, results suggest that compounds 3 and 4 are ER agonists with ER-independent anti-inflammatory properties. Similar ER-independent anti-inflammatory mechanism was reported by Baker et al., (2004) who showed a lack of effect of ICI 182,780 on E2-mediated reductions in iNOS levels. Interestingly author reported that ICI 182,780 pre-treatment reversed E2 inhibition of COX-2. To further confirm ER-independent anti-inflammatory properties of compounds 3 and 4, ER $\beta$  knockdown was performed. In line with ER antagonist results, ER $\beta$  knockdown did not prevent the inhibitory actions of compounds on LPS-stimulated TNF $\alpha$  and IL-6 levels. Hence, reduction of both cytokines is independent of ER $\beta$  activation.

The next protein which tightly controls various inflammatory pathways is SIRT1. Silent Information Regulator TWo protein is the most characterized member of sirtuins family. SIRT1 controls signalling pathways via deacetylation of nucleosomal histones and proteins. SIRT1 transfers the acetyl group from proteins to NAD<sup>+</sup> producing 2'-O-acetyl-ADP-ribose and nicotinamide, thereby reducing the activity of NF- $\kappa$ B and AP-1 (Xie et al., 2013).



Daidzein has been demonstrated to reduce inflammation by upregulation of SIRT1 (Hirasaka et al., 2013). Therefore, the anti-inflammatory properties of daidzein derivatives were assessed after blocking SIRT1 with EX527. Similarly, to Nrf2, SIRT1 inhibition also resulted in increased LPS-induced production of TNF $\alpha$  and IL-6 to 124% and 141%, respectively, compared to LPS control. This is in line with results reported by Yoshizaki et al., (2009) where authors also indicated enhanced pro-inflammatory cytokines expression in knock-down SIRT1 3T3-L1 adipocytes. The increased inflammatory response is caused by lack of SIRT1 negative regulation of NF- $\kappa$ B and AP-1 gene expression (Xie et al., 2013). However, SIRT1 inhibition did not cause nitrite upregulation. Inhibition of SIRT1 did not affect compounds 3 and 4 ability to diminish LPS-induced TNF $\alpha$ , IL-6 and NO level. Therefore, the anti-inflammatory properties of daidzein derivatives are SIRT1-independent.

MAPKs are important proteins involved in transduction of inflammatory response. Abnormal activation of those pathways contributes to disease progression. Hence, their inhibition has been described as a potential treatment strategy for neuroinflammation and neurodegeneration (Kaminska et al., 2009; Kim & Choi, 2010; Krzyzowska et al., 2010). MAPKs modulate activities of several transcription factors, thereby orchestrating inflammatory proteins gene expression. Compounds 3 and 4 did not inhibit LPS-induced phosphorylation of p38, JNK and ERK1/2. These results reflect those of Choi et al., (2012) who also found that daidzein had no effect on p38 and JNK in macrophages. Therefore, daidzein derivatives, similar to daidzein, had no impact on MAPKs. Hence the reduction of pro-inflammatory cytokines and NO is MAPK-independent. This indicates the crucial role of NF- $\kappa$ B in compound 4 inflammatory gene regulation. Moreover, lack of compound 4 effect on MAPKs, and NF- $\kappa$ B inhibition suggests that compound 4 is most likely to target NF- $\kappa$ B pathway downstream of TAK1 because TAK1 is a divergent point for those two pathways (Ajibade, Wang, & Wang, 2013).

Summarizing, compounds 3 and 4 significantly inhibited LPS-induced production of TNF $\alpha$ , IL-6, IL-1 $\beta$  and NO/iNOS in BV2 cells. Moreover, both compounds increased ERE activation, suggesting their role as ER agonists. Reduction of pro-inflammatory mediators by compounds was ER-, Nrf2- and SIRT1-independent. Additionally, both compounds did not decrease MAPKs activation. Compound 3 also did not inhibit NF- $\kappa$ B activity. However, Compound 3 might affect other signalling pathways which modulate the inflammatory response. For example, inhibition of Janus kinase (JAK)/signal transducer and activator of transcription 3 (STAT3) pathway in microglia has been demonstrated to reduce IL-6 and

iNOS. Moreover, isoflavones, including daidzein, were shown to downregulate JAK/STAT signalling (Hämäläinen, Nieminen, Vuorela, Heinonen, & Moilanen, 2007). Another potential mechanism of compound 3 anti-inflammatory effects might induce inhibition of AP-1 downstream of MAPKs. In contrary to compound 3, compound 4 reduced p-NF- $\kappa$ B p65, therefore it may act upstream of phosphorylation of NF- $\kappa$ B p65 but downstream of TAK1 possibly affecting IKK or I $\kappa$ B $\alpha$  phosphorylation, or I $\kappa$ B $\alpha$  degradation. Therefore, chloropropyl triazole group in compound 4 might play a key role in compound specificity to inhibit NF- $\kappa$ B signal transduction. Figure 3.19 summarises the possible pathways by which compounds 1 and 2 induce their anti-inflammatory actions.

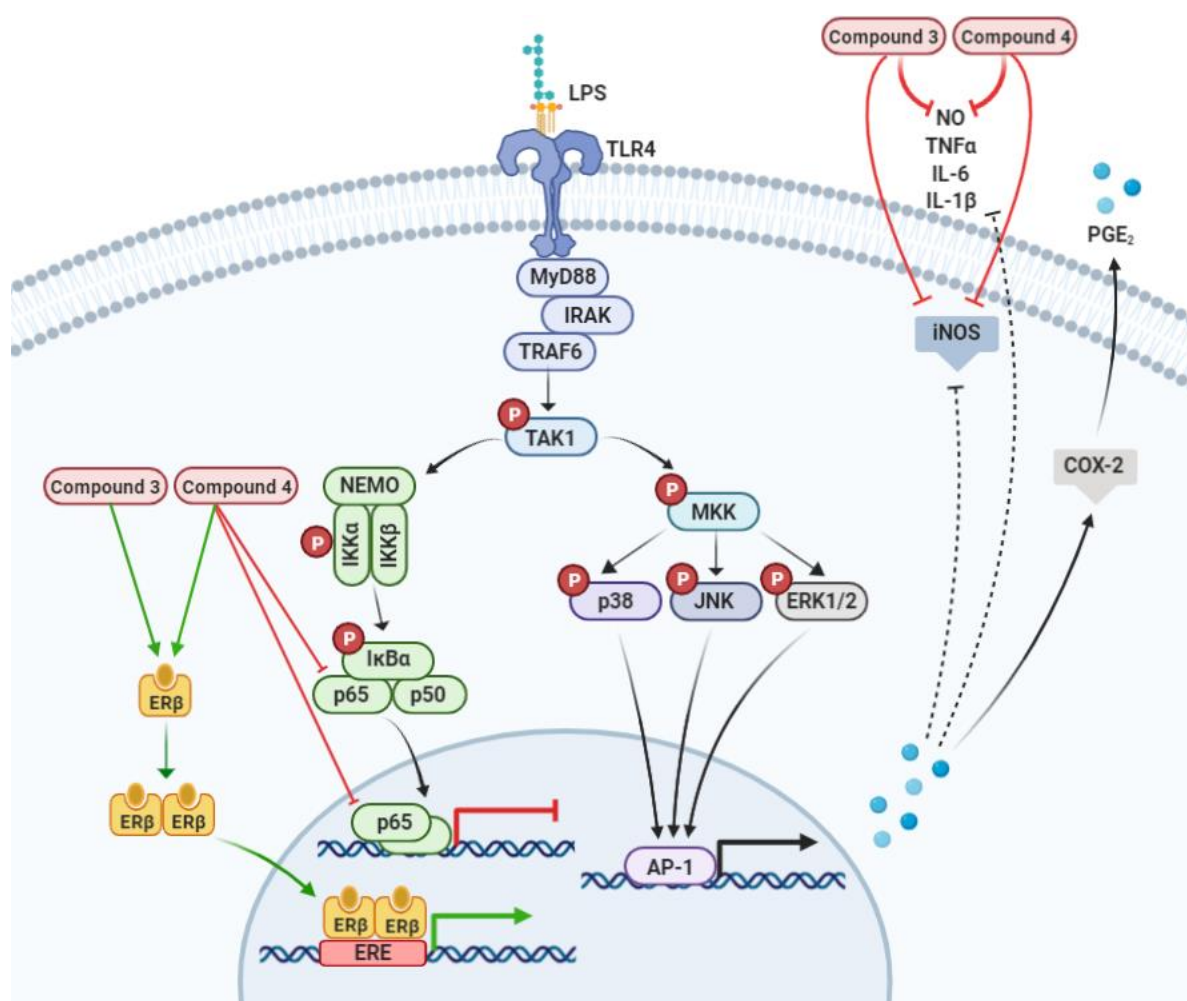


Figure 3.22 Schematic representation of anti-inflammatory actions of compounds 3 and 4.

## 4 Chapter IV - Neuroprotective Properties of Daidzein Derivatives and their Molecular Mechanism

### 4.1 Introduction

#### 4.1.1 Neurons

A neuron is a nerve cell that is designed to transmit the information in the form of electrical or chemical impulses. Structurally, a neuron can be divided into three parts: nerve cell body also known as perikaryon or soma, dendrites and axon which is a single, long protrusion extending from the body of a nerve cell (Figure 4.1). The body of the nerve cell contains all primary cellular organelles, including characteristic for nerve cells Nissl granules which are rough endoplasmic reticulum with richly disseminated ribosomes (Gautam, 2017). Dendrites are branched protoplasmic extensions protruding from perikaryon and are primarily responsible for receiving information flowing into the nerve cell. Information received by dendrite is then transmitted through the axon to other nerve cells. Some of the axons are covered with a special coating called the myelin sheath, which enables much faster transmission of nerve impulses (Uemura, 2015). Neurons communicate with one another using synapses. Ultimately, after stimulation by neurotransmitters, excitation may be triggered, and information may be finally transferred from one nerve cell to another. Since neurons play a pivotal role in processing information, their loss leads to organism dysfunction causing neurological disorders. Selective loss of a particular subset of neurons results in neurodegenerative diseases e.g. loss of cerebral cortical neurons - Alzheimer's disease (AD), substantia nigra neurons - Parkinson's disease (PD), spinal motoneurons - Amyotrophic Lateral Sclerosis (ALS) (Kanazawa, 2001).

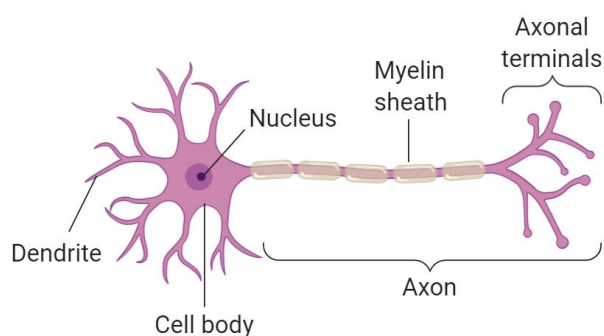


**Figure 4.1 Diagram of a neuron.**

#### 4.1.2 Neuronal death in neuroinflammation

Activated microglia may induce neurotoxicity by a variety of mechanisms (Brown & Vilalta, 2015). One of the mechanisms includes the production of inflammatory cytokines such as TNF $\alpha$ . Excessive production of TNF $\alpha$  not only accelerates inflammation-causing vicious cycle but is also neurotoxic at high concentrations. TNF $\alpha$ , alongside its pro-inflammatory activities, is a death ligand for TNF $\alpha$  receptors whose activation leads to neuronal apoptosis (Brown & Vilalta, 2015). The next factor which becomes neurotoxic when produced in excessive amounts by activated microglia is nitric oxide (NO) synthesized by iNOS (Brown, 2010). Moreover, activated microglia also upregulate NADPH oxidase resulting in increased expression of superoxide (O $^{\ominus}$ ). Nitric oxide and superoxide may react with each other or another free radical to form a mixture of potent ROS and NOS, e.g. peroxynitrite (ONOO $^{\ominus}$ ), hydrogen peroxide (H $_2$ O $_2$ ) (Brown & Vilalta, 2015). Therefore, ROS/NOS may lead to neuronal necrosis mediated via energy depletion or apoptosis mediated by oxidative and nitrosative stress. Necrotic cell death is characterised by rupture of the plasma membrane due to cell swelling (Fricker, Tolkovsky, Borutaite, Coleman, & Brown, 2018). Apoptosis, also known as ‘programmed cell death’ was first introduced in 1964 by Lockshin and Williams (Fricker et al., 2018). Less than a decade later, Kerr, Wyllie, & Currie (1972) described morphological changes associated with apoptosis, including shrinkage of the cell, chromatin condensation, nuclear fragmentation, and formation of apoptotic bodies. Apoptotic induction has been distinguished into two main pathways: the extrinsic pathway and the intrinsic pathway (Figure 4.2) (Elmore, 2007). The extrinsic pathway is initiated by activation of death receptor such as TNFR1 by TNF-related apoptosis-inducing ligand (TRAIL) or Fas ligand (FasL) leading to recruitment of adaptor proteins including tumour necrosis factor receptor type 1-associated death domain protein (TRADD) or Fas-associated death domain protein (FADD) thereby proteolytically activating caspase-8. Active caspase-8 directly activate executioner caspases-3/-6/-7 leading to apoptosis or may also initiate the intrinsic apoptotic pathway through cleavage of Bid into tBid inducing Bax activation (Haase, Pettmann, Raoul, & Henderson, 2008). Intrinsic apoptotic pathway also known as mitochondrial apoptotic pathway is induced by DNA damage, endoplasmic reticulum stress and metabolic stress. Mitochondrial apoptosis is mainly regulated by members of the Bcl-2 family, which include pro-apoptotic proteins: Bax, Bak, Bid and anti-apoptotic proteins: Bcl-2, Bcl-x, Bcl-XL, Bcl-XS (Červinka, 1999). Initiated intrinsic pathway activate Bax proteins leading to mitochondrial outer membrane permeabilization (MOMP) and cytochrome c release.

Released cytochrome c binds to apoptotic protease activating factor 1 (APAF-1) which recruits and cleaves pro-caspase 9. Activated caspase-9 consequently activate downstream executioner caspases-3/-6/-7 causing degradation of cellular proteins and apoptosis (Wu & Bratton, 2013).

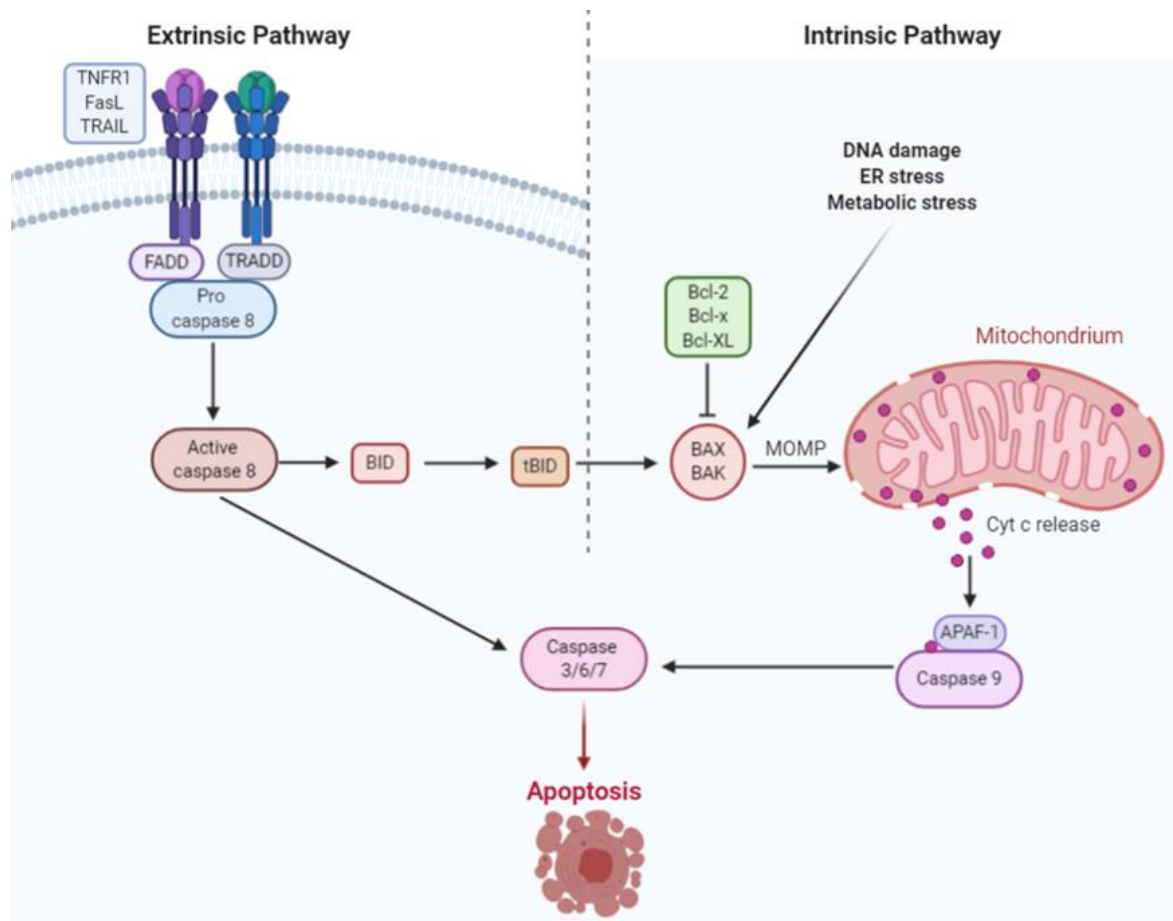


**Figure 4.2 Diagram of the extrinsic and intrinsic apoptotic pathway.** The extrinsic pathway is initiated by activation of death receptors such as TNFR1, FasL, TRAIL leading to recruitment of adaptor proteins TRADD or FADD. TRADD or FAD recruitment cause proteolytic activation of caspase-8, which directly activate executioner caspases-3/6/7 conducting apoptosis. The extrinsic pathway may also initiate the intrinsic apoptotic pathway through caspase-8 cleavage of Bid into tBid inducing Bax activation. Intrinsic apoptotic pathway is induced by DNA damage, endoplasmic reticulum stress and metabolic stress. Initiated intrinsic pathway activates Bax proteins leading to MOMP and cytochrome c release. Released cytochrome c binds to APAF-1 which recruits and cleaves pro-caspase 9. Activated caspase-9 consequently activate downstream executioner caspases-3/6/7 conducting apoptosis.

### 4.1.3 Neuroprotective properties of daidzein

Daidzein expresses many beneficial effects on the brain, including anti-inflammatory, antioxidant and neuroprotective properties. In addition to the reduction of neuroinflammation and oxidative damage which leads to a decrease of neurotoxic factors, daidzein has been shown to directly act on neurons inducing neuroprotection (Ahmed et al., 2017). Neuroprotective effects of daidzein include induction of neuronal survival, development, and function through upregulation of brain-derived neurotrophic factor (BDNF) (Pan, Han, Zhong, & Geng, 2012), choline acetyltransferase (ChAT) (Heo et al., 2006) and arginase 1 (Arg1) (Ma et al., 2010). *In vivo* studies showed that daidzein reduced high-fat diet-induced apoptosis in rat hippocampus (Rivera et al., 2013). Additionally, Stout, Knapp, Banz, Wallace, & Cheatwood, (2013) demonstrated that daidzein enhanced recovery of rats after stroke. *In vitro* studies of daidzein using PC12 neuronal cells presented its inhibitory effect on A $\beta$ -induced cytotoxicity. Moreover, daidzein expressed a neuroprotective effect on mitochondrial caspase-dependent apoptosis via ER $\beta$  and GPR30 activation in primary neocortical, cerebellar and hippocampal neurons (Kajta et al., 2013a). Similarly, Adams, Aksenova, Aksenov, Mactutus, & Booze, (2012) demonstrated that daidzein diminished HIV-1 Tat-induced apoptosis of primary rat cortical neurons through ER-dependent caspase-3/-9 and Bax downregulation. In turn, Hurtado et al., (2012) reported ER-independent neuroprotective actions of daidzein involving activation of PPAR $\gamma$ . Therefore, daidzein's neuroprotective properties might be caused by multiple mechanisms.

Positive biological activities of daidzein encouraged synthesis, and further examination of daidzein derivatives with ethyl ester and chloropropyl triazole functional group inserted into daidzein B-ring at position 4'. The insertion of ethyl ester and chloropropyl triazole functional group created daidzein analogues – compounds 3 and 4 which expressed prominent anti-inflammatory properties in activated microglia; hence this chapter evaluates neuroprotective activities of those compounds.

## **4.2 Methods**

### **4.2.1 HT22 cell culture**

HT22 is an immortalized mouse hippocampal neuronal cell line. HT22 neuronal cells were a kind gift from Dr Jeff Davis (Salk Institute for Biological Studies, California, USA). Cells were cultured in Dulbecco's Modified Eagle's Medium (DMEM; Sigma-Aldrich), 2mM L-glutamine additionally enriched with 10% Gibco™ FBS and 100 mM Gibco™ Sodium Pyruvate (Fisher Scientific). Cells were cultured in a tissue culture flask T-75 (Sarstedt) with standard surface modification for adherent cells. Cells were incubated in a humid atmosphere of 5% CO<sub>2</sub> and 95% air at 37°C. When cells reached approximately 80% confluence, they were washed with Gibco™ Phosphate Buffered Saline (Fisher Scientific) and detached from the vessel using Gibco™ TrypLE™ Express Enzyme (Fisher Scientific) followed by cell counting and subculture.

### **4.2.2 BV2 cell culture**

BV2 mouse brain microglial cells (ICLC ATL03001) were purchased from Interlab Cell Line Collection, Banca Biological Cell Factory, Italy. Cells were cultured in Dulbecco's Modified Eagle's Medium (DMEM, Sigma-Aldrich) already supplemented with 2 mM glutamine and additionally enriched with 10% Gibco™ Fetal Bovine Serum (FBS, Fisher Scientific), and 100 mM Gibco™ Sodium Pyruvate (Fisher Scientific) in a tissue culture flask T-75 (Sarstedt) with standard surface modification for adherent cells. Cells were incubated in a humid atmosphere of 5% CO<sub>2</sub> and 95% air at 37°C. When cells reached approximately 80% confluence, they were washed with Gibco™ Phosphate Buffered Saline (Fisher Scientific) and then adherent cells were dissociated from the vessel using Gibco™ TrypLE™ Express Enzyme (Fisher Scientific) which allowed cell counting and subsequent subculture.

### **4.2.3 HMC3 cell culture**

HMC3 (ATCC®CRL-3304™) were purchased from ATCC, UK. Cells were cultured in Gibco™ Minimum Essential Medium (MEM; Fisher Scientific), supplemented with 10% Gibco™ FBS (Thermo Fisher), and 100 mM Gibco™ Sodium Pyruvate (Thermo Fisher) in a tissue culture flask T-75 (Sarstedt) with standard surface modification for adherent cells. Cells were incubated in a humid atmosphere of 5% CO<sub>2</sub> and 95% air at 37°C. When cells reached approximately 80% confluence, they were washed with Gibco™ Phosphate Buffered

Saline (Fisher Scientific) and detached from the vessel using Gibco™ TrypLE™ Express Enzyme (Fisher Scientific) followed by cell counting and subculture.

#### **4.2.4 SH-SY5Y cell culture**

SH-SY5Y (ATCC® CRL-2266™) cells are neuroblast-like cells subcloned from SK-N-SH, which were initially derived from bone marrow biopsy in 1970<sup>7</sup>. SH-SY5Y cell line model is widely used in vitro neurobiology to test protein functions, transduction pathways, pathology of disease or infection and preliminary drug assessment (Shipley, Mangold, & Szpara, 2016). SH-SY5Y were kindly provided by Dr Patrick McHugh (The University of Huddersfield, UK). Cells were cultured in Gibco™ Minimum Essential Medium (MEM)/ Gibco™ Ham's F-12 Nutrient Mixture (1:1, v:v) (Fisher Scientific) supplemented with 2 mM L-glutamine and additionally enriched with 15% Gibco™ Fetal Bovine Serum (FBS, Fisher Scientific), 100 mM Gibco™ Sodium Pyruvate (Fisher Scientific) and 1% Non-essential Amino Acids (Sigma-Aldrich). Cells were cultured in a tissue culture flask T-75 (Sarstedt) with standard surface modification for adherent cells. Cells were incubated in a humid atmosphere of 5% CO<sub>2</sub> and 95% air at 37°C. When cells reached approximately 80% confluence, they were washed with Gibco™ Phosphate Buffered Saline (Fisher Scientific) and detached from the vessel using Gibco™ TrypLE™ Express Enzyme (Fisher Scientific) followed by cell counting and subculture.

##### **4.2.4.1 Differentiation of SH-SY5Y cells**

Undifferentiated SH-SY5Y cells continuously proliferate and resemble immature neurons; cells express immature neuronal markers and lack mature neuronal phenotype. SH-SY5Y cells can be differentiated to a mature neuron-like phenotype that is characterized by formation and extension of neuritic processes and neuronal markers. The most commonly used differentiation-inducing agent is retinoic acid (RA) and reduced serum medium (Kovalevich & Langford, 2013).

SH-SY5Y cells differentiation was started when cells reached approximately 60% confluence usually 24 hours after seeding cells at a density of  $2 \times 10^4$  cells/ml in multi-well plates (Sarstedt). Cells medium was replaced with freshly prepared differentiation medium: MEM/ Ham's F-12 (1:1, v:v), 1% Gibco™ FBS (Fisher Scientific) and 10 μM of RA (Sigma-Aldrich). Differentiation medium was changed every 48 hours for seven days. After seven



days, neuronal differentiation was monitored microscopically via morphological assessment of neurite outgrowth (Figure 4.3).

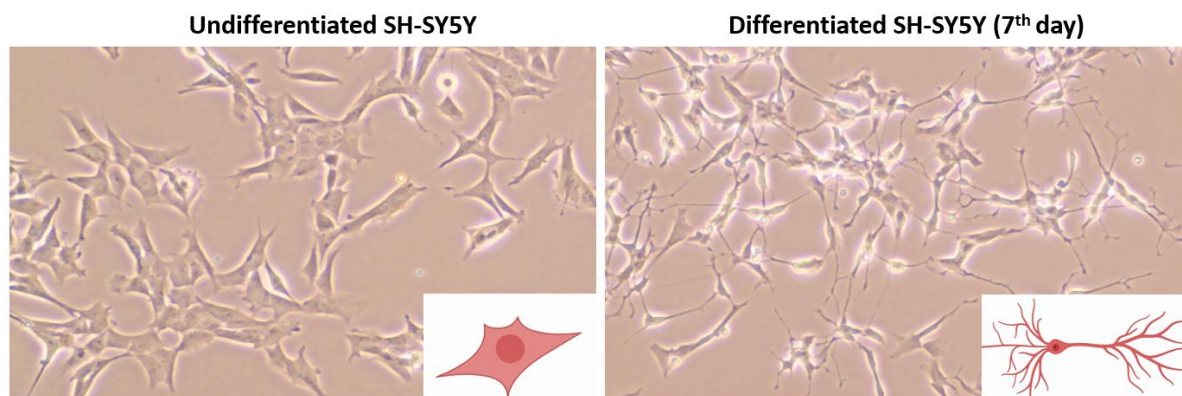


**Figure 4.3** Microscopical assessment of undifferentiated and RA-differentiated SH-SY5Y cells.

#### **4.2.5 XTT cell viability assay**

XTT assay was performed as described in chapter two, section [2.2.3](#)

#### **4.2.6 Selection of the cell model and neurotoxicity-inducing agent for neuroprotection experiments**

##### **4.2.6.1 Conditioned medium experiments**

Conditioned medium is cell-free medium harvested from cultured cells. This medium contains proteins and mediators, which has been secreted by cultured cells, e.g. enzymes, hormones, growth factors, cytokines and ROS/NOS. Conditioned medium is used to assess the impact one cell population to another.

In this study, the conditioned medium from activated microglia was harvested and introduced to neurons in order to induce neurotoxicity.

##### **The effect of BV2 conditioned medium on HT22 viability**

BV2 cells were stimulated with 100 ng/ml and 1000 ng/ml of LPS for 24 hours. Then cell culture medium was collected and centrifuged at  $806 \times g$ . Subsequently, the conditioned medium was introduced to confluent HT22 cells for 24 hours. This was followed by neuronal viability assessment using XTT assay as described in [2.2.3](#). Figure 4.4 indicates that HT22 exposed for 24 hours for the conditioned medium collected from BV2 cells activated with

LPS did not significantly reduce the viability of HT22 when compared to cells exposed medium without LPS stimulation.

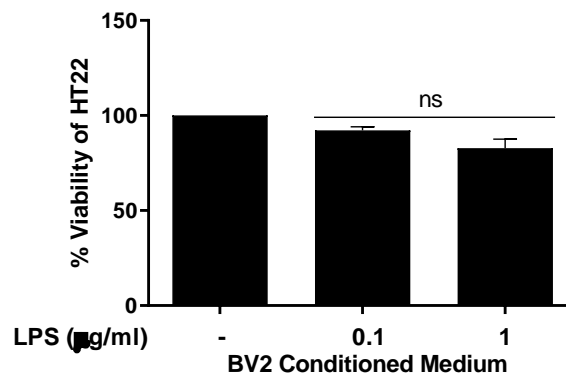


**Figure 4.4 The effect of BV2 conditioned medium on HT22 viability.** BV2 cells were activated with 0.1 µg/ml and 1 µg/ml of LPS for 24 hours. Then cell culture medium was harvested and introduced to HT22 cells for 24 hours, followed by XTT assay. BV2 conditioned medium did not significantly affect the viability of HT22 cells. All values are expressed as a mean ± SEM for N=3. Data were analysed using one-way ANOVA for multiple comparisons with post hoc Student Newman-Keuls test. \*p<0.033 in comparison with untreated control.

#### The effect of HMC3 conditioned medium on HT22 viability

HMC3 cells were treated with 25 ng/ml and 50 ng/ml of Recombinant Human TNF-α Protein (R&D Systems) or 10 ng/ml and 50 ng/ml of Recombinant Human IFN-γ Protein (R&D Systems) for 24 hours. After incubation, HMC3 medium was collected and centrifuged 806 × g for 5 minutes, and the medium was introduced to confluent HT22 cells for 24 hours. Then XTT assay was performed to assess neuronal viability (as indicated in [2.2.3](#)). Conditioned medium collected from HMC3 cells stimulated with TNF-α (25 and 50 ng/ml), or IFN-γ (10 and 50 ng/ml) did not induce HT22 cytotoxicity (Figure 4.5).

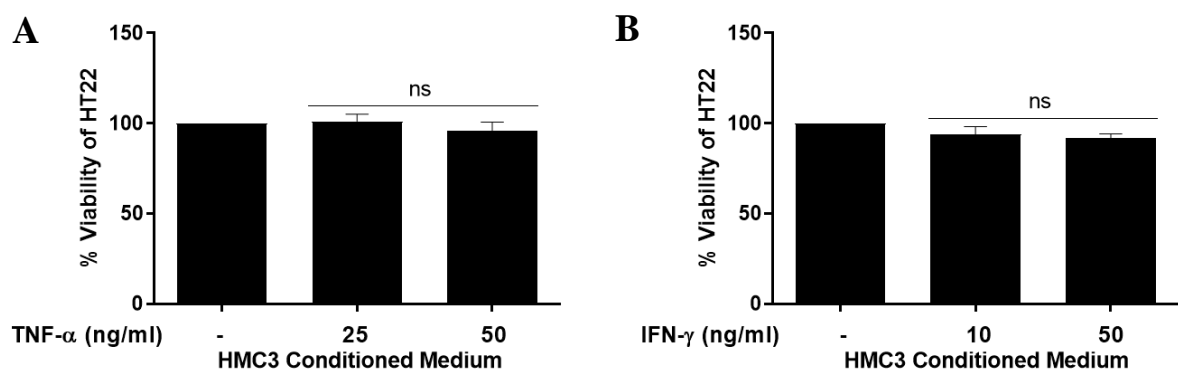


**Figure 4.5 The effect of HMC3 conditioned medium on HT22 viability.** HMC3 cells were activated with TNFα (A) or IFNγ (B) for 24 hours. Then cell culture medium was harvested and introduced to HT22 cells for 24 hours, followed by XTT assay. HMC3 conditioned medium did not significantly affect the viability of HT22 cells. All values are expressed as a mean ± SEM for N=3. Data were analysed using one-way ANOVA for multiple comparisons with post hoc Student Newman-Keuls test. \*p<0.033 in comparison with untreated control.

### The effect of HMC3 conditioned medium on SH-SY5Y viability

HMC3 cells were treated with 25 - 1000 ng/ml of Recombinant Human TNF $\alpha$  Protein (R&D Systems) or 10 - 1000 ng/ml of Recombinant Human IFN $\gamma$  Protein (R&D Systems) for 24 hours. After incubation, HMC3 medium was collected and centrifuged 806  $\times$  g for 5 minutes, and then the medium was introduced to RA-differentiated SH-SY5Y cells for 24 hours. After 24-hour incubation, XTT assay was performed as indicated in [2.2.3](#). Medium collected from HMC3 cells activated with TNF $\alpha$  (25 – 1000 ng/ml) and IFN $\gamma$  (10 – 1000 ng/ml) did not significantly induce cytotoxicity of differentiated SH-SY5Y cells (Figure 4.6).

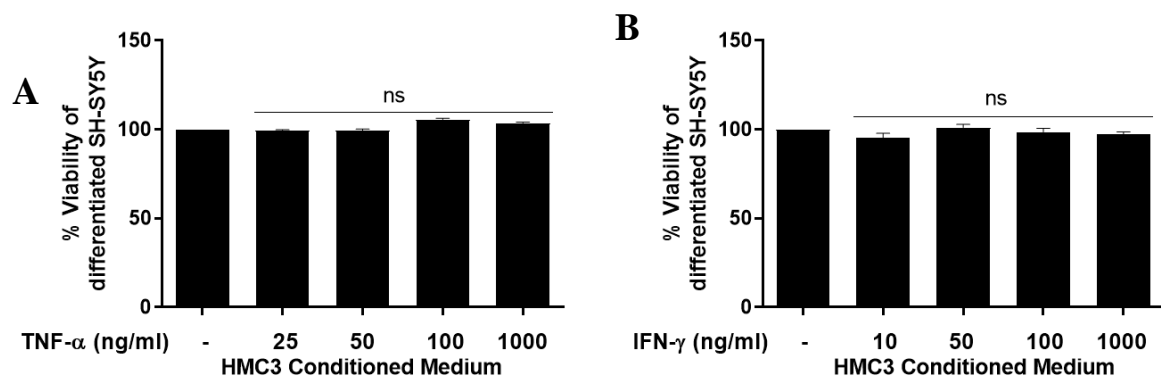


**Figure 4.6 The effect of HMC3 conditioned medium on SH-SY5Y viability.** HMC3 cells were activated with TNF- $\alpha$  (A) or IFN- $\gamma$  (B) for 24 hours. Then cell culture medium was harvested and introduced to differentiated SH-SY5Y cells for 24 hours, and XTT assay was performed. HMC3 conditioned medium did not significantly affect the viability of differentiated SH-SY5Y cells. All values are expressed as a mean  $\pm$  SEM for N=3. Data were analysed using one-way ANOVA for multiple comparisons with post hoc Student Newman-Keuls test. \* $p < 0.033$  in comparison with untreated control.

#### 4.2.6.2 The impact of Amyloid $\beta_{25-35}$ on SH-SY5Y viability

Differentiated and undifferentiated SH-SY5Y cells were incubated with 5 – 40  $\mu\text{M}$  of Amyloid  $\beta$ -Protein Fragment 25-35 (A4559; Sigma-Aldrich) for 24 and 48 hours. Before use,  $\text{A}\beta_{25-35}$  protein was dissolved in sterile water (Fisher Scientific) to final concentration 1 mM. Then  $\text{A}\beta_{25-35}$  solution was incubated five days at  $37^\circ\text{C}$  to induce aggregation of diffusible oligomers. After incubation of SH-SY5Y cells with  $\text{A}\beta_{25-35}$  XTT assay was performed as described in 2.2.3.  $\text{A}\beta_{25-35}$  (5 – 40  $\mu\text{M}$ ) did not reduce the viability of undifferentiated and differentiated SH-SY5Y cells after 24- and 48-hour incubation (Figure 4.7).

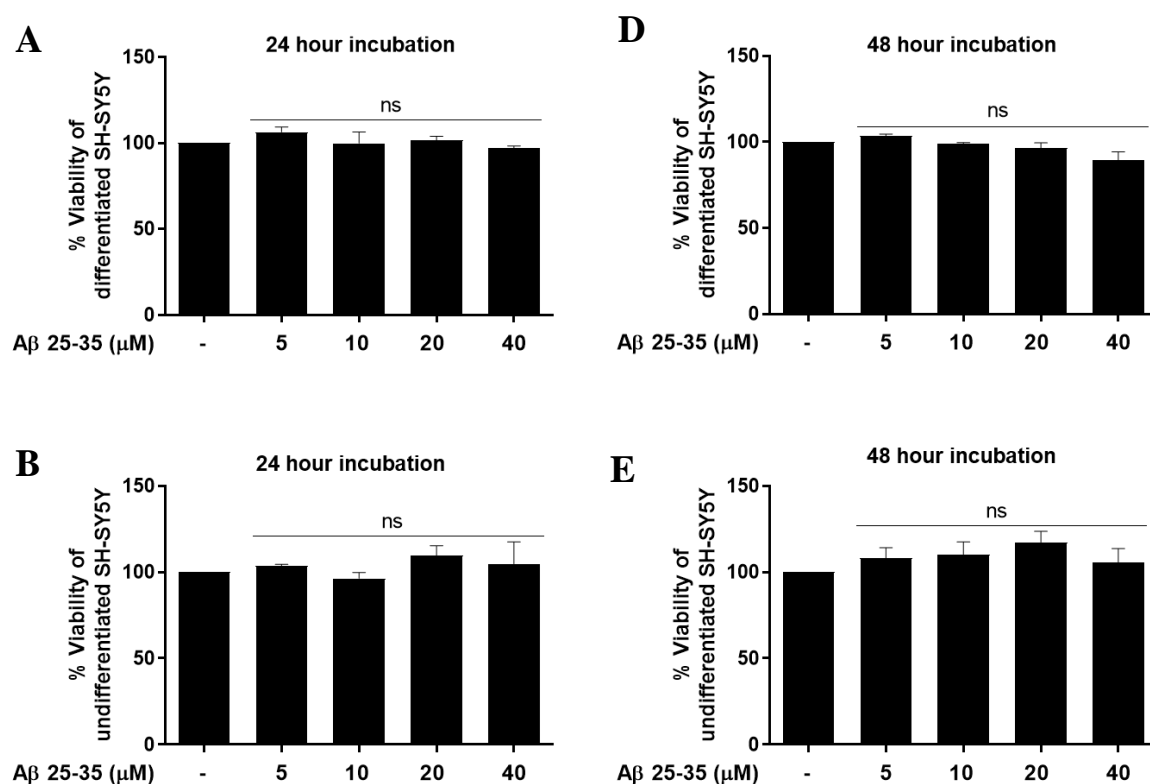


**Figure 4.7 Viability of SH-SY5Y cells after  $\text{A}\beta_{25-35}$  incubation.** Undifferentiated and differentiated SH-SY5Y cells were incubated with  $\text{A}\beta_{25-35}$  protein for 24 (A and B) and 48 (D and E) hours and XTT assay was performed.  $\text{A}\beta_{25-35}$  incubation for 24 hours and 48 hours did not affect the viability of undifferentiated and differentiated SH-SY5Y cells. All values are expressed as a mean  $\pm$  SEM for N=3. Data were analysed using one-way ANOVA for multiple comparisons with post hoc Student Newman-Keuls test. \* $p < 0.033$  in comparison with untreated control.

#### 4.2.6.3 The impact of H<sub>2</sub>O<sub>2</sub> on SH-SY5Y viability

Differentiated SH-SY5Y cells were incubated with 50 – 800  $\mu$ M of Hydrogen Peroxide (Fisher Scientific) for 24 hours, followed by XTT assay performed as indicated in [2.2.3](#). H<sub>2</sub>O<sub>2</sub> significantly ( $p < 0.001$ ) reduced the viability of SH-SY5Y at all tested concentrations (Figure 4.8). As optimal H<sub>2</sub>O<sub>2</sub> concentration to induce SH-SY5Y cell death has been established 50  $\mu$ M of H<sub>2</sub>O<sub>2</sub> because it was the lowest concentration which significantly ( $p < 0.001$ ) reduced neuronal viability.

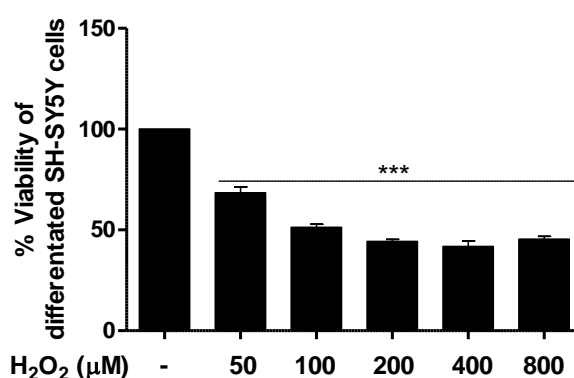


**Figure 4.8 Determination of the optimal H<sub>2</sub>O<sub>2</sub> concentration to induce SH-SY5Y cell death.** Differentiated SH-SY5Y cells were incubated with 50 – 800  $\mu$ M of H<sub>2</sub>O<sub>2</sub> for 24 hours followed XTT assay. H<sub>2</sub>O<sub>2</sub> significantly reduced the viability of differentiated SH-SY5Y cells at all tested concentrations. All values are expressed as a mean  $\pm$  SEM for N=3. Data were analysed using one-way ANOVA for multiple comparisons with post hoc Student Newman-Keuls test. \*\*\* $p < 0.001$  in comparison with untreated control.

#### 4.2.7 Treatment of SH-SY5Y cells with compounds 3 and 4

Before experiments, SH-SY5Y cells were seeded at a density of  $2 \times 10^4$  cells/ml in 200  $\mu$ l/well for 96-well 1 ml/well for 24-well and 2 ml/well for 6-well plate and 5ml/T25 flask (Sarstedt). Then cells were differentiated as indicated in [4.2.4.1](#) after differentiation cell culture medium was changed to serum-free MEM/F12 medium (Fisher Scientific) to reduce the variability of experiments caused by lot to lot variation of serum composition. After 1 – 2 hours of incubation, cells were treated with compounds 3 (2.5, 5, and 10  $\mu$ M) and 4 (5, 10, and 20  $\mu$ M) for 30 minutes. The final concentration of DMSO in cells was constant – 0.01% v/v for all concentrations of compounds and untreated cells (Figure 4.9). Subsequently, cells were treated with 50  $\mu$ M of H<sub>2</sub>O<sub>2</sub> for 24 hours to induce neuronal toxicity.

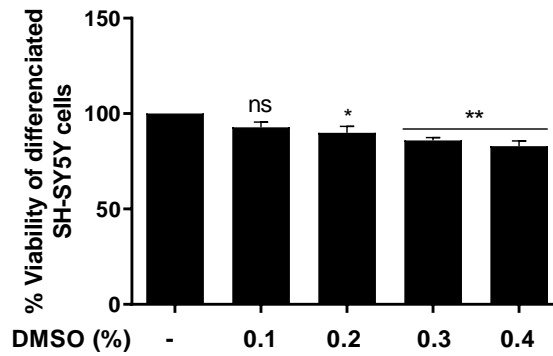


**Figure 4.9 Optimisation of non-toxic concentration of DMSO for differentiated SH-SY5Y cells.** Differentiated SH-SY5Y cells has been exposed to DMSO at final concentration of 0.1%, 0.2%, 0.3% and 0.4% (v/v) for 24 hours. After 24-hour incubation XTT assay was carried out. The final concentration of 0.1% (v/v) of DMSO was not toxic to cells. Concentrations from 0.2% (v/v) of DMSO significantly reduced the viability of SH-SY5Y cells. All values are expressed as a mean  $\pm$  SEM for N=3. Data were analysed using one-way ANOVA for multiple comparisons with post hoc Student Newman-Keuls test. \* $p < 0.033$ , \*\* $p < 0.002$  in comparison with untreated control.

#### 4.2.8 Annexin V-FITC /PI

Annexin V-FITC /PI assay is used to detect and quantify apoptotic cells. This assay relies on the specificity of annexin V to phosphatidylserine (PS) residues, which in viable cells are located in the cytosolic side of the plasma membrane. However, in the early stage of apoptosis, PS residues translocate to the outer part of the membrane allowing its binding to fluorochrome-labelled annexin V and detection of apoptotic cells. Moreover, late apoptosis or necrosis beside translocation of PS into outer layer leads to loss of membrane integrity. This lack of membrane integrity enables another fluorescent agent – propidium iodide (PI) to bind to DNA. PI is not membrane-permeable; hence it stains only late apoptotic and necrotic cells (Schutte, Nuydens, Geerts, & Ramaekers, 1998). Therefore, early apoptotic cells are annexin V positive and PI negative and late apoptotic and necrotic cells are PI-positive (Figure 4.10).

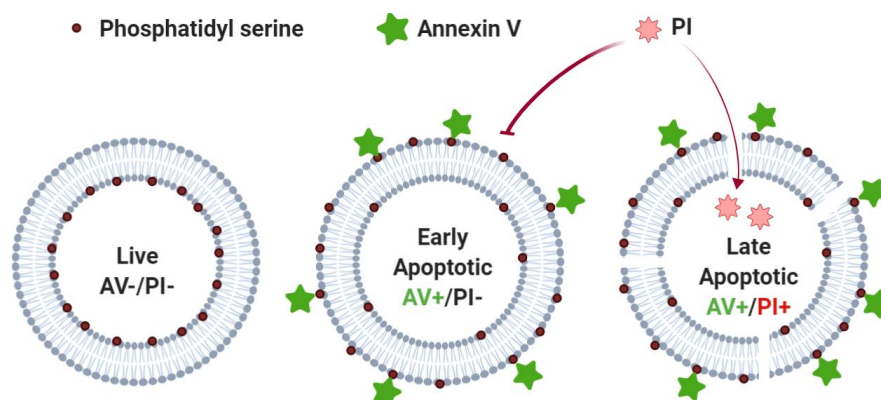


**Figure 4.10 Schematic representation of annexin V/PI staining of live, early apoptotic and late apoptotic/necrotic cells.**

To investigate the effect of compounds on H<sub>2</sub>O<sub>2</sub>-induced neuronal death, dual staining with fluorescent Annexin V and PI has been performed and detected using flow cytometry. Annexin V-FITC Apoptosis Staining / Detection Kit (ab14085) was purchased from Abcam. Before the experiment, SH-SY5Y cells were seeded and differentiated as described in [4.2.4.1](#). Differentiated cells were treated with compounds 3 (2.5, 5, and 10 μM) and 4 (5, 10, and 20 μM) for 30 minutes, followed by induction of cell apoptosis by 50 μM of H<sub>2</sub>O<sub>2</sub>. After 24-hour incubation cells were collected by dissociation from the plate using Gibco™ TrypLE™ Express Enzyme (Fisher Scientific). Subsequently, cells were washed with PBS, centrifuged (400 × g ; 5 minutes) and suspended in 500 μl of 1x Binding Buffer with 5 μL of annexin V-FITC and 5 μL of PI. After 10 minutes of incubation in the dark at room temperature cells were analysed using Guava® easyCyte 5 Benchtop Flow Cytometer. Five thousand events were collected for each sample.

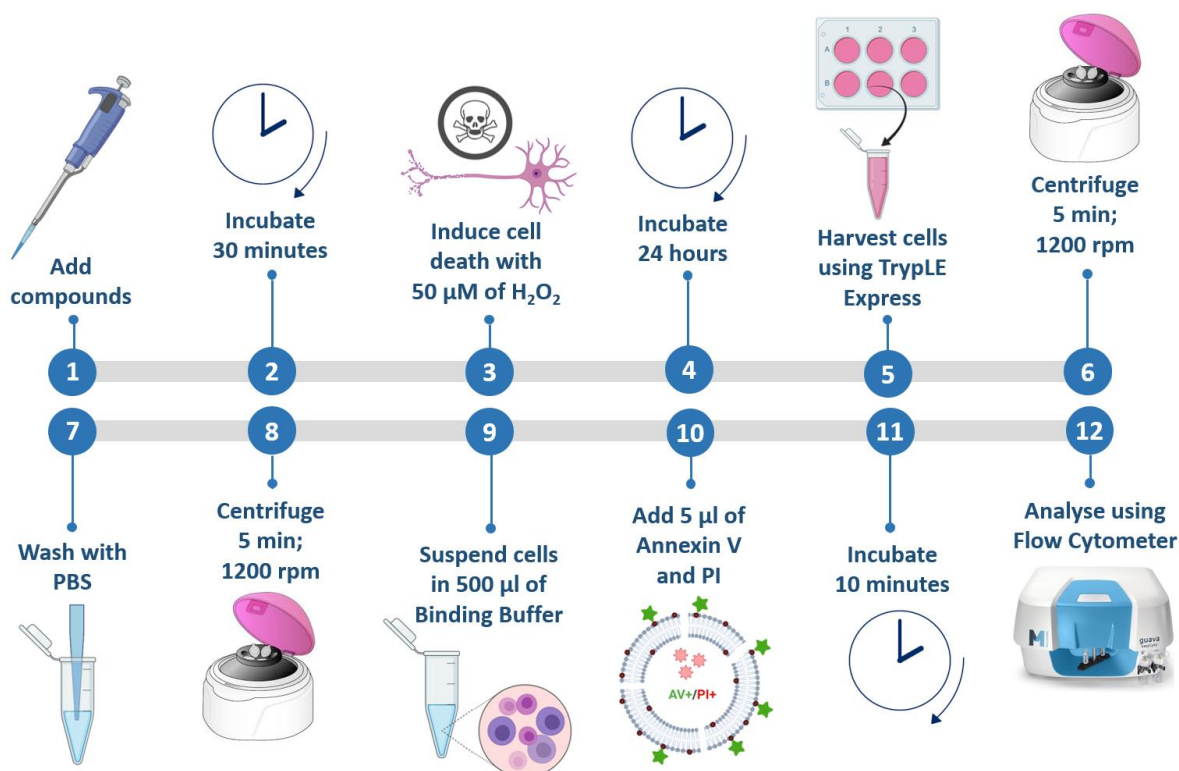


**Figure 4.11** Flowchart of Annexin V/PI staining.

#### 4.2.9 Caspase-3/-7 and -9 activity

Apoptosis is mediated by sequential activation of cysteine-aspartic proteases, also known as caspases. Caspase-9 is initiator caspase of the intrinsic apoptotic pathway. Activated caspase-9 triggers caspase-3 and -7. Caspase-3 and -7 belong to executioner caspases which can be activated by extrinsic and intrinsic (mitochondrial) apoptotic pathways. Activated executioner caspases cleave crucial cellular components and degrade DNA leading to induction of apoptosis (Chowdhury, Tharakan, & Bhat, 2008). Hence caspase-3/-7 activity is directly proportional to cell death.

The activity of caspase-3/-7 and caspase-9 was measured using the Caspase-Glo<sup>®</sup> 3/7 Assay System and Caspase-Glo<sup>®</sup> 9 Assay System (Promega). This technique utilizes Caspase-Glo<sup>®</sup> Reagent to lyse cells and cleave specific caspase-DEVD-aminoluciferin or caspase-LEHD-aminoluciferin substrate for caspase-3/-7 and caspase-9, respectively. This reaction leads to the liberation of aminoluciferin. Consequently aminoluciferin is consumed by luciferase producing a luminescent signal proportional to caspase activity (Promega, n.d.).

Before the experiment, SH-SY5Y cells were seeded at a density of  $2 \times 10^4$  cells/ml in 200  $\mu$ l/well in a white 96-well plate (Sarstedt) and then differentiated as indicated in [4.2.4.1](#). After differentiation, cells were treated with compounds 3 (2.5, 5, and 10  $\mu$ M) and 4 (5, 10, and 20  $\mu$ M) for 30 minutes followed by induction of apoptosis using 50  $\mu$ M of H<sub>2</sub>O<sub>2</sub> for 24 hours. At the end of incubation 100  $\mu$ l of cell culture medium was removed from each well, followed by the addition of 100  $\mu$ l of Caspase-Glo<sup>®</sup> Reagent. Caspase-Glo<sup>®</sup> Reagent was prepared by transferring the contents of the Caspase-Glo<sup>®</sup> Buffer bottle into the amber bottle containing Caspase-Glo<sup>®</sup> Substrate. For the caspase-9 assay, Caspase-Glo<sup>®</sup> 9 Reagent was prepared with proteasome inhibitor - MG-132 to a final concentration of 60  $\mu$ M. Proteasome inhibitor was used to reduce nonspecific background via inhibition of the ATP-independent 20S proteasome activity, which can cleave short peptide substrates such as LEHD. Subsequently, the plate contents were briefly mixed using a plate shaker and incubated 30 minutes for caspase 3/-7 and 90 minutes for caspase-9 before measurement of luminescence (FLUOstar OPTIMA Plate Reader by BMG Labtech).



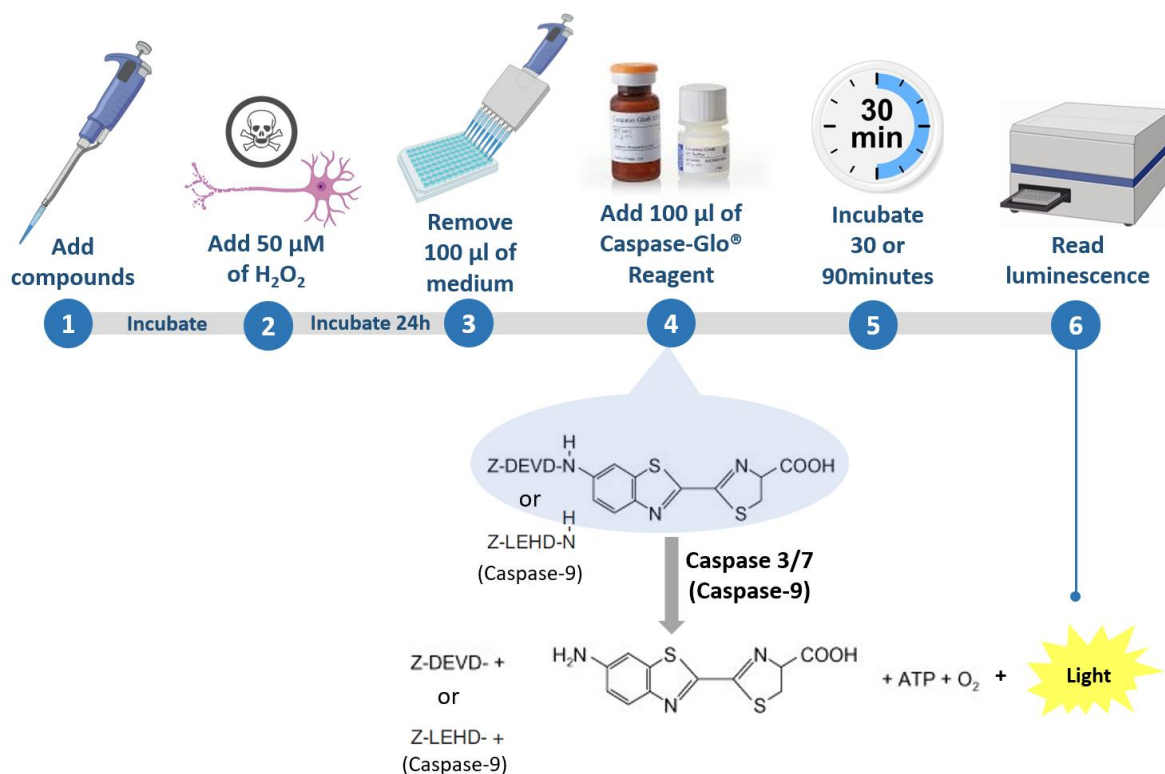


Figure 4.12 Flowchart of Caspase-Glo® 3/7 and 9 Assay System.

#### 4.2.10 Bcl-2 ELISA

SH-SY5Y cells were seeded at a density of  $5 \times 10^4$  cells/ml in 5 ml of MEM/F12 culture medium in tissue culture flask T-25 (Sarstedt) with standard surface modification for adherent cells. This was followed by differentiation and treatment of cells as described in [4.2.4.1](#) and [4.2.6](#). After 24-hour incubation, Bcl-2 ELISA was performed as indicated in [2.2.10](#) using Invitrogen™ Bcl-2 Human ELISA Kit (Fisher Scientific).

#### 4.2.11 Pre-treatment of cells with ER antagonist – ICI 182,780

A common way to evaluate the involvement of proteins or receptors in specific effects expressed by compounds involves the use of antagonists. In previous experiments (chapter three, section [3.3.8](#)), daidzein derivatives have been shown to activate ERE promoter. Therefore, to assess oestrogen receptor contribution to neuroprotective effects of compounds, ICI 182,780 - ERs antagonist was employed. SH-SY5Y cells were seeded and differentiated, as indicated in [4.2.4.1](#). Then, the cell culture medium was changed to serum-free medium followed by 1 – 2-hour incubation. Next cells were incubated with or without 10 nM of ICI 182,780 (Fulvestrant; Sigma-Aldrich) for 30 minutes, then compounds 3 (2.5, 5 and 10 µM) and 4 (5, 10, 20 µM) were added and cells were further incubated 30 minutes. Subsequently,

neuronal death was induced with 50  $\mu\text{M}$  of  $\text{H}_2\text{O}_2$ . After 24-hour incubation XTT assay was performed as described in [2.2.3](#).

#### **4.2.12 Statistical analysis**

Data were analysed using one-way analysis of variance (ANOVA) or two-way ANOVA (for Annexin V/PI data) with post hoc Student-Newman-Keuls test (with multiple comparisons) and are expressed as mean  $\pm$  SEM of at least three independent samples and experiment repetitions (N=3) unless otherwise stated. As statistically significant considered are values \* $p < 0.033$ , \*\* $p < 0.002$ , \*\*\* $p < 0.001$  compared with untreated control or  $\text{H}_2\text{O}_2$  control. Statistical analysis was executed using Graph Pad Prism software version 8.

## 4.3 Results

### 4.3.1 The effect of compounds 3 and 4 on the viability of SH-SY5Y cells

Differentiated SH-SY5Y cells were treated with compounds 3 (2.5, 5 and 10  $\mu\text{M}$ ) and 4 (5, 10, 20  $\mu\text{M}$ ) for 24 hours followed by XTT assay conducted to assess the effect of compounds on the viability of SH-SY5Y cells. Data presented in Figure 4.13 A and B indicate that compounds 3 and 4 at all tested concentrations did not significantly reduce the viability of differentiated SH-SY5Y cells.

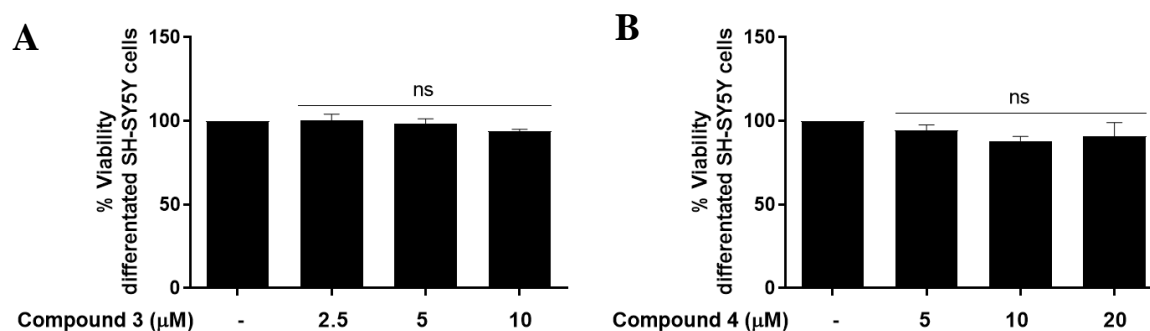


**Figure 4.13 The effect of compounds 3 and 4 on the viability of SH-SY5Y cells.** Differentiated SH-SY5Y cells were treated with compounds 3 (2.5, 5, 10  $\mu\text{M}$ ) and 4 (5, 10, 20  $\mu\text{M}$ ) for 24 hours followed by XTT assay. Compounds 3 (A) and 4 (B) did not affect the viability of differentiated SH-SY5Y cells at any of the tested concentrations. All values are expressed as a mean  $\pm$  SEM for N=3. Data were analysed using one-way ANOVA for multiple comparisons with post hoc Student Newman-Keuls test. \* $p < 0.033$  in comparison with untreated control.

### 4.3.2 The effect of compounds 3 and 4 on H<sub>2</sub>O<sub>2</sub>-induced reduction of SH-SY5Y viability using XTT

To assess if compounds 3 and 4 possess neuroprotective properties, differentiated SH-SY5Y cells were pre-treated with or without compounds followed by induction of neuronal death. Figure 4.12 shows that 50  $\mu$ M of H<sub>2</sub>O<sub>2</sub> induced reduction in neuronal cell viability to 59  $\pm$  9% when compared to the untreated control value of 100%. Compound 3 at 2.5  $\mu$ M significantly ( $p < 0.033$ ) attenuated H<sub>2</sub>O<sub>2</sub>-induced reduction of cell viability to 85  $\pm$  5% when compared to the H<sub>2</sub>O<sub>2</sub> control value of 59%. Compound 3 at concentration 5 and 10  $\mu$ M also significantly ( $p < 0.002$ ) reduced cell death to 99  $\pm$  5% and 95  $\pm$  7% of viable cells, when compared to H<sub>2</sub>O<sub>2</sub> control value of 59% (Figure 4.14 A). Compound 4 significantly ( $p < 0.002$ ) decreased H<sub>2</sub>O<sub>2</sub>-induced reduction of cell viability to 92  $\pm$  5% - 5  $\mu$ M, 85  $\pm$  1% - 10  $\mu$ M and 83  $\pm$  3% - 20  $\mu$ M of viable cells, when compared to H<sub>2</sub>O<sub>2</sub> control value of 59% (Figure 4.14 B).

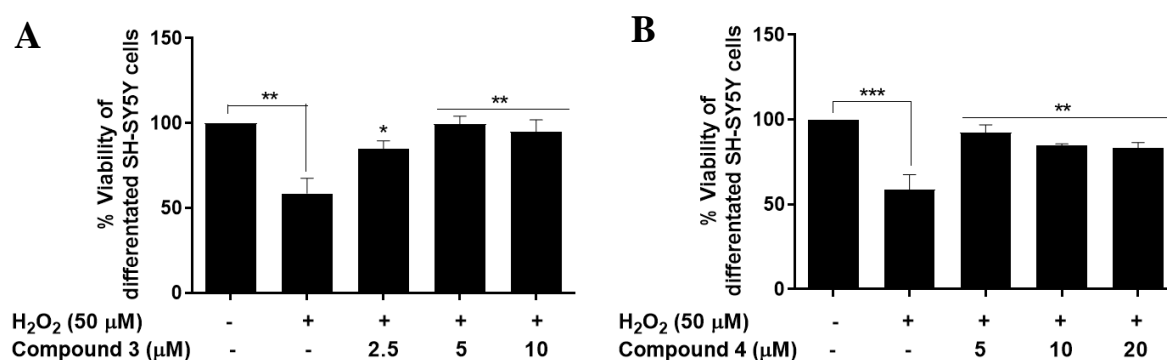
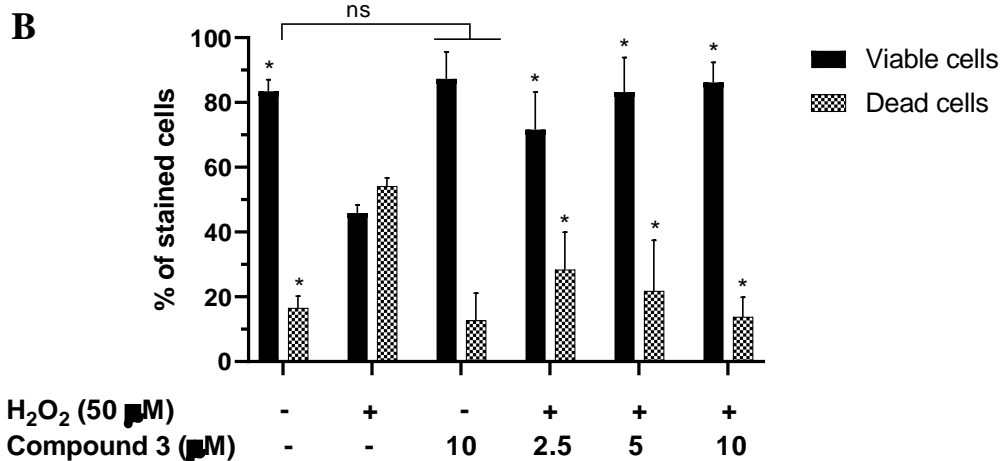
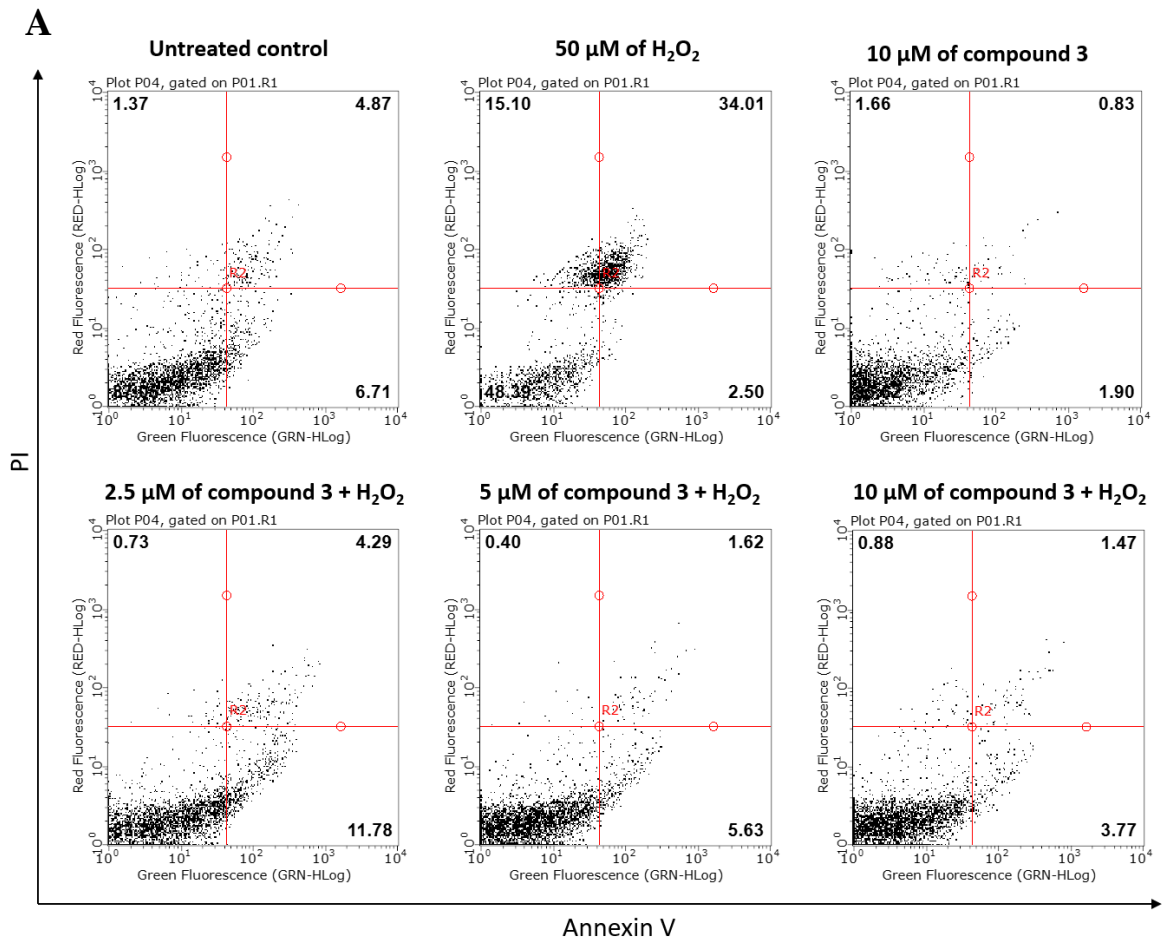


**Figure 4.14** The effect of compounds 3 and 4 on H<sub>2</sub>O<sub>2</sub>-induced reduction of SH-SY5Y cell viability. Differentiated SH-SY5Y cells were treated with compounds 3 (2.5, 5, 10  $\mu$ M) and 4 (5, 10, 20  $\mu$ M) for 30 minutes followed by treatment with 50  $\mu$ M of H<sub>2</sub>O<sub>2</sub> for 24 hours. After 24-hour incubation, XTT assay was performed. Compound 3 (A) and compound 4 (B) attenuated H<sub>2</sub>O<sub>2</sub>-induced decreased cell viability. All values are expressed as a mean  $\pm$  SEM for N=3. Data were analysed using one-way ANOVA for multiple comparisons with post hoc Student Newman-Keuls test. \* $p < 0.033$ , \*\* $p < 0.002$ , \*\*\* $p < 0.001$  in comparison with H<sub>2</sub>O<sub>2</sub> control.

### 4.3.3 The effect of compounds 3 and 4 on H<sub>2</sub>O<sub>2</sub>-induced SH-SY5Y cell death using Annexin V/PI flow cytometry

To further confirm neuroprotective properties of compounds 3 and 4, differentiated SH-SY5Y cells were pre-treated with or without compounds followed by induction of neuronal apoptosis and analysis of cell viability using Annexin V/PI flow cytometry. Figure 4.15 shows that viability of SH-SY5Y cells incubated with H<sub>2</sub>O<sub>2</sub> (50  $\mu$ M) for 24 hours was significantly ( $p < 0.033$ ) decreased to 46  $\pm$  3% compared to untreated cells value of 83  $\pm$  4%. Pre-incubation of cells with compound 3 (2.5, 5 and 10  $\mu$ M) significantly ( $p < 0.033$ )

alleviated H<sub>2</sub>O<sub>2</sub>-induced apoptosis leading to 72 ± 12%, 78 ± 16% and 86 ± 6% of viable cells, respectively, when compared to the H<sub>2</sub>O<sub>2</sub> control (Figure 4.16 B). Similarly, pre-incubation of SH-SY5Y cells with compound 4 (5, 10, 20 μM) significantly (p<0.033) inhibited H<sub>2</sub>O<sub>2</sub>-induced apoptosis when compared to H<sub>2</sub>O<sub>2</sub> control value of 46%. Viability of cells incubated with 5, 10, 20 μM of compound 4 followed by H<sub>2</sub>O<sub>2</sub>-induced apoptosis was 64 ± 3%, 71 ± 2% and 81 ± 7% (Figure 4.16 D).



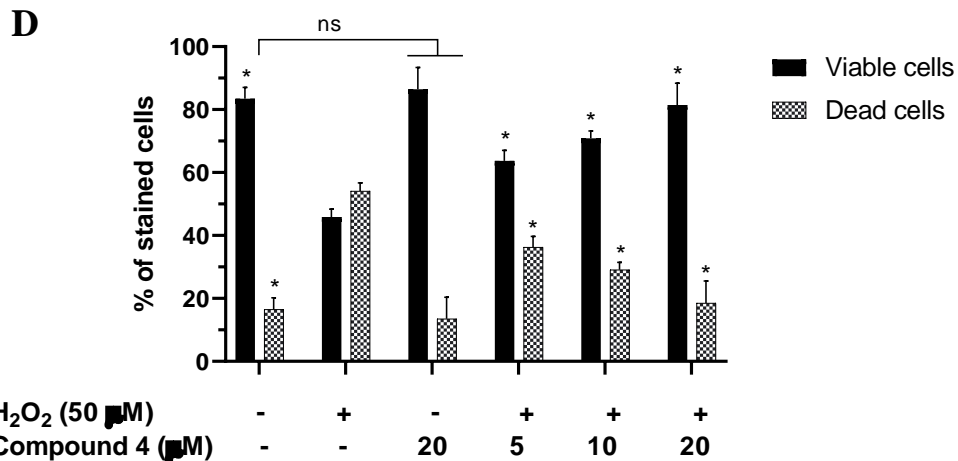
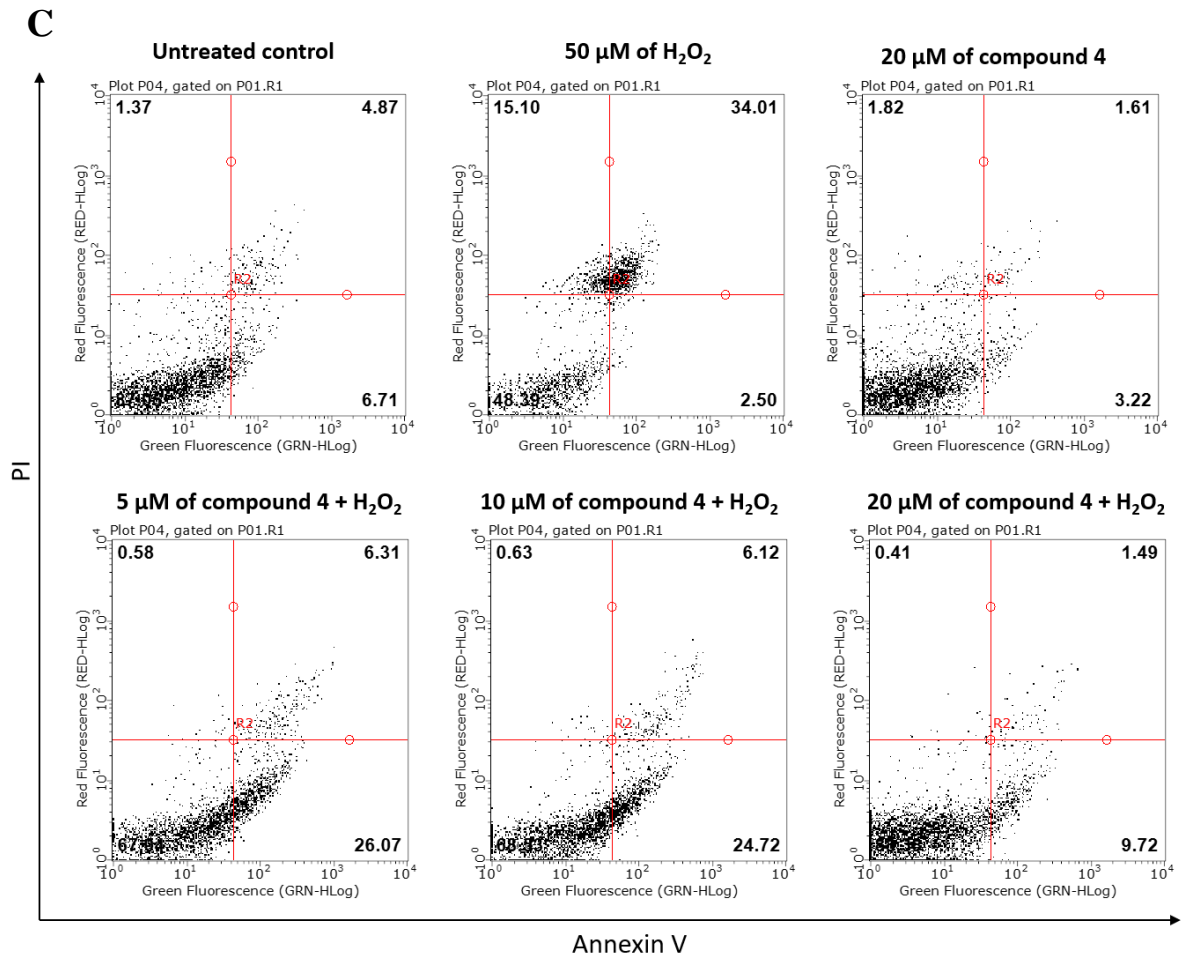


**Figure 4.15 Viability of cells exposed to different concentrations of compounds 3 and 4 followed by  $\text{H}_2\text{O}_2$ -induced apoptosis of SH-SY5Y cells.** Differentiated SH-SY5Y cells were incubated with compounds 3 (2.5, 5, 10  $\mu\text{M}$ ) and 4 (5, 10, 20  $\mu\text{M}$ ) for 30 minutes followed by 50  $\mu\text{M}$  of  $\text{H}_2\text{O}_2$  treatment for 24 hours. After 24-hour incubation cells were harvested and stained with annexin V and PI followed by flow cytometry analysis. (A and C) Representative scatter diagrams of cells stained with annexin V and PI. Compound 3 (B) and compound 4 (D) attenuated  $\text{H}_2\text{O}_2$ -induced apoptosis. All values are expressed as a mean  $\pm$  SEM for  $N=3$ . Data were analysed using two-way ANOVA for multiple comparisons with post hoc Student Newman-Keuls test. \* $p < 0.033$  in comparison with untreated control or  $\text{H}_2\text{O}_2$  control.

#### 4.3.4 The effect of compounds 3 and 4 on H<sub>2</sub>O<sub>2</sub>-induced caspase-3/-7 activity in SH-SY5Y cells

Cell death is coordinated by sequential activation of caspases. Caspase-3/-7 play crucial role in execution-phase of cell apoptosis (Chowdhury et al., 2008). Therefore, to evaluate the neuroprotective properties of compounds 3 and 4 and their impact on the activation of caspase-3/-7, SH-SY5Y cells were treated with compounds followed by H<sub>2</sub>O<sub>2</sub>-induced cell death. Cells incubated with 50  $\mu$ M of H<sub>2</sub>O<sub>2</sub> for 24 hours significantly ( $p < 0.002$ ) increased caspase-3/-7 activity when compared to unstimulated cells. Figure 4.16 A shows that compound 3 did not significantly affect basal caspase-3/-7 activity when compared to untreated cells. However, compound 3 at 2.5, 5 and 10  $\mu$ M significantly ( $p < 0.033$ ) decreased H<sub>2</sub>O<sub>2</sub>-induced caspase-3/-7 activity to  $68 \pm 9\%$ ,  $69 \pm 12\%$  and  $67 \pm 11\%$ , respectively, compared to H<sub>2</sub>O<sub>2</sub> control value of 100%. SH-SY5Y cells incubated with 20  $\mu$ M of compound 4 significantly ( $p < 0.002$ ) reduced basal level of caspase-3/-7 activity when compared to untreated control. Not significant reduction of the basal level of caspase-3/-7 activity was observed in cells treated with 5  $\mu$ M and 10  $\mu$ M of compound 4 when compared to untreated cells. Moreover, cells pre-treated with compound 4 at 5, 10 and 20  $\mu$ M followed by H<sub>2</sub>O<sub>2</sub> incubation significantly ( $p < 0.001$ ) reduced H<sub>2</sub>O<sub>2</sub>-induced caspase-3/-7 activity to  $66 \pm 8\%$ ,  $64 \pm 8\%$  and  $53 \pm 6\%$ , respectively, compared to H<sub>2</sub>O<sub>2</sub> control value of 100% (Figure 4.16 B).

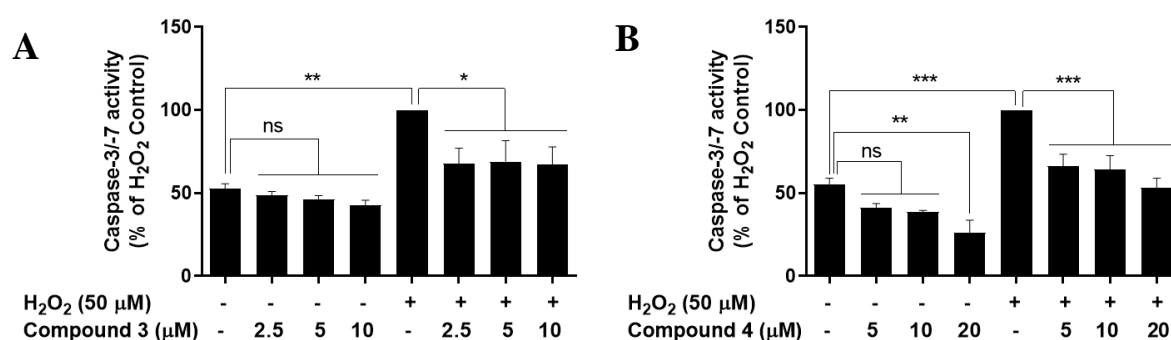


**Figure 4.16** The effect of compounds 3 and 4 on H<sub>2</sub>O<sub>2</sub>-induced caspase 3/7 activity in SH-SY5Y neurons. Differentiated SH-SY5Y cells have been treated with compounds 3 (2.5, 5, and 10  $\mu$ M) and 4 (5, 10, and 20  $\mu$ M) followed by H<sub>2</sub>O<sub>2</sub>-induced cell death. Cells significantly upregulated caspase 3/7 activity when incubated with 50  $\mu$ M of H<sub>2</sub>O<sub>2</sub>. (A) Cells exposed to compound 3 only did not significantly change caspase 3/7 activity. Treatment of cells with compound 3 followed by H<sub>2</sub>O<sub>2</sub>-induced reduction of cell viability result in significant ( $p < 0.033$ ) reduction of caspase 3/7 activity, when compared to H<sub>2</sub>O<sub>2</sub> control. (B) Compound 4 at 20  $\mu$ M significantly ( $p < 0.002$ ) inhibited caspase 3/7 activity when compared to untreated control. Compound 4 significantly ( $p < 0.001$ ) attenuated H<sub>2</sub>O<sub>2</sub>-induced caspase 3/7 activity in cells pre-incubated with 5, 10 and 20  $\mu$ M of the compound. All values are expressed as a mean  $\pm$  SEM for N=3. Data were analysed using one-way ANOVA for multiple comparisons with post hoc Student Newman-Keuls test. \* $p < 0.033$ , \*\* $p < 0.002$ , \*\*\* $p < 0.001$  in comparison with untreated control or H<sub>2</sub>O<sub>2</sub> control.

### 4.3.5 The effect of compounds 3 and 4 on the H<sub>2</sub>O<sub>2</sub>-induced caspase-9 activity in SH-SY5Y cells

Compounds 3 and 4 showed inhibitory activity on caspase-3/-7 activation. Consequently, the effect of compounds 3 and 4 was investigated on the activity of caspase-9 which is an upstream regulator of executioner caspases directing intrinsic apoptotic pathway (Brentnall, Rodriguez-Menocal, De Guevara, Cepero, & Boise, 2013). Data presented in Figure 4.17 show that SH-SY5Y cells treated with 50  $\mu$ M H<sub>2</sub>O<sub>2</sub> significantly ( $p < 0.001$ ) increased caspase-9 activity compared to untreated control. Cells treated only with compounds 3 (2.5, 5, and 10  $\mu$ M) and 4 (5, 10, and 20  $\mu$ M) did not alter the activity of caspase-9 when compared to untreated cells. However, cells pre-incubated with 2.5, 5, and 10  $\mu$ M of compound 3 followed by H<sub>2</sub>O<sub>2</sub> treatment significantly ( $p < 0.002$ ) reduced caspase-9 activity to  $57 \pm 5\%$ ,  $70 \pm 9\%$  and  $72 \pm 7\%$ , respectively, when compared to H<sub>2</sub>O<sub>2</sub> control value of 100%. Similarly, cells pre-incubated with 5, 10, and 20  $\mu$ M of compound 4 followed by H<sub>2</sub>O<sub>2</sub>-induced cells death significantly ( $p < 0.001$ ) inhibited caspase-9 activity to  $58 \pm 8\%$ ,  $51 \pm 2\%$  and  $58 \pm 9\%$ , respectively, compared to H<sub>2</sub>O<sub>2</sub> control value of 100% (Figure 4.17 B).

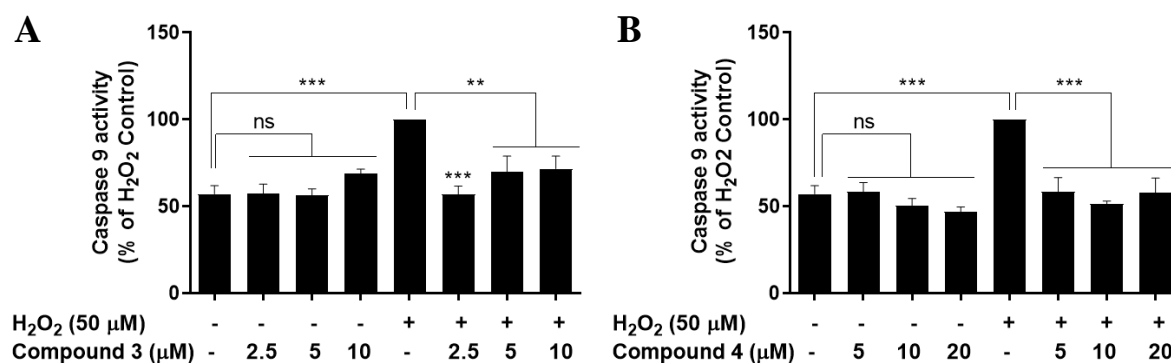


**Figure 4.17** The effect of compounds 3 and 4 on H<sub>2</sub>O<sub>2</sub>-induced caspase-9 activity in SH-SY5Y neurons. Differentiated SH-SY5Y cells have been treated with compounds 3 (2.5, 5, and 10  $\mu$ M) and 4 (5, 10, and 20  $\mu$ M) followed by H<sub>2</sub>O<sub>2</sub>-induced cell death. Cells significantly ( $p < 0.001$ ) upregulated caspase-9 activity when incubated with 50  $\mu$ M of H<sub>2</sub>O<sub>2</sub> compared to untreated control. (A) Compound 3 did not significantly affect caspase-9 activity when compared to untreated cells. Treatment of cells with compound 3 followed by H<sub>2</sub>O<sub>2</sub>-induced reduction of cell viability significantly ( $p < 0.033$ ) reduce of caspase-9 activity, when compared to H<sub>2</sub>O<sub>2</sub> control. (B) Cells incubated with compound 4 did affect caspase-9 activity when compared to untreated control. In turn, cells pre-incubated with compound 4 followed by H<sub>2</sub>O<sub>2</sub> treatment significantly ( $p < 0.001$ ) attenuated H<sub>2</sub>O<sub>2</sub>-induced caspase-9 activity when compared to H<sub>2</sub>O<sub>2</sub> control. All values are expressed as a mean  $\pm$  SEM for N=3. Data were analysed using one-way ANOVA for multiple comparisons with post hoc Student Newman-Keuls test. \* $p < 0.033$ , \*\* $p < 0.002$ , \*\*\* $p < 0.001$  in comparison with untreated control or H<sub>2</sub>O<sub>2</sub> control.



### 4.3.6 The effect of compounds 3 and 4 on the Bcl-2 level in SH-SY5Y cells

Previous results indicated neuroprotective activities of compounds 3 and 4; hence, the further studies sought to determine molecular mechanisms underlying those actions. Bcl-2 is one of the critical regulators of apoptosis promoting cellular survival and inhibiting the actions of pro-apoptotic proteins (Howard et al., 2002). Therefore, the effects of compounds 3 and 4 alone and in combination with H<sub>2</sub>O<sub>2</sub> on Bcl-2 levels were investigated. Differentiated SH-SY5Y cells incubated with 50 μM of H<sub>2</sub>O<sub>2</sub> for 24 hours significantly ( $p < 0.033$ ) reduced Bcl-2 level to  $85 \pm 2\%$  compared to untreated control values of 100%. Figure 4.18 A shows that cells incubated with compound 3 (2.5, 5, and 10 μM) did not significantly affect Bcl-2 production compared to untreated cells. However, SH-SY5Y incubated with compound 3 and H<sub>2</sub>O<sub>2</sub> significantly ( $p < 0.002$ ) upregulated Bcl-2 level to  $113 \pm 4\%$  - 5 μM,  $106 \pm 5\%$  - 10 μM,  $120 \pm 5\%$  - 20 μM, when compared to H<sub>2</sub>O<sub>2</sub> control value of 85%. Figure 4.18 B indicates that compound 4 did not significantly affect Bcl-2 production in SH-SY5Y cells when compared to untreated control value of 100%. Similarly, compound 4 (5, 10 and 20 μM) had no significant ( $p < 0.033$ ) effect on cells pre-incubated with compound followed by H<sub>2</sub>O<sub>2</sub> treatment for 24-hour when compared to H<sub>2</sub>O<sub>2</sub> control.

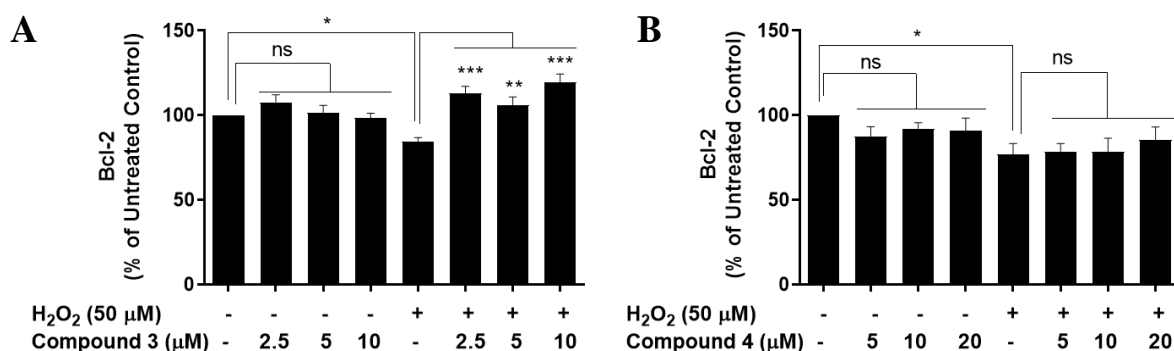


**Figure 4.18** The effect of compounds 3 and 4 on the Bcl-2 level in SH-SY5Y incubated with or without H<sub>2</sub>O<sub>2</sub>. Differentiated SH-SY5Y cells were incubated with compounds (2.5, 5, and 10 μM) and 4 (5, 10, and 20 μM) followed by H<sub>2</sub>O<sub>2</sub>-induced cell death. After 24-hour incubation, whole-cell lysates were collected, and Bcl-2 ELISA was conducted. Significant ( $p < 0.033$ ) reduction of Bcl-2 level was observed in cells incubated with 50 μM of H<sub>2</sub>O<sub>2</sub> for 24 hours when compared to untreated cells. (A) Cells incubated with compound 3 did not significantly increase Bcl-2 level when compared to untreated cells. However, cells pre-treated with compound 3 followed by the addition of 50 μM of H<sub>2</sub>O<sub>2</sub> significantly ( $p < 0.002$ ,  $p < 0.001$ ) increase the level of Bcl-2 when compared to H<sub>2</sub>O<sub>2</sub> control. Compound 4 did not significantly affect Bcl-2 production in SH-SY5Y cells when compared to untreated control. Similarly, compound 4 (5, 10 and 20 μM) had no significant effect on cells pre-incubated with compound followed by addition of H<sub>2</sub>O<sub>2</sub> for 24-hours when compared to H<sub>2</sub>O<sub>2</sub> control. All values are expressed as a mean  $\pm$  SEM for N=3. Data were analysed using one-way ANOVA for multiple comparisons with post hoc Student Newman-Keuls test. \* $p < 0.033$ , \*\* $p < 0.002$ , \*\*\* $p < 0.001$  in comparison with untreated control or H<sub>2</sub>O<sub>2</sub> control.

### 4.3.7 The impact of ER antagonist on neuroprotective properties of compounds 3 and 4 in SH-SY5Y cells

Compounds 3 and 4 showed the ability to induce ERE activity, therefore, to investigate if neuroprotective properties of compounds are ER-dependent, cells were pre-treated with ER antagonist - ICI 182,780 (10 nM) followed by treatment with compounds 3 and 4 and H<sub>2</sub>O<sub>2</sub> (50 μM). XTT assay indicated that SH-SY5Y cells incubated with H<sub>2</sub>O<sub>2</sub> alone or ICI 182,780 followed by H<sub>2</sub>O<sub>2</sub> treatment significantly (p<0.001) reduced cell viability to 75 ± 2% and 80 ± 6%, respectively when compared to unstimulated cells as 100%. Thus, ICI 182,780 did not attenuate H<sub>2</sub>O<sub>2</sub>-induced cell death (Figure 4.19). Figure 4.19 A shows that pre-incubation of cells with or without ICI 182,780 followed by compound 3 and H<sub>2</sub>O<sub>2</sub> treatment significantly (p<0.001) increased cells viability when compared to H<sub>2</sub>O<sub>2</sub> control value of 75%. Figure 4.19 B indicates that pre-incubation of cells with ICI 182,780 did not inhibit increased cells viability caused by treatment with compound 4 followed by H<sub>2</sub>O<sub>2</sub>-induced cell death. Pre-incubation of cells with ER antagonist did not diminish the neuroprotective properties of compounds 3 and 4 in H<sub>2</sub>O<sub>2</sub>-induced cell death in SH-SY5Y cells.

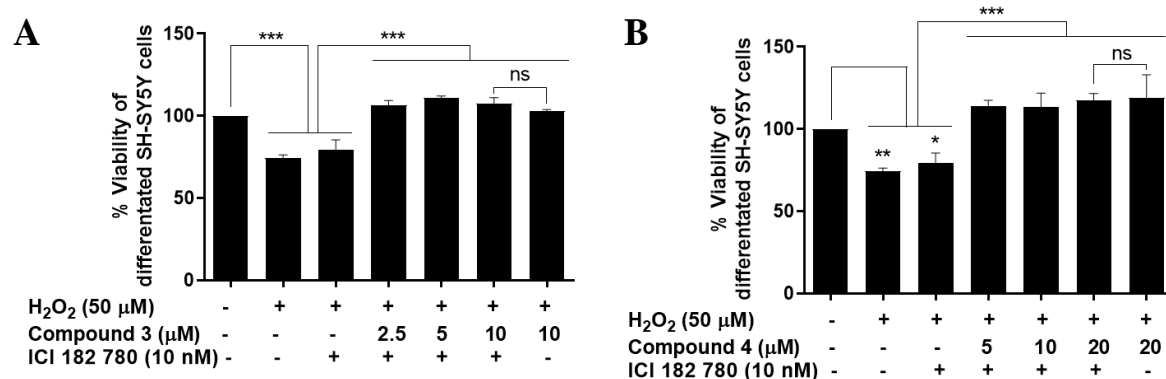


**Figure 4.19 The impact of ER antagonist on neuroprotective properties of compounds 3 and 4 in SH-SY5Y.** Differentiated SH-SY5Y cells were incubated with 10 nM of ICI 182,780 for 30 minutes followed by treatment with compounds 3 (2.5, 5, and 10 μM) and 4 (5, 10, and 20 μM). After 30 minutes of incubation 50 μM of H<sub>2</sub>O<sub>2</sub> was added to reduce cell viability. Subsequently, cells were incubated 24 hours, and XTT assay was conducted. Pre-incubation with ICI 182,780 did not attenuate compounds 3 (A) and 4 (B) ability to increase H<sub>2</sub>O<sub>2</sub>-induced reduction of cell viability. All values are expressed as a mean ± SEM for N=3. Data were analysed using one-way ANOVA for multiple comparisons with post hoc Student Newman-Keuls test. \*p<0.033, \*\*p<0.002, \*\*\*p<0.001 in comparison with untreated control or H<sub>2</sub>O<sub>2</sub> control.

## 4.4 Discussion

Neuronal loss is a pathological feature of neurodegenerative disorders. The most prevalent neurodegenerative disease of modern society is dementia. Globally, 50 million people are living with dementia, and it is estimated that this number will increase to 75 million by 2030 (Prince, Wimo, Guerchet, 2015). Moreover, dementia which includes Alzheimer's disease (AD) is the leading cause of death among women in the United Kingdom (Office for National Statistics, 2020). Therefore, a higher incidence of the AD in women than men has been associated with a decrease of oestrogen level during menopause (Ciesielska, Joniec, & Członkowska, 2002). This hypothesis indicates that oestrogens are important neuroprotective factors which counteract AD development via oestrogen receptor (ER) direct and indirect genomic signalling mechanisms. However, oestrogens may cause detrimental side effects, such as gynaecological and breast cancers. Hence, selective activation of ERs may serve as a potential therapy aiming to reduce neuroinflammation and restore normal physiological brain functions. Phytoestrogens are polyphenolic compounds known to selectively target ERs. Daidzein, which belongs to phytoestrogens family, showed fivefold increased affinity to ER $\beta$  than ER $\alpha$  (Poschner et al., 2017). ER $\alpha$  and ER $\beta$  have different biological activities and expression patterns. Activation of ER $\alpha$  induces proliferation of the uterus and mammary gland, which may cause pathological processes such as endometrial and breast cancer (Zhao, Dahlman-Wright, & Gustafsson, 2008). In contrast, ER $\beta$ -agonists exhibit anticarcinogenic, neuroprotective and cognitive enhancement activities (Paterni, Iliaria, Granchi, Katzenellenbogen, & Minutolo, 2011). Therefore, daidzein's selective oestrogen receptor modulation plays a crucial role in its neuroprotective, anti-inflammatory, anticarcinogenic, and antioxidant properties (Sun et al., 2016).

Compounds 3 and 4 are novel daidzein analogues with ethyl ester and chloropropyl triazole functional group inserted into daidzein B-ring at position 4'. Ethyl ester moiety increases lipid solubility and stability of molecule (Harrold & Zavod, 2014). Moreover, ethyl ester functional group has been found in the structure of various compounds exhibiting neuroprotective activities including glutathione monoethyl ester, lanthionine ketimine-5-ethyl ester, orotic acid ethyl ester and ferulic acid ethyl ester (Akiho et al., 1998; Anderson, Nilsson, Eriksson, & Sims, 2004; Koehler, Shah, Hensley, & Williams, 2018; Sultana, Ravagna, Mohmmad-Abdul, Calabrese, & Butterfield, 2005). The functional group added to compound 4 – chloropropyl triazole provides electron reach system and increase compounds stability. Furthermore, triazole-based compounds have been shown to alleviate

neurodegenerative disorders such as Alzheimer's disease or Parkinson's disease (Marques et al., 2020; Kharb et al., 2011; Xu et al., 2019).

This study presented daidzein derivatives ability to reduce LPS-induced inflammation in BV2 microglia, which suggests that compounds are also neuroprotective through a decrease of neuroinflammation. Further research focused on the examination of direct neuroprotective properties of daidzein derivatives using differentiated SH-SY5Y with H<sub>2</sub>O<sub>2</sub>-induced cytotoxicity. Exposure of cells to H<sub>2</sub>O<sub>2</sub> was demonstrated to induce either apoptosis or necrosis depending on concentration (Troyano et al., 2003). Moderate concentrations of H<sub>2</sub>O<sub>2</sub> trigger apoptosis, while elevated concentrations cause necrosis through direct inactivation of caspases by excessive oxidation (Samali, Nordgren, Zhivotovsky, Peterson, & Orrenius, 1999). Therefore, this study based on viability assays employed the lowest examined H<sub>2</sub>O<sub>2</sub> concentration - 50 μM, which significantly reduced neuronal viability.

Neurodegeneration is associated with inflammation and oxidative stress resulting in excessive production of ROS, including H<sub>2</sub>O<sub>2</sub>. Therefore, H<sub>2</sub>O<sub>2</sub> represents one of the neurotoxic molecules which causes neuronal loss during neurodegeneration. Hence, H<sub>2</sub>O<sub>2</sub> is widely used and studied as an apoptosis-inducing agent (Xiang, Wan, Guo, & Guo, 2016). H<sub>2</sub>O<sub>2</sub> triggers apoptosis via oxidative stress causing damage to proteins, lipids, nucleic acids, and organelles such as mitochondria (Redza-Dutordoir & Averill-Bates, 2016). In the case of mitochondria, H<sub>2</sub>O<sub>2</sub> induces apoptosis through the mitochondrial pathway leading to Bax/Bak activation. Activated Bax causes mitochondrial outer membrane permeabilization, which leads to cytochrome c release. Released cytochrome c allows APAF-1 and pro-caspase-9 recruitment leading to caspase-9 activation which in turn triggers effector caspases-3/-7 activation. Incubation of SH-SY5Y cells with 50 μM of H<sub>2</sub>O<sub>2</sub> significantly decreased cell viability to 60% compared to untreated cells value of 100%. Pre-treatment of SH-SY5Y cells with compounds 3 and 4 prevented H<sub>2</sub>O<sub>2</sub>-induced cell loss. Moreover, both compounds also downregulated caspase-3/-7 activity which coordinates the execution phase of apoptosis by cleaving cellular structures causing characteristic apoptotic cellular breakdown. Therefore, both compounds are neuroprotective against oxidative-stress induced cell death. Similar to the observed effects of its derivatives, daidzein reduced caspase-3 activity in primary neocortical, cerebellar, and hippocampal cell cultures exposed to glutamic acid (Kajta et al., 2013a). Adams et al., (2012) also demonstrated that daidzein attenuated the HIV-1 Tat-induced upregulation of active caspase-3 expression in neuronal cultures.

Previous experiments demonstrating compounds 3 and 4 ability to reduce caspase-3/-7 activity led to further investigation of effect of compounds on upstream caspase-9 which is initiator caspase of intrinsic apoptotic pathway (Li & Yuan, 2008). Both compounds 3 and 4 significantly inhibited H<sub>2</sub>O<sub>2</sub>-induced caspase-9 activity in SH-SY5Y cells. Therefore, both compounds have the ability to inhibit intrinsic apoptotic pathway through caspase-9 inactivation. These results reflect those of Adams et al., (2012) who also found that daidzein and genistein reduced caspase-9 activity in primary cultured cortical neurons with HIV Tat-induced neurotoxicity.

Apoptosis is tightly regulated by Bcl-2 protein where its decrease leads to cell death, and its overexpression protects the cell from apoptosis. Bcl-2 may be neuroprotective by sequestering the activators from engaging Bax and Bak or by binding already activated Bak and Bax thereby blocking the release of cytochrome c from mitochondria (Hata, Engelman, & Faber, 2016). A large body of evidence suggests that Bcl-2 improves neuronal survival following various insults such as glutamate, hydrogen peroxide and MPTP (Howard et al., 2002). Mao et al., (2007) demonstrated that daidzein increased the transcription of Bcl-2 in brain regions of D-galactose-treated mice. Previous experiments presented in this study demonstrated that both daidzein derivatives are neuroprotective against H<sub>2</sub>O<sub>2</sub>-induced apoptosis. Therefore, the effect of compounds was examined on Bcl-2 levels to determine if neuroprotective properties of daidzein derivatives are caused by increased Bcl-2 protein level like in case of the parental compound. Pre-treatment with compound 3 followed by H<sub>2</sub>O<sub>2</sub> treatment resulted in upregulation of Bcl-2 level, compared to H<sub>2</sub>O<sub>2</sub> stimulated cells. Therefore, the increased level of Bcl-2 suggests strong neuroprotective properties of compound 3. In turn, compound 4 did not affect Bcl-2 levels. Hence, chloropropyl triazole moiety at position 4' in daidzein B-ring possibly diminished the compound's ability to upregulate Bcl-2 in contrast to daidzein and daidzein derivative with ethyl ester functional group.

Neuroprotective properties of daidzein have been associated with oestrogen receptor (ER) activation (Adams et al., 2012). Moreover, Kajta et al., (2013a) demonstrated that among ERs - ER $\beta$  plays a crucial function in the inhibition of apoptosis. The cell line used in this study – SH-SY5Y express both ER $\alpha$  and ER $\beta$  (Saeed et al., 2008). Therefore, in order to evaluate if compounds 3 and 4 mediate their neuroprotective activities via ERs activation cells were pre-incubated with ER antagonist - ICI 182,780, followed by treatment with compounds and H<sub>2</sub>O<sub>2</sub>. ICI 182,780 is pure antioestrogen which completely blocks both ER $\alpha$

and ER $\beta$  (He et al., 2011). Viability assays showed that ER antagonist did not block neuroprotective properties of daidzein analogues in SH-SY5Y with H<sub>2</sub>O<sub>2</sub>-induced cell death. Therefore, specific cellular responses inducing neuroprotection triggered by compounds 3 and 4 are ER-independent.

Summarizing, both daidzein derivatives – compounds 3 and 4 blocked H<sub>2</sub>O<sub>2</sub>-induced SH-SY5Y cell death via reduction of caspase-3/-7 and -9 activation. Furthermore, compound 3 increased Bcl-2 protein level, whereas compound 4 did not affect Bcl-2 level. Hence, ethyl ester functional group inserted into daidzein B-ring at position 4' plays a crucial role in the upregulation of Bcl-2 expression. Moreover, pre-incubation of cells with ERs antagonist did not block the neuroprotective properties of both compounds suggesting ER-independent neuroprotective activities. Consequently, daidzein derivatives might serve as a potential treatment to reduce the progressive loss of neurons caused by oxidative stress and thereby slow down the development of neurodegeneration.

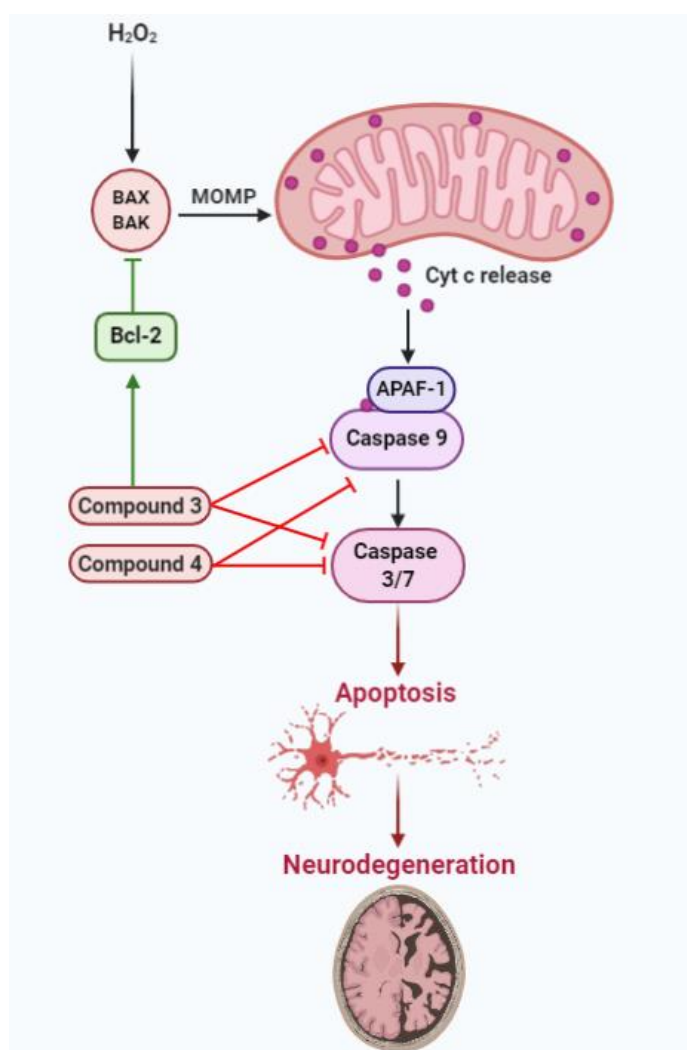


Figure 4.20 Schematic representation of neuroprotective actions of compounds 3 and 4.

## 5 Chapter V - Development of the Human Microglia (HMC3) as a Cellular Model of Neuroinflammation

### 5.1 Introduction

#### 5.1.1 Microglial cell models

Currently, many microglial cell lines are available for investigating neuroinflammation, including primary, cell-derived stem and immortalized microglia. Primary microglia require extensive preparations and have a low proliferation rate; hence, their cultivation is more time consuming, and more expensive than transformed cells. Additionally, isolated microglial cells might lack purity and express phenotypic changes due to the isolation process. The process initially requires a mixed glial culture which leads to microglial phagocytosis of neuronal debris (Timmerman et al., 2018). On the other hand, the use of stem cell-delivered microglia presents different challenges. The challenges may include immature phenotype and lack of CNS exposure which might affect cell function. Furthermore, no consensus over differentiation methodology has been established, and detailed investigation on the effect of specific differentiation methods on receptors expression is required. Moreover, similarly to primary microglia, stem cell-derived microglia involve extensive cultivation methods (Speicher, Wiendl, Meuth, & Pawlowski, 2019). Thereupon, the most common choice, for high-throughput work demanding large numbers of cells, is microglia immortalized by viral transduction with oncogenes (Timmerman et al., 2018).

One of the most widely used transformed cell lines is raf/myc-immortalized murine BV2 cells. Bocchini et al., (1992) established the BV2 cell line as suitable *in vitro* model to study brain activated microglia. Bocchini findings were further supported by Henn et al., (2009) and Lund et al., (2006). Nevertheless, this cell line is not an ideal tool to study human neuroinflammation because of species-specific differences. These differences present with a profound challenge in the translation of studies conducted on rodent cell lines to clinical trials due to insufficient correlation with human genomic changes (Smith & Dragunow, 2014). Mouse and the human genome are on average, only 85% identical (“Why Mouse Matters | NHGRI,” n.d.). Therefore, the ideal microglial cell line model for neuroinflammatory research would be human microglia. However, the use of human microglia is limited due to restrictions of tissue availability. Another challenge for the use of primary human microglia

is limited control over the *antemortem* conditions and *post-mortem* delay leading to phenotypic changes and lack of negative controls (Timmerman et al., 2018). Therefore, an ideal tool which will simultaneously overcome obstacles arising from the usage of primary human microglia and eliminate species differences are immortalized human microglia. Hence, utilisation of immortalized human microglia will provide an opportunity to access more accurate and robust data which will have profound meaning in assessing the therapeutic potential of studied compounds.

### **5.1.2 The human microglial clone 3 cell line**

The human microglial clone 3 cell line (HMC3) was developed by Prof. Tardieu through SV40-dependent immortalization of human embryonic microglial cells (Janabi, Nazila, Peudenier, 1995). American Type Culture Collection (ATCC®) has recently authenticated HMC3 cell line and distributes it under the name HMC3 (ATCC®CRL-3304). HMC3 cells retained most of the morphological and phenotypical properties of primary microglial cells, except for lower phagocytic activity and higher expression of Cluster of Differentiation 68 (CD68) in comparison to primary microglia (Dello Russo et al., 2018). CD68 is a transmembrane glycoprotein mainly associated with lysosomal membrane in microglia (Holness & Simmons, 1993). A higher CD68 expression might indicate increased lysosomal activity. Therefore, HMC3 microglia appear to be a potential alternative for murine cell lines. However, the literature indicates that the transition of research methods used to study murine microglia to HMC3 might not bring the expected results due to species-specific differences (Mestas & Hughes, 2004).

Smith & Dragunow (2014) described that one of the major differences between rodent and human microglia is the level of TLR4 expression. Activation of TLR4 by LPS was considered as gold-standard to induce M1 microglial activation and induce a comprehensive inflammatory response in rodent microglia. However, the same response might not be observed in HMC3 due to lower TLR4 expression in human microglia. Also, during the transition from well-known rodent models to HMC3, there is a difference in the cells ability to express specific mediators which have been used as inflammatory biomarkers. For instance, nitric oxide production is abundant in rodent microglia, whereas in human microglial cells is negligible (Dello Russo et al., 2018). Therefore, this study is aiming to identify ligands which will activate HMC3 cells, leading to the expression of pro-inflammatory mediators and upregulation of inflammatory signalling pathways.



Ligands which were used in this study to induce pro-inflammatory activation of microglia are ODN 2006, IFN $\gamma$ , LPS and TNF $\alpha$ . ODN 2006 is CpG oligonucleotide present in bacterial DNA known to activate human TLR9. This ligand has been chosen because several studies indicated that *Porphyromonas gingivalis* which is a bacterium causing gum disease is a significant risk factor for developing A $\beta$  plaques, dementia, and AD (Dominy et al., 2019; Kamer et al., 2015; Noble et al., 2009). Moreover, Nonnenmacher et al., (2003) indicated that CpG motifs from periodontopathogenic bacteria are immunostimulatory for mouse and human immune cells. Hence, the immunostimulatory activity of TLR9 ligand was tested in HMC3. This study also examined IFN $\gamma$  ability to induce activation of HMC3. Li et al., (2009) demonstrated that HMC3 cells exposed to IFN $\gamma$  (10 ng/ml) upregulate expression of MHCII, CD68 and CD11b. Therefore, this indicates that IFN $\gamma$  might serve as potential ligand inducing HMC3 activation. However, the effect of IFN $\gamma$  on Iba1, NO, TNF $\alpha$ , NF- $\kappa$ B and MAPKs upregulation have not been established up to date. Therefore, this study aimed to evaluate the impact of IFN $\gamma$  on above-mentioned pro-inflammatory mediators and signalling pathways. The next examined ligand was LPS as it is considered as a gold standard to induce activation of murine microglial cells (Horvath, Natile-McMenemy, Alkaitis, & DeLeo, 2008) Therefore, the impact of LPS was examined on HMC3 microglia. The last ligand, which was used to induce M1 activation of HMC3 was TNF $\alpha$ . TNF $\alpha$  is a major proinflammatory cytokine known as “master-regulator” of inflammatory cytokine production. Moreover, this cytokine is upregulated during neurodegenerative disorders, and TNF $\alpha$  receptor expression has been confirmed on microglia and other brain cells. Activation of the TNF $\alpha$  receptor has been associated with NF- $\kappa$ B and AP-1 upregulation and increased expression of pro-inflammatory cytokines (Probert, 2015).

## 5.2 Methods

### 5.2.1 HMC3 cell culture

HMC3 cell culture has been described in chapter four, section [4.2.2](#)

### 5.2.2 Stimulation of HMC3 cells with LPS, IFN $\gamma$ , TNF $\alpha$ and ODN 2006

HMC3 wells were seeded in 24-well plates (Sarstedt) at a density of  $1 \times 10^5$  cells/ml in 1 ml/well and incubated at 37°C until approximately 80% confluent. Subsequently, the Gibco™ MEM cell culture medium was changed to serum-free Gibco™ MEM (Fisher Scientific) to reduce the variability of experiments caused by lot to lot variation of serum composition. This was followed by 2 hours incubation. Subsequently cells were activated using LPS (100 ng/ml – 10  $\mu$ g/ml), IFN $\gamma$  (1 – 10 ng/ml), TNF $\alpha$  (25 – 50 ng/ml), ODN 2006 (1 – 5  $\mu$ M). Lipopolysaccharide (LPS) derived from *Salmonella typhimurium*, S-type (Innaxon Biosciences) was diluted in PBS (Fisher Scientific). Recombinant Human IFN $\gamma$  Protein (R&D Systems) was diluted to desired concentrations in sterile endotoxin-free water. Recombinant Human TNF $\alpha$  Protein (R&D Systems) was prepared in PBS. ODN 2006 - Class B CpG oligonucleotide (Human TLR9 ligand; sequence: 5'-tcgtcgttttgcgttttgcgtt-3') (InvivoGen) was diluted in sterile endotoxin-free water.

### 5.2.3 Treatment of HMC3 microglia with 17 $\beta$ -oestradiol

HMC3 cells were seeded in 6-well plates (Sarstedt) at a density of  $1 \times 10^5$  cells/ml in 2 ml of MEM culture medium per well and incubated at 37°C until approximately 80% confluent. Subsequently, the medium was changed to serum-free MEM to reduce the variability of experiments caused by lot to lot variation of serum composition, and cells were incubated 2 hours after incubation cells were treated with 100 nM of 17 $\beta$ -oestradiol (Sigma-Aldrich) for different time periods 6, 8, 12, and 24 hours.

### 5.2.4 Immunofluorescence

Immunofluorescence assays were conducted as described in [2.2.9](#) with modifications. Experiments were carried out using antibodies listed in Table 5.1. In the case of Alexa Fluor® 488-conjugated primary antibodies, secondary antibody exposure was omitted.

Antibodies	Supplier	Product no.	Dilution
<b>NF-<math>\kappa</math>B p65 (F6)</b>	Santa Cruz Biotechnology	8008	1:100
<b>ER<math>\beta</math> (h-150)</b>	Santa Cruz Biotechnology	8974	1:100
<b>Iba1 (1022-5)</b>	Santa Cruz Biotechnology	32725	1:100
<b>CD14</b>	BioLegend	301817	1:100
<b>TLR4 (H-80)</b>	Santa Cruz Biotechnology	10741	1:100
<b>TLR9</b>	Abcam	62577	1:100

**Table 5.1 The list of antibodies used for immunofluorescence staining.**

### 5.2.5 Griess assay

Griess assay was performed as described in chapter two, section [2.2.5](#)

### 5.2.6 TNF $\alpha$ and IL-6 ELISAs

HMC3 cells were stimulated as described in [5.2.2](#) for 24 hours, and then the TNF $\alpha$  and IL-6 levels were measured using ELISA MAX<sup>TM</sup> Deluxe Set Human TNF- $\alpha$  and ELISA MAX<sup>TM</sup> Deluxe Set Human IL-6 (BioLegend). Experiments were performed as indicated in [2.2.4](#).

### 5.2.7 Western blotting

This procedure has been described in chapter two, section [2.2.6](#)

### 5.2.8 ROS immunofluorescence

DCFDA Cellular ROS Detection Assay allows measuring reactive oxygen species in a cell. This technique uses 2',7' -dichlorofluorescein diacetate (DCFDA) which penetrate the cell membrane, and then is deacetylated by cellular esterase to a non-fluorescent compound, which subsequently is oxidized by ROS into fluorescent 2', 7'-dichlorofluorescein (DCF) allowing fluorescence spectroscopy detection (Kalyanaraman et al., 2012).

Cells were seeded in 8-well cell culture chambers (Sarstedt) at a density of  $1 \times 10^5$  cells/ml in 500  $\mu$ l of MEM culture medium. At approximately 80% confluence, cells were washed with 300  $\mu$ l of Gibco<sup>TM</sup> HBSS/Ca/Mg (Fisher Scientific) and incubated with 250  $\mu$ l of 25

$\mu\text{M}$  of carboxy- $\text{H}_2\text{DCFDA}$  using Invitrogen™ Image-IT™ LIVE Green Reactive Oxygen Species Detection Kit, for microscopy (Fisher Scientific) for 30 minutes. After incubation 250  $\mu\text{l}$  of the serum-free MEM medium was added. This was followed by cells stimulation with LPS (10  $\mu\text{g}/\text{ml}$ ) or  $\text{IFN}\gamma$  (10  $\text{ng}/\text{ml}$ ) for 24-hours incubation at  $37^\circ\text{C}$ . The following day cells were stained with Hoechst 33342 for 5 minutes, which was added at a final concentration of 1  $\mu\text{M}$  to carboxy- $\text{H}_2\text{DCFDA}$  medium solution. At the end of induction, cells were washed with HBSS, and fluorescent images were captured using EVOS® FLoid® Cell Imaging Station and then processed using ImageJ software.

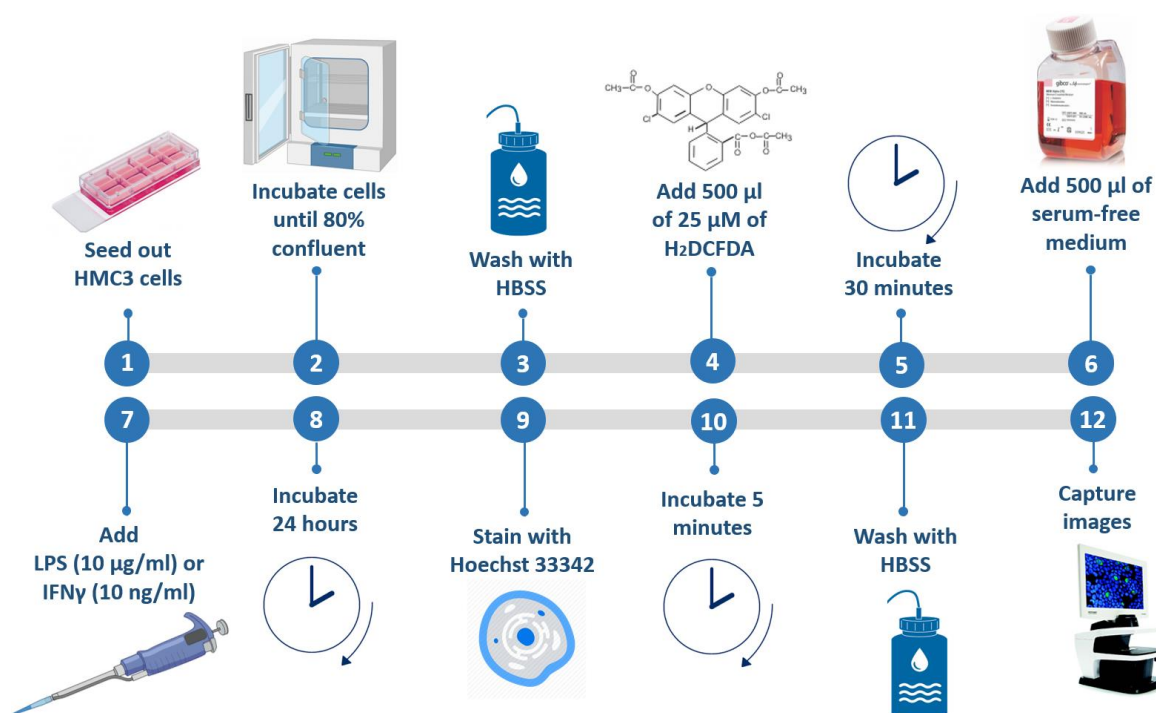


**Figure 5.1** Flowchart of ROS immunofluorescence.

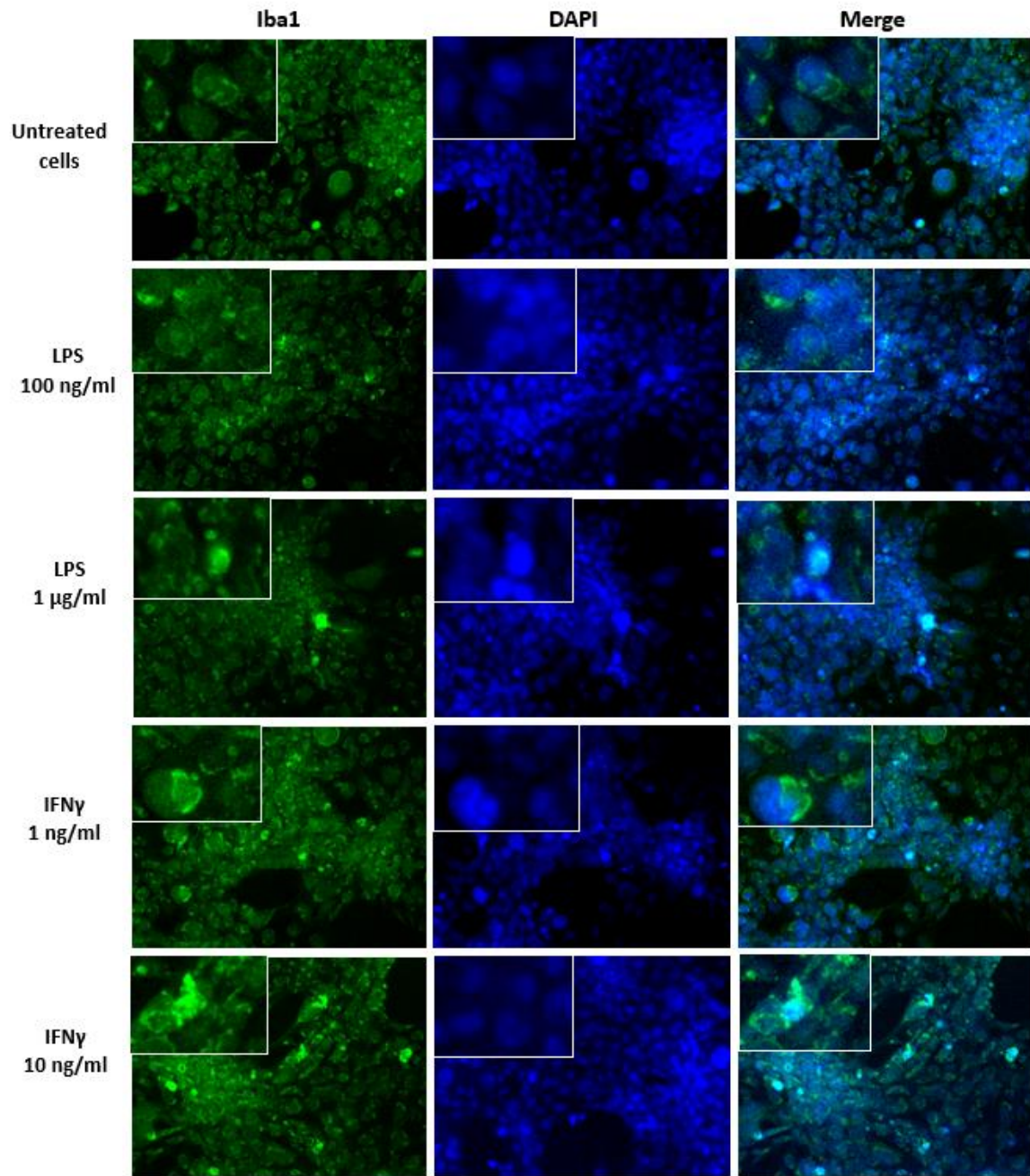
### 5.2.9 Statistical analysis

Data were analysed using one-way analysis of variance (ANOVA) with post hoc Student-Newman-Keuls test (with multiple comparisons) and are expressed as mean  $\pm$  SEM of at least three independent samples and experiment repetitions (N=3) unless otherwise stated. As statistically significant considered are values  $*p < 0.033$ ,  $**p < 0.002$ ,  $***p < 0.001$  compared with untreated control or  $\text{IFN}\gamma$  control or  $\text{TNF}\alpha$  control. Statistical analysis was executed using Graph Pad Prism software version 8.

## **5.3 Results**

### **5.3.1 Expression of Iba1 in HMC3**

Among brain cells, Iba1 is only expressed by microglia. Moreover, its expression is upregulated during cell M1 activation (Daisuke et al., 1998). Therefore, immunofluorescence staining of Iba1 has been carried out to confirm the origin of cells and to determine the effects of LPS and IFN $\gamma$ , ODN 2006, and TNF $\alpha$  on cell activation. Data presented in Figure 5.1 illustrate that untreated HMC3 cells are Iba1-positive. Activation of cells with 100 ng/ml and 1 $\mu$ g/ml of LPS and 1ng/ml of IFN $\gamma$  did not affect Iba1 expression. Whereas HMC3 cells incubated IFN $\gamma$  (10 ng/ml), ODN 2006 (5  $\mu$ M and 10  $\mu$ M) and TNF $\alpha$  (25 ng/ml and 50 ng/ml) present higher Iba1-positive staining than untreated cells.



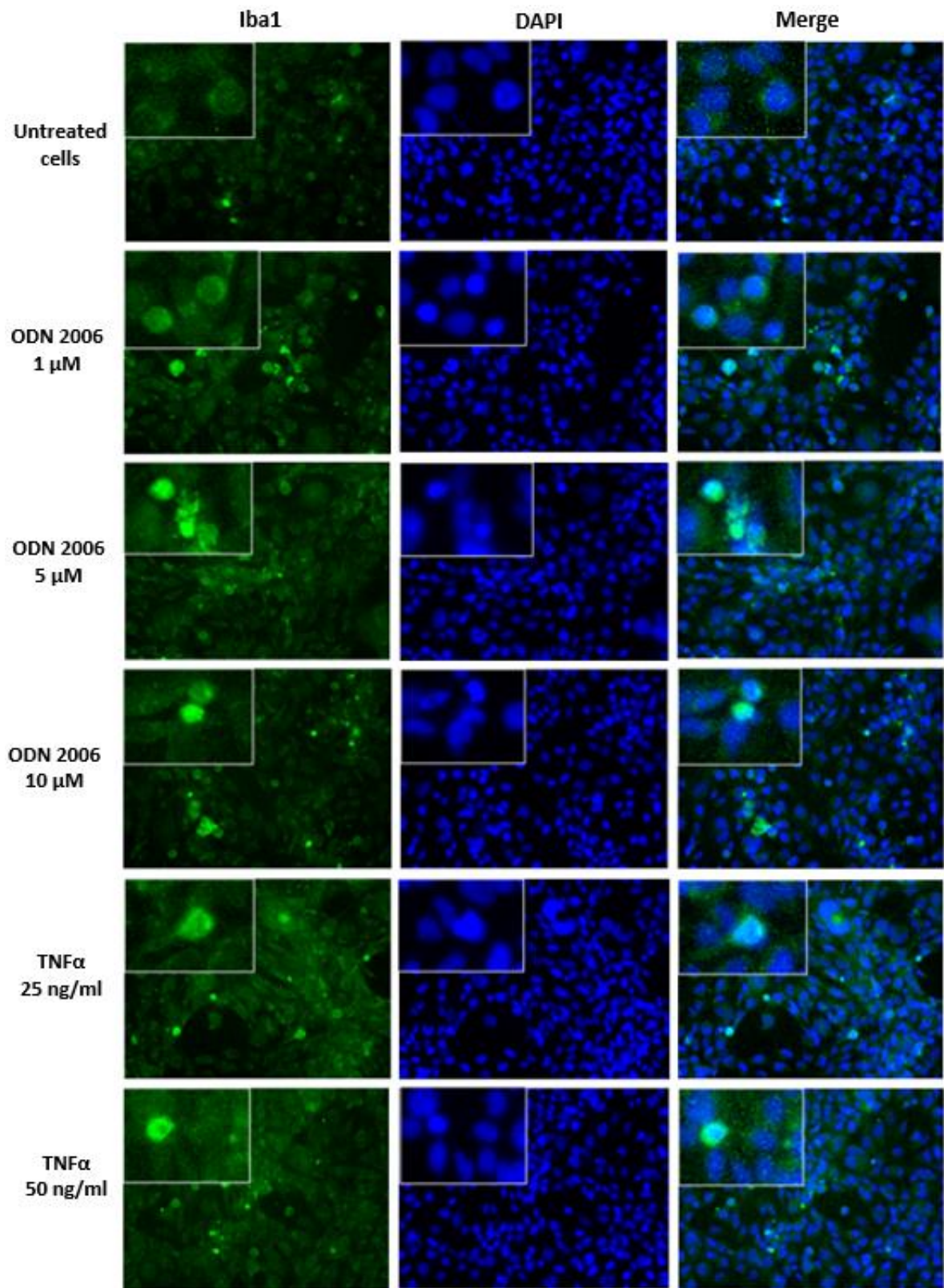


**Figure 5.2 The Iba1 expression in HMC3 cells.** Untreated HMC3 are Iba 1-positive. Stimulation of cells with 100 ng/ml and 1  $\mu$ g/ml of LPS and 1 ng/ml of IFN $\gamma$  did not affect Iba 1 expression. Whereas the exposure of cells to 1  $\mu$ M of ODN 2006 slightly increased Iba 1 expression. Markedly increased production of Iba 1 was observed in cells stimulated with 10 ng/ml of IFN $\gamma$ , 5  $\mu$ M and 10  $\mu$ M of ODN 2006 and 25 ng/ml and 50 ng/ml of TNF $\alpha$ . Cells were counterstained with DAPI and fluorescence images were captured with EVOS<sup>®</sup> FLoid<sup>®</sup> Cell Imaging Station and then processed using ImageJ software.

### 5.3.2 Expression of CD14 in HMC3

CD14 is a cell surface protein which is used as a marker to immunophenotype cells. CD14 is specific to microglia and monocytes. HMC3 cells have been reported to express low levels of CD14 (Etemad, Zamin, Ruitenber, & Filgueira, 2012). Therefore, to further confirm the authenticity of HMC3 cells used in this study, immunofluorescence staining of CD14 was carried out. Data presented in Figure 5.2 shows that untreated HMC3 cells are weakly CD14-positive. Stimulation of HMC3 cells with LPS caused upregulation of CD14 expression.

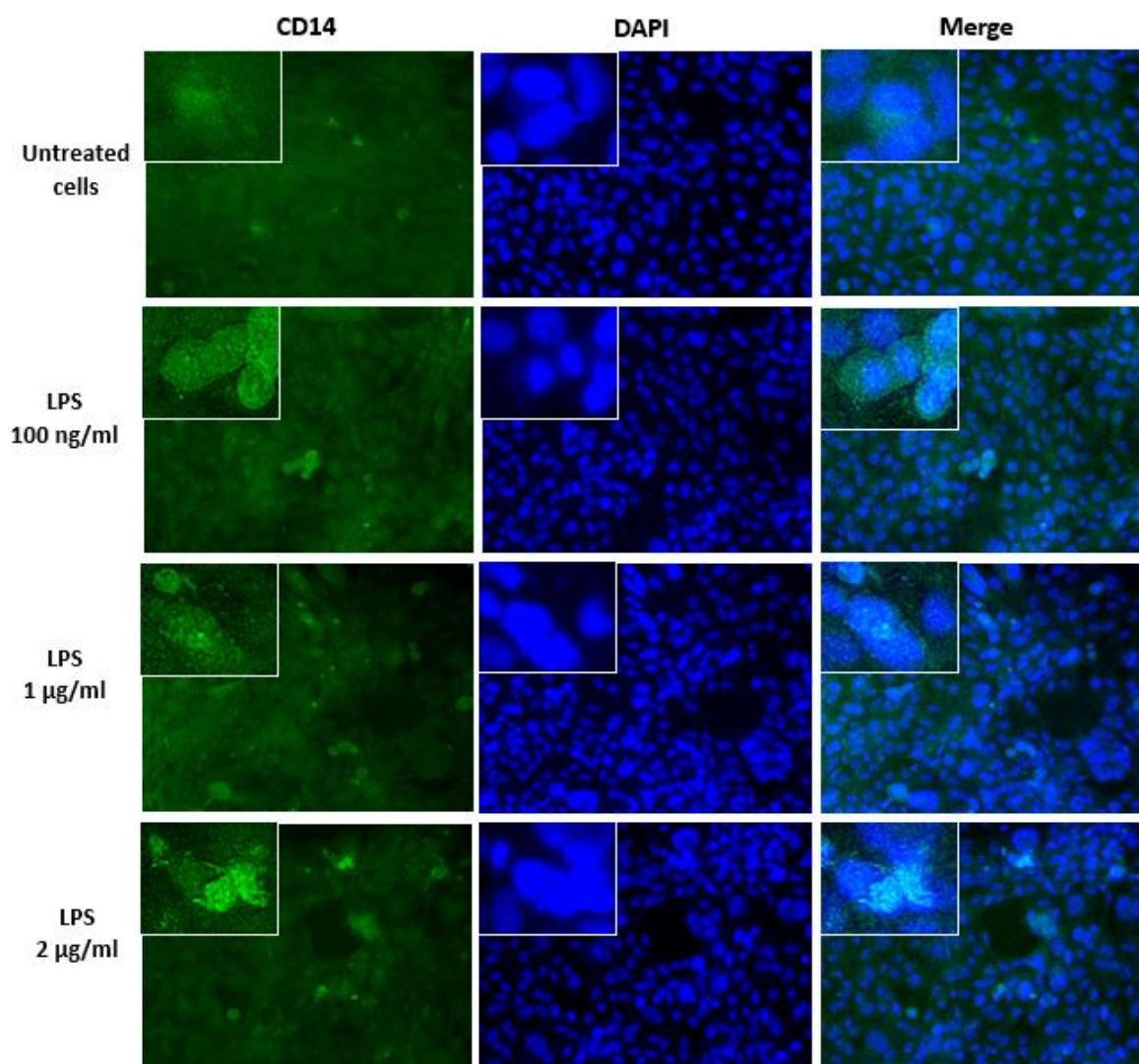


**Figure 5.3 CD14 expression in HMC3 cells.** HMC3 cells were stimulated with or without LPS or IFN $\gamma$  for 24 hours. At the end of incubation immunofluorescent staining of CD14 was performed. Unstimulated cells express are weakly CD14-positive, Whereas stimulation of HMC3 with LPS (100 ng/ml - 2  $\mu$ g/ml) slightly increased CD14 expression. Cells were counterstained with DAPI and fluorescence images were captured with EVOS<sup>®</sup> FLoid<sup>®</sup> Cell Imaging Station and then processed using ImageJ software.



### 5.3.3 Expression of ER $\beta$ and ER $\alpha$ in HMC3 cells

The overall objective of this project was the investigation of anti-inflammatory properties of isoflavone analogues, which belong to a class of phytochemicals known to target oestrogen receptors. Accordingly, to confirm the suitability of HMC3 cell model for this project, their expression of ER $\beta$  and ER $\alpha$  was examined. HMC3 cells were incubated with or without 17 $\beta$ -oestradiol (100 nM) for different time points, and expression of ER $\beta$  and ER $\alpha$  was detected using Western blotting. Data presented in Figure 5.4 show that HMC3 cells express both ERs in the absence of 17 $\beta$ -oestradiol. Moreover, exposure of cells to 17 $\beta$ -oestradiol not significantly increased expression of ER $\beta$  and ER $\alpha$ , with the highest level at 12 hours for ER $\beta$ , and 8-12 hours for ER $\alpha$ . In addition, immunofluorescence staining was used to confirm the expression of ER $\beta$  in HMC3. Consistent with immunoblotting results, immunofluorescence staining also confirmed ER $\beta$  expression in HMC3 cells, with its increased production caused by 17 $\beta$ -oestradiol (Figure 5.5).

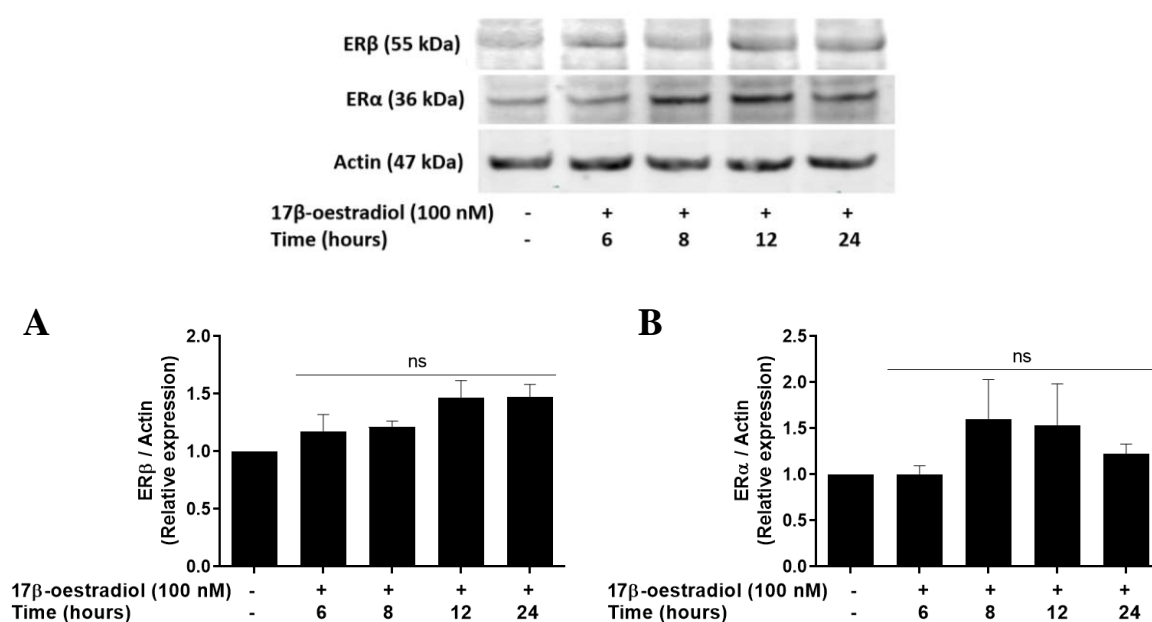


**Figure 5.4 ER $\beta$  and ER $\alpha$  expression in HMC3 cells.** Cells were incubated at different time points with or without 17 $\beta$ -oestradiol (100 nM). After incubation cell lysates were collected, and immunoblotting was conducted with actin used as a loading control. HMC3 cells express ER $\beta$  (A) and ER $\alpha$  (A). Incubation of cells with 17 $\beta$ -oestradiol not significantly increased level of both receptors. Expression of ER $\beta$  after incubation with 17 $\beta$ -oestradiol was the highest at 12 hours and ER $\alpha$  at 8-12 hours. All values are expressed as a mean  $\pm$  SEM for N=3. Data were analysed using one-way ANOVA for multiple comparisons with post hoc Student Newman-Keuls test. \* $p$ <0.033 in comparison with untreated control.

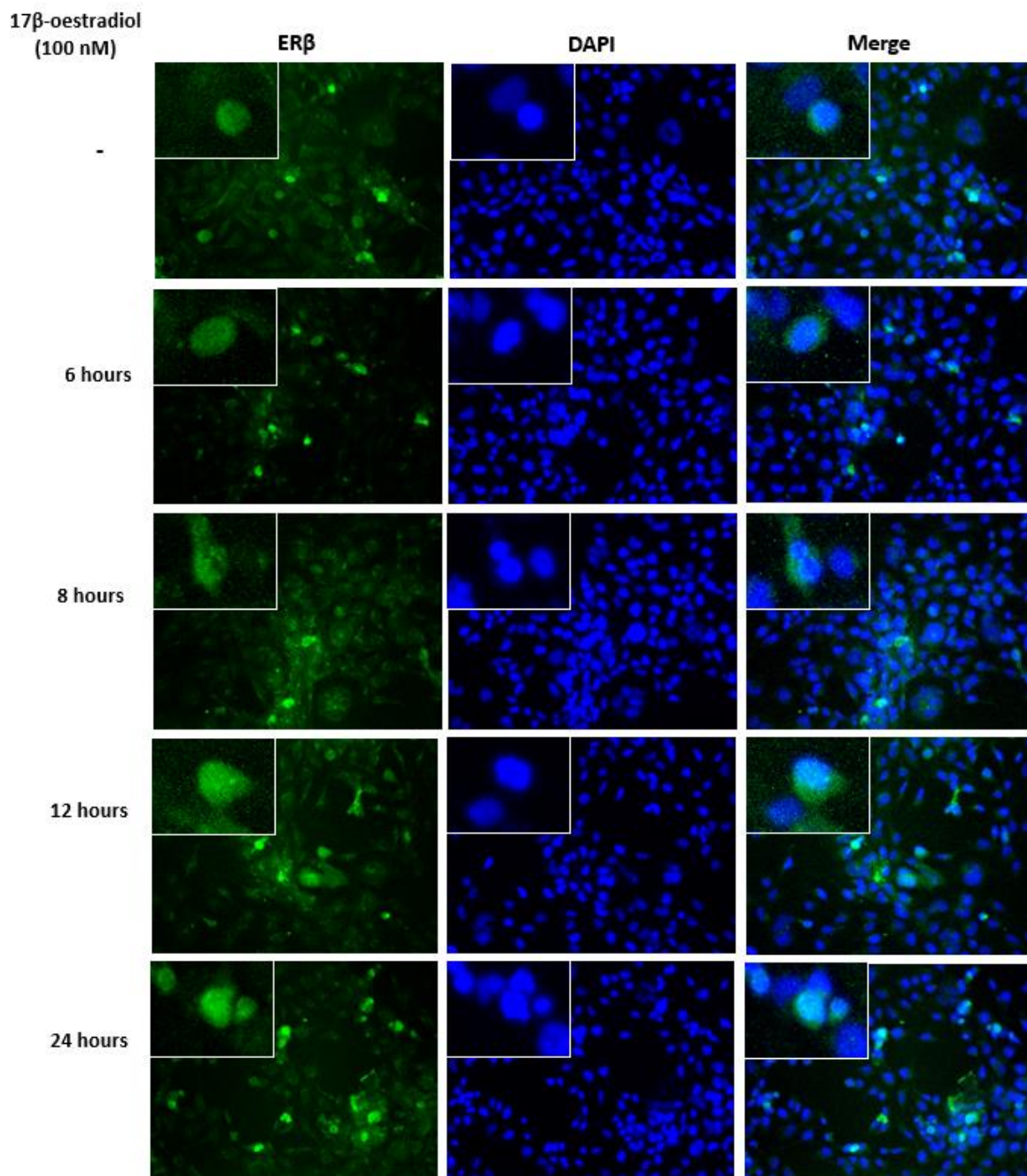


**Figure 5.5 ER $\beta$  expression in HMC3 cells.** Cells were incubated at different time points with or without 17 $\beta$ -oestradiol (100 nM). At the end of the incubation period, immunofluorescence staining of ER $\beta$  was performed. Green colour indicates ER $\beta$ ; blue represents the cell nucleus stained with DAPI. HMC3 are ER $\beta$ -positive. Incubation of cells with 17 $\beta$ -oestradiol increased ER $\beta$  expression. Fluorescence images were captured with EVOS<sup>®</sup> FLoid<sup>®</sup> Cell Imaging Station and then processed using ImageJ software.

### 5.3.4 Expression of TLR4 and TLR9 in HMC3

Toll-like receptors (TLRs) are transmembrane proteins responsible for pathogen recognition and initiation of innate immunity. Activation of TLR4 is widely used to induce microglial activation in murine cell models, and activation of TLR9 by *Porphyromonas gingivalis* is a significant risk factor for developing A $\beta$  plaques, dementia, and AD (Dominy et al., 2019; Kamer et al., 2015; Noble et al., 2009). Therefore, to verify if HMC3 cells express TLR4 and TLR9, immunofluorescence staining of both receptors was performed. Figure 5.6 illustrates that HMC3 cells are weakly TLR4-positive and highly TLR9-positive. Hence, HMC3 cells express a higher level of TLR9 than TLR4.

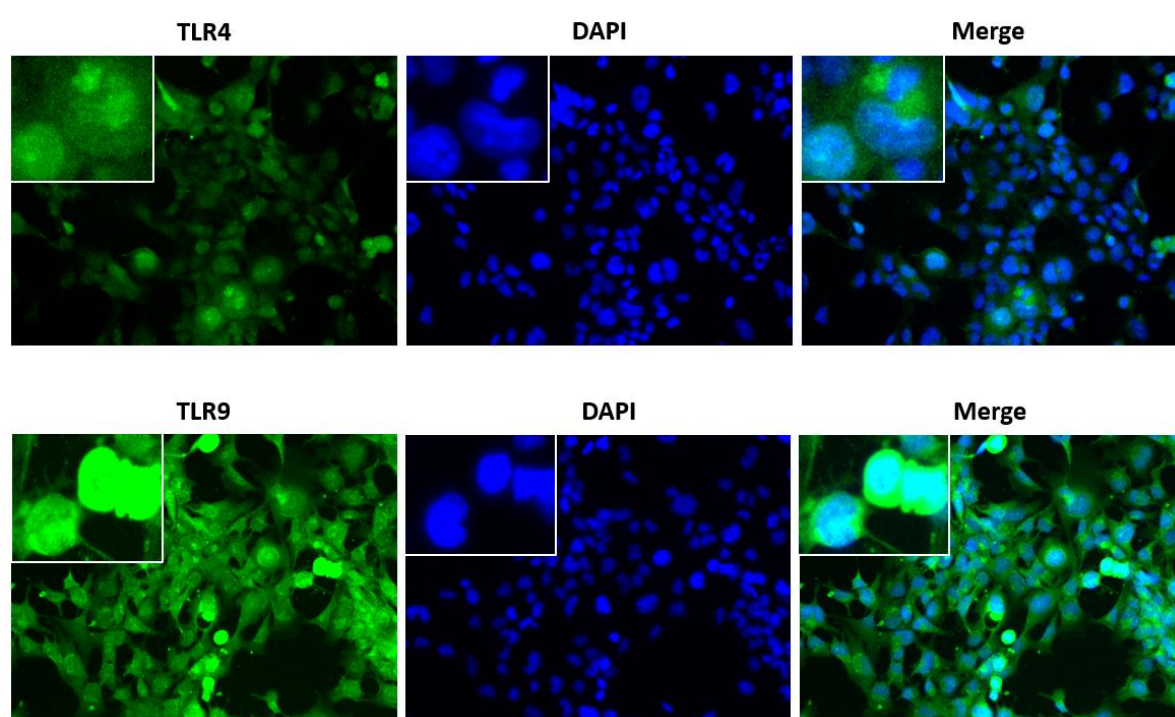


**Figure 5.6 The expression of TLR4 and TLR9 in HMC3 cells.** Untreated HMC3 cells express a low level of TLR4 and high level of TLR9. Green colour indicates TLR4 or TLR9. Cells were counterstained with DAPI (blue colour), and fluorescence images were captured with EVOS® FLoid® Cell Imaging Station and then processed using ImageJ software.

### 5.3.5 ROS production in HMC3

Reactive oxygen species (ROS) are important signalling molecules that play a crucial role in the propagation of neuroinflammation. To determine the effects of LPS and IFN $\gamma$  on ROS production in HMC3, immunofluorescence staining of ROS was performed. Figure 5.7 illustrates that unstimulated cells produced high amounts of ROS and pre-incubation of HMC3 with LPS (10  $\mu$ g/ml) or IFN $\gamma$  (10 ng/ml) did not increase ROS production.

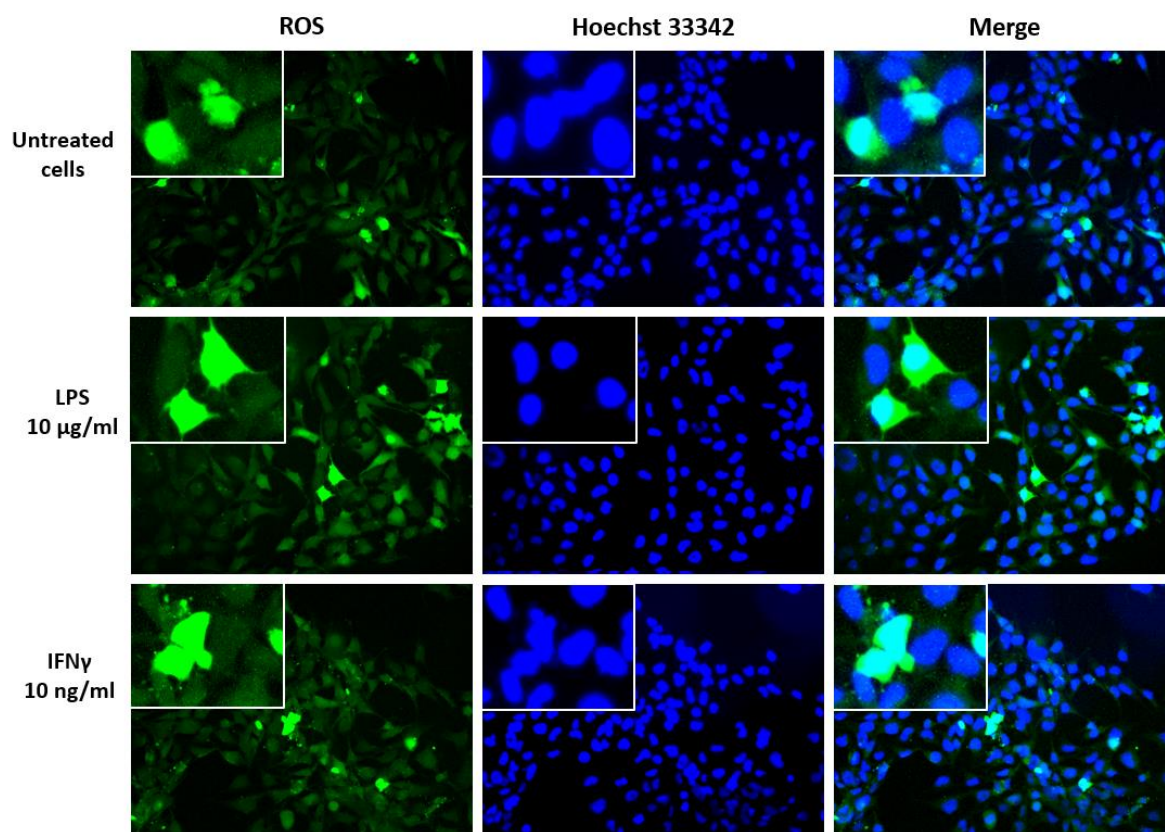


**Figure 5.7 ROS production in HMC3 cells.** Cells were labelled with carboxy-H<sub>2</sub>DCFDA and then stimulated with LPS (10  $\mu$ g/ml) or IFN $\gamma$  (10 ng/ml) for 24 hours. Unstimulated cells and LPS or IFN $\gamma$  activated cells produced a substantial amount of ROS. Cells were counterstained with Hoechst 33342. Fluorescence images were captured with EVOS<sup>®</sup> FLoid<sup>®</sup> Cell Imaging Station and then processed using ImageJ software.

### 5.3.6 The effect of ODN 2006, IFN $\gamma$ , LPS, and TNF $\alpha$ on the production nitrite, IL-6 and TNF $\alpha$

Levels of pro-inflammatory mediators have been widely used to determine the magnitude of inflammation. In order to establish which ligand will induce HMC3 activation, levels of nitrite, IL-6 and TNF $\alpha$  were measured after incubation of cells with ODN 2006 (1, 5 and 10  $\mu$ M), IFN $\gamma$  (10 ng/ml), LPS (1 and 10  $\mu$ g/ml), and TNF $\alpha$  (25 and 50 ng/ml) for 24 hours.

Data presented in Figure 5.8 A show that unstimulated cells produced  $0.25 \pm 0.05$   $\mu$ M of nitrite; its production remained unaffected after incubation with IFN $\gamma$ , LPS, and TNF $\alpha$ . However, ODN 2006 at 1, 5 and 10  $\mu$ M increased in a concentration-dependent manner nitrite production to  $0.33 \pm 0.08$   $\mu$ M,  $0.63 \pm 0.06$   $\mu$ M and  $1.14 \pm 0.07$   $\mu$ M, respectively, compared to untreated control. The only ligand which significantly ( $p < 0.001$ ) upregulated nitrite production was ODN 2006 at 10  $\mu$ M.

Unstimulated cells produced  $67.4 \pm 10.1$  pg/ml of IL-6 (Figure 5.8 B). Interestingly incubation with ODN 2006 at 1, 5 and 10  $\mu$ M reduced IL-6 expression to  $34.9 \pm 13.7$  pg/ml,  $33.4 \pm 9.7$  pg/ml, and  $17.5 \pm 8.5$  pg/ml, respectively, when compared to untreated control. IFN $\gamma$  at 10 ng/ml upregulated the production of IL-6 to  $110.1 \pm 22.4$  pg/ml – approximately 1.6-fold increase when compared to untreated control. LPS at 1  $\mu$ g/ml and 10  $\mu$ g/ml did not significantly affect IL-6 production, and its production was  $54.4 \pm 11.5$  pg/ml and  $46.9 \pm 11.9$  pg/ml, respectively. Only cells stimulated with TNF $\alpha$  at 25 ng/ml and 50 ng/ml significantly ( $p < 0.001$ ) upregulated IL-6 production to  $524.4 \pm 85.70$  pg/ml and  $572.3 \pm 64.2$  pg/ml (~8-fold increase), respectively, when compared to untreated control.

Untreated HMC3 cells produced 27.9 pg/ml of TNF $\alpha$  (Figure 5.8 C). ODN 2006, IFN $\gamma$  and LPS did not significantly affect TNF $\alpha$  level in HMC3 cells. TNF $\alpha$  production was  $21.9 \pm 10.7$  pg/ml,  $18 \pm 12.7$  pg/ml and  $18 \pm 12.3$  pg/ml for 1, 5 and 10  $\mu$ M of ODN 2006, respectively. Cells incubated with IFN $\gamma$  produced  $24.4 \pm 0.7$  pg/ml. TNF $\alpha$  production was  $40.4 \pm 8.3$  pg/ml and  $27.3 \pm 9.4$  pg/ml for cells stimulated with 1  $\mu$ g/ml and 10  $\mu$ g/ml of LPS. Increased production of TNF $\alpha$  was only observed in cells stimulated with 25 and 50 ng/ml of recombinant TNF $\alpha$  protein to  $283.8 \pm 52.54$  pg/ml and  $601.4 \pm 235$  pg/ml, respectively. However, cell-free medium incubated with 25 and 50 ng/ml of recombinant TNF $\alpha$  protein also increased TNF $\alpha$  level to  $437.4 \pm 49.7$  pg/ml and  $657.5 \pm 47.8$  pg/ml - similar level as cells incubated with recombinant TNF $\alpha$  protein. This suggests that reading of TNF $\alpha$  level of

cells incubated with recombinant TNF $\alpha$  protein is false positive because TNF $\alpha$  ELISA kit was detecting recombinant TNF $\alpha$  protein which was used to stimulate cells.

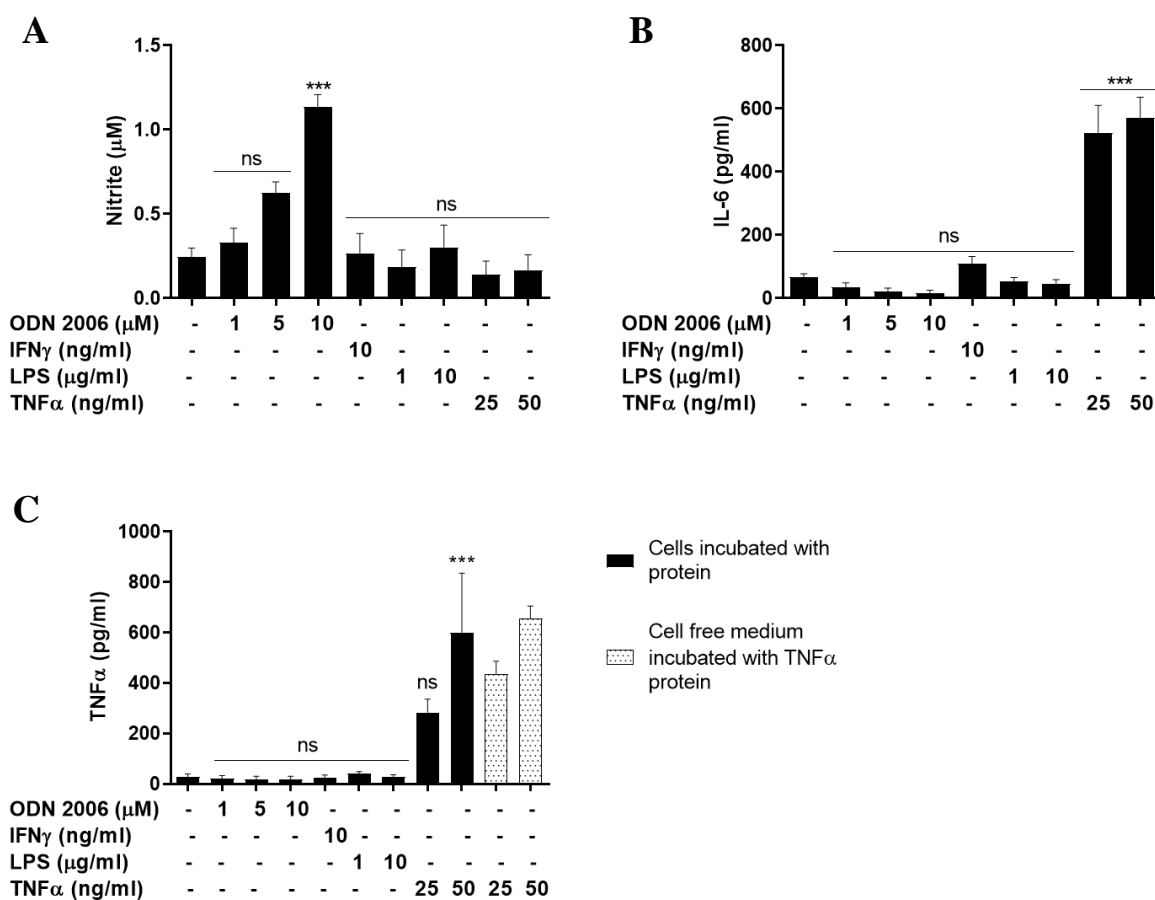


**Figure 5.8** The effect of ODN 2006, IFN $\gamma$ , LPS and TNF $\alpha$  on the production of nitrite, IL-6 and TNF $\alpha$  in HMC3 cells. HMC3 were pre-incubated with or without ODN 2006 (1  $\mu$ M – 10  $\mu$ M), IFN $\gamma$  (10 ng/ml), LPS (1  $\mu$ g/ml and 10  $\mu$ g/ml) and TNF $\alpha$  (25 ng/ml and 50 ng/ml) for 24 hours. At the end of incubation, cell culture supernatants were collected, and Griess assay and ELISAs were performed. (A) Level of nitrite remained unaffected after incubation with IFN $\gamma$ , LPS and TNF $\alpha$ , whereas ODN 2006 increased nitrite production in a concentration-dependent manner. (B) IL-6 production was decreased by ODN 2006, increased by IFN $\gamma$  and TNF $\alpha$  and unaffected by LPS. (C) Level of TNF $\alpha$  was unaffected by ODN 2006, IFN $\gamma$  and LPS; only TNF $\alpha$  protein increased TNF $\alpha$  level. However, cell-free medium incubated with TNF $\alpha$  protein also increased TNF $\alpha$  detection level, suggesting that TNF $\alpha$  ELISA kit detected recombinant TNF $\alpha$  protein used to stimulate cells. All values are expressed as a mean  $\pm$  SEM for N=3. Data were analysed using one-way ANOVA for multiple comparisons with post hoc Student Newman-Keuls test. \*p<0.033, \*\*p<0.002, \*\*\*p<0.001 in comparison with untreated control.

### 5.3.7 NF- $\kappa$ B activation in HMC3 cells

Activation of the NF- $\kappa$ B signalling pathway is widely involved in the modulation of inflammatory response. Its activation has been attributed to the transcription of numerous pro-inflammatory factors such as chemokines, cytokines, pro-inflammatory enzymes (Shih et al., 2015). Consequently, to develop HMC3 as a new model to study neuroinflammation and test molecular mechanisms of potential anti-inflammatory compounds, it was crucial to

establish an agent which will trigger activation of the NF- $\kappa$ B signalling pathway. Therefore, the effect of LPS, IFN $\gamma$ , and TNF $\alpha$  was tested on NF- $\kappa$ B activation.

### 5.3.7.1 The effect of LPS on NF- $\kappa$ B nuclear localisation in HMC3 cells

HMC3 were stimulated with 2  $\mu$ g/ml of LPS for 30, 60, and 90 minutes. After an appropriate time of incubation, immunofluorescent staining of NF- $\kappa$ B p65 was performed. Stimulation of HMC3 cells with 2  $\mu$ g/ml of LPS did not promote NF- $\kappa$ B p65 nuclear localisation at 30, 60 and 90 minutes (Figure 5.9).

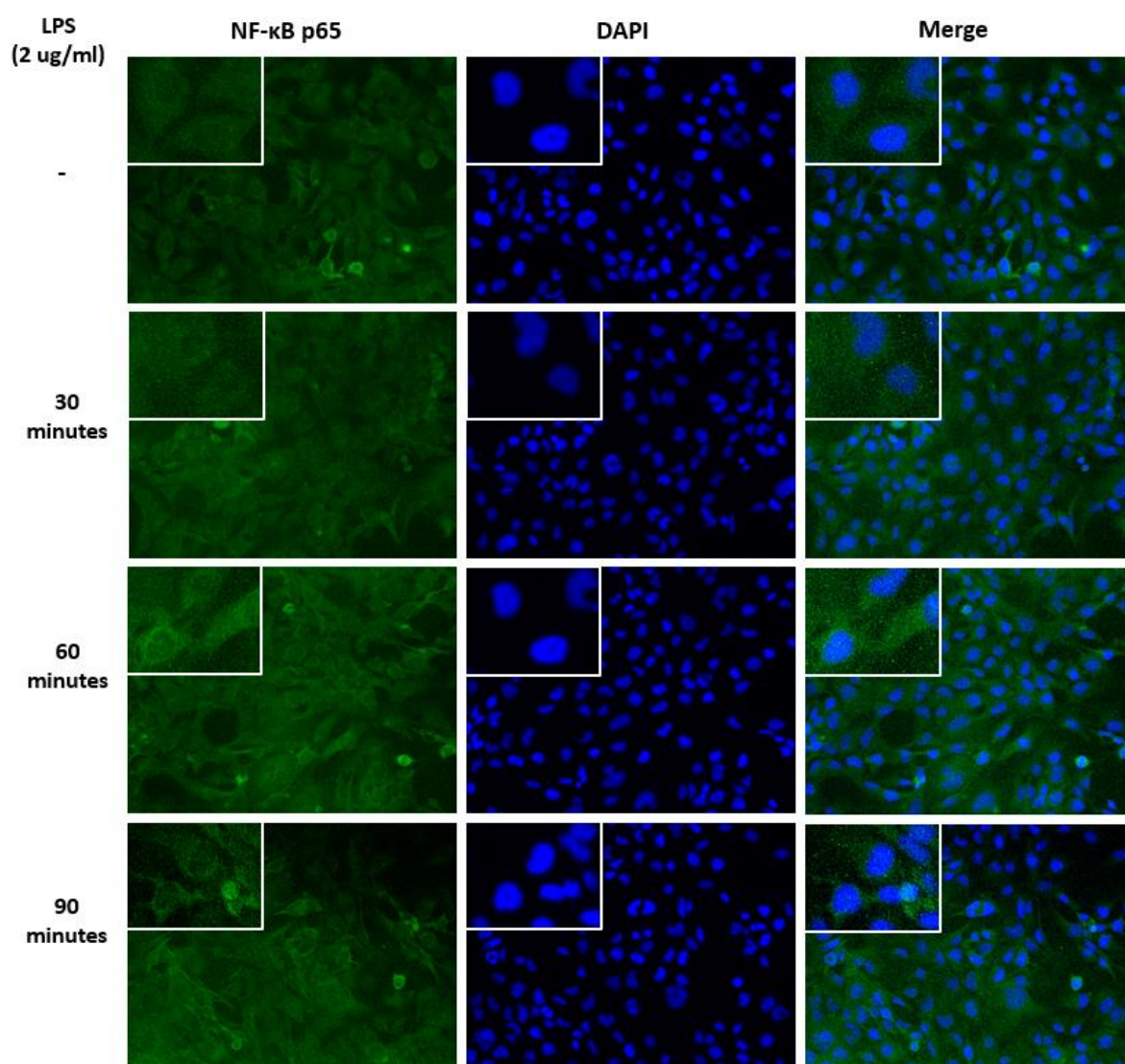


**Figure 5.9** The effect of LPS on NF- $\kappa$ B p65 nuclear localisation in HMC3 cells. Cells were stimulated with LPS (2  $\mu$ g/ml) at different time points (30, 60, and 90 minutes). After incubation time immunofluorescence experiment was performed. LPS did not induce NF- $\kappa$ B p65 nuclear localisation. Cells were counterstained with DAPI; fluorescence images were captured with EVOS<sup>®</sup> FLoid<sup>®</sup> Cell Imaging Station and then processed using ImageJ software.

### 5.3.7.2 The effect of IFN $\gamma$ on NF- $\kappa$ B activation

To verify the impact of IFN $\gamma$  on NF- $\kappa$ B activation immunoblotting and immunofluorescence staining of NF- $\kappa$ B p65 was performed. Immunostaining of NF- $\kappa$ B p65 revealed that IFN $\gamma$  was able to induce NF- $\kappa$ B p65 nuclear localisation at 90 minutes (Figure 5.10).

To further support the ability of IFN $\gamma$  to induce activation of NF- $\kappa$ B pathway immunoblotting and immunostaining of NF- $\kappa$ B p65 was conducted with IFN $\gamma$  and BAY 11-7082 (10  $\mu$ M) which is well established IKK phosphorylation inhibitor. HMC3 were pre-incubated for 30 minutes with or without BAY 11-7082 (10  $\mu$ M) and then stimulated with IFN $\gamma$  (10 ng/ml) for 60, 90 and 120-minutes. Cells incubated only with IFN $\gamma$  for 90 minutes significantly ( $p < 0.033$ ) increased expression of p-NF- $\kappa$ B p65 approximately 1.7-fold when compared to unstimulated cells (Figure 5.11 A). Furthermore, the pre-incubation of cells with BAY 11-7082 followed by IFN $\gamma$  activation significantly ( $p < 0.002$ ) decreased p-NF- $\kappa$ B p65 level approximately 3.2-fold compared to IFN $\gamma$  at 90 minutes. These findings are also supported by immunofluorescence staining of NF- $\kappa$ B p65 showing IFN $\gamma$ -induced nuclear localisation NF- $\kappa$ B p65 which was blocked by pre-incubation of cells with BAY 11-7082 (Figure 5.11 B).



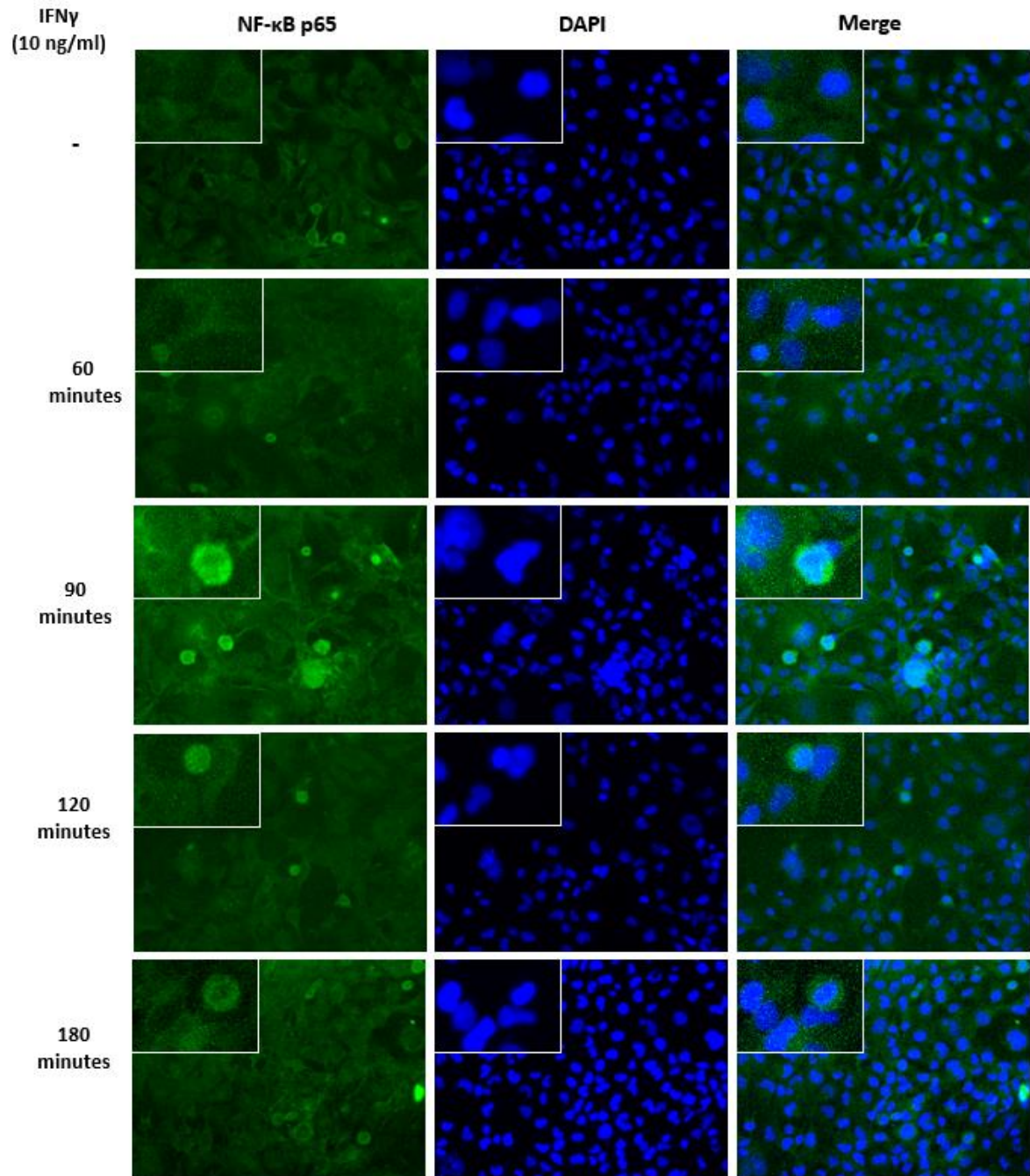


**Figure 5.10** The effect of IFN $\gamma$  on nuclear localisation of NF- $\kappa$ B p65 in HMC3 cells. HMC3 microglia were incubated IFN $\gamma$  (10ng/ml) for different time periods followed by immunofluorescent staining of NF- $\kappa$ B p65 and counterstaining with DAPI. Incubation of cells with IFN $\gamma$  caused nuclear translocation of NF- $\kappa$ B p65 at 90 minutes. Fluorescence images were captured with EVOS<sup>®</sup> FLoid<sup>®</sup> Cell Imaging Station and then processed using ImageJ software.

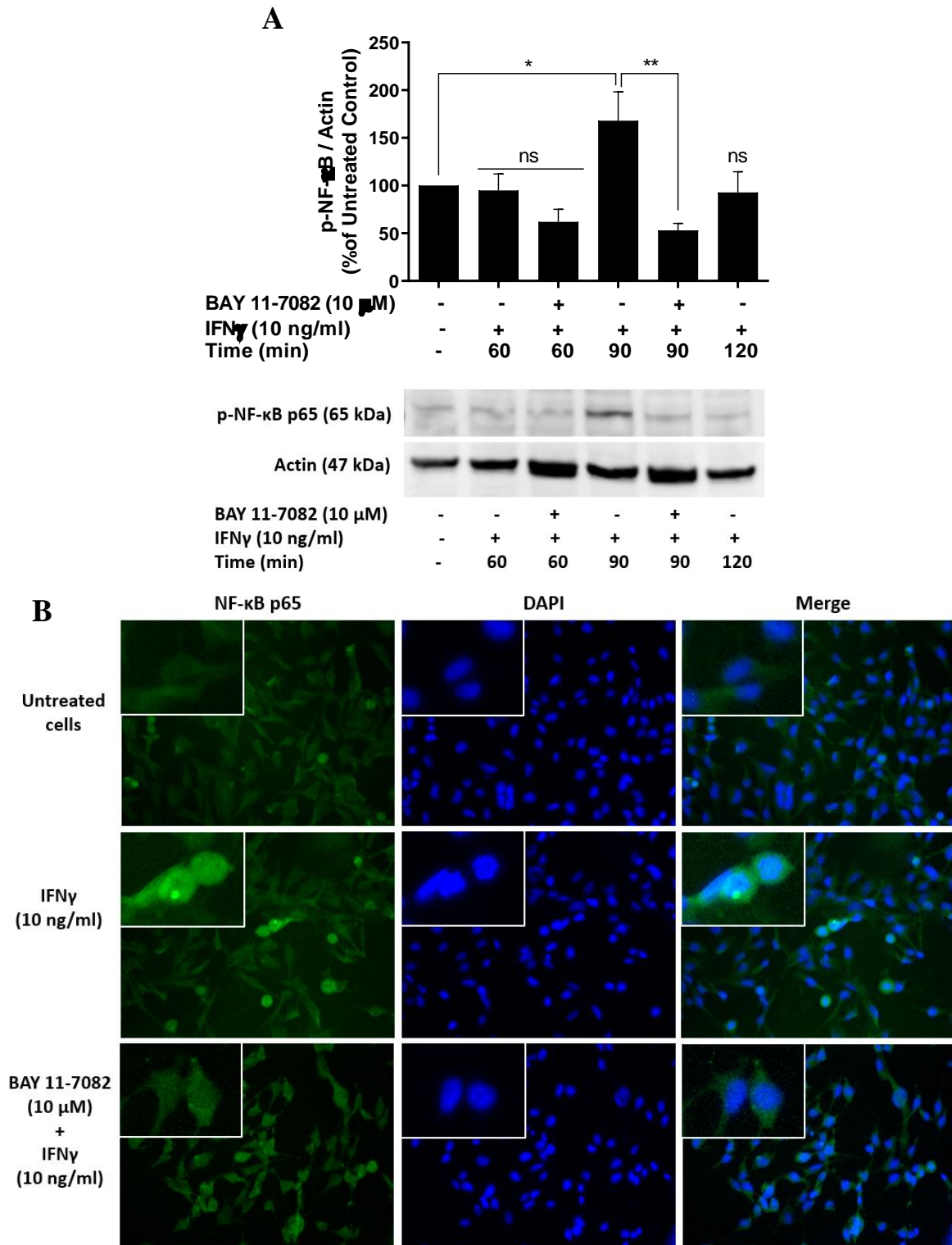


**Figure 5.11** The effect of IFN $\gamma$  alone and IFN $\gamma$  with BAY 11-7082 on phosphorylation of NF- $\kappa$ B p65 in HMC3. Cells were pre-incubated with or without BAY 11-7082 (10  $\mu$ M) for 30 minutes and then activated with IFN $\gamma$  at different time points. (A) At the end of incubation, cell lysates were collected, and Western blots were conducted with actin used as a loading control. The highest phosphorylation occurred at 90 minutes. IFN $\gamma$ -induced NF- $\kappa$ B phosphorylation was blocked BAY 11-7082. (B) After 90 minutes of incubation, NF- $\kappa$ B p65 was stained, and additionally, cells were counterstained with DAPI. IFN $\gamma$  induced nuclear translocation of NF- $\kappa$ B p65, whilst pre-incubation with BAY 11-7082 blocked this activation. Fluorescence images were captured with EVOS® FLoid® Cell Imaging Station and then processed using ImageJ software. All values are expressed as a mean  $\pm$  SEM for N=3. Data were analysed using one-way ANOVA for multiple comparisons with post hoc Student Newman-Keuls test. \*p<0.033, \*\*p<0.002 in comparison with untreated control.

### 5.3.7.3 The effect of TNF $\alpha$ on NF- $\kappa$ B activation in HMC3

The next protein which its effect was tested on NF- $\kappa$ B activation in HMC3 cells was the Recombinant Human TNF $\alpha$  Protein (TNF $\alpha$ ). Cells were activated with 25 ng/ml of TNF $\alpha$  for 30, 45, 60, and 90 minutes. After incubation cell lysates were collected and immunoblotting of p-NF- $\kappa$ B p65 was performed. Stimulation of HMC3 cells with TNF $\alpha$  induced phosphorylation of NF- $\kappa$ B p65 and caused p-NF- $\kappa$ B p65 approximately 3.1-fold increase at all tested time points compared to untreated cells. TNF $\alpha$  induced a significant ( $p < 0.033$ ) increase of p-NF- $\kappa$ B p65 level at 60 minutes – approximately 3.5-fold compared to untreated control (Figure 5.12).

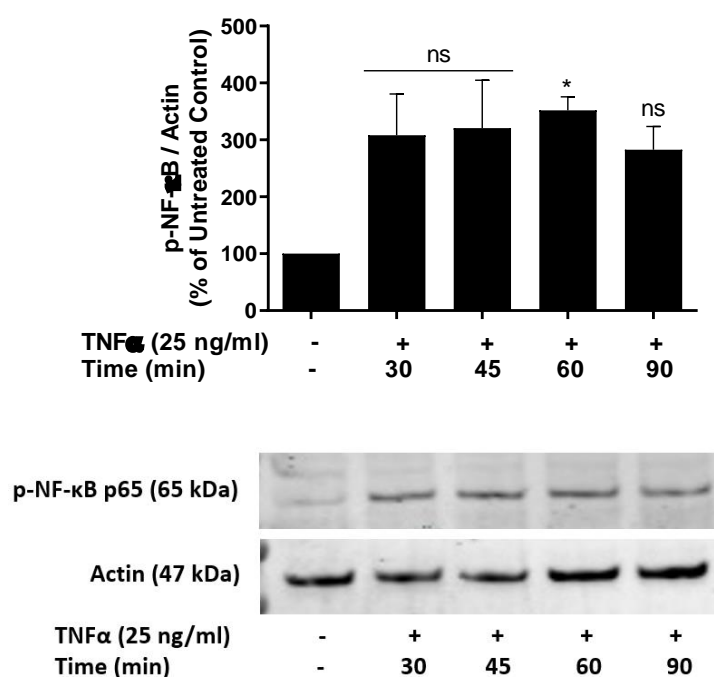


**Figure 5.12** The effect of TNF $\alpha$  on NF- $\kappa$ B p65 phosphorylation in HMC3 cells. Cells were activated with 25 ng/ml of TNF $\alpha$  for 30, 45, 60, and 90 minutes. After incubation cell lysates were collected, and Western blot for p-NF- $\kappa$ B p65 was performed. Actin has been used as a loading control. TNF $\alpha$  protein-induced phosphorylation of NF- $\kappa$ B p65 at 30, 45, 60 and 90 minutes. The highest expression of p-NF- $\kappa$ B was observed at 60 minutes. All values are expressed as a mean  $\pm$  SEM for N=3. Data were analysed using one-way ANOVA for multiple comparisons with post hoc Student Newman-Keuls test. \* $p < 0.033$  in comparison with untreated control.

### 5.3.8 MAPK activation in HMC3 cells

To fully develop HMC3 microglial model to study inflammation, it was crucial to determine not only the type of pro-inflammatory mediators produced by HMC3 cells but also signalling pathways implicated in those events. Accumulating evidence suggests that mitogen-activated protein kinases (MAPKs) regulate the synthesis of various inflammatory mediators, including TNF $\alpha$  and IL-6 (Kaminska, 2005). Therefore, apart from the investigation of NF- $\kappa$ B activation, an attempt was made to examine the effect of IFN $\gamma$  and TNF $\alpha$  on the MAPK signalling pathways: extracellular signal-regulated kinases (ERKs), and p38.

#### 5.3.8.1 The impact of IFN $\gamma$ on p-ERK1/2 in HMC3 cells

To establish the effect of IFN $\gamma$  on ERK1/2 activation in HMC3, cells were incubated with IFN $\gamma$  (10 ng/ml) at different time points (15, 30, 35, 60 and 90 minutes) and cell lysates were collected for Western blot analysis. Stimulation of HMC3 with IFN $\gamma$  not significantly upregulated p-ERK1/2 level with the highest approximately 1.7-fold increase at 90 minutes compared to unstimulated cells (Figure 5.13).

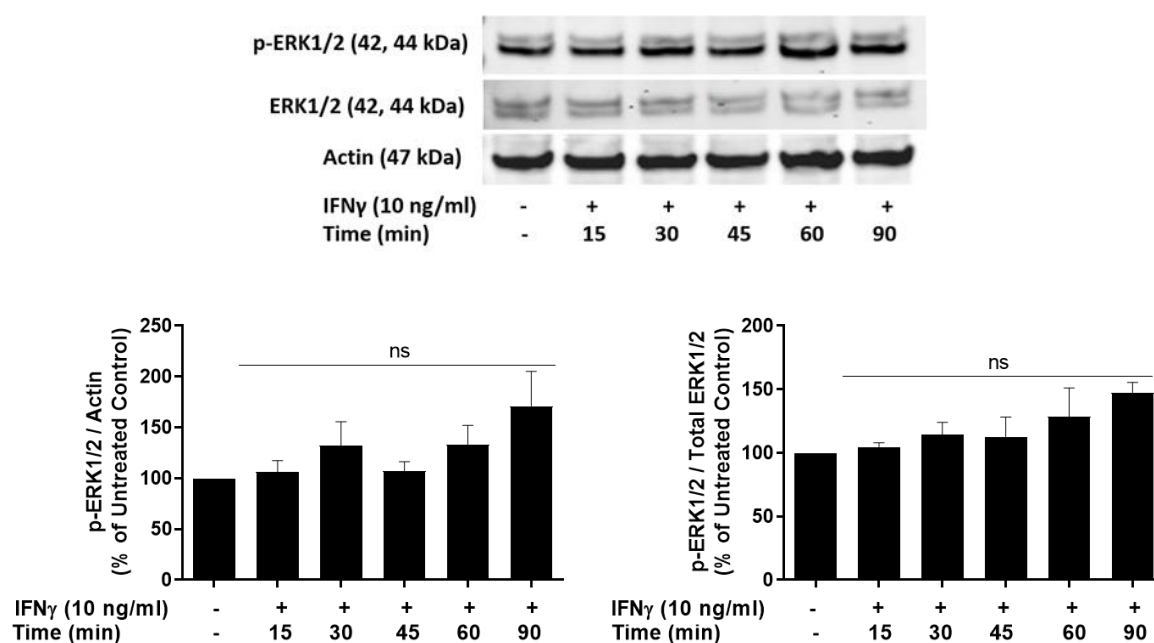


**Figure 5.13 The effect of IFN $\gamma$  on ERK1/2 activation in HMC3 cells.** Cells were activated with IFN $\gamma$  (10 ng/ml) at different time points (15, 30, 35, 60 and 90 minutes) and cell lysates were collected for Western blot analysis. IFN $\gamma$  upregulated p-ERK1/2 production at all tested time points which the highest expression at 90 minutes. Actin and totalERK1/2 were used as a loading control. All values are expressed as a mean  $\pm$  SEM for N=3. Data were analysed using one-way ANOVA for multiple comparisons with post hoc Student Newman-Keuls test. \*p<0.033 in comparison with untreated control.

### 5.3.8.2 The effect of IFN $\gamma$ on p-p38 in HMC3 cells

To determine the effect of IFN $\gamma$  on p38 upregulation in HMC3, cells were incubated with IFN $\gamma$  (10 ng/ml) at different time points (15, 30, 35, 60 and 90 minutes) followed by cell lysates collection and Western blot analysis. IFN $\gamma$  not significantly upregulated p-p38 level at 60 minutes with approximately 1.3-fold increase when compared to untreated cells (Figure 4.12).

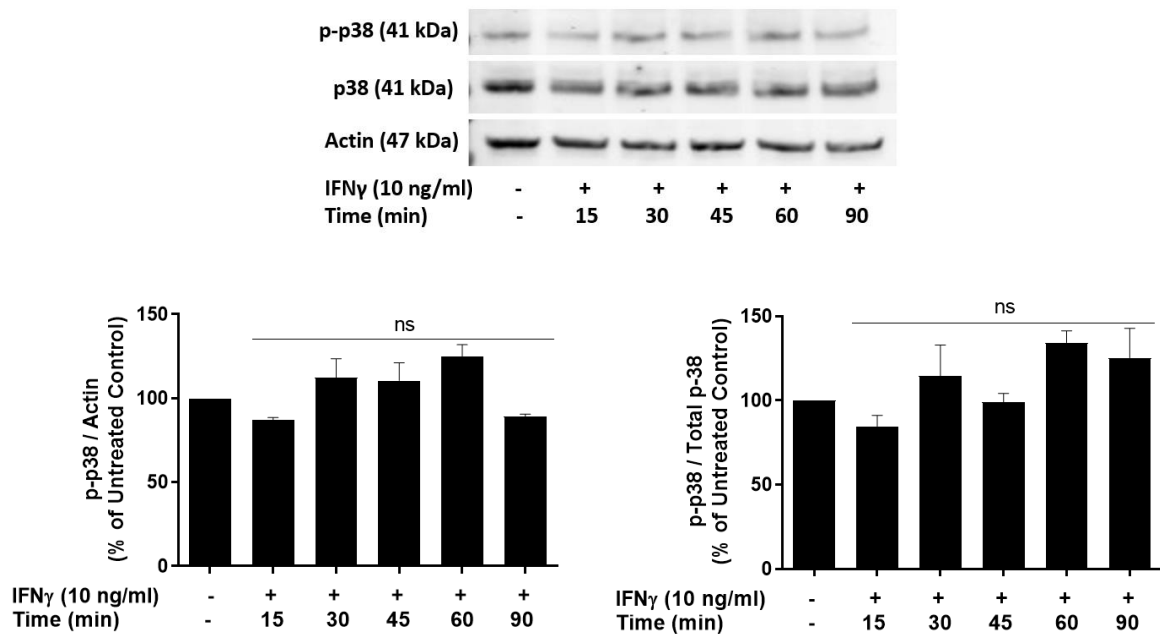


**Figure 5.14** The effect of IFN $\gamma$  on p38 activation in HMC3. Cells were incubated with IFN $\gamma$  (10 ng/ml) at different time points (15, 30, 35, 60 and 90 minutes) and cell lysates were collected for Western blot analysis. IFN $\gamma$  upregulated p-38 production at 60 minutes. Actin and total p38 were used as a loading control. All values are expressed as a mean  $\pm$  SEM for N=3. Data were analysed using one-way ANOVA for multiple comparisons with post hoc Student Newman-Keuls test. \* $p < 0.033$  in comparison with untreated control.

### 5.3.8.3 The effect of TNF $\alpha$ on ERK1/2 activation in HMC3 cells

To establish the effect of TNF $\alpha$  on ERK1/2 activation in HMC3, cells were incubated with TNF $\alpha$  (25 ng/ml) at different time points (15, 30, 35, 60, 90 and 120 minutes) and cell lysates were collected for immunoblotting analysis. Data presented in Figure 5.15 demonstrate that TNF $\alpha$  did not induce a significant increase in p-ERK1/2 level. However, cells incubated with TNF $\alpha$  slightly increased approximately 1.5-fold p-ERK1/2 level at all tested time points when compared to untreated cells. None of these differences was statistically significant.

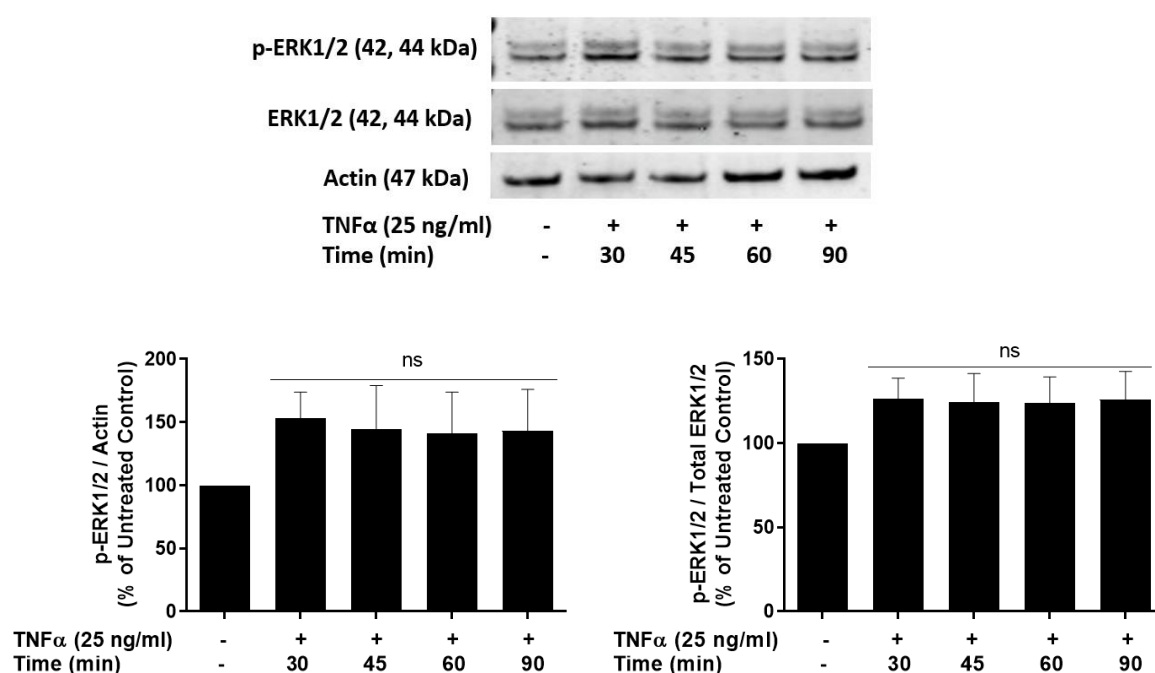


**Figure 5.15 The effect of TNF $\alpha$  on ERK1/2 phosphorylation in HMC3 cells.** Cells were activated with TNF $\alpha$  (25 ng/ml) for different time periods (30, 45, 60, 90 and 120 minutes) followed by cell lysates collection for Western blot analysis. TNF $\alpha$  not significantly induced phosphorylation of ERK1/2 at all tested time periods. Actin and total ERK1/2 were used as a loading control. All values are expressed as a mean  $\pm$  SEM for N=3. Data were analysed using one-way ANOVA for multiple comparisons with post hoc Student Newman-Keuls test. \*p<0.033 in comparison with untreated control.

### 5.3.8.4 The effect TNF $\alpha$ on p38 activation in HMC3

To determine the effect of TNF $\alpha$  on p38 activation in HMC3, cells were incubated with TNF $\alpha$  (25 ng/ml) for different time periods (30, 45, 60, 90 and 120 minutes). Subsequently, cell lysates were collected for p-p38 immunoblotting. Data presented in Figure 5.16 show that TNF $\alpha$  after 60 minutes of incubation significantly ( $p < 0.033$ ) upregulated p-38 phosphorylation approximately 5.8-fold in HMC3 microglia when compared to untreated cells.

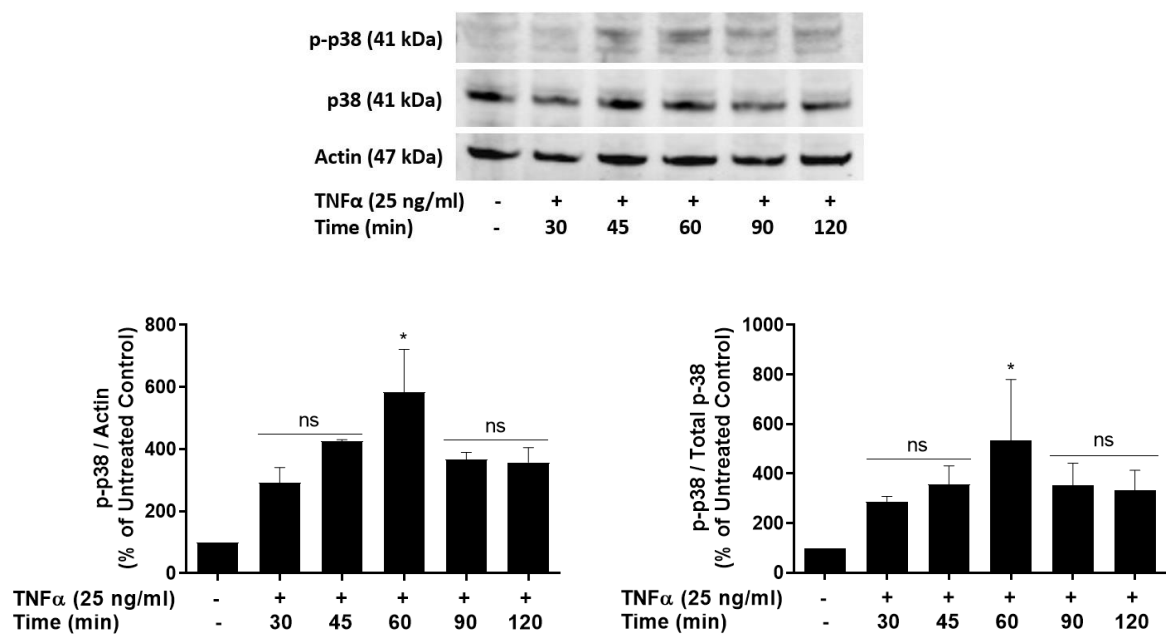


**Figure 5.16 The effect of TNF $\alpha$  on p38 activation in HMC3 cells.** Cells were activated with TNF $\alpha$  (25 ng/ml) for different time periods (30, 45, 60, 90 and 120 minutes) followed by cell lysates collection and p-p38 immunoblotting. TNF $\alpha$  significantly ( $p < 0.033$ ) increased phosphorylation of p-38 at 60 minutes compared to untreated cells. Actin and total p38 were used as a loading control. All values are expressed as a mean  $\pm$  SEM for N=3. Data were analysed using one-way ANOVA for multiple comparisons with post hoc Student Newman-Keuls test. \* $p < 0.033$  in comparison with untreated control.

## 5.4 Discussion

Microglia are the first line of active immune defence in the brain. Hence, they are widely used to study neuroinflammation. Currently, the most common cell lines used for the research are rodent microglial cell lines. In spite of the similarities between rodent microglia and human cells, there are still biochemical and pharmacological differences due to species-specificity (Stansley et al., 2012). Research using human microglia is limited as a result of the restricted availability of human tissue. Therefore, this problem might be solved by the development of immortalized human microglia as an alternative to rodent cells. This study aimed to determine the validity of HMC3 as a suitable cellular model to study neuroinflammation and test potential anti-inflammatory compounds.

To confirm the validity of HMC3 cell line used in this study, immunofluorescence staining of microglial markers was performed. Imai, Ibata, Ito, Ohsawa, & Kohsaka, (1996) reported that ionized calcium-binding adapter molecule 1 (Iba1) protein is monocyte/microglial specific, hence it may serve as a microglial marker for immunostaining. Immunofluorescence experiments confirmed Iba1 expression in untreated - resting cells which in line with results presented by Li et al., (2009) and Etemad, Zamin, Ruitenber, & Filgueira, (2012). To date, no study has investigated the effect of IFN $\gamma$ , ODN 2006, TNF $\alpha$  or LPS on Iba1 expression in HMC3 cells. Immunocytochemistry experiments showed higher Iba1-positive staining in HMC3 cells after incubation with IFN $\gamma$ , ODN 2006 or TNF $\alpha$  and no marked Iba1 increase after LPS exposure as compared with the untreated cells. Daisuke et al., (1998) indicated that Iba1 is upregulated in activated microglia after facial nerve axotomy. Iba1 molecule is essential in membrane ruffling, motility and phagocytosis of microglia (Ohsawa, Imai, Sasaki, & Kohsaka, 2004; Sasaki, Ohsawa, Kanazawa, Kohsaka, & Imai, 2001). Therefore, IFN $\gamma$ , ODN 2006, and TNF $\alpha$  ability to increase Iba1 expression indicate that those proteins can induce HMC3 activation. On the other hand, the lack of Iba1 upregulation by LPS suggests diminished inflammation-inducing properties in human microglia compared to rodent cells. Tao et al., (2018) and Zhang et al., (2019) reported that LPS enhanced Iba1 expression in BV2 cells compared with the non-LPS-treated BV2 cells. Similar results were presented by Duan et al., (2013) where LPS exposure increased Iba1- immunoreactivity in N9 and BV2 cells. Hence murine cells and human microglia respond differently to LPS activation due to species-specific differences.



In line with Etemad et al. (2012), this study also confirms weak CD14 expression in HMC3 cells. Moreover, Janabi, Nazila, Peudenier, (1995) also indicated the same level of CD14 expression in primary human cells. Another study by Lue, Beach, & Walker, (2019) also reported CD14 mRNA expression in human post-mortem isolated microglia. Additionally, in the present study, immunofluorescence staining of HMC3 with CD14 also reveals that LPS stimulation increased CD14-positive staining in HMC3 compared with the non-LPS-treated cells. CD14 is known to act as a co-receptor for LPS hence an increased expression after LPS exposure might serve as a cell's strategy to amplify the inflammatory response. Similarly, Landmann et al. (1996) also reported LPS-induced production of CD14 in human macrophages and monocytes.

This project investigated the anti-inflammatory properties of isoflavones analogues which belong to a class of phytochemicals known to target oestrogen receptors. Therefore, to confirm the suitability of HMC3 cell model for this study, the expression of ER $\beta$  and ER $\alpha$  was examined. Results indicated that HMC3 cells express both ERs, and their expression is upregulated by 17 $\beta$ -oestradiol. A similar observation concerning the increased level of ER $\alpha$  expression caused by 17 $\beta$ -oestradiol was made in human macrophages (Murphy, Guyre, Wira, & Pioli, 2009). On the contrary BV2 cells derived from raf/myc-immortalised murine neonatal microglia were found to selectively express ER $\beta$  (Baker et al., 2004; El-Bakoush & Olajide, 2018b). Whereas as demonstrated in this chapter, HMC3 express both ER, hence HMC3 would be a valuable cell model to test properties and molecular mechanism of molecules which mimic oestrogen by interactions with ERs. Scientific literature shows discrepancies concerning ERs expression in microglia. Wua et al., (2013) indicated that mouse microglia express ER $\beta$ , but not ER $\alpha$ . However, the authors conducted a study using 8-wk-old SJL/J females mice. However, Crain, Nikodemova, & Watters, (2015) argued that mouse microglia are only ER $\alpha$  positive, with no detectable ER $\beta$  mRNA expression. Moreover, the authors did not observe sexual dimorphisms. Studies were conducted using microglia isolated from C57Bl/6 mice at different ages (3- and 21 day-, 7 week-, 4- and 12 months old). Similarly, Sierra, Gottfried-Blackmore, Milner, McEwen, & Bulloch, (2008) reported that microglia isolated from transgenic mouse line p7.2fms-EGFP express of ER $\alpha$ , but not ER $\beta$ . Accordingly, differences in microglial ERs expression might be attributed to cell transformation, developmental stages or species-specific differences.

ROS imbalance has been reported as the cause and effect of neurodegeneration (Hsieh & Yang, 2013; Solleiro-Villavicencio & Rivas-Arancibia, 2018). Rodent microglia have been

extensively demonstrated to highly upregulate ROS after LPS activation (Brabazon, Bermudez, Shaughnessy, Khayrullina, & Byrnes, 2018; Wu et al., 2015). Therefore, an attempt was made to observe ROS production in HMC3 cells. Immunofluorescence staining showed that unstimulated cells produce a sizable amount of ROS and LPS or IFN $\gamma$  stimulation did not markedly further increase the level of ROS compared to that in untreated cells. A similar finding was reported by Li et al., (2009), where the authors showed a constitutive NOX4-dependent ROS generation and downregulated NOX2 mRNA expression in HMC3 cells. Guob et al., (2016) indicated that microglia from post-mortem adult human cortical tissue respond to A $\beta$  by an increase in the production of ROS. Therefore, constitutive ROS production in HMC3 might be attributed to cell transformation leading to an upregulation of genes which in resting primary microglia are not expressed.

Immunocytochemistry experiments indicated that HMC3 cells express a low level of TLR4, which might explain why the HMC3 cells show weak response to LPS stimulation. Interestingly it was reported that human primary microglia are also weakly TLR4-positive when compared to rodent microglial cells (Smith & Dragunow, 2014). Therefore, the reduced sensitivity of human cells to LPS might be caused by the decreased expression of receptors. Immunofluorescence studies also showed higher expression of TLR9 than TLR4 in HMC3. Therefore, the effect of TLR9 ligand - ODN 2006 on HMC3 activation (CpG oligonucleotide) was monitored via the measurement of pro-inflammatory mediators.

Nitric oxide is one of the main biomarkers of neuroinflammation because it plays a vital role in the pathogenesis of inflammation. Nitric oxide production is readily induced in rodent microglia. However, literature shows many discrepancies of human microglia ability to produce nitric oxide (Smith & Dragunow, 2014). Therefore, the effects of ODN 2006, IFN $\gamma$ , LPS and TNF $\alpha$  were examined on nitrite production in HMC3 cells. Griess assay experiment indicated that untreated HMC3 produced 0.25  $\mu$ M of nitrite, and this basal level was not affected by pre-incubation of cells with IFN $\gamma$ , LPS, and TNF $\alpha$ . Similar results were reported by Russo et al., (2018) where scientists also did not report nitrite upregulation in HMC3 cells after stimulation with LPS, LPS/IFN $\gamma$ , IL-1 $\beta$ , and TNF $\alpha$ . Additionally, the authors reported a lack of iNOS expression in both resting and activated HMC3. Moreover, Zhao, Liu, He, Dickson, & Lee, (1998) demonstrated that IL-1 $\beta$  and IFN $\gamma$  stimulated human immature foetal and adult microglia do not express iNOS. In contrast, both foetal and adult human astrocytes upregulated iNOS expression. Therefore, it may be assumed that a high level of NO observed in AD patients is produced by astrocytes and, not by microglia (Janabi, 2002; M. L. Zhao et

al., 1998). Interestingly this study is showing an increase in the level of nitrite in cells activated with ODN 2006 to 0.63  $\mu\text{M}$  and 1.14  $\mu\text{M}$  when incubated with 5  $\mu\text{M}$  and 10  $\mu\text{M}$ , respectively, suggesting that TLR9 activation induced inflammatory response in HMC3 cells. Therefore, the impact of TLR9 ligand was further investigated on TNF $\alpha$  and IL-6 production in HMC3 cells.

Encouraged by results showing ODN 2006 ability to increase the nitrite level in HMC3 cells, production of IL-6 and TNF $\alpha$  was also assessed. The results showed that the non-treated cells contained ~67 pg/ml of IL-6 in the incubation medium, and pre-incubation of cells with ODN 2006 caused a concentration-dependent decrease of IL-6 levels to 33 pg/ml, and 18 pg/ml when incubated with 5 and 10  $\mu\text{M}$ , respectively. On the other hand, IFN $\gamma$  and TNF $\alpha$  increased IL-6 levels to 110 pg/ml (1.6-fold increase) and 524 pg/ml (7.8-fold increase), respectively. Similar findings were reported by Cappoli et al., (2019), who additionally reported an upregulation of IL-6 expression by IL-1 $\beta$ . HMC3 cells exposed to LPS did not alter IL-6 production. Although, primary human embryonic cells have been reported to respond to LPS via slight upregulation of IL-6 (Janabi, Nazila, Peudener, 1995; Sébire et al., 1993). Moreover, Timmerman et al., (2018) indicated that similarly to HMC3 another transformed human microglial cell line - HMO6 lost the ability to LPS-induced secretion of IL-1 $\beta$ , IL-6, and MIP-1 $\alpha$  proteins, but had the ability in producing only IL-8, TNF- $\alpha$  proteins. Therefore, the lack of responsiveness to LPS might be attributed to the transformation process. Consequently, immortalized microglia seem to be less responsive to LPS in comparison to primary cultures.

TNF $\alpha$  is an autoregulatory cytokine able to amplify the inflammatory processes (Yamamoto & Gaynor, 2001). Therefore, this study also assessed the TNF $\alpha$  level in HMC3 cells. Under the resting conditions, TNF $\alpha$  level was 28 pg/ml. When HMC3 cells were incubated with ODN 2006, IFN $\gamma$  and LPS the level of TNF $\alpha$  production did not increase. ELISA detected only the enhanced level of TNF $\alpha$  in recombinant TNF $\alpha$  protein stimulated cells. However, additional control experiments (cell-free medium + recombinant TNF $\alpha$  protein) revealed that the observed detection is a false positive caused by the compatibility of recombinant TNF $\alpha$  protein to capture and deduction antibody used in the ELISA kit. Hence TNF $\alpha$  production induced by recombinant TNF $\alpha$  protein could be assessed using polymerase chain reaction. Low expression of TNF $\alpha$  in unstimulated cells is in line with results presented by Hjorth et al., (2013). Authors also reported a lack of TNF $\alpha$  upregulation after stimulation with A $\beta$ 42. Similarly, TNF $\alpha$  was not detected after incubation with LPS, IFN $\gamma$  and IL-1 $\alpha$  in HMC3 and

primary human microglial cells (Dello Russo et al., 2018; Janabi, Nazila, Peudenier, 1995; Sébire et al., 1993). Nevertheless, Rajalakshmy, Malathi, & Madhavan, (2015) reported that Hepatitis C Virus NS3-induced TNF $\alpha$  production in HMC3 via TLR2 or TLR6 activation. This study showed that activation of TLR4 or TLR9 did not promote uniform inflammatory response when compared to the activation of TLR2 and TLR6.

Consequently, an attempt was made to investigate the effect of LPS, IFN $\gamma$ , and TNF $\alpha$  on NF- $\kappa$ B activation. Immunofluorescence staining of NF- $\kappa$ B p65 revealed that LPS did not induce NF- $\kappa$ B p65 nuclear translocation in HMC3, which is in line with lack of LPS impact on pro-inflammatory mediators' production. Therefore, LPS did not induce HMC3 activation leading to the activation of inflammatory responses. In contrary IFN $\gamma$  and TNF $\alpha$  induced NF- $\kappa$ B activation 1.7-fold and 3.2-fold, respectively. Taking into consideration those activities, the impact of both proteins was also tested on MAPK activation in HMC3 cells. Western blot experiments indicated that IFN $\gamma$  caused slight upregulation of MAPKs pathway inducing phosphorylation of ERK1/2 1.7-fold and phosphorylation of p38 1.3-fold. Whereas TNF $\alpha$  significantly induced phosphorylation of p-38 - 5.8-fold and slightly upregulated phosphorylation of ERK1/2 - 1.5-fold as compared to those in untreated cells.

In summary, TNF $\alpha$  induced broader inflammatory response than IFN $\gamma$  by the higher upregulation of IL-6 production - 524 pg/ml vs 110 pg/ml, respectively. Correspondingly with cytokine release, TNF $\alpha$  also more prominently activated two key inflammatory transduction pathways NF- $\kappa$ B and p38. Therefore, among ODN 2006, IFN $\gamma$ , LPS, and TNF $\alpha$ , TNF $\alpha$  is the most effective protein to induce M1 activation of HMC3 cells.

## 6 Concluding Remarks

The main goal of this presented study was to determine the anti-inflammatory and neuroprotective properties of novel isoflavone analogues using *in vitro* cell models. Neuroinflammation is recognized as a common disease-escalating factor of various neurodegenerative disorders, including dementia such as AD. The most significant known risk factor for AD is ageing. The ageing brain is characterized by the slow deterioration of homeostatic balance and shift towards low grade chronic pro-inflammatory status (Sparkman & Johnson, 2008). Therefore, a progressive increase in neuroinflammation causes sensitisation of brain cells and consequently aggravated inflammatory response to pathogens, aggregated proteins or stress. Intensified inflammatory response leads to increased expression of proinflammatory mediators which at high levels are cytotoxic, causing neuronal damage (Angelova & Brown, 2019). Loss of neuronal cells plays a central role in many chronic neurodegenerative diseases resulting in a combination of cognitive and motor deficits (Subramaniam, 2019). Furthermore, it has been proved that the incidence of AD is higher in women than in men. As a result, the loss of oestrogen during menopause has been associated with the decline of cognitive functions and consequently, neurodegeneration (Ciesielska et al., 2002). This observation led to a hypothesis that oestrogens may serve as potential anti-inflammatory and neuroprotective agents (Villa et al., 2016). However, oestrogens act as agonists of ER $\alpha$  and ER $\beta$ . ER $\alpha$  activation acts as an oncogene and contributes to the development of breast, endometrial and ovarian cancers (Y. Liu, Ma, & Yao, 2020). In turn, activation of ER $\beta$  exerts the opposite role to ER $\alpha$ , serving as a tumour suppressor (Chaurasiya et al., 2020). Hence, selective activation of ER $\beta$  is considered to trigger dual positive biological effects: reduction of neurodegeneration and inhibition of carcinogenesis.

In order to achieve the mentioned positive effects, it is assumed that groups of compounds that are structurally similar to oestrogens could be used. Therefore, from a structural point of view, isoflavones express structural similarity to oestrogen and are confirmed to preferentially bind to ER $\beta$  (Poschner et al., 2017). Biochanin A and daidzein are members of the isoflavone family. They are mainly found in soybean, soy foods, and legumes (Yu et al., 2016). The number of studies demonstrates that Biochanin A and daidzein induce anti-inflammatory, anti-oxidant, neuroprotective and anti-carcinogenic effects (Ahmed et al., 2017; Choi et al., 2012; Raheja et al., 2018; Sun et al., 2016; Sundaresan et al., 2018; Wu et

al., 2018). Although biochanin A has many beneficial pharmacological activities, it is not widely used as a therapeutic agent due to limited bioavailability which is <4% (Raheja et al., 2018). Moreover, natural compounds mainly consist of carbon, hydrogen and oxygen atoms with limited nitrogen and halogen atoms. Therefore, functional groups' modifications might change compound physicochemical properties and intrinsic reactivity of the molecule (Ertl, Altmann, & Mckenna, 2020). Consequently, those moieties could enhance bioavailability, specificity and potency of the molecule. This study assessed anti-inflammatory and neuroprotective properties of four novel isoflavone analogues: two of them were biochanin A derivatives and two daidzein derivatives. Biochanin A analogues were created by modification in position 7'. Both biochanin A derivatives were supplemented with large alkyl chain, which enhances lipophilicity and stability of molecule (Fokialakis et al., 2012; Harrold & Zavod, 2014). The moieties which were introduced are carbamate and dodecenoyl ester in compound 1 and 2, respectively. Daidzein derivatives were created by insertion of the functional group into daidzein B-ring at position 4'. Compound 3 contains ethyl ester moiety, which is known to increase lipid solubility and stability of molecule (Harrold & Zavod, 2014). In turn, compound 4 was created by insertion of the chloropropyl triazole functional group. Introduction of a chlorine atom to compounds has been shown to improve intrinsic biological activity by increasing reactivity and electrophilicity of molecule (Turnbull, 2000). Furthermore, the triazole scaffold is an electron reach system that allows binding with various enzymes and receptors. Moreover, triazoles are remarkably stable towards hydrolysis, oxidative and reductive conditions, and enzymatic degradation (Dheer et al., 2017). Therefore, the presented novel compounds could offer higher stability and specificity, which could enhance their pharmacological properties.

In order to address the main aim of this study, which was the evaluation of anti-inflammatory properties of compounds, the first objective was set to assess the effect of compounds on the level of pro-inflammatory mediators in LPS activated BV2 microglia. It is established that during an inflammatory response, microglia produce large amounts of pro-inflammatory mediators, which further enhance inflammatory response. Therefore, the level of pro-inflammatory mediators is often used as a biomarker to estimate the severity of the disease and verify the effectiveness of potential treatments, in this case, the effectiveness of compounds' anti-inflammatory action. The mediators investigated in this study include TNF $\alpha$ , IL-6, IL-1 $\beta$ , NO, iNOS, COX-2 and PGE $_2$ .

The results of ELISA experiments revealed that compound 1 significantly reduced the level of TNF $\alpha$  when tested at two highest concentrations of 15 and 20  $\mu$ M, whereas compound 2 significantly inhibited TNF $\alpha$  only when tested at 20  $\mu$ M. Similarly, compound 1 significantly reduced IL-6 when used at 10  $\mu$ M, 15  $\mu$ M, and 20  $\mu$ M, while compound 2 reduced IL-6 levels when used at 15  $\mu$ M and 20  $\mu$ M. Moreover, both compounds significantly decreased IL-1 $\beta$  production. In turn, daidzein derivatives (compounds 3 and 4) at all tested concentrations significantly inhibited in a concentration-dependent manner LPS-induced production of TNF $\alpha$ , IL-6, IL-1 $\beta$ . The next biomarkers used to examine the anti-inflammatory properties of compounds were NO and iNOS. Results showed that all tested compounds significantly reduced the level of NO and iNOS in LPS-activated BV2 microglia cells. A large body of evidence suggests that COX-2 and PGE<sub>2</sub> signalling modulate the inflammatory response. Hence COX-2 and PGE<sub>2</sub> also can serve as a biomarker of inflammation (Aïd & Bosetti, 2011; Combrinck et al., 2006; Johansson et al., 2015). Therefore, the effect of all compounds on COX-2 and PGE<sub>2</sub> levels were examined to determine the anti-inflammatory properties of compounds. All four tested compounds did not affect COX-2 and PGE<sub>2</sub> level. Funk & FitzGerald, (2007) demonstrated that selective COX-2 inhibition leads to cardiovascular malfunction due to the increase of platelet aggregation. Therefore, all four compounds might serve as a substitute for commonly used nonsteroidal anti-inflammatory drugs, with a potential for patients with a predisposition to cardiovascular diseases.

Among biochanin A derivatives, compound 2 was the least efficient in the inhibition of pro-inflammatory mediators. The only difference between compound 1 and 2 is the amine group in compound 1. Thus, the amine group might have an impact on the affinity of the compound for the receptors and consequently, its potency. Another factor which can enhance compound 1 activity is the higher polarity of the compound caused by the electronegativity of the N atom. Biochanin A analogues showed weak anti-inflammatory properties. However, in contrast to biochanin A derivatives, daidzein analogues reduced pro-inflammatory mediators at all tested concentrations. Therefore, daidzein analogues produced strong anti-inflammatory effects. This suggests that daidzein derivatives might serve as a potential treatment to reduce neuroinflammation.

The present study was designed to determine the effect of compounds on neuroinflammation and their possible molecular targets, hence next main objective included investigation of the

molecular mechanisms responsible for observed anti-inflammatory activity. The effects of compounds were investigated on ERE, NF- $\kappa$ B and MAPKs including p38, JNK and ERK1/2.

The oestrogen receptor is a transcription factor which is activated by oestrogens and structurally similar compounds such as isoflavones. Experiments confirmed that biochanin A and daidzein analogues upregulated ERE activation. Hence, they might act as ER agonists or trigger ERE activation via ER-ligand independent activation. Ligand-independent activation of ERE can be triggered by protein kinase cascades (Fuentes & Silveyra, 2019). Therefore, further work is needed to determine the exact mechanism of compounds triggering ERE activation. As daidzein derivatives showed the ability to upregulate ERE activity, then ER antagonist – ICI 182,780 was employed to evaluate if anti-inflammatory properties of compounds are ER-dependent. Surprisingly ER antagonist did not diminish daidzein derivatives ability to reduce TNF $\alpha$  and IL-6 production. Similarly, knockdown of ER $\beta$  also did not reverse the anti-inflammatory properties of compounds 3 and 4.

Subsequently, to further determine the mechanism of compounds' action, their effect was examined on NF- $\kappa$ B, which is considered a master regulator of inflammation (Liu et al., 2017). Compounds 1, 2 and 3 did not reduce NF- $\kappa$ B activity. Therefore, the mechanism of action of compounds 1, 2 and 3 is NF- $\kappa$ B-independent. In contrast to compounds 1, 2 and 3, compound 4 inhibited phosphorylation of NF- $\kappa$ B p65 and as expected also blocked NF- $\kappa$ B reporter gene transcription. Therefore, the anti-inflammatory activity of compound 4 is NF- $\kappa$ B-dependent. However, alongside NF- $\kappa$ B inflammatory response is modulated by MAPKs. Thus, the effect of compounds on p38, JNK and ERK1/2 activation was investigated. Compounds 1, 3 and 4 did not decrease phosphorylation of p38, JNK and ERK1/2. Therefore, this suggests that the anti-inflammatory action of compounds is MAPKs-independent. Moreover, TAK1 protein is a divergent point modulating the NF- $\kappa$ B and MAPKs activation (Ajibade et al., 2013). Since compound 4 did not reduce MAPKs phosphorylation, suggesting that the NF- $\kappa$ B signalling pathway is downregulated downstream of TAK1. Therefore, compound 4 might affect NF- $\kappa$ B signal transduction possibly affecting IKK or I $\kappa$ B $\alpha$  phosphorylation, or I $\kappa$ B $\alpha$  degradation.

The inflammatory response can be negatively regulated by activation of Nrf2 and SIRT1 (Ahmed, Luo, Namani, Wang, & Tang, 2017; Xie et al., 2013). However, due to biochanin A analogues' weak anti-inflammatory activity, the effect of Nrf2-, SIRT1- antagonists have not been examined on their anti-inflammatory properties. Therefore, it was investigated if the



anti-inflammatory properties of daidzein analogues are Nrf2- and SIRT1-dependent. Results indicated that antagonists of Nrf2 and SIRT1 did not diminish compounds 3 and 4 ability to reduce pro-inflammatory mediators suggesting their Nrf2- and SIRT1-independent anti-inflammatory properties.

The second main aim of this study was to investigate the effects of novel semi-synthetic compounds on neuroprotection using *in vitro* neuronal cell culture. This study presented that daidzein derivatives reduce LPS-induced inflammation in BV2 microglia, suggesting that compounds are neuroprotective through a decrease of neuroinflammation. Therefore, further research focused on the examination of direct neuroprotective properties of daidzein analogues using differentiated SH-SY5Y with H<sub>2</sub>O<sub>2</sub>-induced cytotoxicity. Results indicated that compounds 3 and 4 inhibited H<sub>2</sub>O<sub>2</sub>-induced apoptosis of differentiated SH-SY5Y cells. Both compounds reduced caspase-3/-7 and -9 activity. Moreover, compound 3 upregulated Bcl-2 level, which suggests that the compound directly inhibits the intrinsic apoptotic pathway preventing Bax/Bak oligomerization and disruption of the outer mitochondrial membrane. The neuroprotective properties of compounds 3 and 4 were unaffected in the presence of ER antagonist. Therefore, novel daidzein analogues express ER-independent neuroprotective properties.

Taken together, all tested compounds serve as ER activators upregulating ERE activity. Biochanin A analogues produced weak anti-inflammatory activity in contrast to daidzein derivatives which expressed strong anti-inflammatory activity in LPS-activated BV2 microglia. Moreover, daidzein analogues inhibited H<sub>2</sub>O<sub>2</sub>-induced neuronal death. Therefore, daidzein derivatives could serve as a potential treatment to alleviate neuroinflammation and neurodegeneration.

Finally, this project also aimed to develop human microglial cells (HMC3) as a cellular model to test the anti-inflammatory properties of compounds. To address that aim, two objectives have been determined. The first objective was to identify ligand, which will induce the release of pro-inflammatory mediators and second objective was to evaluate activated transduction pathways. Among four ligands, including ODN 2006, IFN $\gamma$ , LPS, and TNF $\alpha$ , TNF $\alpha$  induced the broadest inflammatory response in HMC3. Stimulation with TNF $\alpha$  increased production of Iba1, IL-6, and upregulated activation of NF- $\kappa$ B and p38 signalling pathways. Moreover, this study also determined that HMC3 cells express ER $\alpha$  and ER $\beta$  therefore, this cell line can be used to investigate properties of compounds acting via ERs.

## 6.1 Directions for future research

Compounds tested in this study presented exceptional ability to reduce iNOS/NO production. Moreover, only compound 4 suppressed NF- $\kappa$ B activity; thus, this compound reduces iNOS/NO production through transcriptional inhibition of iNOS genes. However, compounds 1, 2 and 3 did not inhibit NF- $\kappa$ B or MAPKs activation. Hence compounds may affect iNOS on post-transcription, translation, and post-translational level. Natural compounds such as andrographolide have been demonstrated to reduce *de novo* iNOS protein synthesis and increase degradation of the iNOS protein (Chiou, Chen, & Lin, 2000). Therefore, to thoroughly examine how compounds decrease iNOS protein level, future experiments could assess the effect of compounds on iNOS mRNA expression, iNOS protein stability analysis and *de novo* protein synthesis. The mRNA iNOS expression can be determined using qPCR. iNOS protein stability could be assessed using the protein synthesis inhibitor cycloheximide to prevent further iNOS protein synthesis. *De novo* iNOS protein synthesis could be determined using the synthetic methionine homolog L-azidohomoalanine (AHA) which incorporates into newly synthesized proteins allowing to covalently label the incorporated AHA with reagents to enable its detection (Chiou et al., 2000).

Moreover, a further study could assess the precise mechanism of compound 4 on NF- $\kappa$ B inhibition. This study provides the following insights for future research: compound 4 reduces phosphorylation of NF- $\kappa$ B p65 and do not affect MAPKs. Therefore, these findings indicate that NF- $\kappa$ B is inhibited downstream of TAK1. Thus, to elucidate the target of compound 4 in NF- $\kappa$ B signal transduction further study should determine the compound's effect on IKK and I $\kappa$ B $\alpha$ .

The precise mechanism of the anti-inflammatory action of compound 3 remains to be elucidated. Therefore, the future investigation could assess the effect of compound 3 on AP-1, JAK/STAT or PPAR $\gamma$ , which could modulate the anti-inflammatory properties of the compound.

This study indicated that all examined compounds activated ERE reporter activity. However, the ERE activation can be triggered by compounds via interaction with ER or ligand-independent phosphorylation of ER and consequently ERE activation. Ligand-independent ERE activation can be induced by phosphorylation of protein kinase cascades such as PKC, PKA and MAPK such as ERK1/2 (Fuentes & Silveyra, 2019). Thus, the mode of ERE

activation by compounds could be assessed by receptor-ligand binding assays or the effect of compounds on phosphorylation of protein kinases.

Compounds ability to act as agonist or antagonist to ER may also depend on co-activator and co-repressor proteins present in the cell. Hence, the same compound can work as ER agonist in one tissue type and as an antagonist in other, e.g. tamoxifen - breast cancer drug act as ER agonist in the uterus and bone and as an antagonist in the breast. Isoflavones were demonstrated to have a higher affinity for ER $\beta$  and act as tumour suppressors (Chaurasiya et al., 2020; Lee, Kim, & Song, 2012; Treeck et al., 2019). Therefore, future studies could investigate the effects of novel isoflavone analogues on breast and gynaecological cancers. Granados-Principal et al., (2015) indicated that inhibition of iNOS might serve as an effective targeted therapy against triple-negative breast cancer hence, as tested compounds showed excellent ability to reduce iNOS/NO than future work could evaluate the effect of compounds on triple-negative breast cancer.

This study presented anti-inflammatory activities of four isoflavone analogues. Therefore, future work could determine relative IC<sub>50</sub> values of compounds which would allow to compare compounds anti-inflammatory properties.

The crucial consideration for compounds targeting CNS should be their blood-brain barrier permeability. Therefore, compounds targeted for neuroinflammation and neurodegeneration should be investigated using drug transport mechanisms with relevance to the CNS. One of the *in vitro* models of the BBB is Immortalized Human Cerebral Microvascular Endothelial Cell Line (hCMEC/D3). BBB permeability may change in pathological conditions, such as Alzheimer's disease (Helms et al., 2016). However, if compounds anti-inflammatory properties would be used as a prevention of neuroinflammation, it would be crucial to investigate compounds ability to penetrate BBB.

## 7 Appendices

### 7.1 Appendix 1: Anti-inflammatory properties of compounds 3 and 4 using HMC3 activated with TNF $\alpha$

Protein which induced the highest level of the inflammatory response in HMC3 cells was TNF $\alpha$  (25 ng/ml). HMC3 incubated with TNF $\alpha$  protein produced a significant amount of IL-6 and activated NF- $\kappa$ B and p-38 signalling pathways. Therefore, the anti-inflammatory properties of compounds 3 and 4 were examined using TNF $\alpha$ -induced inflammation in HMC3 microglia.

#### 7.1.1 Treatment of HMC3 with compounds 3 and 4

HMC3 cells were seeded in 96-well, 24-well plates (Sarstedt) at a density of  $1 \times 10^5$  cells/ml in 200  $\mu$ l/well for 96-well plate and 1 ml/well for 24-well plate of culture medium and incubated until approximately 80% confluent. Then, the cell culture medium was changed to serum-free EMEM and incubated for 1 – 2 hours. Then cells were treated with compounds 3 (2.5, 5 and 10  $\mu$ M) and 4 (5, 10 and 20  $\mu$ M) for 30 minutes (both compounds were kindly provided by Gabriel Mengheres (PhD Researcher supervised by Dr Karl Hemming, Department of Chemical Sciences, The University of Huddersfield). The final concentration of DMSO in cells was kept constant at 0.02% (v/v) for all concentrations of compounds and untreated cells. Subsequently, cells were activated with 25 ng/ml of Recombinant Human TNF $\alpha$  Protein (R&D Systems) and incubated 24 hours.

### 7.1.2 The effect of compounds 3 and 4 on the viability of HMC3 cells

HMC3 cells were incubated with or without 0.02% (v/v) of DMSO and compounds 3 (2.5, 5 and 10  $\mu\text{M}$ ) and 4 (5, 10 and 20  $\mu\text{M}$ ). After 30 minutes of pre-incubation with compounds 25 ng/ml of  $\text{TNF}\alpha$  was added, and cells were further incubated for 24 hours, followed by XTT assay. Figure 7.1 indicates that 0.02% (v/v) of DMSO and compounds 3 and 4 did not affect the viability of HMC3 cells.

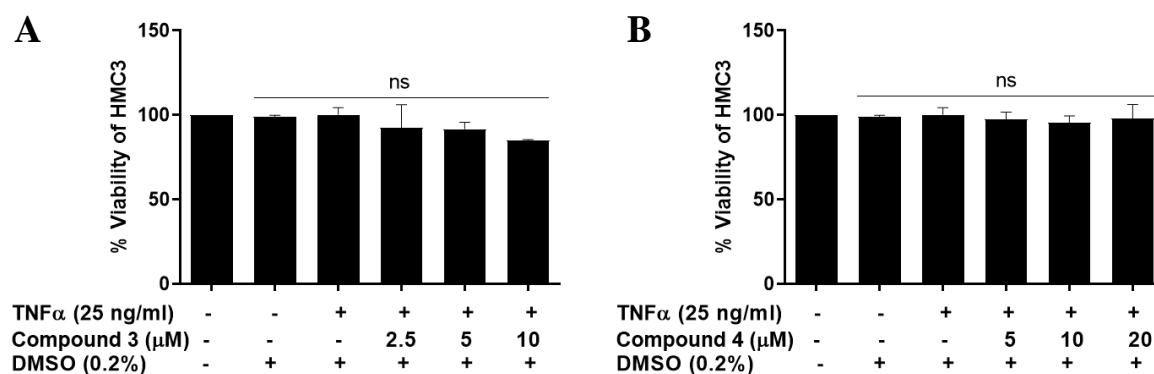


**Figure 7.1** The effect of compounds 3 and 4 on the viability of HMC3 using XTT. HMC3 cells were incubated with or without compounds 3 (2.5, 5 and 10  $\mu\text{M}$ ) and 4 (5, 10 and 20  $\mu\text{M}$ ) for 30 minutes and then activated with  $\text{TNF}\alpha$  (25 ng/ml). Subsequently, HMC3 cells were incubated for 24 hours, and XTT assay was performed. Compounds 3 and 4 at all tested concentrations did not affect the viability of BV2 microglia. All values are expressed as mean  $\pm$  SEM for N=3. Data were analysed using one-way ANOVA for multiple comparisons with post hoc Student Newman-Keuls test. \* $p < 0.033$  in comparison with untreated control.

### 7.1.3 The effect of compounds 3 and 4 on IL-6 production in $\text{TNF}\alpha$ -activated HMC3 microglia

IL-6 is pro-inflammatory cytokine highly upregulated during inflammation. Hence level of IL-6 may serve as an indicator of the severity of inflammations, thus evaluating the effectiveness of molecules to reduce inflammation. To examine if compounds 3 and 4 possess anti-inflammatory properties in  $\text{TNF}\alpha$  activated HMC3, cells were pre-incubated with or without compounds 3 (2.5, 5 and 10  $\mu\text{M}$ ) and 4 (5, 10 and 20  $\mu\text{M}$ ) for 30 minutes followed by  $\text{TNF}\alpha$  activation for 24 hours. ELISA demonstrates that unstimulated cells produced low physiological amounts of IL-6, which was significantly ( $p < 0.001$ ) increased by  $\text{TNF}\alpha$  incubation. Figure 7.2 shows that compound 3 in a concentration-dependent manner enhanced  $\text{TNF}\alpha$ -induced IL-6 level to  $142 \pm 8\%$  - 2.5  $\mu\text{M}$ ,  $143 \pm 11\%$  - 5  $\mu\text{M}$  and  $188 \pm 21\%$  - 10  $\mu\text{M}$ , when compared to  $\text{TNF}\alpha$  control. Compound 4 did not significantly affect IL-6 production in  $\text{TNF}\alpha$  stimulated HMC3 cells. After incubation of cells with 5, 10 and 20  $\mu\text{M}$

of compound 4 IL-6 level was  $109 \pm 5\%$ ,  $106 \pm 9\%$  and  $90 \pm 3\%$ , respectively, when compared to TNF $\alpha$  control as 100% (Figure 7.2 B).

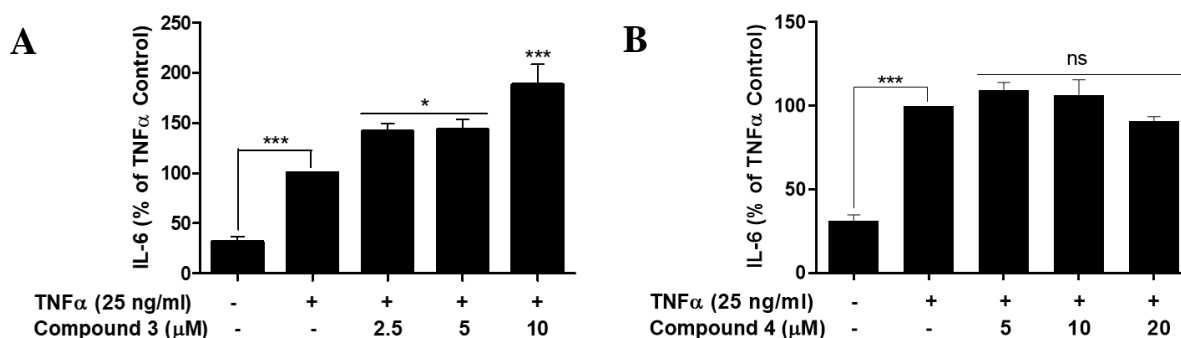


**Figure 7.2** The effect of compounds 3 and 4 on the production of IL-6 in TNF $\alpha$  activated HMC3 cells. HMC3 were pre-incubated for 30 minutes with compounds 3 (2.5, 5 and 10  $\mu$ M) and 4 (5, 10 and 20  $\mu$ M) and then activated with TNF $\alpha$  (ng/ml ng/ml) for 24 hours. After incubation, supernatants were collected, and IL-6 ELISA was performed. Compound 3 significantly in a concentration-dependent manner, increased IL-6 production. Compound 4 did not significantly affect TNF $\alpha$ -induced IL-6 production in HMC3 cells. All values are expressed as a mean  $\pm$  SEM for N=3. Data were analysed using one-way ANOVA for multiple comparisons with post hoc Student Newman-Keuls test. \* $p < 0.033$ , \*\* $p < 0.002$ , \*\*\* $p < 0.001$  in comparison with TNF $\alpha$  control.

Encouraged by the responsiveness of HMC3 cells to TNF $\alpha$ , the effect of daidzein derivatives was examined on TNF $\alpha$ -induced IL-6 production in HMC3. Surprisingly compound 3 in a concentration-dependent manner upregulated TNF $\alpha$ -induced IL-6 production in comparison to TNF $\alpha$  control. Whereas compound 4 had no effect on IL-6 level. Viability assay demonstrates that those actions are caused by pharmacological activities of compounds, not by HMC3 sensitivity to tested molecules. In contrary, the same compounds reduced IL-6 level in LPS-activated BV2 cells. Differential cell response to compounds might be attributed to species-specific differences or HMC3 unknown genetic mutations caused by immortalization leading to unique gene pattern not identical to the human cell type in vivo. An example of HMC3 specific mutations is constitutive NOX4-dependent ROS generation. Therefore, to exclude the effects of unknown mutations caused by cell transformation, single-cell whole-genome sequencing of immortalized cells alongside parental cell lines would be beneficial. Further use of HMC3 in inflammation studies would greatly advance from extensive validation processes, directly comparing primary human microglia to HMC3 investigating an overall pattern of gene activation.

## 7.2 Appendix 2: Figure illustrating the experimental variation that occurs in LPS control

Data presented in Figure 7.3 illustrate experimental variation that occurs in LPS control. Untreated cells produced  $12.5 \pm 0.3$  pg/ml of TNF $\alpha$ . BV2 microglia activated with LPS (100 ng/ml) for 24 hours significantly ( $p < 0.001$ ) increased production of TNF $\alpha$  to  $196.7 \pm 12.5$  pg/ml when compared to untreated cells.

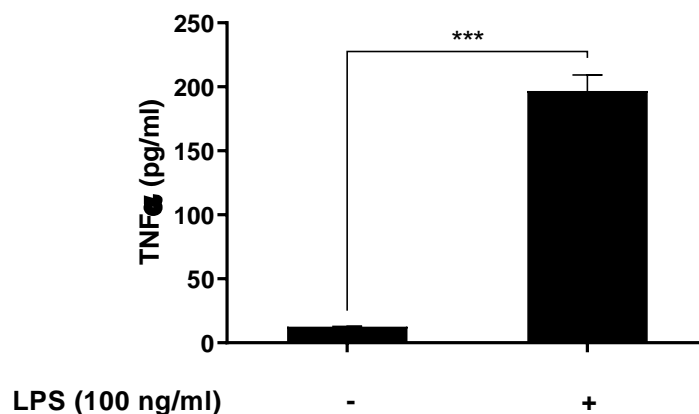


**Figure 7.3 TNF $\alpha$  production in untreated and LPS-activated BV2 microglia.** BV2 microglia were activated with LPS (100 ng/ml) for 24h. After incubation, supernatants were collected, and TNF $\alpha$  ELISAs was performed. Untreated cells produced  $12.5 \pm 0.3$  pg/ml of TNF $\alpha$  and its production was significantly increased by incubation with LPS to  $196.7 \pm 12.5$  pg/ml. All values are expressed as a mean  $\pm$  SEM for N=3. Data were analysed using one-way ANOVA for multiple comparisons with post hoc Student Newman-Keuls test. \*\*\* $p < 0.001$  in comparison with LPS control.

### 7.3 Appendix 3: List of materials used in this study

Materials	Catalog no.	Manufacturer / Supplier
17 $\beta$ -oestradiol	E2758	Sigma-Aldrich
2,2-Diphenyl-1-picrylhydrazyl (free radical), 95%, Alfa Aesar™	11309658	Fisher Scientific
8-well cell culture chamber	94.6140.802	Sarstedt
Amyloid $\beta$ -Protein Fragment 25-35	A4559	Sigma-Aldrich
Annexin V-FITC Apoptosis Staining / Detection Kit	ab14085	Abcam
Aspiration pipette 2 ml for aspiration of liquids	86.1252.011	Sarstedt
Caspase-Glo® 3/7 Assay Systems	G8091	Promega
Caspase-Glo® 9 Assay Systems	G8211	Promega
Cell Lysis Buffer (10x)	9803	Cell Signalling
Cignal ERE Reporter Assay Kit (LUC)	CCS-005L	Qiagen
Cignal NF-kappaB Reporter Assay Kit (LUC)	CCS-013G	Qiagen
Control siRNA-A	sc-37007	Santa Cruz Biotechnology
Dimethyl sulfoxide	10213810	Fisher Scientific
Dual-Glo® Luciferase Assay System	E2920	Promega
Dulbecco's Modified Eagle's Medium	D5796	Sigma-Aldrich
ELISA MAX™ Deluxe Set Human IL-6	430504	BioLegend
ELISA MAX™ Deluxe Set Human TNF- $\alpha$	430204	BioLegend
ELISA MAX™ Deluxe Set Mouse IL-1 $\beta$	432604	BioLegend
ELISA MAX™ Deluxe Set Mouse IL-6	431304	BioLegend
ELISA MAX™ Deluxe Set Mouse TNF- $\alpha$	430904	BioLegend
Er $\beta$ siRNA	sc-35326	Santa Cruz Biotechnology
EX527	E7034	Sigma-Aldrich
Fulvestrant	I4409	Sigma-Aldrich
Gibco™ DPBS	14190250	Fisher Scientific
Gibco™ Fetal Bovine Serum	10500064	Fisher Scientific
Gibco™ Ham's F-12 Nutrient Mix	11500586	Fisher Scientific



Gibco™ HBSS, calcium, magnesium, no phenol red	15266355	Fisher Scientific
Gibco™ MEM	15188319	Fisher Scientific
Gibco™ MEM Non-Essential Amino Acids Solution (100X)	11350912	Fisher Scientific
Gibco™ Opti-MEM™ I Reduced Serum Medium	15392402	Fisher Scientific
Gibco™ Sodium Pyruvate (100 mM)	12539059	Fisher Scientific
Gibco™ TrypLE™ Express Enzyme (1X)	11528856	Fisher Scientific
Griess Reagent System	G2930	Promega
Immobilon-FL PVDF Membrane	IPFL00010	Millipore
Invitrogen™ BCL-2 Human ELISA Kit	15581817	Fisher Scientific
Invitrogen™ Image-IT™ LIVE Green Reactive Oxygen Species Detection Kit, for microscopy	10738994	Fisher Scientific
Invitrogen™ NF-κB p65 (Phospho) [pS536] Human InstantOne™ ELISA Kit	15590787	Fisher Scientific
Invitrogen™ NuPAGE™ 4 to 12%, Bis-Tris, 1.0 mm, Mini Protein Gel	12313623	Fisher Scientific
Invitrogen™ NuPAGE™ Antioxidant	11529166	Fisher Scientific
Invitrogen™ NuPAGE™ LDS Sample Buffer (4X)	11549166	Fisher Scientific
Invitrogen™ NuPAGE™ MES SDS Running Buffer (20X)	11509166	Fisher Scientific
Invitrogen™ NuPAGE™ Sample Reducing Agent (10X)	10424012	Fisher Scientific
Invitrogen™ NuPAGE™ Transfer Buffer (20X)	11539166	Fisher Scientific
Invitrogen™ XTT (2,3-Bis-(2-Methoxy-4-Nitro-5-Sulfophenyl)-2H-Tetrazolium-5-Carboxanilide)	10194032	Fisher Scientific
Invitrogen™ p38 MAPK (Phospho) [pT180/pY182] Multispecies InstantOne™ ELISA Kit	15510777	Fisher Scientific
L-(+)-Ascorbic acid, ACS, >99%, Alfa Aesar™	11393288	Fisher Scientific

LPS from <i>S. typhimurium</i> (S-form)	IAX-100-011-M001	Innaxon Biosciences
Micro tube conical base push cap 0.5 ml	72.699	Sarstedt
Micro tube conical base push cap 1.5 ml	72.690.001	Sarstedt
Microtest plate, 96-well, flat base	82.1581	Sarstedt
ML385	SML1833	Sigma-Aldrich
ODN 2006 Class B CpG oligonucleotide - Human TLR9 ligand	ODN 2006	InvivoGen
Odyssey (TBS) Blocking Buffer	927-50000	LI-COR Biosciences
Phenylmethylsulfonyl fluoride	10837091001	Merck Life Science
PMS, Phenazine methosulfate, 5-Methylphenazinium methyl sulfate	P9625	Sigma-Aldrich
Precision Plus Protein™ Dual Color Standards	161-0374	Bio-Rad Laboratories
Prostaglandin E2 Enzyme Immunoassay Kit	K051-H1	Arbor Assays
Reagent Reservoir, PVC (Sterile)	E2310-1010	Starlab
Recombinant Human IFN-gamma Protein	285-IF	R&D Systems
Recombinant Human TNF-alpha Protein	210-TA	R&D Systems
Retinoic acid	R2625	Sigma-Aldrich
Serological pipette 10 ml	86.1254.001	Sarstedt
Serological pipette 25 ml	86.1685.001	Sarstedt
Serological pipette 5 ml	86.1253.001	Sarstedt
Starter kit - 250 µL Glial-Mag reagent + 3mL Glial-Boost + 1 Super magnetic plate	KGL00250	OZ Biosciences
Thermo Scientific™ Halt™ Phosphatase Inhibitor Single-Use Cocktail	10668304	Fisher Scientific
Thermo Scientific™ Nunc™ MicroWell™ 96-Well, Nunclon Delta-Treated, Flat-Bottom Microplate	10072151	Fisher Scientific
Thermo Scientific™ Pierce™ Coomassie (Bradford) Protein Assay Kit	10270014	Fisher Scientific
Thermo Scientific™ Restore™ Fluorescent Western Blot Stripping Buffer	11577900	Fisher Scientific
Tissue culture flask t75	83.3911.002	Sarstedt

Tissue culture plate, 24 flat well	83.3922	Sarstedt
Tissue culture plate, 6 flat well	83.3920	Sarstedt
Tissue culture plate, 96 flat well	83.3924	Sarstedt
Tris Buffered Saline	sc-24951	Santa Cruz Biotechnology
Tube Conical Base, 50ml	62.547.254	Sarstedt
TWEEN® 20	P9416	Sigma-Aldrich
Water, (DNASE, RNASE free), Fisher BioReagents	10295243	Fisher Scientific

## References

- Abán, C. E., Accialini, P. L., Etcheverry, T., Leguizamón, G. F., Martínez, N. A., & Farina, M. G. (2018). Crosstalk Between Nitric Oxide and Endocannabinoid Signaling Pathways in Normal and Pathological Placentation. *Frontiers in Physiology*, 9(December), 1–9. <https://doi.org/10.3389/fphys.2018.01699>
- Adams, S. M., Aksenova, M. V., Aksenov, M. Y., Mactutus, C. F., & Booze, R. M. (2012). Soy isoflavones genistein and daidzein exert anti-apoptotic actions via a selective ER-mediated mechanism in neurons following HIV-1 Tat1-86 exposure. *PLoS ONE*, 7(5), 38–40. <https://doi.org/10.1371/journal.pone.0037540>
- Ahmed, S. M. U., Luo, L., Namani, A., Wang, X. J., & Tang, X. (2017a). Nrf2 signaling pathway: Pivotal roles in inflammation. *Biochimica et Biophysica Acta - Molecular Basis of Disease*, 1863(2), 585–597. <https://doi.org/10.1016/j.bbadis.2016.11.005>
- Ahmed, S. M. U., Luo, L., Namani, A., Wang, X. J., & Tang, X. (2017b). Nrf2 signaling pathway: Pivotal roles in inflammation. *Biochimica et Biophysica Acta - Molecular Basis of Disease*, 1863(2), 585–597. <https://doi.org/10.1016/j.bbadis.2016.11.005>
- Ahmed, T., Javed, S., Tariq, A., Budzyńska, B., D'Onofrio, G., Daglia, M., ... Nabavi, S. M. (2017). Daidzein and its Effects on Brain. *Curr Med Chem*, 24(4), 365–375.
- Aïd, S., & Bosetti, F. (2011). Targeting cyclooxygenases-1 and -2 in neuroinflammation: Therapeutic implications. *Biochimie*, 93(1), 46–51. <https://doi.org/10.1016/j.biochi.2010.09.009>
- Ajibade, A. A., Wang, H. Y., & Wang, R. F. (2013). Cell type-specific function of TAK1 in innate immune signaling. *Trends in Immunology*, 34(7), 307–316. <https://doi.org/10.1016/j.it.2013.03.007>
- Ajmone-Cat, M. A., Bernardo, A., Greco, A., & Minghetti, L. (2010). Non-steroidal anti-inflammatory drugs and brain inflammation: Effects on microglial functions. *Pharmaceuticals*, 3(6), 1949–1964. <https://doi.org/10.3390/ph3061949>
- Akiho, H., Iwai, A., Katoh-Sudoh, M., Tsukamoto, S., Kazuo, K., & Yamaguchi, T. (1998). Neuroprotective Effect of YM-39558, Orotic Acid Ethylester, in Gerbil Forebrain Ischemia. *The Japanese Journal of Pharmacology*, 76(4), 441–444.
- Anderson, M. F., Nilsson, M., Eriksson, P. S., & Sims, N. R. (2004). Glutathione monoethyl ester provides neuroprotection in a rat model of stroke. *Neuroscience Letters*, 354(2), 163–165. <https://doi.org/10.1016/j.neulet.2003.09.067>
- Andreasson, K. (2010). Emerging roles of PGE2 receptors in models of neurological disease. *Prostaglandins and Other Lipid Mediators*, 91(3–4), 104–112. <https://doi.org/10.1016/j.prostaglandins.2009.04.003>
- Angelova, D. M., & Brown, D. R. (2019). Microglia and the aging brain: are senescent microglia the key to neurodegeneration? *Journal of Neurochemistry*, 151(6), 676–688.

<https://doi.org/10.1111/jnc.14860>

- Arcuri, C., Mecca, C., Bianchi, R., Giambanco, I., & Donato, R. (2017). The pathophysiological role of microglia in dynamic surveillance, phagocytosis and structural remodeling of the developing CNS. *Frontiers in Molecular Neuroscience*, *10*(June), 1–22. <https://doi.org/10.3389/fnmol.2017.00191>
- Arulselvan, P., Fard, M. T., Tan, W. S., Gothai, S., Fakurazi, S., Norhaizan, M. E., & Kumar, S. S. (2016). Role of Antioxidants and Natural Products in Inflammation. *Oxidative Medicine and Cellular Longevity*, *2016*. <https://doi.org/10.1155/2016/5276130>
- Baker, A. E., Brautigam, V. M., & Watters, J. J. (2004a). Estrogen modulates microglial inflammatory mediator production via interactions with estrogen receptor  $\beta$ . *Endocrinology*, *145*(11), 5021–5032. <https://doi.org/10.1210/en.2004-0619>
- Baker, A. E., Brautigam, V. M., & Watters, J. J. (2004b). Estrogen modulates microglial inflammatory mediator production via interactions with estrogen receptor  $\beta$ . *Endocrinology*, *145*(11), 5021–5032. <https://doi.org/10.1210/en.2004-0619>
- Baker, A. E., Brautigam, V. M., & Watters, J. J. (2004c). Estrogen Modulates Microglial Inflammatory Mediator Production via Interactions with Estrogen Receptor  $\beta$ . *Endocrinology*, *145*(11), 5021–5032. <https://doi.org/10.1210/en.2004-0619>
- Bao, T. Z., Han, G. Z., Shim, J. Y., Wen, Y., & Jiang, X. R. (2006). Quantitative structure-activity relationship of various endogenous estrogen metabolites for human estrogen receptor  $\alpha$  and  $\beta$  subtypes: Insights into the structural determinants favoring a differential subtype binding. *Endocrinology*, *147*(9), 4132–4150. <https://doi.org/10.1210/en.2006-0113>
- Basu, A., Krady, J. K., & Levison, S. W. (2004). Interleukin-1: A master regulator of neuroinflammation. *Journal of Neuroscience Research*, *78*(2), 151–156. <https://doi.org/10.1002/jnr.20266>
- Becher, B., Spath, S., & Goverman, J. (2017). Cytokine networks in neuroinflammation. *Nature Reviews Immunology*, *17*(1), 49–59. <https://doi.org/10.1038/nri.2016.123>
- Bevilacqua, M. A., Iovine, B., Iannella, M. L., Gasparri, F., & Monfrecola, G. (2011). Synergic effect of genistein and daidzein on UVB-induced DNA damage: An effective photoprotective combination. *Journal of Biomedicine and Biotechnology*, *2011*. <https://doi.org/10.1155/2011/692846>
- Bhat, N. R., Zhang, P., Lee, J. C., & Hogan, E. L. (1998). Extracellular signal-regulated kinase and p38 subgroups of mitogen- activated protein kinases regulate inducible nitric oxide synthase and tumor necrosis factor- $\alpha$  gene expression in endotoxin-stimulated primary glial cultures. *Journal of Neuroscience*, *18*(5), 1633–1641. <https://doi.org/10.1523/jneurosci.18-05-01633.1998>
- Boraschi, D., & Tagliabue, A. (2013). The interleukin-1 receptor family. *Seminars in Immunology*, *25*(6), 394–407. <https://doi.org/10.1016/j.smim.2013.10.023>

- Brabazon, F., Bermudez, S., Shaughnessy, M., Khayrullina, G., & Byrnes, K. R. (2018). The effects of insulin on the inflammatory activity of BV2 microglia. *PLoS ONE*, *13*(8), 1–13. <https://doi.org/10.1371/journal.pone.0201878>
- Bradford, M. M. (1976). A Rapid and Sensitive Method for the Quantitation of Microgram Quantities of Protein Utilizing the Principle of Protein-Dye Binding. In *ANALYTICAL BIOCHEMISTRY* (Vol. 72).
- Brentnall, M., Rodriguez-Menocal, L., De Guevara, R. L., Cepero, E., & Boise, L. H. (2013). Caspase-9, caspase-3 and caspase-7 have distinct roles during intrinsic apoptosis. *BMC Cell Biology*, *14*(1), 1. <https://doi.org/10.1186/1471-2121-14-32>
- Brown, G. C. (2010). Nitric oxide and neuronal death. *Nitric Oxide - Biology and Chemistry*, *23*(3), 153–165. <https://doi.org/10.1016/j.niox.2010.06.001>
- Brown, G. C., & Vilalta, A. (2015). How microglia kill neurons. *Brain Research*, *1628*, 288–297. <https://doi.org/10.1016/j.brainres.2015.08.031>
- Campbell, I. L., Erta, M., Lim, S. L., Frausto, R., May, U., Rose-John, S., ... Hidalgo, J. (2014). Trans-signaling is a dominant mechanism for the pathogenic actions of interleukin-6 in the brain. *Journal of Neuroscience*, *34*(7), 2503–2513. <https://doi.org/10.1523/JNEUROSCI.2830-13.2014>
- Cappoli, N., Mezzogori, D., Tabolacci, E., Coletta, I., Navarra, P., Pani, G., & Russo, C. Dello. (2019). The mTOR kinase inhibitor rapamycin enhances the expression and release of pro-inflammatory cytokine interleukin 6 modulating the activation of human microglial cells. *EXCLI Journal*, *18*, 779–798. <https://doi.org/10.17179/excli2019-1715>
- Cargnello, M., & Roux, P. P. (2011). Activation and Function of the MAPKs and Their Substrates, the MAPK-Activated Protein Kinases. *Microbiology and Molecular Biology Reviews*, *75*(1), 50–83. <https://doi.org/10.1128/mubr.00031-10>
- Casini, M. L., Marelli, G., Papaleo, E., Ferrari, A., D'Ambrosio, F., & Unfer, V. (2006). Psychological assessment of the effects of treatment with phytoestrogens on postmenopausal women: A randomized, double-blind, crossover, placebo-controlled study. *Fertility and Sterility*, *85*(4), 972–978. <https://doi.org/10.1016/j.fertnstert.2005.09.048>
- Červinka, M. (1999). The role of mitochondria in apoptosis induced in vitro. *General Physiology and Biophysics*, *18*(SPEC. ISS.), 33–40. <https://doi.org/10.1146/annurev-genet-102108-134850>.The
- Chabrier, P. E., Demerlé-Pallardy, C., & Auguet, M. (1999). Nitric oxide synthases: Targets for therapeutic strategies in neurological diseases. *Cellular and Molecular Life Sciences*, *55*(8–9), 1029–1035. <https://doi.org/10.1007/s000180050353>
- Chalaris, A., Garbers, C., Rabe, B., Rose-John, S., & Scheller, J. (2011). The soluble Interleukin 6 receptor: Generation and role in inflammation and cancer. *European Journal of Cell Biology*, *90*(6–7), 484–494. <https://doi.org/10.1016/j.ejcb.2010.10.007>

- Chaurasiya, S., Widmann, S., Botero, C., Lin, C. Y., Gustafsson, J. Å., & Strom, A. M. (2020). Estrogen receptor  $\beta$  exerts tumor suppressive effects in prostate cancer through repression of androgen receptor activity. *PLoS ONE*, *15*(5), 1–13. <https://doi.org/10.1371/journal.pone.0226057>
- Chen, M. N., Lin, C. C., & Liu, C. F. (2015). Efficacy of phytoestrogens for menopausal symptoms: A meta-analysis and systematic review. *Climacteric*, *18*(2), 260–269. <https://doi.org/10.3109/13697137.2014.966241>
- Chen, W. W., Zhang, X., & Huang, W. J. (2016). Role of neuroinflammation in neurodegenerative diseases (Review). *Molecular Medicine Reports*, *13*(4), 3391–3396. <https://doi.org/10.3892/mmr.2016.4948>
- Chiou, W. F., Chen, C. F., & Lin, J. J. (2000). Mechanisms of suppression of inducible nitric oxide synthase (iNOS) expression in RAW 264.7 cells by andrographolide. *British Journal of Pharmacology*, *129*(8), 1553–1560. <https://doi.org/10.1038/sj.bjp.0703191>
- Choi, E. J., & Kim, G. H. (2008). Daidzein causes cell cycle arrest at the G1 and G2/M phases in human breast cancer MCF-7 and MDA-MB-453 cells. *Phytomedicine*, *15*(9), 683–690. <https://doi.org/10.1016/j.phymed.2008.04.006>
- Choi, E. Y., Jin, J. Y., Lee, J. Y., Choi, J. I., Choi, I. S., & Kim, S. J. (2012). Anti-inflammatory effects and the underlying mechanisms of action of daidzein in murine macrophages stimulated with *Prevotella intermedia* lipopolysaccharide. *Journal of Periodontal Research*, *47*(2), 204–211. <https://doi.org/10.1111/j.1600-0765.2011.01422.x>
- Choi, Y., Lee, M. K., Lim, S. Y., Sung, S. H., & Kim, Y. C. (2009). Inhibition of inducible NO synthase, cyclooxygenase-2 and interleukin-1 $\beta$  by torilin is mediated by mitogen-activated protein kinases in microglial BV2 cells. *British Journal of Pharmacology*, *156*(6), 933–940. <https://doi.org/10.1111/j.1476-5381.2009.00022.x>
- Cholerton, B., Gleason, C. E., Baker, L. D., & Asthana, S. (2002). Estrogen and Alzheimer's disease: the story so far. *Drugs & Aging*, *19*(6), 405–427.
- Chowdhury, I., Tharakan, B., & Bhat, G. K. (2008). Caspases - An update. *Comparative Biochemistry and Physiology - B Biochemistry and Molecular Biology*, *151*(1), 10–27. <https://doi.org/10.1016/j.cbpb.2008.05.010>
- Ciesielska, A., Joniec, I., & Członkowska, A. (2002). Rola estrogenów w patogenezie chorób neurodegeneracyjnych. *Farmakoterapia W Psychiatrii I Neurologii*, *2*(E 2), 130–147.
- Cobb, M. H. (2016). *MAP Kinase Pathways: Functions and Modulation*. 1–16. Retrieved from <https://www.semanticscholar.org/paper/MAP-Kinase-Pathways-%3A-Functions-and-Modulation-Cobb/e81798ebf70c233741ada55e0666ea96927e5b4a>
- Combrinck, M., Williams, J., De Berardinis, M. A., Warden, D., Puopolo, M., Smith, A. D., & Minghetti, L. (2006). Levels of CSF prostaglandin E2, cognitive decline, and survival in Alzheimer's disease. *Journal of Neurology, Neurosurgery and Psychiatry*, *77*(1), 85–88. <https://doi.org/10.1136/jnnp.2005.063131>

- Coneski, P. N., & Schoenfisch, M. H. (2012). Nitric oxide release: Part III. Measurement and reporting. *Chemical Society Reviews*, 41(10), 3753–3758. <https://doi.org/10.1039/c2cs15271a>
- Cos, P., De Bruyne, T., Apers, S., Vanden Berghe, D., Pieters, L., & Vlietinck, A. J. (2003). Phytoestrogens: Recent developments. *Planta Medica*, 69(7), 589–599. <https://doi.org/10.1055/s-2003-41122>
- Crain, J. M., Nikodemova, M., & Watters, J. J. (2015). Microglia express distinct M1 and M2 phenotypic markers in the postnatal and adult CNS in male and female mice. *J. Neuroscience*, 91(9), 1143–1151. <https://doi.org/10.1002/jnr.23242>.Microglia
- Cui, J., Shen, Y., & Li, R. (2013). Estrogen synthesis and signaling pathways during aging: From periphery to brain. *Trends in Molecular Medicine*. <https://doi.org/10.1016/j.molmed.2012.12.007>
- Dai, X. jing, Li, N., Yu, L., Chen, Z. yang, Hua, R., Qin, X., & Zhang, Y. M. (2015). Activation of BV2 microglia by lipopolysaccharide triggers an inflammatory reaction in PC12 cell apoptosis through a toll-like receptor 4-dependent pathway. *Cell Stress and Chaperones*, 20(2), 321–331. <https://doi.org/10.1007/s12192-014-0552-1>
- Daisuke, I., Yoshinori, I., Keiko, O., Kazuyuki, N., Yasuo, F., & Shinichi, K. (1998). Microglia-specific localisation of a novel calcium binding protein, Iba1. *Molecular Brain Research*, 57(1), 1–9.
- Dello Russo, C., Cappoli, N., Coletta, I., Mezzogori, D., Paciello, F., Pozzoli, G., ... Battaglia, A. (2018). The human microglial HMC3 cell line: where do we stand? A systematic literature review. *Journal of Neuroinflammation*, 15(1), 259. <https://doi.org/10.1186/s12974-018-1288-0>
- Dheer, D., Singh, V., & Shankar, R. (2017). Medicinal attributes of 1,2,3-triazoles: Current developments. *Bioorganic Chemistry*, 71(January), 30–54. <https://doi.org/10.1016/j.bioorg.2017.01.010>
- Di Meo, S., Reed, T. T., Venditti, P., & Victor, V. M. (2016). Role of ROS and RNS Sources in Physiological and Pathological Conditions. *Oxidative Medicine and Cellular Longevity*, 2016. <https://doi.org/10.1155/2016/1245049>
- Dinkova-Kostova, A. T., Kostov, R. V., & Kazantsev, A. G. (2018). The role of Nrf2 signaling in counteracting neurodegenerative diseases. *FEBS Journal*, 285(19), 3576–3590. <https://doi.org/10.1111/febs.14379>
- Dinkova-Kostova, A. T., & Talalay, P. (2008). Direct and indirect antioxidant properties of inducers of cytoprotective proteins. *Molecular Nutrition and Food Research*, 52(SUPPL. 1), 128–138. <https://doi.org/10.1002/mnfr.200700195>
- DiSabato, D., Quan, N., & Godbout, J. (2016). Neuroinflammation: the devil is in the details. *Journal of Neurochemistry*, 139 Suppl(Suppl 2), 136–153. <https://doi.org/10.1111/jnc.13607>



- Dizhbite, T., Telysheva, G., Jurkjane, V., & Uldis, V. (2004). Characterization of the radical scavenging activity of lignins—natural antioxidants. *Bioresource Technology*, *95*, 309–317.
- Dominy, S. S., Lynch, C., Ermini, F., Benedyk, M., Marczyk, A., Konradi, A., ... Potempa, J. (2019). Porphyromonas gingivalis in Alzheimer's disease brains: Evidence for disease causation and treatment with small-molecule inhibitors. *Science Advances*, *5*(1), 1–22. <https://doi.org/10.1126/sciadv.aau3333>
- Dong, C., Davis, R. J., & Flavell, R. a. (2002). MAP kinases in the immune response. *Annual Review of Immunology*, *20*(1), 55–72. <https://doi.org/10.1146/annurev.immunol.20.091301.131133>
- Duan, L., Chen, B. Y., Sun, X. L., Luo, Z. J., Rao, Z. R., Wang, J. J., & Chen, L. W. (2013). LPS-Induced proNGF Synthesis and Release in the N9 and BV2 Microglial Cells: A New Pathway Underling Microglial Toxicity in Neuroinflammation. *PLoS ONE*, *8*(9). <https://doi.org/10.1371/journal.pone.0073768>
- El-Bakoush, A., & Olajide, O. A. (2018a). Formononetin inhibits neuroinflammation and increases estrogen receptor beta (ER $\beta$ ) protein expression in BV2 microglia. *International Immunopharmacology*, *61*, 325–337. <https://doi.org/10.1016/j.intimp.2018.06.016>
- El-Bakoush, A., & Olajide, O. A. (2018b). Formononetin inhibits neuroinflammation and increases estrogen receptor beta (ER $\beta$ ) protein expression in BV2 microglia. *International Immunopharmacology*, *61*, 325–337. <https://doi.org/10.1016/j.intimp.2018.06.016>
- Elmore, S. (2007). Apoptosis: A Review of Programmed Cell Death. *Toxicologic Pathology*, *35*(4), 495–516. <https://doi.org/10.1080/01926230701320337>
- Engvall, E., & Perlmann, P. (1971). Enzyme-linked immunosorbent assay (ELISA) quantitative assay of immunoglobulin G. *Immunochemistry*, *8*(9), 871–874. [https://doi.org/10.1016/0019-2791\(71\)90454-X](https://doi.org/10.1016/0019-2791(71)90454-X)
- Erickson, M. A., Dohi, K., & Banks, W. A. (2012). Neuroinflammation: A common pathway in CNS diseases as mediated at the blood-brain barrier. *NeuroImmunoModulation*, *19*(2), 121–130. <https://doi.org/10.1159/000330247>
- Erta, M., Quintana, A., & Hidalgo, J. (2012). Interleukin-6, a major cytokine in the central nervous system. *International Journal of Biological Sciences*, *8*(9), 1254–1266. <https://doi.org/10.7150/ijbs.4679>
- Ertl, P., Altmann, E., & Mckenna, J. M. (2020). The Most Common Functional Groups in Bioactive Molecules and How Their Popularity Has Evolved over Time. *Journal of Medicinal Chemistry*, *63*(15), 8408–8418. <https://doi.org/10.1021/acs.jmedchem.0c00754>
- Etemad, S., Zamin, R. M., Ruitenber, M. J., & Filgueira, L. (2012). A novel in vitro human microglia model: Characterization of human monocyte-derived microglia. *Journal of*

*Neuroscience Methods*, 209(1), 79–89. <https://doi.org/10.1016/j.jneumeth.2012.05.025>

- Famitafreshi, H., & Karimian, M. (2020). Prostaglandins as the Agents That Modulate the Course of Brain Disorders. *Degenerative Neurological and Neuromuscular Disease*, 10, 1–13. <https://doi.org/10.2147/dnnd.s240800>
- Fan, L., Pandey, S. C., & Cohen, R. S. (2008). Estrogen affects levels of Bcl-2 protein and mRNA in medial amygdala of ovariectomized rats. *Journal of Neuroscience Research*, 86(16), 3655–3664. <https://doi.org/10.1002/jnr.21801>
- Fokialakis, N., Alexi, X., Aligiannis, N., Siriani, D., Meligova, A. K., Pratsinis, H., ... Alexis, M. N. (2012). Ester and carbamate ester derivatives of Biochanin A: Synthesis and in vitro evaluation of estrogenic and antiproliferative activities. *Bioorganic and Medicinal Chemistry*. <https://doi.org/10.1016/j.bmc.2012.03.012>
- Forrester, S. J., Kikuchi, D. S., Hernandez, M. S., Xu, Q., & Griendling, K. K. (2018). Reactive oxygen species in metabolic and inflammatory signaling. *Circulation Research*, 122(6), 877–902. <https://doi.org/10.1161/CIRCRESAHA.117.311401>
- Franceschi, C., Capri, M., Monti, D., Giunta, S., Olivieri, F., Sevini, F., ... Salvioli, S. (2007). Inflammaging and anti-inflammaging: A systemic perspective on aging and longevity emerged from studies in humans. *Mechanisms of Ageing and Development*, 128(1), 92–105.
- Fricker, M., Tolkovsky, A. M., Borutaite, V., Coleman, M., & Brown, G. C. (2018). Neuronal cell death. *Physiological Reviews*, 98(2), 813–880. <https://doi.org/10.1152/physrev.00011.2017>
- Froyen, E. B., & Steinberg, F. M. (2010). Soy isoflavones increase quinone reductase in hepa-1c1c7 cells via estrogen receptor beta and nuclear factor erythroid 2-related factor 2 binding to the antioxidant response element. *Journal of Nutritional Biochemistry*, 843–848.
- Fuentes, N., & Silveyra, P. (2019). Estrogen receptor signaling mechanisms. *Advances in Protein Chemistry and Structural Biology*, 116(Figure 1), 135–170. <https://doi.org/10.1016/bs.apcsb.2019.01.001>
- Funk, C. D., & FitzGerald, G. A. (2007). COX-2 inhibitors and cardiovascular risk. *Journal of Cardiovascular Pharmacology*, 50(5), 470–479. <https://doi.org/10.1097/FJC.0b013e318157f72d>
- Galien, R., & Garcia, T. (1997). Estrogen receptor impairs interleukin-6 expression by preventing protein binding on the NF-κB site. *Nucleic Acids Research*, 25(12), 2424–2429. <https://doi.org/10.1093/nar/25.12.2424>
- Galimberti, D., & Scarpini, E. (2012). Progress in Alzheimer's disease. *Journal of Neurology*, 259(2), 201–211. <https://doi.org/10.1007/s00415-011-6145-3>
- Gao, Q. G., Zhou, L. P., Lee, V. H. Y., Chan, H. Y., Man, C. W. Y., & Wong, M. S. (2019). Ginsenoside Rg1 activates ligand-independent estrogenic effects via rapid estrogen

- receptor signaling pathway. *Journal of Ginseng Research*, 43(4), 527–538. <https://doi.org/10.1016/j.jgr.2018.03.004>
- Gaschler, M. M., & Stockwell, B. R. (2017). Lipid peroxidation in cell death. *Biochemical and Biophysical Research Communications*, 482(3), 419–425. <https://doi.org/10.1016/j.bbrc.2016.10.086>
- Gautam, A. (2017). Nerve Cells. *Encyclopedia of Animal Cognition and Behavior*, 6–9. <https://doi.org/10.1007/978-3-319-47829-6>
- Ghosh, A. K., & Brindisi, M. (2015). Organic Carbamates in Drug Design and Medicinal Chemistry. *Journal of Medicinal Chemistry*, 58(7), 2895–2940. <https://doi.org/10.1021/jm501371s>
- Ginhoux, F., & Prinz, M. (2015). Origin of microglia: Current concepts and past controversies. *Cold Spring Harbor Perspectives in Biology*, 7(8), 1–15. <https://doi.org/10.1101/cshperspect.a020537>
- Gleason, C. E., Carlsson, C. M., Barnet, J. H., Meade, S. A., Setchell, K. D. R., Atwood, C. S., ... Asthana, S. (2009). A preliminary study of the safety, feasibility and cognitive efficacy of soy isoflavone supplements in older men and women. *Age and Ageing*, 38(1), 86–93. <https://doi.org/10.1093/ageing/afn227>
- Granados-Principal, S., Liu, Y., Guevara, M. L., Blanco, E., Choi, D. S., Qian, W., ... Chang, J. C. (2015). Inhibition of iNOS as a novel effective targeted therapy against triple-negative breast cancer. *Breast Cancer Research*, 17(1). <https://doi.org/10.1186/s13058-015-0527-x>
- Gray, S. C., Kinghorn, K. J., & Woodling, N. S. (2020). Shifting equilibriums in Alzheimer's disease: The complex roles of microglia in neuroinflammation, neuronal survival and neurogenesis. *Neural Regeneration Research*, 15(7), 1208–1219. <https://doi.org/10.4103/1673-5374.272571>
- Guo, Q., Rimbach, G., Moini, H., Weber, S., & Packer, L. (2002). ESR and cell culture studies on free radical-scavenging and antioxidant activities of isoflavonoids. *Toxicology*, 179(1–2), 171–180. [https://doi.org/10.1016/S0300-483X\(02\)00241-X](https://doi.org/10.1016/S0300-483X(02)00241-X)
- Guo, Z. (2017). The modification of natural products for medical use. *Acta Pharmaceutica Sinica B*, 7(2), 119–136. <https://doi.org/10.1016/j.apsb.2016.06.003>
- Guob, L., Rezvaniana, A., Kukreja, L., Hoveydaia, R., Bigio, E. H., Mesulama, M.-M., ... Geula, C. J. El. (2016). Postmortem Adult Human Microglia Proliferate in Culture to High Passage and Maintain Their Response to Amyloid- $\beta$ . *J Alzheimers Dis*, 54(3), 1157–1167. <https://doi.org/10.1097/CCM.0b013e31823da96d>. Hydrogen
- Gupta, S. C., Sundaram, C., Reuter, S., & Aggarwal, B. B. (2010). Inhibiting NF- $\kappa$ B Activation by Small Molecules As a Therapeutic Strategy. *Biochim Biophys Acta*, 1799(10–12), 775–787. <https://doi.org/10.1016/j.bbagr.2010.05.004>. Inhibiting
- Haase, G., Pettmann, B., Raoul, C., & Henderson, C. E. (2008). Signaling by death receptors

- in the nervous system. *Current Opinion in Neurobiology*, 18(3), 284–291. <https://doi.org/10.1016/j.conb.2008.07.013>
- Haegeman, G. (2003). Inhibition of signal transduction pathways involved in inflammation. *European Respiratory Journal, Supplement*, 22(44), 16–19. <https://doi.org/10.1183/09031936.03.00000503a>
- Hämäläinen, M., Nieminen, R., Vuorela, P., Heinonen, M., & Moilanen, E. (2007a). Anti-Inflammatory Effects of Flavonoids: Genistein, Kaempferol, Quercetin, and Daidzein Inhibit STAT-1 and NF- $\kappa$ B Activations, Whereas Flavone, Isorhamnetin, Naringenin, and Pelargonidin Inhibit only NF- $\kappa$ B. *Mediators of Inflammation*, 2007, 1–10. Retrieved from <http://www.hindawi.com/journals/mi/2007/045673/abs/>
- Hämäläinen, M., Nieminen, R., Vuorela, P., Heinonen, M., & Moilanen, E. (2007b). Anti-inflammatory effects of flavonoids: Genistein, kaempferol, quercetin, and daidzein inhibit STAT-1 and NF- $\kappa$ B activations, whereas flavone, isorhamnetin, naringenin, and pelargonidin inhibit only NF- $\kappa$ B activation along with their inhibitory effect on i. *Mediators of Inflammation*, 2007. <https://doi.org/10.1155/2007/45673>
- Harnish, D. C., Scicchitano, M. S., Adelman, S. J., Lyttle, C. R., & Karathanasis, S. K. (2000). The role of CBP in estrogen receptor cross-talk with nuclear factor- $\kappa$ B in HepG2 cells. *Endocrinology*, 141(9), 3403–3411. <https://doi.org/10.1210/endo.141.9.7646>
- Harrold, M. W., & Zavod, R. M. (2014). Basic Concepts in Medicinal Chemistry. *Drug Development and Industrial Pharmacy*, 40(7), 988–988. <https://doi.org/10.3109/03639045.2013.789908>
- Hata, A. N., Engelman, J., & Faber, A. (2016). Targeted Anti-Cancer Therapeutics. *Cancer Discov*, 5(5), 475–487. <https://doi.org/10.1158/2159-8290.CD-15-0011>.The
- He, F., Ru, X., & Wen, T. (2020). NRF2, a transcription factor for stress response and beyond. *International Journal of Molecular Sciences*, 21(13), 1–23. <https://doi.org/10.3390/ijms21134777>
- He, H., Yang, F., Wang, X., Zeng, X., Hu, Q., Huang, J., & Feng, J. (2011). Complete estrogen receptor blocker ICI182,780 promotes the proliferation of vascular smooth muscle cells. *Acta Biochimica et Biophysica Sinica*, 43(2), 118–123. <https://doi.org/10.1093/abbs/gmq119>
- Helms, H. C., Abbott, N. J., Burek, M., Cecchelli, R., Couraud, P. O., Deli, M. A., ... Brodin, B. (2016). In vitro models of the blood-brain barrier: An overview of commonly used brain endothelial cell culture models and guidelines for their use. *Journal of Cerebral Blood Flow and Metabolism*, 36(5), 862–890. <https://doi.org/10.1177/0271678X16630991>
- Helmut, K., Hanisch, U. K., Noda, M., & Verkhratsky, A. (2011). Physiology of microglia. *Physiological Reviews*, 91(2), 461–553. <https://doi.org/10.1152/physrev.00011.2010>
- Henn, A., Lund, S., Hedtjärn, M., Schrattenholz, A., Pörzgen, P., & Leist, M. (2009). The

- Suitability of BV2 Cells as Alternative Model System for Primary Microglia Cultures or for Animal Experiments Examining Brain Inflammation Doerenkamp-Zbinden Chair for alternative in vitro methods to replace animal experiments. *Altex*, 26(January), 83–94.
- Heo, H. J., Suh, Y. M., Kim, M. J., Choi, S. J., Mun, N. S., Kim, H. K., ... Shin, D. H. (2006). Daidzein activates choline acetyltransferase from MC-IXC cells and improves drug-induced amnesia. *Bioscience, Biotechnology and Biochemistry*, 70(1), 107–111. <https://doi.org/10.1271/bbb.70.107>
- Hewett, S. J., Jackman, N. A., Claycomb, R. J., Neuroscience, P. I., & Haven, N. (2012). Interleukin-1 $\beta$  in Central Nervous System Injury and Repair Sandra. *Eur J Neurodegener Dis*, 1(2), 195–211. <https://doi.org/10.1016/j.ygyno.2014.12.035>. Pharmacologic
- Himamura, T. S., Umikura, Y. S., Amazaki, T. Y., Ada, A. T., Ashiwagi, T. K., Shikawa, H. I., ... Keda, H. U. (2014). *Applicability of the DPPH Assay for Evaluating the Antioxidant Capacity of Food Additives – Inter-laboratory Evaluation Study*. 30(July). <https://doi.org/10.2116/analsci.30.717>
- Hjorth, E., Zhu, M., Toro, V. C., Vedin, I., Palmblad, J., Cederholm, T., ... Schultzberg, M. (2013). Omega-3 fatty acids enhance phagocytosis of alzheimer's disease-related amyloid- $\beta$ 42 by human microglia and decrease inflammatory markers. *Journal of Alzheimer's Disease*, 35(4), 697–713. <https://doi.org/10.3233/JAD-130131>
- Holness, C. L., & Simmons, D. L. (1993). Molecular cloning of CD68, a human macrophage marker related to lysosomal glycoproteins. *Blood*, 81(6), 1607–1613. <https://doi.org/10.1182/blood.v81.6.1607.bloodjournal8161607>
- Horvath, R. J., Natile-McMenemy, N., Alkaitis, M. S., & DeLeo, J. A. (2008). Differential migration, LPS-induced cytokine, chemokine, and NO expression in immortalized BV-2 and HAPI cell lines and primary microglial cultures. *Journal of Neurochemistry*, 107(2), 557–569. <https://doi.org/10.1111/j.1471-4159.2008.05633.x>
- Howard, S., Bottino, C., Brooke, S., Cheng, E., Giffard, R. G., & Sapolsky, R. (2002). Neuroprotective effects of bcl-2 overexpression in hippocampal cultures: Interactions with pathways of oxidative damage. *Journal of Neurochemistry*, 83(4), 914–923. <https://doi.org/10.1046/j.1471-4159.2002.01198.x>
- Hsieh, H. L., & Yang, C. M. (2013). Role of redox signaling in neuroinflammation and neurodegenerative diseases. *BioMed Research International*, 2013. <https://doi.org/10.1155/2013/484613>
- Huang, S. Y., Xin, H., Sun, J., Li, R., Zhang, X. M., & Zhao, D. (2013). Estrogen receptor  $\beta$  agonist diarylpropionitrile inhibits lipopolysaccharide-induced regulated on activation normal T cell expressed and secreted (RANTES) production in macrophages by repressing nuclear factor kb activation. *Fertility and Sterility*, 100(1), 234–240. <https://doi.org/10.1016/j.fertnstert.2013.02.052>
- Hurtado, O., Ballesteros, I., Cuartero, M. I., Moraga, A., Pradillo, J. M., Ramírez-Franco, J.,

- ... Moro, M. A. (2012). Daidzein has neuroprotective effects through ligand-binding-independent PPAR $\gamma$  activation. *Neurochemistry International*, 61(1), 119–127. <https://doi.org/10.1016/j.neuint.2012.04.007>
- Hussain, R., Zubair, H., Pursell, S., & Shahab, M. (2018). Neurodegenerative diseases: Regenerative mechanisms and novel therapeutic approaches. *Brain Sciences*, 8(9). <https://doi.org/10.3390/brainsci8090177>
- Imai, Y., Ibata, I., Ito, D., Ohsawa, K., & Kohsaka, S. (1996). A novel gene *iba1* in the major histocompatibility complex class III region encoding an EF hand protein expressed in a monocytic lineage. *Biochemical and Biophysical Research Communications*, 224(3), 855–862. <https://doi.org/10.1006/bbrc.1996.1112>
- Ishihara, Y., Itoh, K., Ishida, A., & Yamazaki, T. (2015). Selective estrogen-receptor modulators suppress microglial activation and neuronal cell death via an estrogen receptor-dependent pathway. *Journal of Steroid Biochemistry and Molecular Biology*, 145, 85–93. <https://doi.org/10.1016/j.jsbmb.2014.10.002>
- Jack, C. S., Arbour, N., Manusow, J., Montgrain, V., Blain, M., McCrea, E., ... Antel, J. P. (2005). TLR Signaling Tailors Innate Immune Responses in Human Microglia and Astrocytes. *The Journal of Immunology*, 175(7), 4320–4330. <https://doi.org/10.4049/jimmunol.175.7.4320>
- Janabi, Nazila, Peudenier, S. (1995). Establishment of human microglial cell lines after transfection of primary cultures of embryonic microglial cells with the SV40 large T antigen. *Neuroscience Letters*, Vol. 195, pp. 105–108.
- Janabi, N. (2002). Selective Inhibition of Cyclooxygenase-2 Expression by 15-Deoxy-12,14,12,14-prostaglandin J2 in Activated Human Astrocytes, But Not in Human Brain Macrophages. *The Journal of Immunology*, 168(9), 4747–4755. <https://doi.org/10.4049/jimmunol.168.9.4747>
- Jantaratnotai, N., Utaisincharoen, P., Sanvarinda, P., Thampithak, A., & Sanvarinda, Y. (2013). Phytoestrogens mediated anti-inflammatory effect through suppression of IRF-1 and pSTAT1 expressions in lipopolysaccharide-activated microglia. *International Immunopharmacology*, 17(2), 483–488. <https://doi.org/10.1016/j.intimp.2013.07.013>
- Jin, S. E., Son, Y. K., Min, B. S., Jung, H. A., & Choi, J. S. (2012). Anti-inflammatory and antioxidant activities of constituents isolated from *Pueraria lobata* roots. *Archives of Pharmacal Research*, 35(5), 823–837. <https://doi.org/10.1007/s12272-012-0508-x>
- Johansson, J. U., Woodling, N. S., Shi, J., Andreasson, K. I., North, T., & Francisco, S. S. (2015). *Inflammatory Cyclooxygenase Activity and PGE 2 Signaling in Models of Alzheimer 's Disease*. 125–131.
- Jones, S. V., & Kounatidis, I. (2017). Nuclear factor-kappa B and Alzheimer disease, unifying genetic and environmental risk factors from cell to humans. *Frontiers in Immunology*, 8(DEC). <https://doi.org/10.3389/fimmu.2017.01805>
- Joshua-Tor, L. (2004). siRNAs at RISC. *Structure*, 12(7), 1120–1122.

<https://doi.org/10.1016/j.str.2004.06.008>

- Kajta, M., Rzemieniec, J., Litwa, E., Lason, W., Lenartowicz, M., Krzeptowski, W., & Wojtowicz, A. (2013a). The key involvement of estrogen receptor  $\beta$  and G-protein-coupled receptor 30 in the neuroprotective action of daidzein. *Neuroscience*, 238, 345–360.
- Kajta, M., Rzemieniec, J., Litwa, E., Lason, W., Lenartowicz, M., Krzeptowski, W., & Wojtowicz, A. K. (2013b). The key involvement of estrogen receptor  $\beta$  and G-protein-coupled receptor 30 in the neuroprotective action of daidzein. *Neuroscience*, 238, 345–360. <https://doi.org/10.1016/j.neuroscience.2013.02.005>
- Kalaitzidis, D., & Gilmore, T. D. (2005). Transcription factor cross-talk: The estrogen receptor and NF- $\kappa$ B. *Trends in Endocrinology and Metabolism*, 16(2), 46–52. <https://doi.org/10.1016/j.tem.2005.01.004>
- Kamer, A. R., Pirraglia, E., Tsui, W., Rusinek, H., Vallabhajosula, S., Mosconi, L., ... de Leon, M. J. (2015). Periodontal disease associates with higher brain amyloid load in normal elderly. *Neurobiology of Aging*, 36(2), 627–633. <https://doi.org/10.1016/j.neurobiolaging.2014.10.038>
- Kaminska, B. (2005). MAPK signalling pathways as molecular targets for anti-inflammatory therapy - From molecular mechanisms to therapeutic benefits. *Biochimica et Biophysica Acta - Proteins and Proteomics*, 1754(1–2), 253–262. <https://doi.org/10.1016/j.bbapap.2005.08.017>
- Kaminska, B., Gozdz, A., Zawadzka, M., Ellert-Miklaszewska, A., & Lipko, M. (2009). MAPK signal transduction underlying brain inflammation and gliosis as therapeutic target. *Anatomical Record*, 292(12), 1902–1913. <https://doi.org/10.1002/ar.21047>
- Kampkötter, A., Chovolou, Y., Kulawik, A., Röhrdanz, E., Weber, N., Proksch, P., & Wätjen, W. (2008). Isoflavone daidzein possesses no antioxidant activities in cell-free assays but induces the antioxidant enzyme catalase. *Nutrition Research*, 28(9), 620–628. <https://doi.org/10.1016/j.nutres.2008.06.002>
- Kanazawa, I. (2001). How do neurons die in neurodegenerative diseases? *Trends in Molecular Medicine*, 7(8), 339–344. [https://doi.org/10.1016/S1471-4914\(01\)02017-2](https://doi.org/10.1016/S1471-4914(01)02017-2)
- Kedare, S. B., & Singh, R. P. (2011). Genesis and development of DPPH method of antioxidant assay. *Journal of Food Science and Technology*, 48(4), 412–422. <https://doi.org/10.1007/s13197-011-0251-1>
- Kerr, J. F. R., Wyllie, A. H., & Currie, A. R. (1972). Apoptosis: A Basic Biological Phenomenon with Wideranging Implications in Tissue Kinetics. *British Journal of Cancer*, 26, 239–257. <https://doi.org/10.1111/j.1365-2796.2005.01570.x>
- Kharb, R., Sharma, P. C., & Yar, M. S. (2011). Pharmacological significance of triazole scaffold. *Journal of Enzyme Inhibition and Medicinal Chemistry*, 26(1), 1–21. <https://doi.org/10.3109/14756360903524304>

- Kim, E. K., & Choi, E. J. (2010). Pathological roles of MAPK signaling pathways in human diseases. *Biochimica et Biophysica Acta - Molecular Basis of Disease*, 1802(4), 396–405. <https://doi.org/10.1016/j.bbadis.2009.12.009>
- Kim, J. W., Jin, Y. C., Kim, Y. M., Rhie, S., Kim, H. J., Seo, H. G., ... Chang, K. C. (2009). Daidzein administration in vivo reduces myocardial injury in a rat ischemia/reperfusion model by inhibiting NF- $\kappa$ B activation. *Life Sciences*, 84(7–8), 227–234. <https://doi.org/10.1016/j.lfs.2008.12.005>
- Kim, S.-W., Lee, H.-K., Shin, J.-H., & Lee, J.-K. (2013). Up-down Regulation of HO-1 and iNOS Gene Expressions by Ethyl Pyruvate via Recruiting p300 to Nrf2 and Depriving It from p65. *Free Radical Biology and Medicine*, 65, 468–476.
- Kładna, A., Berczyński, P., Kruk, I., Piechowska, T., & Aboul-Enein, H. Y. (2016). Studies on the antioxidant properties of some phytoestrogens. *Luminescence*, (December 2015), 1201–1206. <https://doi.org/10.1002/bio.3091>
- Koehler, D., Shah, Z. A., Hensley, K., & Williams, F. E. (2018). Lanthionine ketimine-5-ethyl ester provides neuroprotection in a zebrafish model of okadaic acid-induced Alzheimer's disease. *Neurochemistry International*, 115, 61–68. <https://doi.org/10.1016/j.neuint.2018.02.002>
- Kovalevich, J., & Langford, D. (2013). Considerations for the Use of SH-SY5Y Neuroblastoma Cells in Neurobiology. *Methods Mol Biol*, 9–21. [https://doi.org/10.1007/978-1-62703-640-5\\_2](https://doi.org/10.1007/978-1-62703-640-5_2)
- Krzyzowska, M., Swiatek, W., Fijalkowska, B., Niemialtowski, M., & Schollenberger, A. (2010). The Role of Map Kinases in Immune Response. *Advances in Cell Biology*, 2(3), 125–138. <https://doi.org/10.2478/v10052-010-0007-5>
- Kuiper, G. G. J. M., Lemmen, J. G., Carlsson, B., Corton, J. C., Safe, S. H., Van Der Saag, P. T., ... Gustafsson, J. Å. (1998). Interaction of estrogenic chemicals and phytoestrogens with estrogen receptor  $\beta$ . *Endocrinology*, 139(10), 4252–4263. <https://doi.org/10.1210/endo.139.10.6216>
- Kyriakidis, I., & Papaioannidou, P. (2016). Estrogen receptor beta and ovarian cancer: a key to pathogenesis and response to therapy. *Archives of Gynecology and Obstetrics*, 293(6), 1161–1168. <https://doi.org/10.1007/s00404-016-4027-8>
- Łabuzek, K., Skrudlik, E., Gabryel, B., & Okopień, B. (2015). Anti-inflammatory microglial cell function in the light of the latest scientific research. *Annales Academiae Medicae Silesiensis*, 69, 99–110. <https://doi.org/10.18794/aams/32608>
- Lan, Y. L., Zou, S., Wang, X., Lou, J. C., Xing, J. S., Yu, M., & Zhang, B. (2017). Update on the therapeutic significance of estrogen receptor beta in malignant gliomas. *Oncotarget*, 8(46), 81686–81696. <https://doi.org/10.18632/oncotarget.20970>
- Landmann, R., Knopf, H. P., Link, S., Sansano, S., Schumann, R., & Zimmerli, W. (1996). Human monocyte CD14 is upregulated by lipopolysaccharide. *Infection and Immunity*, 64(5), 1762–1769.



- Lawrence, T. (2009). The nuclear factor NF-kappaB pathway in inflammation. *Cold Spring Harbor Perspectives in Biology*, 1(6), 1–10. <https://doi.org/10.1101/cshperspect.a001651>
- Lee, J. K., & Kim, N. J. (2017). Recent advances in the inhibition of p38 MAPK as a potential strategy for the treatment of Alzheimer's disease. *Molecules*, 22(8). <https://doi.org/10.3390/molecules22081287>
- Lepenietier, G., Hracsko, Z., Unger, M., Van Griensven, M., Grummel, V., Krumbholz, M., ... Kowarik, M. C. (2019). Cytokine and immune cell profiling in the cerebrospinal fluid of patients with neuro-inflammatory diseases. *Journal of Neuroinflammation*, 16(1), 1–11. <https://doi.org/10.1186/s12974-019-1601-6>
- Li, B., Bedard, K., Sorce, S., Hinz, B., Dubois-Dauphin, M., & Krause, K. H. (2009). NOX4 expression in human microglia leads to constitutive generation of reactive oxygen species and to constitutive il-6 expression. *Journal of Innate Immunity*, 1(6), 570–581. <https://doi.org/10.1159/000235563>
- Li, J., & Yuan, J. (2008). Caspases in apoptosis and beyond. *Oncogene*, 27(48), 6194–6206. <https://doi.org/10.1038/onc.2008.297>
- Liang, F., Cao, W., Huang, Y., Fang, Y., Cheng, Y., Pan, S., & Xu, X. (2019). Isoflavone biochanin A, a novel nuclear factor erythroid 2-related factor 2 (Nrf2)-antioxidant response element activator, protects against oxidative damage in HepG2 cells. *BioFactors*, 45(4), 563–574. <https://doi.org/10.1002/biof.1514>
- Liang, J., Tian, Y. X., Fu, L. M., Wang, T. H., Li, H. J., Wang, P., ... Skibsted, L. H. (2008). Daidzein as an antioxidant of lipid: Effects of the microenvironment in relation to chemical structure. *Journal of Agricultural and Food Chemistry*, 56(21), 10376–10383. <https://doi.org/10.1021/jf801907m>
- Liu, F., Su, Y., Li, B., & Ni, B. (2003). Regulation of amyloid precursor protein expression and secretion via activation of ERK1/2 by hepatocyte growth factor in HEK293 cells transfected with APP751. *Experimental Cell Research*, 287(2), 387–396. [https://doi.org/10.1016/S0014-4827\(03\)00152-6](https://doi.org/10.1016/S0014-4827(03)00152-6)
- Liu, M. H., Lin, Y. S., Sheu, S. Y., & Sun, J. S. (2009). Anti-inflammatory effects of daidzein on primary astroglial cell culture. *Nutritional Neuroscience*, 12(3), 123–134. <https://doi.org/10.1179/147683009X423274>
- Liu, T., Zhang, L., Joo, D., & Sun, S.-C. (2017). NF-κB signaling in inflammation. *Signal Transduction and Targeted Therapy*, 2(April), 17023. <https://doi.org/10.1038/sigtrans.2017.23>
- Liu, Y., Ma, H., & Yao, J. (2020). ERα, a key target for cancer therapy: A review. *OncoTargets and Therapy*, 13, 2183–2191. <https://doi.org/10.2147/OTT.S236532>
- Loera-Valencia, R., Cedazo-Minguez, A., Kenigsberg, P. A., Page, G., Duarte, A. I., Giusti, P., ... Winblad, B. (2019). Current and emerging avenues for Alzheimer's disease drug targets. *Journal of Internal Medicine*, 286(4), 398–437.

<https://doi.org/10.1111/joim.12959>

- Lopez-Castejon, G., & Brough, D. (2011). Understanding the mechanism of IL-1 $\beta$  secretion. *Cytokine and Growth Factor Reviews*, 22(4), 189–195. <https://doi.org/10.1016/j.cytogfr.2011.10.001>
- Lue, L.-F., Beach, T. G., & Walker, D. G. (2019). Alzheimer's disease research using human microglia. *Cells*, 8(8), 1–19. <https://doi.org/10.3390/cells8080838> LK - <http://sfx.library.uu.nl/utrecht?sid=EMBASE&issn=20734409&id=doi:10.3390%2Fcells8080838&atitle=Alzheimer%E2%80%99s+disease+research+using+human+microglia&stitle=Cells&title=Cells&volume=8&issue=8&spage=&epage=&aualast=Lue&aufirst=Lih-Fen&auint=L.-F.&aufull=Lue+L.-F.&coden=&isbn=&pages=-&date=2019&aunit1=L&aunitm=-F>
- Lund, S., Christensen, K. V., Hedtj rn, M., Mortensen, A. L., Hagberg, H., Falsig, J., ... Leist, M. (2006). The dynamics of the LPS triggered inflammatory response of murine microglia under different culture and in vivo conditions. *Journal of Neuroimmunology*, 180(1–2), 71–87. <https://doi.org/10.1016/j.jneuroim.2006.07.007>
- Ma, M. W., Wang, J., Zhang, Q., Wang, R., Dhandapani, K. M., Vadlamudi, R. K., & Brann, D. W. (2017). NADPH oxidase in brain injury and neurodegenerative disorders. *Molecular Neurodegeneration*, 12(1), 1–28. <https://doi.org/10.1186/s13024-017-0150-7>
- Ma, T. C., Campana, A., Lange, P. S., Lee, H. H., Banerjee, K., Barney Bryson, J., ... Ratan, R. R. (2010). A large-scale chemical screen for regulators of the arginase 1 promoter identifies the soy isoflavone daidzein as a clinically approved small molecule that can promote neuronal protection or regeneration via a cAMP-independent pathway. *Journal of Neuroscience*, 30(2), 739–748. <https://doi.org/10.1523/JNEUROSCI.5266-09.2010>
- Mahesha, H. G., Singh, S. A., & Rao, A. G. A. (2007). Inhibition of lipoxygenase by soy isoflavones: Evidence of isoflavones as redox inhibitors. *Archives of Biochemistry and Biophysics*, 461(2), 176–185. <https://doi.org/10.1016/j.abb.2007.02.013>
- Mahmood, T., & Yang, P. C. (2012). Western blot: Technique, theory, and trouble shooting. *North American Journal of Medical Sciences*, 4(9), 429–434. <https://doi.org/10.4103/1947-2714.100998>
- Malgorzata, K., Weronika, S., Beata, F., Marek, N., & Ada, S. (2009). Rola kinaz MAP w odpowiedzi immunologicznej. *Postepy Biologii Komorki*, 36(2), 295–308.
- Malkiewicz, M. A., Szarmach, A., Sabisz, A., Cubała, W. J., Szurowska, E., & Winklewski, P. J. (2019). Blood-brain barrier permeability and physical exercise. *Journal of Neuroinflammation*, 16(1), 1–16. <https://doi.org/10.1186/s12974-019-1403-x>
- Mao, Z., Zheng, Y. L., Zhang, Y. Q., Han, B. P., Zhu, X. W., Chang, Q., & Hu, X. Bin. (2007). The anti-apoptosis effects of daidzein in the brain of D-galactose treated mice. *Molecules*, 12(7), 1455–1470. <https://doi.org/10.3390/12071455>
- McQuade, A., & Blurton-Jones, M. (2019). Microglia in Alzheimer's Disease: Exploring

- How Genetics and Phenotype Influence Risk. *Journal of Molecular Biology*, 431(9), 1805–1817. <https://doi.org/10.1016/j.jmb.2019.01.045>
- Mestas, J., & Hughes, C. C. W. (2004). Of mice and not men: differences between mouse and human immunology. *Journal of Immunology (Baltimore, Md. : 1950)*, 172(5), 2731–2738. <https://doi.org/10.4049/jimmunol.172.5.2731>
- Minghetti, L. (2004). Cyclooxygenase-2 ( COX-2 ) in Inflammatory and Degenerative Brain Diseases. *Journal of Neuropathology and Experimental Neurology*, 63(9), 901–910.
- Moon, Y. J., Sagawa, K., Frederick, K., Zhang, S., & Morris, M. E. (2006). Pharmacokinetics and Bioavailability of the Isoflavone Biochanin A in Rats. *The AAPS Journal*, 8(3). Retrieved from <http://www.aapsj.org>
- Mrak, R. E., & Griffin, W. S. T. (2005). Glia and their cytokines in progression of neurodegeneration. *Neurobiology of Aging*, 26(3), 349–354. <https://doi.org/10.1016/j.neurobiolaging.2004.05.010>
- Mubarak, M. (2019). Tumor Necrosis Factor Alpha: A Major Cytokine of Brain Neuroinflammation. In *Cytokines* (pp. 1–9). <https://doi.org/http://dx.doi.org/10.5772/57353>
- Munoz, L., & Ammit, A. J. (2010). Targeting p38 MAPK pathway for the treatment of Alzheimer's disease. *Neuropharmacology*, 58(3), 561–568. <https://doi.org/10.1016/j.neuropharm.2009.11.010>
- Munro, I. C., Harwood, M., Hlywka, J. J., Stephen, A. M., Doull, J., Flamm, W. G., & Adlercreutz, H. (2003). Soy isoflavones: A safety review. *Nutrition Reviews*, 61(1), 1–33. <https://doi.org/10.1301/nr.2003.janr.1-33>
- Murphy, A. J., Guyre, P. M., Wira, C. R., & Pioli, P. A. (2009). *Estradiol Regulates Expression of Estrogen Receptor ER  $\alpha$  46 in Human Macrophages*. 4(5). <https://doi.org/10.1371/journal.pone.0005539>
- Nimse, S. B., & Pal, D. (2015). Free radicals, natural antioxidants, and their reaction mechanisms. *RSC Advances*, 5(35), 27986–28006. <https://doi.org/10.1039/c4ra13315c>
- Noble, J. M., Borrell, L. N., Papapanou, P. N., Elkind, M. S. V., Scarmeas, N., & Wright, C. B. (2009). Periodontitis is associated with cognitive impairment among older adults: Analysis of NHANES-III. *Journal of Neurology, Neurosurgery and Psychiatry*, 80(11), 1206–1211. <https://doi.org/10.1136/jnnp.2009.174029>
- Nonnenmacher, C., Dalpke, A., Zimmermann, S., Flores-de-Jacoby, L., Mutters, R., & Heeg, K. (2003). DNA from periodontopathogenic bacteria is immunostimulatory for mouse and human immune cells. *Infection and Immunity*, 71(2), 850–856. <https://doi.org/10.1128/IAI.71.2.850-856.2003>
- Nynca, A., Swigonska, S., Piasecka, J., Kolomycka, A., Kaminska, B., Radziewicz-Pigiel, M., ... Ciereszko, R. E. (2013). Biochanin A affects steroidogenesis and estrogen receptor- $\beta$  expression in porcine granulosa cells. *Theriogenology*, 80(7), 821–828.

<https://doi.org/10.1016/j.theriogenology.2013.07.009>

- Office for National Statistics. (2020). *Leading causes of death, UK: 2001 to 2018*. 1–8. Retrieved from <https://www.ons.gov.uk/peoplepopulationandcommunity/healthandsocialcare/causesofdeath/datasets/leadingcausesofdeathuk>
- Ohsawa, K., Imai, Y., Sasaki, Y., & Kohsaka, S. (2004). Microglia/macrophage-specific protein Ibal binds to fimbrin and enhances its actin-bundling activity. *Journal of Neurochemistry*, 88(4), 844–856. <https://doi.org/10.1046/j.1471-4159.2003.02213.x>
- Olmos, G., & Lladó, J. (2014). Tumor necrosis factor alpha: A link between neuroinflammation and excitotoxicity. *Mediators of Inflammation*, 2014(May). <https://doi.org/10.1155/2014/861231>
- Overk, C. R., Yao, P., Chadwick, L. R., Nikolic, D., Sun, Y., Cuendet, M. A., ... Bolton, J. L. (2005). Comparison of the in vitro estrogenic activities of compounds from hops (*Humulus lupulus*) and red clover (*Trifolium pratense*). *Journal of Agricultural and Food Chemistry*, 53(16), 6246–6253. <https://doi.org/10.1021/jf050448p>
- Pacher, P., Beckman, J. S., & Liaudet, L. (2007). Nitric Oxide and Peroxynitrite in Health and Disease. *Physiological Reviews*, 87(1), 315–424. <https://doi.org/10.1152/physrev.00029.2006>
- Pallauf, K., Duckstein, N., Hasler, M., Klotz, L. O., & Rimbach, G. (2017). Flavonoids as Putative Inducers of the Transcription Factors Nrf2, FoxO, and PPAR  $\gamma$ . *Oxidative Medicine and Cellular Longevity*, 2017, 14–16. <https://doi.org/10.1155/2017/4397340>
- Pan, H., Wang, H., Wang, X., Zhu, L., & Mao, L. (2012). The absence of Nrf2 enhances NF- $\kappa$ B-dependent inflammation following scratch injury in mouse primary cultured astrocytes. *Mediators of Inflammation*, 2012. <https://doi.org/10.1155/2012/217580>
- Pan, M., Han, H., Zhong, C., & Geng, Q. (2012). Effects of genistein and daidzein on hippocampus neuronal cell proliferation and bdnf expression in h19-7 neural cell line. *Journal of Nutrition, Health and Aging*, 16(4), 389–394. <https://doi.org/10.1007/s12603-011-0140-3>
- Panche, A. N., Diwan, A. D., & Chandra, S. R. (2016). Flavonoids: An overview. *Journal of Nutritional Science*, 5. <https://doi.org/10.1017/jns.2016.41>
- Park, J., Pillinger, M., & Abramson, S. (2006). Prostaglandin E2 synthesis and secretion: The role of PGE2 synthases. *Clinical Immunology*, 119(3), 229–240.
- Paterni, Iliaria. Granchi, C., Katzenellenbogen, J., & Minutolo, F. (2011). *Estrogen Receptors Alpha and Beta Subtype-Selective Ligands and Clinical Potential*. 18(11), 1492–1501. <https://doi.org/10.1016/j.str.2010.08.012>.Structure
- Peixoto, C., Nunes, A., & Rapôso, C. (2017). The Role of NO/cGMP Signaling on Neuroinflammation: A New Therapeutic Opportunity. *Mechanisms of Neuroinflammation*.

- Pelzer, T., Neumann, M., De Jager, T., Jazbutyte, V., & Neyses, L. (2001). Estrogen effects in the myocardium: Inhibition of NF- $\kappa$ B DNA binding by estrogen receptor- $\alpha$  and - $\beta$ . *Biochemical and Biophysical Research Communications*, 286(5), 1153–1157. <https://doi.org/10.1006/bbrc.2001.5519>
- Peng, Y., Shi, Y., Zhang, H., Mine, Y., & Tsao, R. (2017). Anti-inflammatory and anti-oxidative activities of daidzein and its sulfonic acid ester derivatives. *Journal of Functional Foods*, 35, 635–640. <https://doi.org/10.1016/j.jff.2017.06.027>
- Perry, V. H., & Teeling, J. (2013). Microglia and macrophages of the central nervous system: The contribution of microglia priming and systemic inflammation to chronic neurodegeneration. *Seminars in Immunopathology*, 35(5), 601–612. <https://doi.org/10.1007/s00281-013-0382-8>
- Poschner, S., Maier-Salamon, A., Zehl, M., Wackerlig, J., Dobusch, D., Pachmann, B., ... Jäger, W. (2017). The Impacts of Genistein and Daidzein on Estrogen Conjugations in Human Breast Cancer Cells: A targeted metabolomics approach. *Frontiers in Pharmacology*, 8(OCT), 1–11. <https://doi.org/10.3389/fphar.2017.00699>
- Prince M, Wimo A, Guerchet M, A. D. I. (2015). World Alzheimer Report 2015: The Global Impact of Dementia | Alzheimer's Disease International. *World Alzheimer Report 2015*, 1–87. Retrieved from <https://www.alz.co.uk/research/worldalzheimerreport2015summary.pdf>
- Probert, L. (2015). TNF and its receptors in the CNS: The essential, the desirable and the deleterious effects. *Neuroscience*, 302, 2–22. <https://doi.org/10.1016/j.neuroscience.2015.06.038>
- Promega. (n.d.). *Caspase-Glo*® 3/7 Assay.
- Raheja, S., Girdhar, A., Lather, V., & Pandita, D. (2018). Biochanin A: A phytoestrogen with therapeutic potential. *Trends in Food Science and Technology*, 79(June), 55–66. <https://doi.org/10.1016/j.tifs.2018.07.001>
- Rahman, S., & Islam, R. (2011). Mammalian Sirt1: Insights on its biological functions. *Cell Communication and Signaling*, 9, 1–8. <https://doi.org/10.1186/1478-811X-9-11>
- Rajalakshmy, A. R., Malathi, J., & Madhavan, H. N. (2015). Hepatitis C virus NS3 mediated microglial inflammation via TLR2/TLR6 MyD88/NF- $\kappa$ B pathway and toll like receptor ligand treatment furnished immune tolerance. *PLoS ONE*, 10(5), 1–18. <https://doi.org/10.1371/journal.pone.0125419>
- Redza-Dutordoir, M., & Averill-Bates, D. A. (2016). Activation of apoptosis signalling pathways by reactive oxygen species. *Biochimica et Biophysica Acta - Molecular Cell Research*, 1863(12), 2977–2992. <https://doi.org/10.1016/j.bbamcr.2016.09.012>
- Ricciotti, Emanuela and FitzGerald, G. A. (2012). NIH Public Access. *NIH Public Access*, 31(5), 986–1000. <https://doi.org/10.1161/ATVBAHA.110.207449.Prostaglandins>
- Rimbach, G., De Pascual-Teresa, S., Ewins, B. A., Matsugo, S., Uchida, Y., Minihane, A.

- M., ... Weinberg, P. D. (2003). Antioxidant and free radical scavenging activity of isoflavone metabolites. *Xenobiotica*, 33(9), 913–925. <https://doi.org/10.1080/0049825031000150444>
- Rivera, P., Pérez-Martín, M., Pavón, F. J., Serrano, A., Crespillo, A., Cifuentes, M., ... Suárez, J. (2013). Pharmacological Administration of the Isoflavone Daidzein Enhances Cell Proliferation and Reduces High Fat Diet-Induced Apoptosis and Gliosis in the Rat Hippocampus. *PLoS ONE*, 8(5). <https://doi.org/10.1371/journal.pone.0064750>
- Rogers, J., Cooper, N. R., Webster, S., Schultz, J., McGeer, P. L., Styren, S. D., ... Lieberburg, I. (1992). Complement activation by  $\beta$ -amyloid in Alzheimer disease. *Proceedings of the National Academy of Sciences of the United States of America*, 89(21), 10016–10020. <https://doi.org/10.1073/pnas.89.21.10016>
- Romera-Castillo, C., & Jafféab, R. (2015). Free radical scavenging (antioxidant activity) of natural dissolved organic matter. *Marine Chemistry*, 177(4), 668–676.
- Ronkina, N., Menon, M. B., Schwermann, J., Tiedje, C., Hitti, E., Kotlyarov, A., & Gaestel, M. (2010). MAPKAP kinases MK2 and MK3 in inflammation: Complex regulation of TNF biosynthesis via expression and phosphorylation of tristetraprolin. *Biochemical Pharmacology*, 80(12), 1915–1920. <https://doi.org/10.1016/j.bcp.2010.06.021>
- Rothaug, M., Becker-Pauly, C., & Rose-John, S. (2016). The role of interleukin-6 signaling in nervous tissue. *Biochimica et Biophysica Acta - Molecular Cell Research*, 1863(6), 1218–1227. <https://doi.org/10.1016/j.bbamcr.2016.03.018>
- Rubio-Perez, J. M., & Morillas-Ruiz, J. M. (2012). A Review: Inflammatory Process in Alzheimer's Disease, Role of Cytokines. *The Scientific World Journal*, 2012, 1–15. <https://doi.org/10.1100/2012/756357>
- Saeed, U., Durgadoss, L., Valli, R. K., Joshi, D. C., Joshi, P. G., & Ravindranath, V. (2008). Knockdown of cytosolic glutaredoxin 1 leads to loss of mitochondrial membrane potential: Implication in neurodegenerative diseases. *PLoS ONE*, 3(6). <https://doi.org/10.1371/journal.pone.0002459>
- Samali, A., Nordgren, H., Zhivotovsky, B., Peterson, E., & Orrenius, S. (1999). A comparative study of apoptosis and necrosis in HepG2 cells: Oxidant-induced caspase inactivation leads to necrosis. *Biochemical and Biophysical Research Communications*, 255(1), 6–11. <https://doi.org/10.1006/bbrc.1998.0139>
- Sarniak, A., Lipińska, J., Tytman, K., & Lipińska, S. (2016). Endogenne mechanizmy powstawania reaktywnych form tlenu (ROS). *Postepy Higieny i Medycyny Doswiadczalnej*, 70(503), 1150–1165. <https://doi.org/10.5604/17322693.1224259>
- Sasaki, Y., Ohsawa, K., Kanazawa, H., Kohsaka, S., & Imai, Y. (2001). Iba1 is an actin-cross-linking protein in macrophages/microglia. *Biochemical and Biophysical Research Communications*, 286(2), 292–297. <https://doi.org/10.1006/bbrc.2001.5388>
- Scheller, J., Chalaris, A., Schmidt-Arras, D., & Rose-John, S. (2011). The pro- and anti-inflammatory properties of the cytokine interleukin-6. *Biochimica et Biophysica Acta -*

- Schutte, B., Nuydens, R., Geerts, H., & Ramaekers, F. (1998). Annexin V binding assay as a tool to measure apoptosis in differentiated neuronal cells. *Journal of Neuroscience Methods*, 86(1), 63–69. [https://doi.org/10.1016/S0165-0270\(98\)00147-2](https://doi.org/10.1016/S0165-0270(98)00147-2)
- Schwartz, N., Verma, A., Bivens, C. B., Schwartz, Z., & Boyan, B. D. (2016). Rapid steroid hormone actions via membrane receptors. *Biochimica et Biophysica Acta - Molecular Cell Research*, 1863(9), 2289–2298. <https://doi.org/10.1016/j.bbamcr.2016.06.004>
- Scudiero, D. a, Shoemaker, R. H., Paull, K. D., Scudiere, D. a, Paul, K. D., Monks, A., ... Boyd, M. R. (1988). *Evaluation of a Soluble Tetrazolium / Formazan Assay for Cell Growth and Drug Sensitivity in Culture Using Human and Other Tumor Cell Lines Evaluation of a Soluble Tetrazolium / Formazan Assay for Cell Growth and Drug Sensitivity in Culture Using Human an.* 4827–4833.
- Sébire, G., Emilie, D., Wallon, C., Héry, C., Devergne, O., Delfraissy, J., ... Tardieu, M. (1993). In vitro production of IL-6, IL-1 beta, and tumor necrosis factor-alpha by human embryonic microglial and neural cells. *The Journal of Immunology*, 150(4), 1517–1523.
- Sedger, L. M., & McDermott, M. F. (2014). TNF and TNF-receptors: From mediators of cell death and inflammation to therapeutic giants - past, present and future. *Cytokine and Growth Factor Reviews*, 25(4), 453–472. <https://doi.org/10.1016/j.cytogfr.2014.07.016>
- Shaftel, S. S., Griffin, W. S. T., & Kerry, K. M. (2008). The role of interleukin-1 in neuroinflammation and Alzheimer disease: An evolving perspective. *Journal of Neuroinflammation*, 5, 1–12. <https://doi.org/10.1186/1742-2094-5-7>
- Shao, J., Liu, T., Xie, Q. R., Zhang, T., Yu, H., Wang, B., ... Xia, W. (2013). Adjudin attenuates lipopolysaccharide (LPS)- and ischemia-induced microglial activation. *Journal of Neuroimmunology*, 254(1–2), 83–90. <https://doi.org/10.1016/j.jneuroim.2012.09.012>
- Sharma, O. P., & Bhat, T. K. (2009). DPPH antioxidant assay revisited. *Food Chemistry*, 113(4), 1202–1205. <https://doi.org/10.1016/j.foodchem.2008.08.008>
- Sherif, H. S., & Gebreyohannes, B. T. (2018). Synthesis, Characterization, and Antioxidant Activities of Genistein, Biochanin A, and Their Analogues. *Journal of Chemistry*, 2018, 2–8. <https://doi.org/10.1155/2018/4032105>
- Shih, R.-H., Wang, C.-Y., & Yang, C.-M. (2015). NF-kappaB Signaling Pathways in Neurological Inflammation: A Mini Review. *Frontiers in Molecular Neuroscience*, 8(December), 1–8. <https://doi.org/10.3389/fnmol.2015.00077>
- Shipley, M. M., Mangold, C. A., & Szpara, M. L. (2016). Differentiation of the SH-SY5Y Human Neuroblastoma Cell Line. *J. Vis. Exp*, (108), 53193. <https://doi.org/10.3791/53193>
- Sidorova, Y., Beshpalov, M., Raitio, M., Lampinen, J., & Scientific, T. F. (2009). *Using a*

*Thermo Scientific Microplate Photometer to Choose an Optimum Reagent for Cytotoxicity Assays.* Retrieved from <https://assets.thermofisher.com/TFS-Assets/LCD/Application-Notes/D10327~.pdf>

- Sierra, A., Gottfried-Blackmore, A. C., McEwen, B. S., & Bulloch, K. (2007). Microglia Derived from Aging Mice Exhibit an Altered Inflammatory Profil. *Glia*, *55*, 412–424. <https://doi.org/10.1002/glia>
- Sierra, Amanda, Gottfried-Blackmore, A., Milner, T. A., McEwen, B. S., & Bulloch, K. (2008). Steroid hormone receptor expression and function in microglia. *Glia*, *56*(6), 659–674. <https://doi.org/10.1002/glia.20644>
- Singer, C. A., Pang, P. A., Dobie, D. J., & Dorsa, D. M. (1996). Estrogen increases GAP-43 (neuromodulin) mRNA in the preoptic area of aged rats. *Neurobiology of Aging*, *17*(4), 661–663. [https://doi.org/10.1016/0197-4580\(96\)00063-2](https://doi.org/10.1016/0197-4580(96)00063-2)
- Singh, A., Venkannagari, S., Oh, K. H., Zhang, Y.-Q., Rohde, J. M., Liu, L., ... Xu, X. (2016). Small molecule inhibitor of NRF2 selectively intervenes therapeutic resistance in KEAP1-deficient NSCLC tumors *Anju*. *11*(11), 3214–3225. <https://doi.org/10.1021/acscchembio.6b00651.Small>
- Singh, A., Venkannagari, S., Oh, K. H., Zhang, Y. Q., Rohde, J. M., Liu, L., ... Biswal, S. (2016). Small molecule inhibitor of NRF2 selectively intervenes therapeutic resistance in KEAP1-deficient NSCLC tumors. *ACS Chemical Biology*, *11*(11), 3214–3225. <https://doi.org/10.1021/acscchembio.6b00651>
- Singh, C. K., Chhabra, G., Ndiaye, M. A., Garcia-Peterson, L. M., MacK, N. J., & Ahmad, N. (2018). The Role of Sirtuins in Antioxidant and Redox Signaling. *Antioxidants and Redox Signaling*, *28*(8), 643–661. <https://doi.org/10.1089/ars.2017.7290>
- Sirotkin, A. V. (2014). Phytoestrogens and their effects. *European Journal of Pharmacology*, *741*(1), 230–236. <https://doi.org/10.1016/j.ejphar.2014.07.057>
- Smith, A. M., & Dragunow, M. (2014). The human side of microglia. *Trends in Neurosciences*, *37*(3), 125–135. <https://doi.org/10.1016/j.tins.2013.12.001>
- Smith, C. L., & O'Malley, B. W. (2004). Coregulator Function: A Key to Understanding Tissue Specificity of Selective Receptor Modulators. *Endocrine Reviews*, *25*(1), 45–71. <https://doi.org/10.1210/er.2003-0023>
- Smolders, S., Kessels, S., Smolders, S. M. T., Poulhes, F., Zelphati, O., Sapet, C., & Brône, B. (2018). Magnetofection is superior to other chemical transfection methods in a microglial cell line. *Journal of Neuroscience Methods*, *293*, 169–173. <https://doi.org/10.1016/j.jneumeth.2017.09.017>
- Sochocka, M., Diniz, B. S., & Leszek, J. (2017). Inflammatory Response in the CNS: Friend or Foe? *Molecular Neurobiology*, *54*(10), 8071–8089. <https://doi.org/10.1007/s12035-016-0297-1>
- Solleiro-Villavicencio, H., & Rivas-Arancibia, S. (2018). Effect of chronic oxidative stress



- on neuroinflammatory response mediated by CD4+T cells in neurodegenerative diseases. *Frontiers in Cellular Neuroscience*, 12(April), 1–13. <https://doi.org/10.3389/fncel.2018.00114>
- Soni, M., Rahardjo, T. B. W., Soekardi, R., Sulistyowati, Y., Lestariningsih, Yesufu-Udechuku, A., ... Hogervorst, E. (2014). Phytoestrogens and cognitive function: A review. *Maturitas*, 77(3), 209–220. <https://doi.org/10.1016/j.maturitas.2013.12.010>
- Sparkman, N. L., & Johnson, R. W. (2008). The Effects of Infection or Stress. *NeuroImmunoModulation*, 15(4–6), 323–330. <https://doi.org/10.1159/000156474.Neuroinflammation>
- Speicher, A. M., Wiendl, H., Meuth, S. G., & Pawlowski, M. (2019). Generating microglia from human pluripotent stem cells: Novel in vitro models for the study of neurodegeneration. *Molecular Neurodegeneration*, 14(1), 1–16. <https://doi.org/10.1186/s13024-019-0347-z>
- Speir, E., Yu, Z. X., Takeda, K., Ferrans, V. J., & Cannon, R. O. (2000a). Antioxidant effect of estrogen on cytomegalovirus-induced gene expression in coronary artery smooth muscle cells. *Circulation*, 102(24), 2990–2996. <https://doi.org/10.1161/01.CIR.102.24.2990>
- Speir, E., Yu, Z. X., Takeda, K., Ferrans, V. J., & Cannon, R. O. (2000b). Competition for p300 regulates transcription by estrogen receptors and nuclear factor-κB in human coronary smooth muscle cells. *Circulation Research*, 87(11), 1006–1011. <https://doi.org/10.1161/01.RES.87.11.1006>
- Stansley, B., Post, J., & Hensley, K. (2012). A comparative review of cell culture systems for the study of microglial biology in Alzheimer's disease. *Journal of Neuroinflammation*, 9(1), 1. <https://doi.org/10.1186/1742-2094-9-115>
- Stein, B., & Yang, M. X. (1995). Repression of the interleukin-6 promoter by estrogen receptor is mediated by NF-kappa B and C/EBP beta. *Molecular and Cellular Biology*, 15(9), 4971–4979. <https://doi.org/10.1128/mcb.15.9.4971>
- Stout, J., Knapp, A., Banz, W., Wallace, D., & Cheatwood, J. (2013). Subcutaneous daidzein administration enhances recovery of skilled ladder walking performance following stroke in rats. *Behavioural Brain Research*, 256, 428–431.
- Stout, J. M., Knapp, A. N., Banz, W. J., Wallace, D. G., & Cheatwood, J. L. (2013). Subcutaneous daidzein administration enhances recovery of skilled ladder walking performance following stroke in rats. *Behavioural Brain Research*, 256, 428–431. <https://doi.org/10.1016/j.bbr.2013.08.027>
- Su, F., Bai, F., & Zhang, Z. (2016). Inflammatory Cytokines and Alzheimer's Disease: A Review from the Perspective of Genetic Polymorphisms. *Neuroscience Bulletin*, 32(5), 469–480. <https://doi.org/10.1007/s12264-016-0055-4>
- Subedi, L., Ji, E., Shin, D., Jin, J., Yeo, J. H., & Kim, S. Y. (2017). Equol, a dietary daidzein gut metabolite attenuates microglial activation and potentiates neuroprotection in vitro.

*Nutrients*, 9(3), 1–16. <https://doi.org/10.3390/nu9030207>

- Subramaniam, S. (2019). Selective neuronal death in neurodegenerative diseases: The ongoing mystery. *Yale Journal of Biology and Medicine*, 92(4), 695–705.
- Subramaniam, S., & Unsicker, K. (2010). ERK and cell death: ERK1/2 in neuronal death. *FEBS Journal*, 277(1), 22–29. <https://doi.org/10.1111/j.1742-4658.2009.07367.x>
- Sultana, R., Ravagna, A., Mohmmad-Abdul, H., Calabrese, V., & Butterfield, D. A. (2005). Ferulic acid ethyl ester protects neurons against amyloid  $\beta$ -peptide(1-42)-induced oxidative stress and neurotoxicity: Relationship to antioxidant activity. *Journal of Neurochemistry*, 92(4), 749–758. <https://doi.org/10.1111/j.1471-4159.2004.02899.x>
- Sun, J., & Nan, G. (2017a). The extracellular signal-regulated kinase 1/2 pathway in neurological diseases: A potential therapeutic target (Review). *International Journal of Molecular Medicine*, 39(6), 1338–1346. <https://doi.org/10.3892/ijmm.2017.2962>
- Sun, J., & Nan, G. (2017b, June 1). The extracellular signal-regulated kinase 1/2 pathway in neurological diseases: A potential therapeutic target (Review). *International Journal of Molecular Medicine*, Vol. 39, pp. 1338–1346. <https://doi.org/10.3892/ijmm.2017.2962>
- Sun, M. Y., Ye, Y., Xiao, L., Rahman, K., Xia, W., & Zhang, H. (2016). Daidzein: A review of pharmacological effects. *African Journal of Traditional, Complementary and Alternative Medicines*, 13(3), 117–132. <https://doi.org/10.4314/ajtcam.v13i3.15>
- Sundaresan, A., Radhiga, T., & Deivasigamani, B. (2018). Biological Activity of Biochanin A: A Review. *Asian Journal of Pharmacy and Pharmacology*, 4(1), 1–5. <https://doi.org/10.31024/ajpp.2018.4.1.1>
- Tao, X., Li, N., Liu, F., Hu, Y., Liu, J., & Zhang, Y. M. (2018). In vitro examination of microglia-neuron crosstalk with BV2 cells, and primary cultures of glia and hypothalamic neurons. *Heliyon*, 4(8), 1–14. <https://doi.org/10.1016/j.heliyon.2018.e00730>
- Tham, D. M., Gardner, C. D., & Haskell, W. L. (2011). Potential Health Benefits of Dietary Phytoestrogens: A Review of the Clinical, Epidemiological, and Mechanistic Evidence<sup>1</sup>. <Http://Dx.Doi.Org/10.1210/Jcem.83.7.4752>, 83(7), 2223–2235. <https://doi.org/10.1210/jc.83.7.2223>
- Timmerman, R., Burm, S. M., & Bajramovic, J. J. (2018). An Overview of in vitro Methods to Study Microglia. *Frontiers in Cellular Neuroscience*, 12(August), 1–12. <https://doi.org/10.3389/fncel.2018.00242>
- Tong, C. K., & Vidyadaran, S. (2016). Role of microglia in embryonic neurogenesis. *Experimental Biology and Medicine*, 241(15), 1669–1675. <https://doi.org/10.1177/1535370216664430>
- Treeck, O., Diepolder, E., Skrzypczak, M., Schüler-Toprak, S., & Ortmann, O. (2019). Knockdown of estrogen receptor  $\beta$  increases proliferation and affects the transcriptome of endometrial adenocarcinoma cells. *BMC Cancer*, 19(1), 1–11.

<https://doi.org/10.1186/s12885-019-5928-2>

- Tremblay, M. È., Lecours, C., Samson, L., Sánchez-Zafra, V., & Sierra, A. (2015). From the Cajal alumni Achúcarro and Río-Hortega to the rediscovery of never-resting microglia. *Frontiers in Neuroanatomy*, 9(APR), 1–10. <https://doi.org/10.3389/fnana.2015.00045>
- Tripathi, P., Tripathi, P., Kashyap, L., & Singh, V. (2007). The role of nitric oxide in inflammatory reactions. *FEMS Immunology and Medical Microbiology*, 51(3), 443–452. <https://doi.org/10.1111/j.1574-695X.2007.00329.x>
- Turnbull, M. D. (2000). “Influence of chlorine substituents on biological activity of chemicals”: A comment. *Pest Management Science*, 56(1), 22–23. [https://doi.org/10.1002/\(SICI\)1526-4998\(200001\)56:1<22::AID-PS127>3.0.CO;2-I](https://doi.org/10.1002/(SICI)1526-4998(200001)56:1<22::AID-PS127>3.0.CO;2-I)
- Tzagarakis-Foster, C., Geleziunas, R., Lomri, A., An, J., & Leitman, D. C. (2002). Estradiol represses human T-cell leukemia virus type 1 Tax activation of tumor necrosis factor- $\alpha$  gene transcription. *Journal of Biological Chemistry*, 277(47), 44772–44777. <https://doi.org/10.1074/jbc.M205355200>
- Uemura, E. (2015). Structure and Function of Neurons and Neuroglia. *Fundamentals of Canine Neuroanatomy and Neurophysiology*, 11–37.
- Veldman, C. M., Cantorna, M. T., & DeLuca, H. F. (2001). Eating soya improves human memory. *Psychopharmacology*, 157(4), 430–436. <https://doi.org/10.1007/s002130100845>
- Villa, A., Vegeto, E., Poletti, A., & Maggi, A. (2016). Estrogens, neuroinflammation, and neurodegeneration. *Endocrine Reviews*, 37(4), 372–402. <https://doi.org/10.1210/er.2016-1007>
- Vrtačnik, P., Ostanek, B., Mencej-Bedrač, S., & Marc, J. (2014). The many faces of estrogen signaling. *Biochimica Medica*, 24(3), 329–342. <https://doi.org/10.11613/BM.2014.035>
- Wang, J., He, C., Wu, W. Y., Chen, F., Wu, Y. Y., Li, W. Z., ... Yin, Y. Y. (2015). Biochanin A protects dopaminergic neurons against lipopolysaccharide-induced damage and oxidative stress in a rat model of Parkinson’s disease. *Pharmacology Biochemistry and Behavior*, 138, 96–103. <https://doi.org/10.1016/j.pbb.2015.09.013>
- Wang, W., Tan, M., Yu, J., & Tan, L. (2015). *Imported from* <https://www.ncbi.nlm.nih.gov/pubmed/26207229/?i=2&from=/28431620/related>. 3(10), 1–15. <https://doi.org/10.3978/J.ISSN.2305-5839.2015.03.49>
- Wang, Y. J., Zheng, Y. L., Lu, J., Chen, G. Q., Wang, X. H., Feng, J., ... Sun, Q. J. (2010). Purple sweet potato color suppresses lipopolysaccharide-induced acute inflammatory response in mouse brain. *Neurochemistry International*, 56(3), 424–430. <https://doi.org/10.1016/j.neuint.2009.11.016>
- Wardyn, J. D., Ponsford, A. H., & Sanderson, C. M. (2015). Dissecting molecular cross-talk between Nrf2 and NF- $\kappa$ B response pathways. *Biochemical Society Transactions*, 43, 621–626. <https://doi.org/10.1042/BST20150014>

- Weemen, B. K., & Schuurs, A. H. W. M. (1971). Immunoassay Using Antigen - Enzyme Conjugates. *FEBS Letters*, *15*(3), 232–236. <https://doi.org/10.5055/jom.2019.0521>
- Weiser, M. J., Foradori, C. D., & Handa, R. J. (2008). Estrogen receptor beta in the brain: from form to function. *Brain Res Rev*, *57*(2), 309–320. <https://doi.org/10.1016/j.brainresrev.2007.05.013>
- Why Mouse Matters | NHGRI. (n.d.). Retrieved April 13, 2020, from <https://www.genome.gov/10001345/importance-of-mouse-genome>
- Wojda, I. (2012). Szlaki kinaz białkowych MAP - ewolucja i rola w przebiegu wybranych chorób neurozwyrodnieniowych. *Postępy Biochemii*, *58*(1), 79–90.
- Wojtera, M., Kłoszewska, I., Sobów, T., & Liberski, P. P. (2006). Immunologiczne aspekty choroby Alzheimera. *Aktualności Neurologiczne*, *6*(2), 108–115.
- Woodling, N. S., & Andreasson, K. I. (2016). Untangling the Web: Toxic and Protective Effects of Neuroinflammation and PGE2 Signaling in Alzheimer's Disease. *ACS Chem Neurosci*, *7*(4), 454–463. <https://doi.org/10.1016/j.gde.2016.03.011>
- Wu, C. C., & Bratton, S. B. (2013). Regulation of the intrinsic apoptosis pathway by reactive oxygen species. *Antioxidants and Redox Signaling*, *19*(6), 546–558. <https://doi.org/10.1089/ars.2012.4905>
- Wu, L. Y., Ye, Z. N., Zhuang, Z., Gao, Y., Tang, C., Zhou, C. H., ... Shi, J. X. (2018). Biochanin a reduces inflammatory injury and neuronal apoptosis following subarachnoid hemorrhage via suppression of the TLRs/TIRAP/MyD88/NF-κB pathway. *Behavioural Neurology*, 2018. <https://doi.org/10.1155/2018/1960106>
- Wu, W. Y., Wu, Y. Y., Huang, H., He, C., Li, W. Z., Wang, H. L., ... Yin, Y. Y. (2015). Biochanin A attenuates LPS-induced pro-inflammatory responses and inhibits the activation of the MAPK pathway in BV2 microglial cells. *International Journal of Molecular Medicine*, *35*(2), 391–398. <https://doi.org/10.3892/ijmm.2014.2020>
- Wua, W. F., Tana, X. J., Daia, Y. B., Krishnan, V., Warner, M., & Gustafsson, J. Å. (2013). Targeting estrogen receptor β in microglia and T cells to treat experimental autoimmune encephalomyelitis. *Proceedings of the National Academy of Sciences of the United States of America*, *110*(9), 3543–3548. <https://doi.org/10.1073/pnas.1300313110>
- Xia, Q., Hu, Q., Wang, H., Yang, H., Gao, F., Ren, H., ... Wang, G. (2015). Induction of COX-2-PGE2 synthesis by activation of the MAPK/ERK pathway contributes to neuronal death triggered by TDP-43-depleted microglia. *Cell Death & Disease*, *6*, e1702. <https://doi.org/10.1038/cddis.2015.69>
- Xiang, J., Wan, C., Guo, R., & Guo, D. (2016). Is Hydrogen Peroxide a Suitable Apoptosis Inducer for All Cell Types? *BioMed Research International*, 2016. <https://doi.org/10.1155/2016/7343965>
- Xiao, B. X., Feng, L., Cao, F. R., Pan, R. Le, Liao, Y. H., Liu, X. M., & Chang, Q. (2016). Pharmacokinetic profiles of the five isoflavonoids from *Pueraria lobata* roots in the CSF

- and plasma of rats. *Journal of Ethnopharmacology*, 184, 22–29. <https://doi.org/10.1016/j.jep.2016.02.027>
- Xie, J., Zhang, X., & Zhang, L. (2013). Negative regulation of inflammation by SIRT1. *Pharmacological Research*, 67(1), 60–67. <https://doi.org/10.1016/j.phrs.2012.10.010>
- Xu, M., Peng, Y., Zhu, L., Wang, S., Ji, J., & Rakesh, K. P. (2019). Triazole derivatives as inhibitors of Alzheimer's disease: Current developments and structure-activity relationships. *European Journal of Medicinal Chemistry*, 180, 656–672. <https://doi.org/10.1016/j.ejmech.2019.07.059>
- Xue, M., Zhang, K., Mu, K., Xu, J., Yang, H., Liu, Y., ... Zhuang, T. (2019). Regulation of estrogen signaling and breast cancer proliferation by an ubiquitin ligase TRIM56. *Oncogenesis*, 8(5). <https://doi.org/10.1038/s41389-019-0139-x>
- Yamamoto, Y., & Gaynor, R. B. (2001). Therapeutic potential of inhibition of the NF- $\kappa$ B pathway in the treatment of inflammation and cancer. *Journal of Clinical Investigation*, 107(2), 135–142. <https://doi.org/10.1172/JCI11914>
- Yang, Y., Kim, S. C., Yu, T., Yi, Y.-S., Rhee, M. H., Sung, G.-H., ... Cho, J. Y. (2014). Functional Roles of p38 Mitogen-Activated Protein Kinase in Macrophage-Mediated Inflammatory Responses. *Mediators of Inflammation*, 2014. <https://doi.org/10.1155/2014/270302>
- Yarza, R., Vela, S., Solas, M., & Ramirez, M. J. (2016). c-Jun N-terminal kinase (JNK) signaling as a therapeutic target for Alzheimer's disease. *Frontiers in Pharmacology*, 6(JAN), 1–12. <https://doi.org/10.3389/fphar.2015.00321>
- Yu, C., Zhang, P., Lou, L., & Wang, Y. (2019). Perspectives Regarding the Role of Biochanin A in Humans. *Frontiers in Pharmacology*, 10(July), 1–11. <https://doi.org/10.3389/fphar.2019.00793>
- Yu, J., Bi, X., Yu, B., & Chen, D. (2016). Isoflavones: Anti-inflammatory benefit and possible caveats. *Nutrients*, 8(6), 1–16. <https://doi.org/10.3390/nu8060361>
- Yuste, J. E., Tarragon, E., Campuzano, C. M., & Ros-Bernal, F. (2015). Implications of glial nitric oxide in neurodegenerative diseases. *Frontiers in Cellular Neuroscience*, 9(August), 1–13. <https://doi.org/10.3389/fncel.2015.00322>
- Zárate, S., Stevnsner, T., & Gredilla, R. (2017). Role of estrogen and other sex hormones in brain aging. Neuroprotection and DNA repair. *Frontiers in Aging Neuroscience*, 9(DEC), 1–22. <https://doi.org/10.3389/fnagi.2017.00430>
- Zhang, B., Wei, Y. Z., Wang, G. Q., Li, D. Di, Shi, J. S., & Zhang, F. (2019). Targeting MAPK pathways by naringenin modulates microglia M1/M2 polarization in lipopolysaccharide-stimulated cultures. *Frontiers in Cellular Neuroscience*, 12(January), 1–11. <https://doi.org/10.3389/fncel.2018.00531>
- Zhang, Y., & Chen, W. an. (2014). Biochanin A Inhibits Lipopolysaccharide-Induced Inflammatory Cytokines and Mediators Production in BV2 Microglia. *Neurochemical*

*Research*, 40(1), 165–171. <https://doi.org/10.1007/s11064-014-1480-2>

Zhao, C., Dahlman-Wright, K., & Gustafsson, J. A. (2008). Estrogen receptor beta: an overview and update. *Nuclear Receptor Signaling*, 6, 1–10. <https://doi.org/10.1621/nrs.06003>

Zhao, L., Mao, Z., & Diaz Brinton, R. (2009). *A Select Combination of Clinically Relevant Phytoestrogens Enhances Estrogen Receptor-Binding Selectivity and Neuroprotective Activities in Vitro and in Vivo*. <https://doi.org/10.1210/en.2008-0715>

Zhao, M. L., Liu, J. S. h., He, D., Dickson, D. W., & Lee, S. C. (1998). Inducible nitric oxide synthase expression is selectively induced in astrocytes isolated from adult human brain. *Brain Research*, 813(2), 402–405. [https://doi.org/10.1016/S0006-8993\(98\)01023-3](https://doi.org/10.1016/S0006-8993(98)01023-3)

Zhao, X., Allison, D., Condon, B., Zhang, F., Gheyi, T., Zhang, A., ... Luz, J. G. (2013). The 2.5 Å crystal structure of the SIRT1 catalytic domain bound to nicotinamide adenine dinucleotide (NAD<sup>+</sup>) and an indole (EX527 analogue) reveals a novel mechanism of histone deacetylase inhibition. *Journal of Medicinal Chemistry*, 56(3), 963–969. <https://doi.org/10.1021/jm301431y>

Zhou, C.-H., & Wang, Y. (2012). Recent Researches in Triazole Compounds as Medicinal Drugs. *Current Medicinal Chemistry*, 19(2), 239–280. <https://doi.org/10.2174/092986712803414213>